



Kent Academic Repository

Delezene, Lucas K., Skinner, Matthew M., Bailey, Shara E., Brophy, Juliet K., Elliott, Marina C., Gurtov, Alia, Irish, Joel D., Moggi-Cecchi, Jacopo, de Ruiten, Darryl J., Hawks, John and others (2023) *Descriptive catalog of Homo naledi dental remains from the 2013 to 2015 excavations of the Dinaledi Chamber, site U.W. 101, within the Rising Star cave system, South Africa*. *Journal of human evolution*, 180 . ISSN 0047-2484.

Downloaded from

<https://kar.kent.ac.uk/101593/> The University of Kent's Academic Repository KAR

The version of record is available from

<https://doi.org/10.1016/j.jhevol.2023.103372>

This document version

Author's Accepted Manuscript

DOI for this version

Licence for this version

CC BY-NC-ND (Attribution-NonCommercial-NoDerivatives)

Additional information

Versions of research works

Versions of Record

If this version is the version of record, it is the same as the published version available on the publisher's web site. Cite as the published version.

Author Accepted Manuscripts

If this document is identified as the Author Accepted Manuscript it is the version after peer review but before type setting, copy editing or publisher branding. Cite as Surname, Initial. (Year) 'Title of article'. To be published in **Title of Journal**, Volume and issue numbers [peer-reviewed accepted version]. Available at: DOI or URL (Accessed: date).

Enquiries

If you have questions about this document contact ResearchSupport@kent.ac.uk. Please include the URL of the record in KAR. If you believe that your, or a third party's rights have been compromised through this document please see our [Take Down policy](https://www.kent.ac.uk/guides/kar-the-kent-academic-repository#policies) (available from <https://www.kent.ac.uk/guides/kar-the-kent-academic-repository#policies>).

Descriptive catalogue of *Homo naledi* dental remains from the 2013–2015 excavations of the Dinaledi Chamber, Site U.W. 101, within the Rising Star cave system, South Africa

Lucas K. Delezene^{a, b, *}, Matthew M. Skinner^{b, c, d}, Shara Bailey^{d, e}, Juliet K. Brophy^{b, f}, Marina Elliott^{b, g}, Alia Gurtov^h, Joel D. Irish^{b, i}, Jacopo Moggi-Cecchi^j, Darryl J. de Ruiter^{b, k}, J. Hawks^{b, l}, Lee R. Berger^{m, b}

^a *Department of Anthropology, University of Arkansas, Fayetteville, AR 72701, USA*

^b *Centre for the Exploration of the Deep Human Journey, University of the Witwatersrand, Private Bag 3, WITS 2050, South Africa*

^c *School of Anthropology and Conservation, University of Kent, Marlowe Building, Canterbury, CT2 7NR, UK*

^d *Department of Human Evolution, Max Planck Institute for Evolutionary Anthropology, Deutscher Platz 6, 04103 Leipzig, Germany*

^e *Department of Anthropology, Center for the Study of Human Origins, New York University, New York, NY 10003, USA*

^f *Department of Geography and Anthropology, Louisiana State University, Baton Rouge, LA 70803, USA*

^g *Department of Archaeology, Simon Fraser University, 8888 University Drive, Burnaby, B.C. V5A 1S6, USA*

^h *Stripe, Inc., 199 Water Street, 30th Floor, New York, NY 10038, USA.*

ⁱ *School of Biological and Environmental Sciences, Liverpool John Moores University, Liverpool L3 3AF, UK*

^j *Laboratory of Anthropology, Department of Biology, University of Florence, Via del Proconsolo 12, Firenze 50122, Italy*

^k *Department of Anthropology, Texas A&M University, College Station, TX 77843, USA*

^l *Department of Anthropology, University of Wisconsin-Madison. Madison, WI 53706, USA*

^m *National Geographic Society, 1145 17th Street NW, Washington DC 20036, USA.*

***Corresponding author.**

E-mail address: delezene@uark.edu (L.K. Delezene).

1 **Descriptive catalogue of *Homo naledi* dental remains from the 2013–2015**
2 **excavations of the Dinaledi Chamber, Site U.W. 101, within the Rising Star cave**
3 **system, South Africa**

4
5 **Abstract**

6 More than 150 hominin teeth, dated to ~241–330 thousand years ago, were recovered
7 during the 2013–2015 excavations of the Dinaledi Chamber of the Rising Star cave
8 system, South Africa. These fossils comprise the first large single-site sample of hominin
9 teeth from the Middle Pleistocene of Africa. Though scattered remains attributable to
10 *Homo sapiens*, or their possible lineal ancestors, are known from older and younger sites
11 across the continent, the distinctive morphological feature set of the Dinaledi teeth
12 supports the recognition of a novel hominin species, *Homo naledi*. This material provides
13 evidence of African *Homo* lineage diversity that lasts until at least the Middle
14 Pleistocene. Here, a catalogue, anatomical descriptions, and details of preservation and
15 taphonomic alteration are provided for the Dinaledi teeth. Where possible, provisional
16 associations among teeth are also proposed. To facilitate future research, we also provide
17 access to a catalogue of surface files of the Rising Star jaws and teeth.

18

19 **Keywords:** Middle Pleistocene; hominin; crown and root morphology; μ CT

20 **1. Introduction**

21 For nearly a century, fossil discoveries in South Africa have shaped our
22 understanding of hominin evolution (Dart, 1925). Nowhere is this more evident than in
23 studies of Plio-Pleistocene dental morphology, for the caves of South Africa (e.g., Taung,
24 Sterkfontein, Makapansgat, Kromdraai, Swartkrans, Gladysvale, Drimolen, Gondolin,
25 and Malapa) have yielded hundreds of teeth of *Australopithecus* and *Paranthropus* (e.g.,
26 Robinson, 1956; Berger et al., 1993, 2010; Menter et al., 1999; Moggi-Cecchi et al.,
27 2006, 2010; Martin et al., 2021; Rak et al., 2021). The pioneering work of Broom (1938)
28 and Robinson (1954, 1956), which detailed and contrasted the morphology of
29 *Australopithecus africanus* and *Paranthropus robustus*, influenced early hypotheses of
30 dental and dietary evolution and set the stage for the recognition of dentally primitive
31 species of *Homo* and other ‘australopithecine’ taxa in eastern and southern Africa (e.g.,
32 Broom and Robinson, 1949; Robinson, 1953; Leakey, 1959; Leakey et al., 1964; Tobias,
33 1965; Hughes and Tobias, 1977; Johanson et al., 1978; Berger et al., 2010; Irish et al.,
34 2013).

35 Yet, amid a rich record of *Australopithecus* and *Paranthropus*, the dental
36 evidence for extinct species of *Homo* in South Africa is comparatively sparse (e.g.,
37 Clarke, 1985; Grine et al., 1996, 2009; Moggi-Cecchi et al., 1998; Kuman and Clarke,
38 2000; Grine, 2005; Curnoe and Tobias, 2006). Broom and Robinson (1949) argued that
39 the SK 15 mandible represents a species of nonrobust hominin contemporaneous with *P.*
40 *robustus* in the Swartkrans deposits and erected the name *Telanthropus capensis* for that
41 taxon. Robinson (1953) considered other Swartkrans specimens (e.g., SK 18, SK 45, SK
42 80) to also belong to *Telanthropus*. These individuals and a few others from Swartkrans

43 (Clarke, 1977a, 1977b; Grine et al., 2009), and a handful of jaws, teeth, and crania from
44 Sterkfontein and Drimolen, are attributed to early *Homo* by some (Hughes and Tobias,
45 1977; Clarke, 1985; Moggi-Cecchi et al., 1998, 2010; Curnoe and Tobias, 2006; Kimbel,
46 2009; Herries et al., 2020). Despite this evidence, the taxonomic reality and identity of
47 South African early *Homo* is debated. Various sources highlight affinities of some of the
48 Swartkrans, Sterkfontein, and Drimolen *Homo* material with *Homo erectus* (*Homo*
49 *ergaster* to some) and/or *Homo habilis* from eastern Africa or suggest that these fossils
50 are phenotypically distinct from contemporary eastern African *Homo* (e.g., Grine et al.,
51 1996, 2009; Kuman and Clarke, 2000; Grine, 2005; Davies et al., 2020; Herries et al.,
52 2020). Whether specimens like Stw 53 and Stw 80 from Sterkfontein represent *Homo* or
53 the same ‘nonrobust’ taxon sampled at Swartkrans and Drimolen is unclear (e.g., Smith
54 and Grine, 2008; Davies et al., 2020). In fact, recent research casts doubts on the
55 attribution of many of the Swartkrans, Sterkfontein, Kromdraai, and Drimolen teeth to
56 early *Homo*, including SK 15 and Stw 53, leaving very few dental specimens that are
57 unequivocally early *Homo* in the South African fossil record (Zanolli et al., 2022).

58 The record of teeth from South Africa that bridges the temporal and phylogenetic
59 gap from early *Homo* to *Homo sapiens* is also patchy, especially in comparison to
60 similarly aged European (e.g., Martín-Torres et al., 2012), northern African (e.g.,
61 Hublin et al., 2017), and Levantine (e.g., Vandermeersch, 1981) material, and the
62 southern African specimens tend to be isolated and with poor chronological resolution
63 (Berger et al., 2017). For example, an approximately one million-year-old M¹ from
64 Cornelia-Uitzek, which is associated Acheulean tools, is argued to resemble South
65 African early *Homo* specimens (Brink et al., 2012). Among southern African teeth argued

66 to derive from the Middle Pleistocene are those in the Cave of Hearths mandible (e.g.,
67 Davies et al., 2019b, 2020), which is likely associated with Late Acheulean artifacts
68 (Curnoe, 2009; McNabb, 2009) and argued by Tobias (1971) to represent *Homo*
69 *rhodesiensis* (*Homo heidelbergensis* or archaic *Homo sapiens* in other taxonomic
70 schemes). From the Lincoln Cave of Sterkfontein, Stw 585 may be associated with
71 Middle Stone Age stone tools and is referred to as “perhaps archaic *Homo sapiens*”
72 (Reynolds et al., 2007: 267). Small samples of teeth from sites along the Eastern Cape
73 coast (e.g., Grine and Klein, 1993; Berger and Parkington, 1995; Stynder et al., 2001) and
74 an isolated third molar spatially associated with the Florisbad cranium could represent *H.*
75 *rhodesiensis*, *Homo helmei*, or even early *H. sapiens* (Dreyer, 1935; Rightmire, 1978;
76 Kuman and Clarke, 1986; Grün et al., 1996). The dental record from the Late Pleistocene
77 is also sparse; yet, specimens attributable to *H. sapiens* are documented from sites that
78 dot the South African coast (e.g., Die Kelders, Diepkloof, Pinnacle Point, Blombos,
79 Klasies River Mouth, Ysterfontein) and from scattered inland sites (e.g., Equus Cave,
80 Hofmeyr, Sibudu) that are argued to show an association between *H. sapiens* and the
81 Middle Stone Age to Late Stone Age transition (e.g., Marean et al., 2004; Smith et al.,
82 2006; Grine et al., 2007, 2017a, 2017b, 2021; Harvati et al., 2015; Grine, 2016; Riga et
83 al., 2018; Will et al., 2019; Niespolo et al., 2021).

84 The ~241–330-thousand-year-old fossils from the Dinaledi Chamber of the Rising
85 Star cave system provide the first assemblage of South African Middle Pleistocene-aged
86 (Dirks et al., 2017; Robbins et al., 2021) *Homo* teeth that begins to approach the
87 abundance of the older *P. robustus* and *A. africanus* samples from the region. The
88 Dinaledi fossils are all attributed to *Homo naledi* (Berger et al., 2015). Given that the

89 previously known Middle Pleistocene southern African fossils could be argued to be *H.*
90 *sapiens* or their lineal ancestors (e.g., Rightmire, 2008; Bailey and Hublin, 2013; but see
91 Grün et al., 2020), it is perhaps surprising that the Dinaledi dental and skeletal material is
92 morphologically quite distinct from contemporaneous Eurasian and other African Middle
93 Pleistocene *Homo* samples. The short stature, small body mass, and absolute and relative
94 encephalization of *H. naledi* are on par with *Australopithecus* and *Paranthropus*;
95 additionally, its curved manual phalanges and an *Australopithecus*-like hip are out of step
96 with fossils attributed to *H. sapiens* and *H. neanderthalensis* (Harcourt-Smith et al., 2015;
97 Kivell et al., 2015; Feuerriegel et al., 2017; Garvin et al., 2017; Hawks et al., 2017;
98 Marchi et al., 2017; VanSickle et al., 2018). However, relative to *Australopithecus*, and
99 possibly early *Homo*, *H. naledi* is argued to share derived features with humans,
100 including aspects of endocast morphology (e.g., “extensive occipital petalial asymmetry”;
101 Holloway et al., 2018: 5740), derived carpal shapes (e.g., “a boot-shaped trapezoid with
102 an expanded palmar non-articular surface; Kivell et al., 2015: 5), low magnitude sexual
103 size dimorphism, an elongated lower limb, and low relative limb joint size (Garvin et al.,
104 2017; Hawks et al., 2017; Prabhat et al., 2021). Thus, the emerging picture is that *H.*
105 *naledi* is not simply a relict species of ‘early’ *Homo* that survived into the Middle
106 Pleistocene, but, rather, a species with a distinct cluster of traits, some of which are
107 candidate autapomorphies (e.g., pillars on the superior aspect of the femoral neck, strong
108 distal attachment of the pes anserinus (Marchi et al., 2017), larger P₃ than P₄ (Davies et
109 al., 2020)). Thus, *H. naledi* cannot be slotted easily into a scenario whereby all Middle
110 Pleistocene African *Homo* populations were ancestral to extant humans; instead, the

111 unique trait pattern of *H. naledi* points toward a deep history of *Homo* lineage diversity in
112 the Pleistocene (Dembo et al., 2016; see also Grün et al., 2020).

113 Through 2015, the Dinaledi Chamber has yielded more than 190 catalogued
114 whole or fragmentary teeth, including those in situ in eight mandibles and one maxilla of
115 variable preservation (Table 1; Berger et al., 2015). The current Dinaledi dental
116 collection represents nearly all anatomical parts, as only the mandibular deciduous central
117 incisor is currently unrepresented. The sample captures individuals that range in age from
118 infant to older adult (Berger et al., 2015; Bolter et al., 2018). Already, the Dinaledi dental
119 collection has contributed to discussions of sample demography (Bolter et al., 2018), diet
120 and ecology (i.e., Towle et al., 2017; Berthaume et al., 2018; Ungar and Berger, 2018),
121 sexual dimorphism and sample-level variation (Garvin et al., 2017), growth and
122 development (Cofran and Walker, 2017; Guatelli-Steinberg et al., 2018; Skinner, 2019),
123 the status of *H. naledi* as a distinct species of *Homo* (e.g., Skinner et al., 2016; Irish et al.,
124 2018; Bailey et al., 2019; Davies et al., 2019a, 2019b, 2020; Kupczik et al., 2019; Brophy
125 et al., 2021), and the phylogenetic place of *H. naledi* (Dembo et al., 2016; Irish and
126 Grabowski, 2021).

127 Here, we provide a descriptive catalogue, with accompanying three-dimensional
128 surface models derived from micro-computerized tomographic scans, of the Dinaledi
129 dental assemblage as collected through 2015. We refrain from extensive interspecific
130 comparisons, as focused analyses of some aspects of dental morphology are provided in
131 Berthaume et al. (2018), Guatelli-Steinberg et al. (2018), Irish et al. (2018), Bailey et al.,
132 (2019), Davies et al. (2019a, 2019b, 2020), Kupczik et al. (2019), Brophy et al. (2020),
133 and in forthcoming work. We do not systematically apply a standardized trait scoring

134 system, like the Arizona State University Dental Anthropology System (ASUDAS), to
135 nonmetric variation. For interested researchers, ASUDAS summary data for this sample
136 of *H. naledi* teeth can be found in Irish et al. (2018: Table 1; SOM Table S2). Individual
137 trait expression should be discernable in the multiple high-resolution views provided of
138 each tooth. Where appropriate to elucidate anatomical features, and when such
139 comparisons could be made with the original material, we also examined the *H. naledi*
140 fossils from the Lesedi Chamber, site U.W. 102 (e.g., Hawks et al., 2017).

141 This paper is intended to stand as the canonical catalogue of the U.W. 101
142 Dinaledi Chamber dental assemblage, to document the state of preservation for each
143 element at the time of publication, and to stand as a reference for and to stimulate future
144 research on the *H. naledi* teeth.

145

146 **2. Materials and methods**

147 *2.1. Provenience*

148 All specimens were collected from 2013 to 2015 from the Dinaledi Chamber (site
149 U.W. 101) within the karstic Rising Star cave system. The site is in the Cradle of
150 Humankind UNESCO World Heritage area in the Gauteng Province, South Africa, and is
151 near other well-known hominin bearing sites (e.g., Swartkrans and Sterkfontein; Dirks et
152 al., 2015, 2017; Kruger et al., 2016). The fossils were either collected from the surface of
153 the chamber floor or retrieved from localized excavations (Berger et al., 2015). Details of
154 the geology of the chamber and the methods of excavation are presented in Dirks et al.
155 (2015). The fossils described are curated in the PalaeoSciences Building at the University
156 of the Witwatersrand, Johannesburg, South Africa.

157

158 *2.2. Specimens*

159 With three exceptions, the teeth described here are those that comprise the
160 published paratype series of *H. naledi* from the Dinaledi Chamber that are iterated in
161 Berger et al. (2015: Supplementary File 1). Three paratype teeth, U.W. 101-020, U.W.
162 101-344, and U.W. 101-347, are not included in this monograph because they are from a
163 spatially discrete collection locus, the ‘Hill Antechamber,’ that is now considered to be
164 separate from the Dinaledi Chamber. The three Hill Antechamber teeth are being
165 examined as part of the material excavated after 2015 (e.g., Elliott et al., 2018). Where
166 differences occur, the specimen numbers and identification of the teeth herein supersede
167 that published in Berger et al. (2015).

168

169 *2.3. Assessment of visible anatomy and scanning procedures*

170 An inventory and description of the preserved visible anatomy is provided for all
171 accessioned dental specimens (Table 1). All teeth were examined with a low
172 magnification hand lens (10×). Where appropriate, micro-computerized tomographic
173 (μCT) scans were consulted to clarify anatomical detail and to assess structures obscured
174 by matrix or adhering bone. The teeth and jaws were scanned with a Nikon Metrology
175 XTH 225/320 μCT scanner housed in the PalaeoSciences Building at the University of
176 the Witwatersrand. Scanning parameters varied slightly by specimen but were 110–130
177 kV, 100–130 mA, 1500–2000 projections, 1–2 frame averaging, 1–2 mm Aluminium
178 filter. The isometric voxel size ranged between 0.027 and 0.036 mm³. Crown lengths and
179 breadths were measured with fine-pointed digital calipers and root lengths and

180 interproximal facet sizes were measured with either calipers or digitally from three-
181 dimensional models derived from μ CT scans using the three-dimensional measuring tool
182 in AvizoLite v. 9.1 (Thermo Fisher Scientific, Waltham). The extent of occlusal and
183 incisal macrowear follows the delineations of stages outlined in Smith (1984).

184 In contrast to the common condition at other South African hominin-bearing sites,
185 the Dinaledi tooth crowns are mostly complete, unbroken, and not deformed in shape
186 postmortem. Microcracks are present in the enamel but have not altered crown shapes.
187 Taphonomic modification, though minimal, is typically associated with the breakage of
188 the roots and the abrasion of their external surfaces. Where such damage is present, it is
189 noted. Many of the *H. naledi* crowns feature antemortem occlusal enamel chipping and
190 such damage is identified in the descriptions. Towle et al. (2017) assessed chipping
191 independently of this study and provide a summary of chipping frequency in their study.

192

193 *2.4. Assessment of antimeres and metameres*

194 The Dinaledi fossils are derived from a commingled assemblage (Dirks et al.,
195 2015) and many of the teeth were excavated as isolated specimens in close spatial
196 association. In some instances, isolated teeth belonging to a single individual (e.g., the
197 U.W. 101-1126, U.W. 101-1131, U.W. 101-1132, and U.W. 101-1333 anterior
198 mandibular teeth) were excavated in near-anatomical position. In most cases, though,
199 spatial proximity is a poor guide as to whether specimens belong to the same individual.
200 In addition, it is evident that there are duplicated teeth representing similarly aged
201 individuals as judged by dental wear and crown developmental status (e.g., the U.W. 101-
202 809 and U.W. 101-814 left M₁s), which complicates attempts to associate isolated, non-

203 articulating, and non-occluding teeth into biological individuals. Thus, a conservative
204 approach to assigning specimens to individuals is taken. Antimeres are proposed based
205 on morphological similarity. Metameric associations are proposed based on the
206 congruency of interproximal facets and consistencies in occlusal wear. In the case of
207 tooth germs, associations based on development status are proposed cautiously. By taking
208 such an approach, many teeth are likely left unlinked to others that could represent the
209 same individual. All proposed associations are provisional and will certainly require
210 revision with the recovery of additional teeth in future excavations.

211

212 *2.5. Abbreviations*

213 The following anatomical abbreviations are used throughout the text:

214 L = left

215 R = right

216 IC = incisocervically

217 OC = occlusocervically

218 MD = mesiodistal/ly

219 BL = buccolingual/ly

220 LaL = labiolingual/ly

221 Prd = Protoconid

222 Med = Metaconid

223 Hyd = Hypoconid

224 End = Entoconid

225 Hld = Hypoconulid

- 226 Pa = Paracone
227 Pr = Protocone
228 Me = Metacone
229 Hy = Hypocone
230 C5 = cusp five, maxillary molar
231 C6 = tuberculum sextum, mandibular molar
232 C7 = tuberculum intermedium, mandibular molar
233 Fa = anterior fovea
234 Fp = posterior fovea
235 MMR = mesial marginal ridge
236 DMR = distal marginal ridge
237 Mlg = median longitudinal groove
238 Co = crista obliqua/distal trigone crest
239 IPF = interproximal contact facet
240 EDJ = enamel-dentine junction
241 OES = outer enamel surface

242

243 **3. Descriptions**

244 As most of the Dinaledi teeth were recovered as isolated specimens, we describe
245 the isolated specimens by tooth class and present them in ascending order according to
246 their accession number. Where specimens with separate accession numbers have been
247 physically refit to one another, they are described together as a single specimen. Teeth
248 found in jaws are described together as a single specimen following the descriptions of

249 the isolated teeth. A companion database of images and viewable ply surface files derived
250 from μ CT scans is available at <https://human-fossil-record.org/>.

251

252 *3.1. Deciduous maxillary central incisors*

253 A single pair of proposed antimeric dI¹s is known from the Dinaledi Chamber
254 deposits. Morphologically, the crowns are simple and lack prominent marginal ridges or
255 features on the lingual face.

256

257 U.W. 101-544C: RdI¹ (Fig. 1A; Table 1) A narrow ribbon of dentine is exposed along the
258 incisal surface (stage 3). A flat, teardrop shaped mesial IPF (2.5 mm IC by 1.5 mm LaL)
259 sits near the incisal edge of the mesial shoulder. No distal IPF is present. The crown is
260 short and wide with weak labial convexity at mid-crown but a more-or-less straight incisal
261 edge. In mesial and distal views, the labial face exhibits only minor IC curvature. In
262 lingual view, weak marginal ridges are visible on the incisal half of the crown. These
263 become indistinct as they extend towards the mesially-displaced and bulbous basal
264 eminence. There is also a faint median lingual ridge, accentuated by mesial and distal
265 furrows. The mesial fossa is narrower and deeper than the distal fossa.

266 The LaL-flattened root is nearly complete, just missing the tip so that the root
267 canal is exposed and is abraded externally. The maximum height preserved is 9.4 mm. In
268 labial and lingual views, the root tilts slightly distally.

269 This specimen is proposed as the antimere of U.W. 101-1331. It shares a
270 specimen number with U.W. 101-544A (RdP⁴) and U.W. 101-544B (crown incomplete
271 RC¹) because they were excavated in close spatial proximity. Though all represent sub-

272 adults, it is unlikely that they represent a single individual. Both U.W. 101-544B and
273 U.W. 101-544C have proposed antimeres in the assemblage and are likely attributable to
274 the nearly complete mixed dentition associated with the U.W. 101-1400 mandible and its
275 associated antimeres and occluding teeth, which have erupted dP4s and nearly crown-
276 complete M1s; this would preclude the developing RdP⁴ germ, U.W. 101-544A, from
277 belonging to the same individual as U.W. 101-544B and U.W. 101-544C. However, from
278 a modern human perspective, the developmental status of U.W. 101-544A is not
279 inconsistent with attribution to the same individual as U.W. 101-544B and U.W. 101-
280 544C (AlQahtani et al., 2010). The possible association of U.W. 101-544B and U.W.
281 101-544C with U.W. 101-1400 are given a detailed treatment in the Discussion.

282

283 U.W. 101-1331: LdI¹ (Fig. 1B; Table 1) A narrow ribbon of dentine is exposed along the
284 incisal surface (stage 3). It also exhibits a flat, teardrop shaped mesial IPF (1.5 mm LaL
285 by 2.5 mm IC). No distal IPF is present. The crown is short and wide with weak labial
286 convexity at mid-crown but a more-or-less straight incisal edge. In mesial and distal views,
287 it exhibits only minor IC curvature. Lingually, weak marginal ridges are visible on the
288 incisal half of the crown, accentuated by faint mesial and distal furrows, and become
289 indistinct as they blend into the domed basal eminence.

290 The LaL-flattened root is nearly complete, just missing the tip so that the root
291 canal is exposed. In labial view, the preserved root is 9.4 mm in height. The root is
292 slightly abraded on its external surface.

293 This is likely the antimeres of U.W. 101-544C, to which it is nearly identical in
294 morphology and state of wear. These specimens are hypothesized to represent the same

295 individual as the U.W. 101-1400 mandible and other isolated deciduous and permanent
296 teeth. These associations are given in more detail in the Discussion.

297

298 *3.2. Deciduous maxillary lateral incisor*

299 A single dI² is represented in the recovered Dinaledi Chamber material. Like the
300 dI¹s, the dI² crown is simple and lacks prominent marginal ridges or features on the
301 lingual face.

302

303 U.W. 101-1304: LdI² (Fig. 2; Table 1) Wear blunted the incisal edge and exposed a thin
304 line of dentine and the DMR is worn along its surface (stage 1). No IPFs are present. In
305 labial and lingual views, the crown is asymmetrical with an incisal edge that is strongly
306 angled distally, resulting in lower distal and higher mesial aspects. The mesial corner is
307 rounded, and the distal corner is more angular. The marginal ridges are apparent,
308 especially so the mesial, which is much longer than the distal. There is a shallow groove
309 adjacent to the MMR. The median lingual ridge is indistinct and blends into a dome-like
310 basal eminence that occupies much of the lingual surface.

311 The root is nearly complete (8.0 mm in preserved height) but is broken before its
312 apex. The root is obliquely oriented relative to the crown, with its major cross-sectional
313 axis running mesiolabial to distolingual. The root is somewhat flattened LaL. A shallow
314 groove runs along the length of the distal surface.

315 Based upon developmental status, including the absence of IPFs, this specimen is
316 likely associated with the U.W. 101-1287A LdC¹.

317

318 3.3. *Deciduous maxillary canines*

319 Three dC¹s are known from the Dinaledi Chamber deposits. These include a pair
320 of proposed antimeres, U.W. 101-728 and U.W. 101-1287A, and an isolated specimen,
321 U.W. 101-595. The proposed antimeres are nearly identical, while U.W. 101-595 departs
322 slightly from the morphology seen in the others. In all crowns, the shoulders are placed at
323 approximately midcrown and the mesial and distal crests angle sharply from the
324 shoulders to meet at a centrally placed apex. The lingual and distal faces lack notable
325 features.

326

327 U.W. 101-595: LdC¹ (Fig. 3A; Table 1) The apex is slightly worn, exposing a dentine pit,
328 as are the mesial and distal tubercles (stage 2). A small mesial IPF is visible, but one is
329 not detectable distally. In occlusal view, the cervical outline is ovoid with the major axis
330 MD and the minor axis LaL. In this view, the apex is more distally placed because of the
331 longer mesial edge. The crown is moderately convex at mid-crown but has a straight
332 occlusal edge. In mesial and distal views, the crown is only mildly convex with a swollen
333 basal cingulum. In labial and lingual views, the crown is pentagonal, with a straight, if
334 not slightly angled, cervical line, vertical mesial and distal shoulders, and angled mesial
335 and distal edges that meet at a high apex, which sits very slightly mesial to the transverse
336 axis. On the lingual aspect, there is a weak, slightly mesially offset, median ridge. The
337 mesial and distal shoulders are quite prominent, forming distinct tubercles. They are
338 delineated lingually by mesial and distal grooves and are associated with mesial and
339 distal marginal ridges originating from the cingulum. The mesial tubercle is higher and
340 larger than the distal tubercle. Labially, the mesial and distal tubercles are associated with

341 weak mesial and distal furrows, with the distal furrow slightly more prominent. The
342 prominence of the tubercles departs from the condition in the other deciduous maxillary
343 canines (i.e., U.W. 101-728 and U.W. 101-1287A) in the Dinaledi assemblage.

344 The root is slightly abraded and is preserved for approximately 9.6 mm in labial
345 view, where it is broken just before the apex. The root extends straight from the crown. It
346 is circular in cross section near the cervix and pinches near the apex, with its major axis
347 MD and minor axis LaL.

348

349 U.W. 101-728: RdC¹ (Fig. 3B; Table 1) The apex is slightly blunted, exposing a pinpoint-
350 sized dentine pit. Minor wear facets, with no dentine exposure, are also visible along the
351 mesial and distal crests (stage 1). There is a teardrop shaped distal IPF (approximately 1.5
352 mm IC by 1.5 mm LaL) and no mesial IPF. In apical view, the crown is ovoid, longer
353 MD than LaL, and the apex is more-or-less centrally placed. In labial and lingual views,
354 the crown is pentagonal in outline with a straight cervical margin and angled mesial and
355 distal crests. The mesial edge is slightly convex, while the distal edge is slightly concave.
356 In lingual view, there is a slightly elevated, wide median ridge that merges with a weak,
357 rounded basal cingulum. Weak mesial and barely perceptible distal fossae border the
358 median lingual ridge. In labial view, there is a faint distal furrow associated with a slight
359 projection of the distal shoulder.

360 The root is slightly abraded and missing its apex. In labial view, the root of the
361 canine is preserved for approximately 10.2 mm where it is broken just before the apex.
362 The root is ovoid in cross section and compressed LaL. It extends nearly directly above
363 the crown with a slight distal tilt.

364 This is proposed as the antimere of U.W. 101-1287A. The specimens are nearly
365 identical in morphology and size. The only significant difference is that the small distal
366 IPF of U.W. 101-728 is lacking on U.W. 101-1287A. These teeth are also proposed to
367 belong to the nearly complete mixed dentition that includes the U.W. 101-1400
368 mandibular dentition and its antimeres.

369

370 U.W. 101-1287A: LdC¹ (Fig. 3C; Table 1) The tip of the apex is blunted by wear with a
371 small dentine pit exposed on its distal aspect. The wear facet continues along the distal
372 crest (stage 2). No IPFs are detectable. In occlusal view, the apex is offset to the mesial of
373 center and the crown is ovoid in profile, with the major axis MD and minor axis LaL. In
374 lingual and labial views, the crown is pentagonal, with vertical mesial and distal
375 shoulders and steeply angled mesial and distal edges. From the labial aspect, the crown
376 apex is slightly mesial of center. On the lingual aspect, the median ridge is slightly
377 swollen and set off by weak mesial and distal furrows. The mesial lingual fossa is a weak
378 groove adjacent to a faint MMR. The distal lingual fossa is barely perceptible and slightly
379 obscured by wear. Labially, a vertical mesial furrow is barely visible, while the distal
380 furrow, which associated with the distal shoulder, is wider and more distinct. Neither the
381 mesial and distal shoulders have distinct apices, as they do in U.W. 101-595, and they
382 lack sharp edges.

383 The root is broken near its apex and measures 11.6 mm as preserved. The exposed
384 root canal is filled with sediment. The root is ovoid in cross section and longer MD than
385 LaL.

386 This is proposed as the antimere of U.W. 101-728. The specimen is, however,
387 slightly less worn than the RdC¹, lacking a distinct wear facet along the mesial crest, and
388 it also lacks a distal IPF, which is present on the RdC¹. Based upon developmental status
389 and the lack of adjoining IPFs on both teeth, this specimen is proposed to be associated
390 with the U.W. 101-1304 LdI². Despite sharing an accession number based on the spatial
391 proximity of their recovery, this specimen and U.W. 101-1287B (RM₁) cannot represent
392 the same biological individual, as U.W. 101-1287B belongs to the mandibular dentition
393 represented by U.W. 101-1142, which has a completely erupted and worn permanent
394 dentition, while U.W. 101-1287A represents a young subadult with light wear on its
395 deciduous canines.

396

397 *3.4. Deciduous maxillary third premolars*

398 A pair of proposed antimeric dP³s, U.W. 101-823 and U.W. 101-1377, are known
399 from the Dinaledi Chamber material. Both feature four well developed main cusps, a
400 pentagonal occlusal outline, a beak-like mesial projection formed by the MMR, a
401 continuous Co separating the hypocone from the trigone, a thick epicrista extending from
402 the mesial crest of the Pa into the Fa, and a weakly-expressed Carabelli's feature.

403

404 U.W. 101-823: RdP³ (Fig. 4A; Table 1) A small oval mesial IPF (1.5 mm BL by 1.0 mm
405 OC) is located buccal to the midline. A distal IPF is absent. The crown is minimally worn
406 with small facets present on the lingual face of the Pa and the apex and mesial crest of the
407 Pr and small dentine pits are exposed over the Pr and Me (stage 2). The crown exhibits
408 four well-developed cusps having the following size relationships: Pr > Pa ≥ Me > Hy.

409 The Hy is conical in shape and equal in height to the Me. In occlusal view, the crown is a
410 squat pentagon in outline, reflecting the distolingually projecting Hy and well-developed,
411 obliquely-angled mesiobuccal and mesiolingual aspects. The MMR is high and sharp. A
412 thick epicrista, with a distinct tubercle and free apex, is separated from the MMR and the
413 Pa essential ridge by distinct furrows. The well-developed MMR and epicrista form a
414 mesiobuccal projection. An uninterrupted Co separates the Hy from the trigone. The
415 DMR is thick, but is much lower than the MMR, and encloses a small, BL-oriented,
416 groove-like Fp that is continuous with the groove separating the Hy and Me. There is a
417 weak Carabelli's feature on the mesiolingual aspect of the Pr that takes the form of a v-
418 shaped furrow and associated crest. The lingual groove is a narrow cleft near the occlusal
419 margin and continues as a deep groove until it terminates at about mid-crown. The buccal
420 groove is short and faint, extending about one-quarter of the crown height.

421 Three widely splayed roots are partially preserved. The remaining height of the
422 distobuccal root is 6.7 mm, and that of the mesiobuccal is 4.8 mm. Both the mesiobuccal
423 and distobuccal roots are longest BL and narrowest MD and rise nearly directly above the
424 crown. The MD-elongated lingual root leans over the crown and 5.8 mm of its height
425 remain in lingual view.

426 Based on similarities in morphology and wear status, this is the proposed antimere
427 of U.W. 101-1377. Unlike U.W. 101-1377, however, this specimen possesses a mesial
428 IPF.

429

430 U.W. 101-1377: LdP³ (Fig. 4B; Table 1) An enamel chip sits at mesiobuccal aspect of the
431 Pa at the intersection with the MMR. No IPFs are observed. The mesial cusps are lightly

432 worn, with a dentine pit exposed over the Pr and Pa and a wear facet visible on the mesial
433 crest of the Pr (Stage 2). The crown is molariform, with four well-developed cusps
434 arranged in size as Pr > Pa > Me > Hy. The Hy is large, conical in shape, and as high as
435 the Me. In occlusal view, the crown is shaped like a pentagon, which reflects the large
436 and distolingually projecting Hy and well-developed, obliquely angled mesiobuccal and
437 distobuccal aspects. The MMR is high and well developed. Just distal to the MMR is a
438 deep groove separating it from a thick epicrista that forms a distinct tubercle observed
439 from the buccal aspect. The combination of the well-developed MMR and epicrista
440 contributes to a mesiobuccal projection of the occlusal surface. A tall and uninterrupted
441 Co extends between the Pr and Me. The DMR is thick and rounded, but is much lower
442 than the Co, and bounds a small, groove-like and BL-oriented Fp that is continuous with
443 the distal occlusal groove separating the Hy and Me. There is a weak Carabelli's feature
444 on the mesiolingual aspect of the Pr that takes the form of a v-shaped furrow. The lingual
445 groove is deep near the occlusal margin until it terminates at mid-crown. The buccal
446 groove is a faint indentation that quickly fades below the occlusal surface.

447 Three widely splayed roots are partially preserved. The lingual root is completely
448 broken away, the distal buccal root is broken at about half its height, and the mesial
449 buccal root is broken near its apex. Both the mesiobuccal and distobuccal roots are
450 longest LaL and narrowest MD. The preserved height of the distobuccal root is 5.4 mm in
451 buccal view, and the mesiobuccal is 9.9 mm.

452 This specimen is proposed as the antimere of U.W. 101-823. Further, it is
453 proposed to be associated with the U.W. 101-1376 LdP⁴. Both specimens lack IPFs,
454 which is consistent with this assignment, and were excavated within centimeters of each

455 other. Further, these teeth are proposed to be associated with the mixed dentition of U.W.
456 101-1400 and other isolated teeth.

457

458 *3.5. Deciduous maxillary fourth premolars*

459 Four dP⁴s, representing a minimum of three individuals, are known from the
460 Dinaledi Chamber deposits. Two of them are proposed as antimeres, U.W. 101-1376 and
461 U.W. 101-1687, while the other two, U.W. 101-384 and U.W. 101-544A, must represent
462 two additional individuals given differences in their crown developmental and macrowear
463 statuses. The four teeth present a consistent morphological pattern featuring four well-
464 developed cusps, a continuous Co, slightly rhomboidal occlusal profile with a Hy that
465 projects distolingually, and weak Carabelli's expression.

466

467 U.W. 101-384: RdP⁴ (Fig. 5A; Table 1) Enamel chipping to the occlusal edge of the
468 MMR sits just above the mesial IPF and another chip is found on the buccal aspect of the
469 Me. An oval mesial IPF (3.5 mm LaL by 1.5 mm OC) and a larger circular distal IPF (3.1
470 mm LaL by 3.7 mm OC) are present. Dentine patches are exposed on all cusps (stage 4).
471 The dentine pool over the Pr is the largest, extending from the distal crest, broadening
472 over the apex, continuing along its mesial crest, and curving buccally to include the
473 region of the Fa. The four main cusps are well developed and have the following size
474 relationships: Pr > Pa > Me > Hy. The occlusal outline is rhomboidal and mildly skewed,
475 as the Hy projects distolingually. A trace of the groove separating the Pa and Me remains,
476 as does a portion of the groove separating the Pa and Pr and a small portion of the groove
477 delineating the Hy and terminating at the Fp remains as well. A short, shallow buccal

478 groove extends about half the distance of the crown. On the lingual surface, a small deep
479 pit is all that remains of what was likely a deep lingual groove.

480

481 U.W. 101-544A: RdP⁴ germ (Fig. 5B; Table 1) This is an unerupted crown with no trace
482 of root formation. There is some post-depositional damage to the fragile cervix lingually
483 and distally; though, the germ does not appear to be crown complete. The Hy broke away
484 from the trigon postmortem and is refit to the crown. The break follows the contour of the
485 lingual groove and parallels the Co onto the buccal side where the Me, a distal accessory
486 ridge, and DMR meet. A deep crack remains and widens on the lingual aspect and, even
487 though refit, the Hy is shifted slightly distally. The morphology is not affected by this
488 damage, but the MD measurement is adjusted to account for this damage.

489 All four principal cusps are well developed and there is no hint of accessory
490 cusps. In size, the cusp sizes are approximately Pr > Pa > Me > Hy. The Hy is large and
491 conical in shape, nearly as high as the other three cusps, and projects distolingually,
492 which gives the crown a rhomboidal occlusal outline. The mesial edge is slightly convex,
493 while the buccal and lingual profiles are fairly straight with mild indentations for the
494 lingual and buccal grooves. The essential ridges of the Pr, Me, and Hy are indistinct. The
495 Pa has a narrow mesial accessory ridge, and the Pr has a short, but distinct, mesial
496 accessory ridge that meets the mesial accessory ridge of the Pa at the central fovea. These
497 accessory ridges define the distal extent of the Fa, which takes the form of a BL-oriented
498 groove. The mesial aspect of the Fa is defined by a thick and rounded MMR that features
499 two mesial accessory tubercles: the paraconule and mesial accessory tubercle (Scott and
500 Turner, 1997; Scott and Irish, 2017). These tubercles extend into the Fa as short ridges.

501 The Fp is a small pit defined by an indistinct DMR. The Co is continuous. A small
502 Carabelli's feature is present and takes the form of a weak obliquely oriented ridge
503 associated with a small pit at its base. The buccal groove is shallow and extends
504 approximately one-quarter of the distance to the cervix. The lingual groove cannot be
505 accurately assessed due to the crown damage.

506 This specimen shares a specimen number with another deciduous tooth (U.W.
507 101-544C; RdI¹) and crown incomplete RC¹ (U.W. 101-544B) because they were
508 excavated in close spatial proximity. Though all represent sub-adults, it is unlikely that
509 they represent a single individual. For example, U.W. 101-544B and U.W. 101-544C
510 have proposed antimeres in the assemblage and are likely attributable to the nearly
511 complete mixed dentition associated with the U.W. 101-1400 mandible and its associated
512 antimeres and occluding teeth, which have erupted dP4s and nearly crown-complete M1s;
513 this would preclude the developing RdP⁴ germ, U.W. 101-544A, from belonging to the
514 same individual as U.W. 101-544B and U.W. 101-544C. However, from a modern
515 human perspective, the developmental status of U.W. 101-544A is not inconsistent with
516 attribution to the same individual as U.W. 101-544B and U.W. 101-544C (AlQahtani et
517 al., 2010). The possible association of U.W. 101-544B and U.W. 101-544C with U.W.
518 101-1400 are given a detailed treatment in the Discussion.

519

520 U.W. 101-1376: LdP⁴ (Fig. 5C; Table 1) The crown is unworn (stage 1) and no IPFs are
521 present. The crown possesses four well-developed cusps with the following size
522 relationships: Pr > Pa ≥ Me ≥ Hy. The Hy is relatively large and projects distolingually,
523 giving the crown a rhomboidal, mildly skewed outline. All cusps are high. The cusps

524 comprising the trigone are of equal height and the Hy only slightly lower. The cusps are
525 also widely spaced, and their tips are placed at the edge of the occlusal margin. The Pr
526 has a weakly-developed essential ridge and a larger mesial accessory ridge that forms a
527 protoconule with a free apex. The Pa has a weakly-developed essential ridge and a
528 narrower, sharper mesial accessory ridge. In addition to the protoconule, a second
529 marginal tubercle—the mesial accessory tubercle (Scott and Turner, 1997)—sits along
530 the MMR. Compared to the low, rather indistinct DMR, the MMR is high and prominent.
531 The Co is high, sharp, and continuous. It is separated from the trigone by a deep occlusal
532 groove that continues onto the lingual surface for about half the height of the crown. The
533 Hy has a faint essential ridge and a short distal accessory ridge. A Carabelli's feature,
534 consisting of a faint v-shaped ridge and groove, is limited to the mesiolingual corner. The
535 buccal groove is a shallow indentation at the occlusal surface that fades at mid-crown.

536 Portions of three widely splayed roots are preserved: two buccal and one lingual.
537 The mesiobuccal root is broken near the cervix, while the distobuccal and lingual roots
538 are broken at about half their length. The distobuccal root measures 4.8 mm from the
539 cervix, the mesial buccal root measures 2.5 mm, and the lingual root measures 3.3 mm.
540 The lingual root is BL compressed, while the two buccal roots are MD compressed.

541 The specimen is proposed to be associated with the U.W. 101-1377 LdP³. Both
542 specimens lack IPFs, which is consistent with this assignment, and further, the teeth,
543 though isolated, were excavated within centimeters of each other. This specimen is
544 proposed as the antimere of the U.W. 101-1687 RdP⁴. The other RdP⁴ in the assemblage,
545 U.W. 101-544A, lacks any trace of root development and appears to be crown
546 incomplete. Thus, U.W. 101-1687 and U.W. 101-1376 represent a slightly older

547 individual. Further, it is proposed that U.W. 101-1376/1687 belong to the mixed dentition
548 represented by U.W. 101-1400 and other isolated teeth.

549

550 U.W. 101-1687: RdP⁴ (Fig. 5D; Table 1) Neither mesial nor distal IPFs are present and
551 the crown is lightly worn (stage 1). The crown is rhomboidal in outline and only mildly
552 skewed by the distolingual projection of the Hy. Four well-developed cusps are present
553 with the following size relationship: $Pr > Pa \geq Me \geq Hy$. The cusp apices are high, with
554 the cusps comprising the trigone equal in height and the Hy only slightly lower. The
555 cusps are also widely spaced, and all cusp tips are oriented towards the edge of the
556 occlusal margin. The Pr has a weakly-developed essential ridge and a pair of weak mesial
557 accessory ridges. In addition to the Pa essential ridge, mesial and distal accessory ridges
558 are present. The Me essential ridge merges with the distal margin of the Pr to form a
559 high, sharp, and incompletely bisected Co. The Hy is separated from the trigone by a
560 deep occlusal groove that continues as the lingual groove, which disappears at mid-
561 crown. The buccal groove is a faint depression throughout. The MMR is thick and
562 continuous. Two small tubercles (mesial marginal tubercle and the mesial Pa tubercle)
563 rise from the MMR near the center of the crown. The low and indistinct DMR is
564 separated from the occlusal basin by a thin groove-like Fp. A small Carabelli's feature
565 presents as an obliquely angled swelling and groove on the mesiolingual corner.

566 Portions of three widely splayed roots, two buccal and one lingual, are preserved.

567 All three roots are broken near the cervix and the mesiobuccal root canal is filled with
568 sediment. Approximately 2.7 mm of the lingual root is preserved, 4.0 mm of the
569 mesiobuccal root is preserved, and the distobuccal root is broken away at the cervix.

570 This is the proposed antimere of U.W. 101-1376. The configuration of the mesial
571 portion of the Pr differs between the teeth, though. Along the mesial Pr crest of this
572 specimen are small crests extending into the Fa, while in U.W. 101-1376 the crests are
573 replaced by a more prominent protoconule. The configuration of the Carabelli's feature
574 of this specimen differs from its proposed antimere, where the feature is more v-shaped.
575 This tooth also likely belongs to a mixed dentition that includes U.W. 101-1400.

576

577 *3.6. Deciduous mandibular lateral incisor*

578 A single dI₂ is currently known from the Dinaledi Chamber deposits. The crown
579 is simple in form, with weak marginal ridges and a featureless lingual fossa.

580

581 U.W. 101-1612: RdI₂ (Fig. 6; Table 1) An ovoid mesial IPF (0.9 mm LaL by 1.1 mm IC)
582 is present, but no distal IPF is detectable. The crown is only minimally worn with a short,
583 thin line of dentine exposed on the mid-section of the incisal edge (stage 1). The crown is
584 tall and narrow. In labial view, the crown lacks prominent features and is slightly convex
585 IC. It is asymmetrical in both labial and lingual views with a marked distal slope and
586 curved distal corner. The mesial and incisal edges, on the other hand, are nearly
587 perpendicular to each other. The incisal edge is straight, and the mid-crown is mildly
588 convex. On the lingual surface, there are weak marginal ridges that gradually disappear
589 as they reach cervically. The lingual fossa is featureless.

590 The root is missing its tip. In the labial view, its preserved height is 9.2 mm. The
591 root is teardrop shaped in cross-section and is MD flattened. A shallow groove runs along
592 the length of its distal aspect. The root tip deflects slightly mesially.

593 This specimen is proposed to be part of the group of teeth that also includes the
594 U.W. 101-1400 mandible and associated specimens.

595

596 *3.7. Deciduous mandibular canines*

597 Three isolated dC₁s (U.W. 101-824, U.W. 101-1571, U.W. 101-1611) and a
598 fourth found in the U.W. 101-1400 mandible are known from the Dinaledi Chamber
599 deposits. Collectively, these teeth represent at least three individuals. The morphology of
600 the dC₁ is best discerned from the two lightly worn proposed antimeres, U.W. 101-1400
601 and U.W. 101-1611, with the two more worn specimens consistent with the pattern. In
602 labial view, the dC₁ crown is asymmetric in profile, with a short, convex mesial crest
603 meeting a mesial shoulder that sits more apically than the distal shoulder. The distal crest
604 is longer, nearly vertical, and terminates in a tubercle. The crown apex is slightly offset
605 distally. The morphology of the deciduous canine mirrors that of the permanent canine.

606

607 U.W. 101-824: LdC₁ (Fig. 7A; Table 1) The apex of the crown is chipped labially.
608 Despite the presence of occlusal wear, neither mesial nor distal IPFs are detectable. A
609 large dentine pool is exposed at the crown apex and narrows along the distal crest (stage
610 3–4). The crown is asymmetrical in lingual and labial view: it has a high, mesially placed
611 apex from which the occlusal edge slopes distally. The distal edge is notably longer than
612 the mesial and terminates at a small tubercle delineated by labial and lingual furrows. On
613 the lingual surface, the basal cingulum is rounded and weakly developed. The bulk of this
614 prominence is distally placed in occlusal view.

615 The root is abraded on all sides and broken at its apex. The root is ovoid in cross
616 section and wider MD than LaL. The maximum preserved height, approximately 10.3
617 mm, exists distolabially.

618

619 U.W. 101-1571: LdC₁ (Fig. 7B; Table 1) A small IPF is present distally and a larger (1.5
620 mm LaL by 2.2 mm OC) teardrop shaped mesial IPF is present. Wear is evident, as the
621 apex is blunted and dentine is exposed here and slightly along the mesial crest (stage 4).
622 The distal tubercle is flattened by wear, but no dentine is exposed. The morphology of the
623 remaining crown resembles the other, better-preserved, mandibular deciduous canines.
624 The crown is asymmetrical and, based on the size of the occlusal dentine exposure, the
625 original cusp was likely high. The distal tubercle is intact and is circumscribed by weak
626 labial and lingual fossae. The cervical eminence is weak, and a broad lingual ridge
627 divides the crown into mesial and distal fossae. The preserved mesial fossa is small and
628 appears as a shallow depression. The distal fossa is also quite shallow and appears as a
629 small feature adjacent to the DMR and distal tubercle.

630 The root is broken at a sharply oblique lingual-to-labial angle. Along the buccal
631 face, approximately 4.7 mm of root remain. Sediment fills the pulp chamber.

632

633 U.W. 101-1611: RdC₁ (Fig. 7C; Table 1) The crown is minimally worn, with a small
634 facet on the apex and a longer facet running along the distal crest. Neither facet exposes
635 any dentine (stage 1). The crown is ovoid in occlusal view. In labial and lingual views,
636 the crown is asymmetrical with a short, high mesial shoulder and a long distal edge
637 terminating in a tubercle. The mesial crest is convex, while the distal is steeply angled

638 and slightly concave because of wear. The crown apex is slightly offset distally. In
639 lingual view, the crown possesses a broad dull median lingual ridge that narrows as it
640 approaches the apex. The mesial and distal fossae are both shallow, with the distal
641 narrower and more groove-like. In labial view there is a weak distal fossa associated with
642 the tubercle.

643 The root is broken at its apex. Approximately 9.3 mm of root remains in labial
644 view. The root is ovoid in cross-section and somewhat flattened LaL.

645 The tooth is consistent in morphology with its proposed antimere in the U.W.
646 101-1400 mandible.

647

648 3.8. *Deciduous mandibular third premolar*

649 A proposed antimeric pair of dP_{3S} is currently known from the Dinaledi Chamber
650 deposits. One is in situ in the U.W. 101-1400 mandible, while its antimere, U.W. 101-
651 1685, is isolated. Morphologically, both present a molarized occlusal pattern, with five
652 main cusps present. The crowns are elongated MD compared to the BL breadth and are
653 slightly BL broader across the talonid than the trigonid. A strong mesial trigonid crest
654 extends into the Fa, creating a narrow, groove-like, Fa that parallels the MMR and mesial
655 crest of the Pr. Both lack a protostylid and accessory cusps. The mesial and distal roots
656 are both plate-like.

657

658 U.W. 101-1685: RdP₃ (Fig. 8; Table 1) The RdP₃ is preserved in a small, mostly lingual,
659 portion of the mandibular corpus, which retains a portion of the crypt of the P₃. There is
660 an enamel chip distally along the DMR between the End and Hld. There is a small distal

661 IPF offset buccally, but no facet is detectable mesially. The crown shows light wear with
662 a small facet visible on the buccal aspect of the Prd cusp tip, and small dentine pits are
663 exposed on the End, Hyd, and Hld (stage 2). There is also a small facet, with no dentine
664 exposed, on the distoocclusal portion of the Hld. The occlusal outline is rectangular,
665 being MD elongated and BL narrow. The crown possesses five well-developed cusps
666 with following size relationships: Prd > Hyd > Med > End > Hld. The talonid is wider
667 than the trigonid and the trigonid cusp apices reach higher than those of the talonid. The
668 Med cusp tip is higher than that of the Prd. The Prd cusp tip sits mesial to that of the Med
669 and is internally placed close to the central groove. The MMR is thick and separated from
670 the Prd and Med by shallow and deep grooves, respectively. Two cuspules,
671 premetaconulid and mesioconulid, rise from the MMR and are delineated by weak
672 grooves. The buccal segment of the MMR is thicker than the lingual and, where the two
673 portions meet at an angle, their junction is marked by a groove. The thick MMR is
674 continuous with the mesial Prd crest and passes mesially to a strong mesial trigonid crest
675 emanating from the Prd; thus, the Fa exists as a narrow groove running between these
676 crests. The midtrigonid crest is separated from the Med by a groove. Near the occlusal
677 surface, the mesiobuccal groove is a deep narrow cleft and then it opens up at mid-crown.
678 The deep mesiobuccal groove and associated v-shaped furrow contribute to the waisted
679 appearance in occlusal view. There is a detectable distobuccal groove only at the occlusal
680 surface. There is a minor mesiolingual groove that extends less than 1.5 mm cervically
681 from the mesial Med crest. The distolingual groove is faint across its course. A faint
682 groove adjacent to the MMR is visible in buccal view. The buccal face presents a slight
683 cervical prominence, but the surface is smooth; no protostylid is present.

684 Plate-like mesial and distal roots are present. The apex of the mesial root is
685 closed. The mesial root is preserved in its entirety and is 9.4 mm in height along its
686 buccal edge. The distal root is also preserved in its entirety and is 9.3 mm in height. The
687 roots are widely splayed, and with the adhering mandible, preserve a portion of the crypt
688 of the P₃.

689 This is the antimere of the LdP₃ preserved in the U.W. 101-1400 mandible.
690 Further, it articulates with U.W. 101-1686 (RdP₄).

691

692 *3.9. Deciduous mandibular fourth premolar*

693 A proposed antimeric pair of dP_{4s} is currently known from the Dinaledi Chamber
694 deposits. One is in situ in the U.W. 101-1400 mandible, while the other, U.W. 101-1686,
695 is isolated. Morphologically, both present a molarized occlusal pattern, with five main
696 cusps present. In comparison to the associated dP_{3s}, the Hld is relatively larger and the
697 BL breadth across the talonid is noticeably greater than the breadth across the trigonid.
698 As with the dP₃, a strong midtrigonid crest is present; however, on the dP₄ it is
699 continuous between the mesial crests of the Med and Prd and completely bounds the Fa
700 distally. Both lack accessory cusps and have faint protostylids. The mesial and distal
701 roots are both plate-like.

702

703 U.W. 101-1686: RdP₄ (Fig. 9; Table 1) The crown surface is lightly worn, with a small
704 wear facet visible along the mesial Prd crest (stage 1). The occlusal outline is rectangular,
705 being MD elongated and BL narrow. Five primary cusps are present and the talonid is
706 wider than the trigonid. The cusps have the following size relationships: Med > Hyd >

707 Prd > End > Hld. The MMR is thick and three small cuspules (preprotoconulid,
708 mesioconulid and premetaconulid) outlined by shallow occlusal and mesial grooves rise
709 from the MMR. The Prd and Med each have prominent mesial crests, which meet to form
710 a mesial trigonid crest separated from the MMR and essential ridges of the Prd and Med
711 by deep grooves. The Med exhibits an incipient postmetaconulid. The essential ridge of
712 the Hyd is bifurcated. The substantially larger mesial portion constricts slightly in the
713 middle and then expands before terminating at the central groove. The End possesses a
714 weak mesial accessory ridge. The components of the DMR originating from the Hld and
715 End meet at an angle and delineate a narrow and weak Fp. The mesiolingual groove is
716 short and shallow terminating about one-quarter the distance to the cervix. In addition,
717 there are short and shallow lingual vertical furrows associated with the cuspules of the
718 MMR and with the postmetaconulid. The mesiobuccal groove is deep, forms a wide v-
719 shaped fovea near the occlusal edge, and terminates at approximately mid-crown. A deep
720 distobuccal groove terminates approximately mid-crown. A short cingular swelling sits
721 on the buccal face of the Hld and terminates at the distobuccal groove. A faint swelling
722 mesiolingually may represent a weakly expressed protostylid.

723 The broken mesial root is refit to the crown (not evident in Fig. 9). The mesial
724 root is damaged apically, and lingual and buccal root canals are exposed. As preserved, in
725 the mesial view the buccal aspect of the root is 7.5 mm, the lingual aspect is 7.3 mm, and
726 the maximum BL width is 9.8 mm. The lingual and buccal aspects of the root are rounded
727 tubes with a MD thin section of root stretched between them. The distal root is broken so
728 that only a 2.2 mm section remains distobuccally.

729 This specimen is morphologically very similar to its proposed antimere, the LdP₄
730 of U.W. 101-1400. However, the two teeth differ in the configuration of accessory ridges
731 on the lingual face of the Hyd, with U.W. 101-1400 having three discernible crests and
732 U.W. 101-1686 only two. Further, this specimen is associated with the U.W. 101-1685
733 RdP₃. Their reciprocal IPFs are a good match.

734

735 *3.10. Permanent maxillary central incisors*

736 Five isolated I¹s, representing at least four individuals, are known from the
737 Dinaledi Chamber deposits. A fifth individual is represented by the I¹ found in situ in the
738 U.W. 101-1277 maxilla. All known I¹s from the Dinaledi Chamber are worn across the
739 incisal edge to such an extent that dentine is exposed. The I¹s present a consistent
740 morphological pattern characterized by a featureless lingual fossa, weak basal eminence,
741 and low marginal ridges.

742

743 U.W. 101-038: RI¹ (Fig. 10A; Table 1) There is a large teardrop shaped mesial IPF (3.0
744 mm along its major axis by 1.8 mm across its minor axis). A small vertical ovoid distal
745 IPF, less than 1.0 mm in all dimensions, is also present. A thin line of dentine is exposed
746 along most of the incisal edge, but it does not quite extend to the distal margin (stage 3–
747 4). Labially, the crown is featureless and mildly convex at midcrown. Lingually, the
748 crown exhibits mild basal swelling. Weak tuberculum dentale, expressed as finger-like
749 extensions, emanate from the basal swelling, extend into the otherwise featureless lingual
750 fossa, and terminate at or just before the incisal edge. Both the MMR and DMR are

751 weakly expressed, giving the tooth a mild shovel shape. The MMR is cut short by the
752 encroachment of the mesial IPF. The DMR is slightly more prominent than the MMR.

753 The apex of the root is broken away. In labial view, approximately 14.2 mm of
754 the root is preserved. The root is broader LaL than MD, has subtle depressions running
755 along both the mesial and distal faces, and, especially apparent apically in labial and
756 lingual views, tilts slightly distally.

757 This specimen and U.W. 101-039 were both found on a rock and had been
758 arranged by cavers prior to excavation (see area D in Dirks et al., 2015: Figure 6B).

759

760 U.W. 101-591: LI¹ (Fig. 10B; Table 1) Most of the mesial IPF has been removed by
761 wear; the remaining portion (3.0 mm LaL by 1.0 mm IC) merges with the incisal edge.
762 The distal IPF (2.8 mm by 1.2 mm) is obliquely oriented relative to the crown. A thick,
763 wide band of dentine is exposed along the entire incisal surface (stage 4) and there is a
764 steep lingual slope to the wear plane. An enamel chip is located incisal to the distal IPF.
765 The basal eminence is slight and bulbous and the median lingual ridge flat. These two
766 features occupy most of the remaining lingual face; though, shallow grooves delineating
767 the marginal ridges are visible near the incisal edge. Labially, the crown is minimally
768 convex at midcrown.

769 Especially distally and mesially, the root is abraded and cracked across its
770 exposed surface. Further, it is broken just before its apex (12.7 mm in preserved height),
771 exposing the canal. The root is ovoid in cross section with its major axis LaL and minor
772 axis MD.

773

774 U.W. 101-931: LI¹ (Fig. 10C; Table 1) There is a larger teardrop shaped mesial IPF (3.1
775 mm LaL by 4.1 mm IC) and a smaller distal IPF (1.8 mm by 3.6 mm). A thin strip of
776 dentine, which does not extend to the mesial and distal edges, is exposed along the incisal
777 surface (stage 3–4). The labial face is minimally convex MD and IC. On the lingual
778 surface, a weak lingual basal eminence is slightly offset mesially. Faint finger-like ridges
779 extend towards, and in some cases reach, the incisal edge. The crown is weakly shovel-
780 shaped with low, rounded marginal ridges that become indistinct where they merge with
781 the basal cingulum. The DMR is stronger than the MMR. Linear hypoplasias are
782 observed in the cervical third of the crown (for a discussion of hypoplasias on this
783 specimen, see also Skinner, 2019).

784 The root is abraded across most of its surface and its apex is missing, exposing the
785 canal. Labially, 14.2 mm of the root are preserved. At the cervix, the root is rounded in
786 profile and tapers towards its apex to become more compressed MD.

787 The mesial IPF fits well with the IPF of its proposed antimere, U.W. 101-1012,
788 while the distal IPF is a reasonable match for that of the mesial facet of U.W. 101-932.
789 As U.W. 101-932 has proposed antimere, U.W. 101-709, that also fits well with U.W.
790 101-1012, this tooth likely belongs to a complete set of maxillary incisors (U.W. 101-
791 709, -931, -932, and -1012) and antimeric canines (U.W. 101-706 and U.W. 101-816).
792 This attribution is consistent with the fit of their respective IPFs, incisal wear, and
793 morphological status as antimeres.

794

795 U.W. 101-1012: RI¹ (Fig. 10D; Table 1) Two enamel chips are missing from the lingual
796 aspect adjacent to the mesial IPF. There is a large teardrop shaped mesial IPF (4.1 mm

797 LaL by 3.1 mm IC) sitting at the incisal edge where it squares off the mesial corner. A
798 smaller distal IPF (3.6 mm LaL by 1.8 mm IC) is also present. A thin strip of dentine is
799 exposed along the incisal edge (stage 2). Labially, the crown is featureless, and the crown
800 is minimally convex both IC and MD at midcrown. Lingually, faint finger-like
801 projections reach into the lingual fossa and fade prior to the incisal edge. The crown is
802 mildly shovel-shaped with weak marginal ridges. The DMR is more prominent than the
803 MMR. Linear hypoplasias are visible in the cervical third of the crown (for a discussion
804 of hypoplasias on this specimen, see also Skinner, 2019).

805 The root is abraded across most of its surface, and it is broken at its apex,
806 exposing the root canal. On the labial aspect, 14.0 mm of root is preserved. Near the
807 cervix, the root is rounded in cross section and tapers apically to become compressed
808 MD. The apex of the root is distally inclined.

809 The mesial IPF is a good match with that of U.W. 101-931, its proposed antimere.
810 The distal IPF is consistent in size and shape with that of U.W. 101-709. This tooth likely
811 belongs to a complete set of maxillary incisors (U.W. 101-709, -931, -932, and -1012)
812 and antimeric canines (U.W. 101-706 and U.W. 101-816). This attribution is consistent
813 with the fit of their respective IPFs, incisal wear, and morphological status as anteriors.

814

815 U.W. 101-1558: RI¹ (Fig. 10E; Table 1) Neither mesial nor distal IPFs are preserved. The
816 crown has a large dentine exposure and a complete enamel ring (stage 5). The incisal
817 wear has a distolingual inclination. The preserved labial face is flat and featureless. No
818 marginal ridges are preserved.

819 The root is broken just before its apex and the root canal is exposed. The
820 maximum root height is 14.5 mm. Cementum is cracked and flaking off the external
821 surface, especially labially. The root is ovoid, being compressed MD.

822

823 *3.11. Permanent maxillary lateral incisors*

824 Seven isolated I²s are known from the Dinaledi Chamber deposits. Additionally,
825 an I² is in situ in the U.W. 101-1277 maxilla. Collectively, these eight I²s represent at
826 least six individuals. They present a consistent morphological pattern characterized by a
827 featureless lingual fossa, weak basal eminence, and low marginal ridges. The incisal edge
828 is straight, but the crown is moderately MD convex at mid-crown and only slightly
829 convex IC. In labial and lingual views, the I² crown flares incisally, with squared mesial
830 and convex distal edges.

831

832 U.W. 101-073: RI² (Fig. 11A; Table 1) A small mesial IPF (approximately 1.5 mm IC by
833 1.0 mm LaL) is present; however, no distal IPF is detected. The crown is well preserved
834 and exhibits minimal wear: the incisal surface is polished, but no dentine is exposed
835 (stage 1). The incisal edge is minimally convex, but the tooth is moderately convex at
836 mid-crown. A subtle notch is present in the center of the incisal margin. This divot
837 resembles more pronounced notches seen on less worn maxillary (i.e., U.W. 101-1588)
838 and mandibular (i.e., U.W. 101-1075, U.W. 101-1131, and U.W. 101-1400) lateral
839 incisors. In both labial and lingual view, the mesial edge is perpendicular, while the distal
840 edge is rounded. Lingually, there is a lingual fossa, but the marginal ridges are faint,
841 merging into a slightly swollen basal cingulum that is more prominent than the marginal

842 ridges. Within the lingual fossa are trace ridges, with the ridge nearest the DMR being the
843 most prominent among them.

844 The root is broken just before the apex and its surface is abraded. In labial view,
845 the remaining root is 12.3 mm in height. The root is compressed MD, with a shallow
846 invagination along the distal face. In lingual and labial views, the root tilts subtly distally.

847 This is a possible antimere of the U.W. 101-1588 LI². The teeth are similar
848 morphologically, in their wear status, and in the presence of small mesial IPF and
849 absence of a distal IPF.

850

851 U.W. 101-417: LI² (Fig. 11B; Table 1) The root broke from the crown near the cervical
852 line and the two portions have been refit. The fit is mostly flush, except distally where the
853 joint is not clean. A small mesial IPF (2.6 mm IC by 1.0 mm LaL) is adjacent to the
854 MMR and continues to the incisal edge. No distal IPF is visible. A line of dentine extends
855 along the incisal edge (stage 3). The wear facet angles distally so that the preserved
856 crown height is shorter distally than mesially. In incisal view the crown is moderately
857 convex, while in mesial or distal view the crown and root are only minimally convex.
858 Labially, the crown is featureless except for minor linear hypoplastic defects in the
859 cervical third. Lingually, the faint MMR and DMR converge at the base and circumscribe
860 a shallow, featureless lingual fossa. There is a slight lingual basal eminence that is offset
861 distally.

862 In addition to the damage near the cervix, the root is broken at the apex, which
863 exposes the sediment-filled canal. From the labial cervix, the preserved root height is

864 16.8 mm. In cross section, the root is longer LaL than MD and has a subtle groove
865 running along the distal face.
866
867 U.W. 101-709: R1² (Fig. 11C; Table 1) The mesial IPF (approximately 2.3 mm LaL by
868 3.3 mm IC) is larger than the distal IPF (2.7 mm by a maximum of 1.2 mm). The distal
869 IPF is complex in shape and has two facets strongly angled relative to each other so that
870 one facet is placed more incisally, having eaten into the DMR, and faces lingually, while
871 the other is placed more cervically on the distal edge. The incisal edge itself is polished
872 but no dentine is exposed (stage 1). The incisal edge is straight, but the tooth is
873 moderately convex at mid-crown. It is only slightly convex IC. In labial and lingual
874 views, the crown flares incisally with a squared mesial and convex distal edge. The labial
875 face is featureless. Lingually, the crown exhibits weak shoveling and the marginal ridges
876 circumscribe a shallow lingual fossa. There is a single, faint finger-like extension from
877 the basal cingulum that ends at a distolingual wear facet. Though worn, a dip can be seen
878 near the center of the incisal edge. This feature matches the morphology seen in less worn
879 *H. naledi* I₂s (e.g., U.W.101-1131 and U.W. 101-1400) and I₂s (i.e., U.W. 101-1588).

880 The root is broken just before its apex, exposing the root canal. The preserved
881 labial height is 11.2 mm. The root is elliptical in cross section, broader LaL than MD.
882 The root tilts slightly distally, especially apically.

883 This specimen is proposed as the antimere of U.W. 101-932. They are similar in
884 morphology, degree of occlusal wear, and even in the complex shape of their distal IPFs.
885 Tentative associations are made with other anterior teeth. The mesial IPF possibly
886 matches that of U.W. 101-1012 and the distal IPF is proposed to fit U.W. 101-816. If

887 these proposals are true, then this tooth belongs to a complete set of maxillary incisors
888 (U.W. 101-709, -931, -932, and -1012) and a set of antimeric maxillary canines (U.W.
889 101-706 and U.W. 101-816).

890

891 U.W. 101-932: LI² (Fig. 11D; Table 1) The distal IPF is small and sits near just superior
892 to the distal shoulder. The mesial IPF is larger (2.2 mm LaL by 3.3 mm IC). The incisal
893 edge is lightly worn with no dentine exposure. The lingual face has moderate facets near
894 the incisal edge, and there is a small facet on the distolingual near the distal IPF (stage 1).
895 The mesial border is perpendicular to the incisal edge, and the distal border is convex in
896 labial and lingual views. In occlusal view, the crown is straight at the incisal edge and
897 moderately convex mid-crown. The labial face is featureless except for a faint distolabial
898 depression near the incisal margin. The lingual face has a moderately elevated basal
899 eminence and slight marginal ridges that are stronger as they approach the incisal edge.
900 There are two faint finger-like extensions from the basal eminence that terminate at the
901 lingual wear facets.

902 The root is missing its apex. What is preserved is abraded and deflects distally.
903 The root is ovoid in cross section with its major axis LaL and minor axis MD. The
904 preserved root measures 11.3 mm in height from the labial aspect.

905 The mesial IPF of this specimen is a good fit for U.W. 101-931 LI¹. Based on
906 similarities in wear and morphology, this specimen is a reasonable antimeric of U.W. 101-
907 709. This tooth likely belongs to a complete set of maxillary incisors (U.W. 101-709, -
908 931, -932, and -1012) and antimeric canines (U.W. 101-706 and U.W. 101-816). This

909 attribution is consistent with the fit of their respective IPFs, incisal wear, and
910 morphological status as antimeres.
911
912 U.W. 101-952: LI² (Fig. 12A; Table 1) There is a large mesial IPF that reaches the worn
913 incisal edge (2.1 mm LaL by 2.6 mm IC). Distally, a small IPF (approximately 0.7 mm
914 LaL by 2.4 mm IC) is present along the DMR near the incisal edge. A distinct line of
915 dentine is exposed across much of the incisal edge (stage 3). The labial face is featureless
916 and moderately convex mid-crown. Lingually, there are weak marginal ridges that merge
917 with the basal cingulum, forming a pit. The lingual fossa is shallow with trace fingerlike
918 extensions arising from a weak basal eminence. Linear hypoplasias are observable in the
919 cervical third (for a discussion of hypoplasias on this specimen, see also Skinner, 2019).

920 The root is broken and a fragment of root that fits neatly onto the fresh break is
921 refit (not apparent in Fig. 12A or in the surface files). Other than the fracture, the root is
922 well preserved, with some abrasion apparent near the apex of the root. The root is ovoid
923 in cross section, with wide shallow depressions running along both mesial and distal
924 faces. The preserved maximum height of the root is 19.0 mm in labial view.

925

926 U.W. 101-1588: LI² (Fig. 12B; Table 1) There is a small mesial IPF (1.2 mm LaL by 2.2
927 mm IC) that sits adjacent to the MMR and near the incisal edge. No distal IPF is
928 detectable. The crown is lightly worn, with facets along the incisal edge and the lingual
929 face, but no dentine is exposed (stage 1). Labially, the crown is featureless. It is
930 moderately convex at mid-crown but has a straight incisal edge. Lingually, there are trace
931 marginal ridges and a shallow lingual fossa. The lingual basal eminence is low and

932 rounded. As with some other *H. naledi* lateral incisors, maxillary and mandibular (e.g.,
933 U.W. 101-1075, U.W. 101-1400), a distinct notch sits in the center of the incisal edge.
934 The mesial corner is nearly perpendicular, while that of the distal shoulder is gently
935 curved.

936 The root is well preserved, with a break at the apex exposing the root canal. The
937 root is MD compressed and ovoid in cross section. There is a shallow groove running
938 along the distal face. The maximum preserved height is 14.9 mm.

939 This is the possible antimere of U.W. 101-073. The two teeth are similar in
940 morphology and wear status, including the presence of small mesial IPF and absence of a
941 distal IPF. The lingual wear facet is, however, more pronounced on U.W. 101-1588 and
942 the incisal notch less pronounced on U.W. 101-073; though, the topography of the labial
943 face suggests that a notch was present on U.W. 101-073 in the unworn state.

944

945 U.W. 101-1684: LI² (Fig. 12C; Table 1) The incisal edge is chipped mesially. Neither
946 mesial IPFs is preserved at this level wear. A very small distal IPF remains. The crown is
947 heavily worn and with a wide dentine exposure and complete enamel rim (stage 5). The
948 labial face is featureless and flat. Lingually, what remains of the MMR and DMR is faint,
949 and the lingual fossa is shallow. The basal eminence is low and rounded and offset
950 mesially.

951 The root is broken obliquely so that the labial portion is longer than the lingual.
952 The root is also abraded, especially mesially. In labial view, 11.7 mm of the root remains,
953 while 5.1 mm remains along the lingual aspect. The root is MD compressed and ovoid in
954 cross section. Its apex deflects distally.

955 The tiny distal IPF possibly matches an equally small IPF on the U.W. 101-1556
956 LC¹. Further, their degree of macrowear is consistent. Thus, tentatively, U.W. 101-1684
957 is proposed to belong to the associated left teeth U.W. 101-1556, -1560, and -1561.

958

959 *3.12. Permanent maxillary canines*

960 Eleven isolated maxillary canines are known from the Dinaledi Chamber deposits.
961 Additionally, a C¹ is found in situ in the U.W. 101-1277 maxilla. Collectively, they
962 represent at least eight individuals. The maxillary canines present a consistent
963 morphological and macrowear pattern. The crown appears tall relative to its small base.
964 In labial view, the crown is asymmetric because the mesial shoulder sits more apically
965 than the distal shoulder and the mesial crest is shorter than the distal. In addition, the
966 mesial shoulder is more angular than the rounded distal shoulder. The marginal ridges on
967 the lingual face are weak and the lingual fossa is relatively featureless except for
968 occasional faint ridging. At early stages of wear, the mesial crest of the crown is blunted,
969 and the asymmetry of the labial crown profile is maintained. As wear progresses, the
970 apex becomes blunted, and the wear surface becomes planar. At early stages of wear, a
971 distinctive wear facet is frequently present on the distolingual face where it extends from
972 the crown apex, runs parallel to the distal edge, and may extend onto the DMR near the
973 distal shoulder.

974

975 U.W. 101-337: RC¹ (Fig. 13A; Table 1) No IPFs are visible mesially or distally. The
976 apex of the tooth is chipped, and wear blunted the apex, exposing a small patch of
977 dentine; further, a moderately sized facet has flattened the mesial crest (stage 1). A very

978 small wear facet is present on the lingual face adjacent to the distal crest at about its
979 midpoint. The placement of the facet suggests that it represents the earliest phase of
980 similar facets on *H. naledi* canines at more advanced stages of wear (i.e., U.W. 101-412,
981 U.W. 101-501, U.W. 101-706, U.W. 101-908). The crown is tall relative to its narrow
982 basal width (Table 1). The crown exhibits moderate labial convexity and is minimally
983 convex in mesial and distal views. In labial view, the crown is asymmetric because the
984 mesial shoulder sits more apically than the distal shoulder and the mesial crest is shorter
985 than the distal. In addition, the mesial shoulder is more angular than the rounded distal
986 shoulder. There are only faint mesial and distal vertical grooves; otherwise, the labial
987 face is featureless. Lingually, the MMR is better defined, thicker and rounder than the
988 DMR. A moderately-developed distal accessory ridge originates on the occlusal edge and
989 merges with a thin and sharp ridge extending from the weak basal eminence. There is a
990 weaker and more rounded mesial accessory lingual ridge that runs parallel to the MMR
991 and becomes more topographically prominent near the occlusal edge. These accessory
992 ridges divide the lingual face into a groove-like mesial lingual fossa and larger, more
993 triangular distal and central fossae. Multiple linear hypoplasias are present along the
994 cervical third of the lingual and labial faces (for a discussion of hypoplasias on this
995 specimen, see also Skinner, 2019).

996 The root is mildly abraded on its external surface and is broken at about two-
997 thirds of its maximum length, which exposes the sediment packed root canal. In labial
998 view, 11.5 mm of root remain. The root is slightly dumbbell shaped in cross section with
999 faint grooves running the length of the root distally and mesially. The mesial depression
1000 is slightly deeper. In labial view, the root tilts distally.

1001

1002 U.W. 101-412: LC¹ (Fig. 13B; Table 1) An enamel chip is present on the distal shoulder
1003 just above the distal IPF. The distal IPF (2.9 mm IC by 1.5 mm LaL) is adjacent to the
1004 DMR, below the apex of the shoulder. A tiny mesial IPF is present at the apex of the
1005 mesial shoulder where it is offset lingually. The cusp apex is worn exposing an oval patch
1006 of dentine. This occlusal facet extends onto the mesial aspect of the crown. In addition,
1007 there is a moderately-sized wear facet on the distolingual face that extends from the apex,
1008 running parallel to the distal edge and onto the DMR and extending slightly past the
1009 distal shoulder (stage 3–4). Although moderately worn, the original crown contour is
1010 largely preserved. The labial face is moderately convex MD at mid-crown and only
1011 slightly convex IC. As preserved, the apex is offset distal to the midpoint of the crown.
1012 The mesial and distal labial grooves are faint. Lingually, the MMR is wider and better
1013 developed than the DMR. Both are bordered by vertical grooves separating them from a
1014 swollen, but undefined, median lingual ridge. The basal lingual surface is flat. Linear
1015 hypoplasias are evident labially and lingually near the cervix (for a discussion of
1016 hypoplasias on this specimen, see also Skinner, 2019).

1017 The distally curving root is broken just before its apex and measures 16.3 mm in
1018 height along its labial aspect. In cross section, the root is ovoid with shallow depression
1019 running along the mesial side of the root.

1020 This is a possible antimere of U.W. 101-908. They are similar, but not identical,
1021 in morphology, size, and in the degree and pattern of wear. Both have wear facets on
1022 their lingual faces and dentine exposed at their apices. The specimens, however, differ in
1023 their lingual surface morphology, with U.W. 101-908 having a mesial accessory ridge.

1024 Further, the mesial IPF on U.W. 101-908 is much larger than on U.W. 101-412 and U.W.
1025 101-908 is slightly more heavily worn apically, which may point to it deriving from a
1026 slightly older individual.

1027

1028 U.W. 101-501: LC¹ (Fig. 13C; Table 1) Consistent with the early stages of apical wear,
1029 there are no IPFs visible mesially or distally. There is a tiny wear facet on the crown
1030 apex, and small facets are present on the distal accessory ridge and along the mesial
1031 occlusal crest (stage 1). The crown is tall relative to its narrow base (Table 1). The crown
1032 is asymmetric: the mesial shoulder sits more apically than the distal shoulder and the
1033 mesial edge is shorter and less steeply angled. The crown apex is placed near the MD
1034 midpoint. The crown has slight labial convexity at the occlusal edge and moderate
1035 convexity mid-crown. In mesial and distal views, it is mildly IC convex. The labial face
1036 presents faint mesial and distal vertical grooves. The lingual face also exhibits a moderate
1037 MMR and weaker DMR. There is no distinct median ridge but there are faint mesial and
1038 distal accessory ridges. These ridges converge in the middle of the lingual face, from
1039 which they angle vertically before fading into the basal portion of the crown. A narrow
1040 groove between these ridges maintains their independence, thus creating a tripartite
1041 lingual fossa. The mesial lingual fossa is a groove adjacent to the MMR, the central
1042 lingual fossa is shallow, and diamond shaped, and the distal lingual fossa is broader and
1043 shallow. Multiple mild hypoplastic defects in the cervical half of the labial crown face.

1044 The root is broken just before its apex, about 11.5 mm in preserved height, and
1045 the exposed canal is packed with sediment. The root surface is abraded in patches. The
1046 root is elliptical in cross section with its major axis LaL, and minor axis MD. Subtle

1047 grooves run along the mesial and distal faces of the root, with the mesial groove deeper
1048 than the distal. In labial view, the remaining root tilts distally.
1049
1050 U.W. 101- 544B: RC¹ germ (Fig. 13D; Table 1) This crown is about two-thirds complete.
1051 The mesial shoulder is complete and is associated with a shallow labial groove.
1052 Lingually, it is associated with a moderate marginal ridge and groove. The median
1053 lingual ridge is faint and bipartite, with central and mesial branches. The distal edge is
1054 nearly vertical and the distal shoulder (if present—see U.W. 101-1548, presumed
1055 antimere) is not yet developed.

1056 This is the antimere of the crown U.W. 101-1548 canine germ. This specimen
1057 shares a specimen number with U.W. 101-544A (RdP⁴) and U.W. 101-544C (RdI¹)
1058 because they were excavated in close spatial proximity. Though all represent sub-adults,
1059 it is unlikely that they represent a single individual. Both U.W. 101-544B and U.W. 101-
1060 544C have proposed anteriors in the assemblage and are likely attributable to the nearly
1061 complete mixed dentition associated with the U.W. 101-1400 mandible and its associated
1062 anteriors and occluding teeth, which have erupted dP4s and nearly crown-complete M1s;
1063 this would preclude the developing RdP⁴ germ, U.W. 101-544A, from belonging to the
1064 same individual as U.W. 101-544B and U.W. 101-544C. However, from a modern
1065 human perspective, the developmental status of U.W. 101-544A is not inconsistent with
1066 attribution to the same individual as U.W. 101-544B and U.W. 101-544C (AlQahtani et
1067 al., 2010). The possible associations of U.W. 101-544B and U.W. 101-544C with U.W.
1068 101-1400 are given detailed treatment in the Discussion.
1069

1070 U.W. 101-706: LC¹ (Fig. 14A; Table 1) The crown has a small mesial IPF (1.3 mm IC by
1071 1.7 mm LaL). Distally, a small facet (2.0 mm along the DMR axis by <1.0 mm
1072 perpendicular to the DMR) is visible on the lingual face of the DMR at its most apical
1073 extent; this may represent an IPF. Wear blunted the mesial edge, but crown height is not
1074 affected (stage 1). As in other *H. naledi* maxillary canines (i.e., U.W. 101-337, U.W. 101-
1075 908, U.W. 101-412, and U.W. 101-510), a distinct wear facet is present on the lingual
1076 face distally near the occlusal margin. Here, the facet extends along the distal crest to
1077 slightly more than half its length. This facet resulted from contact with mesial protoconid
1078 crest of the P₃ and is independent of the small facet distally that may represent an IPF. In
1079 labial view, the crown appears tall relative to its narrow base (Table 1). The crown is
1080 asymmetric in profile, with the mesial shoulder placed more apically than the distal;
1081 correspondingly, the mesial crest is shorter than the distal. The apex is placed near the
1082 MD midpoint of the crown. The crown exhibits moderate mid-crown convexity in
1083 occlusal view and moderate IC convexity in mesial view. The labial surface features a
1084 weak vertical mesial groove and a shallow distal v-shaped furrow. The lingual surface
1085 features weak distal and mesial accessory ridges. These ridges, as well as the marginal
1086 ridges, merge into a basal swelling mid-crown. There are no distinct lingual fossae;
1087 rather, the marginal ridges are delineated by shallow grooves. There are two prominent
1088 hypoplastic defects located in the cervical third of the labial surface (for a discussion of
1089 hypoplasias on this specimen, see also Skinner, 2019).

1090 The root is abraded across most of its surfaces and is also broken at about two-
1091 thirds its length, exposing the canal. In labial view, the maximum root height is 9.3 mm.

1092 The root is a rounded ellipse in cross section, with a wide and shallow invagination along
1093 the mesial face.

1094 The mesial IPF is a potential fit for U.W. 101-932. Further, this specimen is
1095 proposed as the antimere of U.W. 101-816. Their morphology and degree of wear are
1096 similar, as are the patterns of hypoplasias near the labial cervix. There is a conspicuous
1097 difference in their wear patterns though, with U.W. 101-706 having a wear facet on the
1098 lingual face that is lacking on U.W. 101-816. Thus, these canines either represent the
1099 same individual with asymmetric patterns of wear or are different individuals at
1100 approximately the same state of wear. This tooth could belong to a complete set of
1101 maxillary incisors (U.W. 101-709, -931, -932, and -1012) and a set of antimeric canines
1102 (U.W. 101-706 and U.W. 101-816). This attribution is consistent with the fit of their
1103 respective IPFs, incisal wear, and morphological status as antimeres.

1104

1105 U.W. 101-816: RC¹ (Fig. 14B; Table 1) There is a small IPF (1.8 mm by 1.0 mm) just
1106 below the mesial shoulder. There is no distal IPF. Additional wear facets are observed
1107 lingually along the DMR and the mesial crest (stage 1). Unlike other *H. naledi* maxillary
1108 canines at comparable occlusal wear, there is no wear facet on the lingual face adjacent to
1109 the distal crest. The crown is tall relative to its narrow base (Table 1). In occlusal view,
1110 the crown is straight at the occlusal edge but moderately convex mid-crown; it also has
1111 moderate IC convexity. The crown is asymmetric in lingual and labial profiles, with the
1112 mesial shoulder higher and the mesial crest shorter than the distal. There are shallow
1113 mesial and distal labial grooves. Lingually, the MMR and DMR emerge from a broad flat
1114 cervical region and increase in expression as they approach the mesial and distal edges.

1115 Two weak finger-like projections extend into the lingual fossa. The mesial lingual ridge
1116 is truncated by the mesial edge wear. The distal lingual ridge ultimately intersects the
1117 distal crest. There are no distinct lingual fossae; rather, the mesial and distal marginal
1118 ridges are delineated by shallow grooves and the area between the lingual ridges is
1119 essentially flat. There are prominent linear hypoplasias in the cervical third of the crown
1120 (for a discussion of hypoplasias on this specimen, see also Skinner, 2019).

1121 The root tilts distally. It is abraded across most of its surfaces and only about half
1122 its length is preserved. In labial view, the maximum height of the preserved root is 9.2
1123 mm. In cross section, the root is ovoid with a shallow groove along the mesial face.

1124 Based on similarities in crown morphology and size, as well as the number and
1125 position of hypoplastic defects, U.W. 101-706 is proposed as the antimere of this
1126 specimen. The canines do differ slightly in the pattern of wear, with U.W. 101-706
1127 having a distolingual wear facet. Further, the mesial IPF of this specimen is a potential fit
1128 for the U.W. 101-709 I² distal facet. This tooth could belong to a complete set of
1129 maxillary incisors (U.W. 101-709, -931, -932, and -1012) and a set of antimeric canines
1130 (U.W. 101-706 and U.W. 101-816). This attribution is consistent with the fit of their
1131 respective IPFs, incisal wear, and morphological status as antimeres.

1132

1133 U.W. 101-908: RC¹ (Fig. 14C; Table 1) Enamel chips are present at the occlusal ends of
1134 both IPFs. The mesial IPF (2.7 mm by 1.7 mm) is teardrop shaped and placed at the apex
1135 of the shoulder. The distal IPF is larger and more elongated (3.5 mm by 1.9 mm) and
1136 placed very near the apex of the shoulder. As in other maxillary canines of similar
1137 occlusal wear stage, distinct mesial and distal wear planes meet so that the worn apex is

1138 offset distally in labial view. In this manner, the wear planes reflect the contours of the
1139 unworn crown. The apex is flattened by wear and a small dentine pit is exposed (stage 2).
1140 Wear is more extensive along the mesial crest than along the distal and the mesial wear
1141 plane dips lingually as well. A wear facet is also present on the distolingual face,
1142 extending from the DMR to the distal lingual ridge. The maximum MD length of this
1143 facet is 3.3 mm, and its maximum IC height is 2.7 mm. Though worn, in labial view the
1144 crown appears tall relative to its narrow basal size. Curvature at midcrown is minimal.
1145 The mesial and distal labial grooves are quite faint; otherwise, the labial face is
1146 morphologically featureless. Lingually, the flat median lingual ridge and faint mesial
1147 accessory ridge create narrow grooves adjacent to the MMR and DMR and between the
1148 accessory ridge and median lingual ridge. Linear hypoplasias are evident along cervical
1149 third of the lingual and labial faces (for a discussion of hypoplasias on this specimen, see
1150 also Skinner, 2019).

1151 The root is slightly abraded along its mesial surface and the apex of the root is
1152 broken, which exposes a bit of the root canal. Nearly the complete height (18.3 mm in
1153 labial view) of the distally tilting root is preserved. There is a slight depression along the
1154 mesial side of the root; otherwise, the root is a rounded ellipse in cross section, with the
1155 major axis LaL and the minor axis MD. The root is broadest labially and narrows
1156 lingually.

1157 This specimen is the probable antimere of U.W. 101-412. They are similar, but
1158 not identical, in morphology, size, and the degree and pattern of wear. Differences are
1159 seen in their lingual surface morphology, with the mesial accessory ridge absent on U.W.

1160 101-412, and the development of the IPF for the I² on U.W. 101-908 and its near absence
1161 on U.W. 101-412. Further, U.W. 101-908 is slightly more worn than U.W. 101-412.

1162

1163 U.W. 101-1403: RC¹ root (Fig. 14D; Table 1) This specimen was recovered near U.W.
1164 101-1401 (RP⁴) and U.W. 101-1402 (RP³). It is a large root fragment missing its crown,
1165 which broke away. Its ovoid cross-sectional shape, size, and morphology match that of
1166 other maxillary canines and this attribution is consistent with its excavated position
1167 relative to U.W. 101-1401 and U.W. 101-1402. The root is damaged below the position
1168 of the missing crown. Damage is also evident on the labial face as a v-shaped missing
1169 section. Cracks are apparent in the cementum covering the root. Its maximum preserved
1170 height is 17.5 mm, its maximum LaL width is 9.2 mm, and its MD length is 6.0 mm.

1171 This specimen is proposed to be associated with the U.W. 101-1401 and U.W.
1172 101-1402 maxillary premolars. These premolars have proposed antimeres, U.W. 101-
1173 1560 and U.W. 101-1561, that articulate with a LC¹, U.W. 101-1556. Thus, U.W. 101-
1174 1403 and U.W. 101-1556 are tentatively proposed as antimeres. This proposal cannot be
1175 validated with comparisons of crown morphology, as U.W. 101-1403 lacks a crown, but
1176 is consistent with their root sizes and shapes and with the relative thickness of cementum
1177 covering their roots.

1178

1179 U.W. 101-1510: RC¹? (Fig. 15A; Table 1) This specimen preserves the remnant of a
1180 heavily worn crown and root that is ovoid in cross section. Remnants of an enamel ring
1181 remain labially and lingually, while none is preserved mesially and distally (stage 7).
1182 Assuming this is a right tooth, there is a strong distal angle to the occlusal wear and the

1183 root has a distal inclination. The preserved LaL dimension approximates the maximum
1184 LaL dimension of the crown in the unworn state, but the MD dimension is reduced
1185 relative to the unworn state. The root is abraded across its surface and broken before the
1186 apex. The maximum height of the preserved root is 16.2 mm along the labial edge; this is,
1187 however, not the full length of the root, as the apex is broken.

1188 The shape, size, and tilt of the root suggest that it is an upper right canine. The
1189 contour of the cervical line and the strong MD wear gradient is inconsistent with
1190 attribution to any incisor. In addition, the measured LaL breadth exceeds that of every
1191 incisor and mandibular canine in the assemblage and falls within the range of maxillary
1192 canines (range = 8.2–9.7 mm), supporting attribution to that class. The root height is also
1193 consistent with this attribution.

1194

1195 U.W. 101-1548: LC¹ germ (Fig. 15B; Table 1) Approximately two-thirds of this crown is
1196 complete. The mesial shoulder is complete and is associated with a shallow labial groove.
1197 Lingually, this feature is associated with a moderately-developed groove and marginal
1198 ridge. The median lingual ridge is moderately developed and bipartite, with central and
1199 mesial branches. The apex of the distal shoulder is developed, suggesting asymmetry
1200 seen in other *H. naledi* maxillary canines. This specimen is the antimere of U.W. 101-
1201 544B and attributable to the mixed dentition present in the mandible of U.W. 101-1400
1202 mandible and the antimeres of those teeth.

1203

1204 U.W. 101-1556: LC¹ (Fig. 15C; Table 1) A large distal IPF (approximately 5.4 mm along
1205 the DMR by 2.1 mm LaL at the occlusal edge) extends along much of the length of the

1206 distal aspect of the DMR; its OC height is reduced by apical wear. A tiny IPF is present
1207 mesially at the very apex of the preserved MMR. Wear has removed the crown to nearly
1208 the level of the mesial shoulder and dentine is exposed across the entirety of the occlusal
1209 surface (stage 5). There is a slight distolingual inclination to the wear plane and, in labial
1210 view, there are distinct mesial and distal occlusal wear planes that meet at a slight angle
1211 at mid-crown. A remnant of a shallow distal labial groove is present but no trace of a
1212 mesial labial groove is visible. Lingually, a remnant of the mesial fossa is visible as a
1213 small pit. There are linear hypoplasias near the cervix labially (for a discussion of
1214 hypoplasias on this specimen, see also Skinner, 2019).

1215 The root surface is covered in extensively cracked cementum. There is minor
1216 abrasion on the root surface, especially distally. The apex of the root is broken. The
1217 maximum preserved root height is 15.6 mm. The root is ovoid in cross section and MD
1218 compressed. There are shallow invaginations running along the mesial and distal
1219 surfaces, with the mesial slightly deeper than the distal. The root deflects distally.

1220 The root fits well in the preserved alveolus of the U.W. 101-859 maxillary
1221 fragment; however, we do not consider this a conclusive association. In addition, the
1222 distal IPF is a perfect match for the mesial IPF of the U.W. 101-1560 LP³, which itself
1223 articulates distally with U.W. 101-1561, and the two teeth were removed from the same
1224 mass of sediment and fragments (block U.W. 101-1477) that was recovered *en bloc*.
1225 Thus, U.W. 101-1556, -1560, and -1561 belong to the same individual. The U.W. 101-
1226 1560 and -1561 premolars have proposed antimeres, U.W. 101-1401 and U.W. 101-1402,
1227 that are associated with a canine root, U.W. 101-1403. If these proposed associations are
1228 correct, then U.W. 101-1403 and U.W. 101-1556 are antimeres; though, there is no

1229 morphological means to confirm this proposal given the absence of a crown for U.W.
1230 101-1403. Both U.W. 101-1403 and U.W. 101-1556 come from individuals with
1231 advanced apical wear and both roots are covered in a thick layer of cementum. The tiny
1232 mesial IPF and state of macrowear match the tiny distal IPF and state of macrowear on
1233 the U.W. 101-1684 LI²; a tentative association between them is proposed.

1234

1235 *3.13. Permanent maxillary third premolars*

1236 Eight isolated P³s and one preserved in situ in the U.W. 101-1277 maxilla are
1237 known from the Dinaledi Chamber. Collectively, they represent at least seven
1238 individuals. The *H. naledi* P³s present a consistent morphological pattern. In occlusal
1239 view, the crown profile is slightly asymmetric, with the Pr marginally smaller than the
1240 Pa, especially along the MD axis. The lingual margin is more convex than the straighter
1241 buccal margin. The buccal grooves are both shallow and present only in the occlusal third
1242 of the crown height. In addition to a low essential crest, weak mesial and distal accessory
1243 ridges are present on the Pa, which creates a trilobate Pa face. Except for U.W. 101-786
1244 and U.W. 101-1004, with a single canal, the other P³s have three distinct root canals: two
1245 buccal and one lingual. The roots are individualized externally to varying degrees,
1246 showing greater separation in U.W. 101-037, U.W. 101-182, U.W. 101-729, and U.W.
1247 101-1107 than in U.W. 101-1402 and U.W. 101-1560. Even the single rooted specimens
1248 show external clefts in the root mass that hint at the multirooted morphology seen in the
1249 other specimens.

1250

1251 U.W. 101-037: RP³ (Fig. 16A; Table 1) Enamel chipping is present at the occlusal
1252 margin near the mesial IPF and another chip sits on the lingual side of the mesial Pr crest.
1253 A large IPF is present distally (4.2 mm BL by 2.8 mm OC) and a much smaller one sits
1254 mesially (3.2 mm BL by 2.1 mm OC) and is offset buccal to the center of the crown. The
1255 crown is moderately worn with small pits of dentine exposed over the Pa and Pr (stage 2).
1256 The morphological features have been smoothed over by wear, but the ridge and fissure
1257 pattern remain. The occlusal outline is a rounded rectangle, and the Pr is smaller than the
1258 Pa, especially in its MD length. An abbreviated distolingual corner contributes to the
1259 asymmetry of the occlusal profile. The lingual margin is more tightly convex, and the
1260 buccal margin is straighter, although indented by shallow mesiobuccal and distobuccal
1261 grooves. These vertical grooves delineate mesial and distal ridges on the buccal face,
1262 which become imperceptible at mid-crown. Though worn, subtle mesial and distal
1263 accessory ridges (sensu Scott and Irish, 2017) arise from either side of the Pa. Both ridges
1264 terminate at the Mlg. The essential ridge of the Pa is worn but appears to have been
1265 broad; thus, in combination with the accessory ridges, the Pa face is trilobate. The Mlg
1266 curves around the Pa mesially and distally. It is deeper mesially, suggesting the presence
1267 of a pit-like Fa. The lingual crown is featureless.

1268 Two buccal roots and one lingual root are present. All roots are broken at their
1269 tips and the exposed surfaces are stained by adhering matrix. The buccal roots are both
1270 compressed with their major axis BL and minor axis MD. The lingual root is larger in
1271 cross sectional area with its major axis running from mesiolingual to distobuccal. The
1272 buccal roots are vertically oriented above the crown, and, in buccal view, their apices
1273 flare apart MD. The taller lingual root angles out lingually over the crown. The lingual

1274 root canal is individuated from the buccal roots near the cervix, while the buccal root
1275 canals become separated at about one-third of their heights from the cervix. The mesial
1276 buccal root is 10.7 mm in preserved height, while the distal buccal root is 11.9 mm in
1277 preserved height, and 11.1 mm of the lingual root remains.

1278 This isolated tooth is identified as a P³, and not a P⁴, by the combination of
1279 asymmetry in IPF size and orientation and the crown asymmetry in occlusal view.

1280

1281 U.W. 101-182: RP³ (Fig. 16B; Table 1) The occlusal surface is lightly worn: small facets
1282 are visible on the ridges extending from the Pa. The apex of the Pr is also rounded by
1283 wear (stage 1–2). Neither mesial nor distal IPFs are visible. The Pa is slightly larger than
1284 the Pr and its apex sits distal to that of the Pr. The crown has an abbreviated distolingual
1285 corner, which yields an asymmetrical crown outline. The Pa has three distinct occlusal
1286 ridges. None of the ridges connects directly to the center of Pa apex; the relief of the
1287 ridges is slightly reduced by occlusal wear, and they are similarly prominent at this state
1288 of wear. All ridges terminate at the MIg. The Pr does not have accessory ridges and the
1289 essential ridge is not well defined. The MMR is distinct but mostly limited to the region
1290 mesial to the Pr, where it bulges out mesially. A groove-like Fa is formed between the
1291 MMR and the mesial-most ridge of the Pa. It is continuous with the MIg. The DMR is not
1292 well defined. The MIg broadens at its distal-most extent where it terminates as a small
1293 pit. Subtle mesiobuccal and distobuccal grooves are present, with the mesial deeper than
1294 the distal. Both disappear before mid-crown. The lingual face is smooth and
1295 unremarkable.

1296 Portions of three roots are preserved. Minor abrasion is present on the
1297 mesiolingual corner of the lingual root and on the mesial surface of the mesiobuccal root.
1298 There is single nearly circular lingual root, with its major axis mesiobuccal to
1299 distolingual, and two buccal roots that are compressed MD in cross section. The lingual
1300 root is nearly complete except for a small portion that has broken away near the apex.
1301 The remaining lingual root is 10.2 mm in height. The distobuccal root is broken at
1302 approximately half its height, about 3.9 mm from the cervix, while the mesiobuccal root
1303 is broken much nearer its apex, preserving 7.2 mm of its height. The lingual root tilts out
1304 over the crown, while the buccal roots, as preserved, extend nearly vertically from the
1305 crown.

1306 This isolated tooth is likely a P³. This identification is supported by the crown
1307 asymmetry in occlusal view and the mesial flare of the MMR, which tends to be flatter on
1308 inferred P⁴s. However, the absence of IPFs makes this attribution less certain.

1309

1310 U.W. 101-729: RP³ (Fig. 16C; Table 1) No IPFs are present. A tiny facet is present on the
1311 mesial aspect of the Pa (stage 1), which indicates that the crown was like erupting at
1312 death and had just begun occlusal contact. The crown profile is slightly asymmetric, with
1313 a more tightly convex lingual margin and Pr that is nearly equal in size and height to the
1314 Pa; the Pr apex is mesial to that of the Pa. The Pr essential crest is indistinct, and it lacks
1315 accessory ridges. As in other *H. naledi* maxillary premolars, the Pa possesses two ridges
1316 that originate on either side of the cusp apex and terminate at the MIg. Another minor
1317 ridge is merged with the distal Pa ridge and could be considered the essential ridge, but it
1318 does not continue to the apex of the Pa either. The mesial ridge of the Pa is more

1319 topographically prominent than the distal ridge. A third ridge arises from the junction of
1320 the distal Pa crest and DMR and encroaches on the space that would be occupied by the
1321 Fp. The MMR dips just buccal to the MIg and blends into the undefined mesial ridge of
1322 the Pr. Viewed mesially, the MMR is v-shaped with the deepest point of the v set buccal
1323 to the midpoint of the crown. The Pa mesial accessory ridge is hypertrophied, delineated
1324 from the MMR by a groove-like Fa; the groove crosses onto the buccal face as a shallow
1325 vertical indentation. In mesial view, this lingual aspect of the MMR appears as a tubercle-
1326 like bulge. The Fp is undefined. The DMR is low and rounded and barely elevated on the
1327 occlusal surface and the FP is a poorly defined pit. Mesio Buccal and distobuccal grooves
1328 are each shallow and become imperceptible at mid-crown. The lingual face is featureless.

1329 The tooth has three roots: two buccal roots and one lingual. The roots are cracked
1330 on their external surfaces. Slightly less than half the root mass is preserved, and the root
1331 canals are packed with sediment. The buccal roots run parallel to each other and are
1332 compressed and joined by a thin sheath of dentine. They are approximately the same size
1333 in cross sectional area. The larger lingual root is ovoid in cross section, with its major
1334 axis running mesiolingual-to-distobuccal. It flares out lingually. The preserved height of
1335 the lingual root is 5.9 mm, while that of the distobuccal root is 7.8 mm and that of the
1336 mesio Buccal root 5.5 mm.

1337

1338 U.W. 101-786: LP³ (Fig. 16D; Table 1) Enamel chipping is observed on the occlusal
1339 surface just above an ovoid distal IPF (3.4 mm BL by 1.8 mm OC). There is no mesial
1340 IPF. There is light occlusal wear on the Pa and Pr apices, on the Pa mesial accessory
1341 ridge, and on the distal portion of tan accessory ridge extending from the junction of the

1342 distal Pa crest and DMR (stage 1). The occlusal profile is slightly asymmetric, with a
1343 more tightly convex lingual profile and straighter buccal profile slightly indented by the
1344 buccal grooves. The crown is longer MD along the Pa than along the Pr. The cusps are
1345 sub-equal in height and the Pr apex is mesial to that of the Pa. The MMR is low and
1346 rounded and the buccal and lingual segments dip where they meet so that the MMR is v-
1347 shaped in mesial view with its low point buccal to the midpoint of the crown. The
1348 essential lobe of the Pr is poorly developed. Two ridges are present on the Pa face and
1349 neither connects directly to the apex of the crown. The mesial of the two ridges has a
1350 slight extension that crosses the Mlg and helps to define the Fa distally. The distal of the
1351 two Pa ridges terminates at the Mlg. Wide and shallow buccal grooves are associated
1352 with the mesial and distal Pa ridges; both fade at mid-crown. The lingual face is
1353 featureless.

1354 Unlike some other *H. naledi* maxillary premolars, only a single root, with two
1355 distinct radicals, extends above the crown. It is abraded along most of its external surface
1356 and is broken before its apex, exposing the root canal. The preserved buccal root height is
1357 10.2 mm. The root is compressed MD and longer BL with a wide and shallow groove
1358 running along the mesial face, a narrower and deeper groove running the length of the
1359 distal face and a narrower but shallow groove running along the buccal face.

1360 The U.W. 101-1004 RP³ is proposed as the antimere of this tooth. Their crown
1361 morphologies are similar as are their root morphologies; for example, some of the *H.*
1362 *naledi* P³s show a splaying of the roots but U.W. 101-786 and U.W. 101-1004 do not.
1363

1364 U.W. 101-1004: RP³ (Fig. 17A; Table 1) A distal IPF (5.1 mm BL by 2.1 mm OC)
1365 reaches the occlusal margin. A smaller mesial IPF (2.8 mm BL by 1.9 mm OC) is evident
1366 near midcrown extending nearly to the cervix. Occlusal wear is minimal, but the crown
1367 apices and occlusal ridges have been blunted (stage 1). In occlusal view, the crown is
1368 nearly symmetric, with the Pr only slightly shorter MD than the Pa and the two cusps are
1369 nearly equal in area. The essential ridges of both cusps are indistinct. A well-developed
1370 accessory ridge extends towards the MIg from the intersection of the distal Pa crest and
1371 DMR. The groove-like Fa is continuous with the MIg and passes mesial to the Pa. The
1372 MMR is a continuous rim and reaches most cervically just mesial to the Pa. In occlusal
1373 view, the MMR arcs from the Pr to reach its most mesial extent adjacent to the Pa. The
1374 Fp is scarcely more than a pit at the end of the MIg bounded by a low and dull DMR and
1375 the distal accessory ridge of the Pa. The mesio- and distobuccal grooves are shallow, with
1376 the distobuccal groove slightly deeper; both fade away approximately mid-crown. No
1377 lingual grooves are present.

1378 The single root is broken near its apex, exposing the root canal, and the root
1379 surface is abraded. The preserved root measures 11.9 mm along the buccal face. The root
1380 has a cleft running along the buccal aspect and subtle depressions evident along mesial
1381 and distal faces, giving it a slight figure-of-eight cross section.

1382 The U.W. 101-786 LP³ is proposed as the antimere of this tooth. Their crown
1383 morphologies are similar as are their root morphologies; for example, some of the *H.*
1384 *naledi* P³s show a splaying of the roots but U.W. 101-786 and U.W. 101-1004 do not.
1385

1386 U.W. 101-1107: LP³ (Fig. 17B; Table 1) An enamel chip is missing just mesial to the Pa
1387 apex. No IPFs are visible mesially or distally. The crown is minimally worn with wear
1388 facets visible on the Pr apex, as well as mesial and distal to it. A small facet is also visible
1389 on the DMR (stage 1). The Pr is slightly smaller in area and MD length than the Pa. The
1390 buccal profile is pinched in association with shallow mesiobuccal and distobuccal
1391 grooves, while the lingual profile is continuous and more tightly convex. The marginal
1392 ridges are restricted to the Pa and the DMR is slightly broader than the MMR. As in other
1393 inferred P³s, the MMR flares as it passes mesial to the Pa. There is no essential ridge on
1394 the apex; instead, mesial and distal ridges arise on either side of the Pa apex. A fissure-
1395 like Fa is restricted to the Pa and is nearly continuous with the Mlg, separated by a slight
1396 crest connecting the MMR and mesial Pa accessory crest. Both buccal grooves are
1397 shallow and extend less than a third of the way down the buccal face before they become
1398 imperceptible.

1399 Parts of three damaged roots are preserved. Significant abrasion is evident near
1400 the broken edges of the root apices and along the mesial side of lingual and mesiobuccal
1401 roots. Breaks expose the root canals. What remains of the distobuccal root is 6.4 mm, that
1402 of the mesiobuccal root is 6.3 mm, and that of the lingual root is 9.6 mm. The
1403 mesiobuccal and distobuccal roots are similar in cross-sectional area and are both MD
1404 compressed. The lingual root is ovoid in cross section and is larger than both buccal
1405 roots. The buccal roots extend vertically from the crown, while the lingual root deflects
1406 lingually. The buccal roots flare apart to a greater extent than other *H. naledi* maxillary
1407 premolars.
1408

1409 U.W. 101-1402: RP³ (Fig. 17C; Table 1) Enamel chipping is visible along the mesial and
1410 distal margins. The chip in the distal IPF matches the chipping on the mesial IPF of the
1411 U.W. 101-1401 RP⁴. The distal IPF is large (5.4 mm BL by 2.3 mm OC), while the
1412 mesial IPF is small (2.4 mm BL by 0.8 mm OC). Dentine is exposed over the Pa and Pr
1413 apices. The pool of dentine on the Pa extends distally, while that of the Pr extends
1414 mesially and is paired with a thin strip of dentine along the distal crest (stage 4–5). Trace
1415 remnants of the mesiobuccal and distobuccal grooves are palpable. They are more
1416 pronounced than on the U.W. 101-1401 RP⁴ associated with this specimen. The occlusal
1417 morphology has been removed by wear and only a short, thin groove of the Fa remains
1418 mesial to the Pa.

1419 A bit of the alveolus remains attached to the root mass distally. The roots are
1420 broken at their apices. Three roots are present: a single lingual root and two buccal roots.
1421 The roots are tightly compressed into a single external mass, much like U.W. 101-1401.
1422 The μ CT scans show three distinct canals associated with lingual, mesiobuccal, and
1423 distobuccal roots. The lingual root has a slight distal inclination. The mesiobuccal root is
1424 also inclined distally. All roots are MD compressed, with the buccal roots more
1425 compressed than the lingual. The maximum height of the preserved lingual root is 11.1
1426 mm. The maximum mesiobuccal root height is 12.4 mm, and the maximum distobuccal
1427 root height is 9.4 mm.

1428 This specimen was near U.W. 101-1401 (RP⁴) when excavated and has a good
1429 distal articulation with it. It is the proposed antimere of U.W. 101-1560; though, that
1430 determination is difficult to confirm given their advanced wear state. This specimen was
1431 also excavated near the U.W. 101-1403 RC¹, which lacks a crown, but is consistent with

1432 attribution to a maxillary canine. We provisionally propose that U.W. 101-1401, -1402,
1433 and -1403 belong to the same individual.

1434

1435 U.W. 101-1560: LP³ (Fig. 17D; Table 1) There is enamel chipping along the mesial and
1436 distal margins. There is a large obliquely oriented mesial IPF (5.7 mm along the long
1437 oblique axis by approximately 2.4 mm OC near the center of the IPF) and a smaller distal
1438 IPF (4.7 mm BL by 2.0 mm OC). The occlusal morphology has been obliterated by wear.
1439 The moderate-sized pool of dentine on the Pa extends along its distal crest, while that of
1440 the Pr occurs over the apex with an additional strip along the mesial crest (stage 4–5).
1441 The occlusal profile is fairly symmetric, and the Pr and Pa are nearly equal in area. As
1442 judged by the dentine exposures, the Pr apex was placed well mesial to that of the Pa.
1443 Remnants of the mesiobuccal and distobuccal grooves are preserved.

1444 Three roots are present: a mesiobuccal, distobuccal, and lingual root. The roots
1445 are covered in cementum, which is flaking off, and their apices are all broken away;
1446 though, only the lingual root canal is exposed. The preserved height of the lingual root is
1447 10.1 mm, that of mesiobuccal root is 10.6 mm, and that of the distobuccal root is 9.6 mm.
1448 The buccal roots are inclined distolingually, especially near their apices, while the lingual
1449 root is more vertically oriented. The buccal roots are ovoid in cross section, being MD
1450 compressed, while the lingual root is rounder. All three roots are tightly pressed together.
1451 The buccal roots are joined near the cervix, but a cleft develops between them towards
1452 their apices. The μ CT scans indicate that the three roots share a common canal for about
1453 half their lengths before the common canal splits almost simultaneously into three
1454 separate canals.

1455 The shape of the mesial IPF is a perfect fit for the distal IPF of the U.W. 101-
1456 1556 LC¹. This specimen also articulates distally with U.W.101-1561. Further, this is the
1457 proposed antimere of U.W. 101-1402. Given the advanced state of wear of both
1458 specimens, it is, however, difficult to confirm their status as antimeres; in fact, their wear
1459 patterns are not identical, with U.W. 101-1402 having a dentinal exposure along the distal
1460 Pr crest that is absent in U.W. 101-1560.

1461

1462 *3.14. Permanent maxillary fourth premolars*

1463 Eight isolated P⁴s and one in situ in the U.W. 101-1277 maxilla represent at least
1464 seven individuals in the Dinaledi Chamber deposits. The P⁴s present a consistent
1465 morphological pattern. The crown is mildly asymmetric in occlusal outline, as the Pa
1466 slightly exceeds the Pr in area, and the lingual and buccal profiles are similar in their
1467 curvature. The buccal grooves are shallow and only present in the occlusal third of the
1468 crown height. The number and shape of the roots differs between individuals. Some
1469 specimens (e.g., U.W. 101-277, U.W. 101-1362) have three clearly distinct roots
1470 externally, while others (e.g., U.W. 101-1401, U.W. 101-1561) have multiple distinct
1471 root canals but show weak separation of the radicals externally. In all, there is a single
1472 canal in the cervical third of the root mass and the canals become distinct apically. In
1473 some (e.g., U.W. 101-334), the roots are broken near enough to the cervix that it is
1474 difficult to discern if the tooth would have been multirooted.

1475

1476 U.W. 101-277: LP⁴ (Fig. 18A; Table 1) Occlusal enamel chipping is evident along the
1477 MMR and another chip is evident along the DMR. Large, BL-oblong semicircular IPFs

1478 are visible mesially (6.0 mm BL by 3.0 mm OC) and distally (5.6 mm BL and 2.3 mm
1479 OC). Wear has polished the occlusal surface, flattening the cusp apices, but no dentine is
1480 exposed (stage 1–2). Despite the moderate wear, much of the occlusal morphology is
1481 preserved. In occlusal view, the crown is mildly asymmetric in outline, as the Pa slightly
1482 exceeds the Pr in area, and the lingual and buccal profiles are similar in the curvature.
1483 The buccal profile is somewhat lobate. The Pa possesses three occlusal ridges that are
1484 nearly equal in size: the essential ridge widens as it reaches the Pa apex. The mesial and
1485 distal accessory ridges are thinner. The mesial accessory ridge crosses the Mlg and
1486 merges with the essential ridge of the Pr. The Pa essential ridge and distal accessory
1487 ridge, on the other hand, terminate at the Mlg. The Pr also likely possessed mesial and
1488 distal accessory ridges based on the deep occlusal grooves that are preserved. A short,
1489 thin crest extends mesially from the Pr accessory ridge and connects to the MMR, while
1490 the distal accessory ridge terminates at the Mlg. The MMR expression is obscured by
1491 wear and chipping but an Fa, expressed as a narrow groove confined to the Pa with a
1492 short buccal segment preserved, is present. Distally, the Mlg merges with a BL-oriented
1493 groove that curves around the distal accessory ridge of the Pa. The DMR is dulled by
1494 wear but is thick and rounded. The mesial and distal Pa accessory crests are associated
1495 with mesiobuccal and distobuccal grooves, which are both palpable but shallow. The
1496 distal groove is deeper than the mesial groove. Both fade away about mid-crown, but the
1497 distal groove extends a bit farther along the crown.

1498 Portions of three roots are present. Some abrasion is evident on the mesial and
1499 distal aspects of the lingual root, near the preserved apex of the mesial buccal root on its
1500 mesial face, and along the distal face of the distobuccal root. Both buccal roots are

1501 broken, exposing their root canals. The lingual root, which leans over the lingual face and
1502 cants distally as well, is nearly circular in cross section, with its major axis mesiolingual
1503 to distobuccal. The two buccal roots are pressed together and do not splay apart apically
1504 as preserved. They extend nearly directly above the crown, are compressed in cross
1505 section, being broader BL than MD. The mesial buccal root is slightly broader BL than is
1506 the distal buccal root. The buccal roots share a common canal near the cervix; however,
1507 the canals are fully individualized before the break and the radicals themselves begin to
1508 differentiate just prior to the break. The lingual root is preserved completely and
1509 measures 15.8 mm in height lingually. The mesiobuccal and distobuccal roots are each
1510 broken at slightly more than half of their height. The preserved mesiobuccal root is 7.8
1511 mm long and the preserved distobuccal root is 9.2 mm long.

1512 This specimen is considered a P⁴ based on its crown morphology, the placement
1513 and size of its IPFs, and because it likely articulates distally with the U.W. 101-1676
1514 LM¹. The shapes and sizes of their IPFs are a good match. Additionally, if they are
1515 associated, both specimens have enamel chips occlusal to their congruent IPFs.

1516

1517 U.W. 101-333: LP⁴ (Fig. 18B; Table 1) The crown is unworn, with neither occlusal nor
1518 interproximal wear present (stage 1). The occlusal profile is nearly symmetrical, with
1519 similarly sized cusps and the apex of the Pa offset slightly mesial to the Pr. Though both
1520 are dull, the MMR is narrower than the rounded DMR, which is associated with a slight
1521 distobuccal cuspule. Similar to other *H. naledi* P⁴s, two ridges are visible on the face of
1522 the Pa and neither connects to the apex of the cusp. The mesial ridge is pinched in near its
1523 origin occlusally and becomes wider towards the MIg. The Fp is a groove extending

1524 buccally to the distal crest of the Pa and lingually past the MIg as a small pit. The Fa is a
1525 groove adjacent to the mesial Pa ridge and contiguous with the MIg. There is a faint
1526 cuspule at the distal terminus of the MIg. On the buccal face, the mesiobuccal groove is
1527 barely detectable even at the occlusal margin, while the distobuccal groove is wider and
1528 deeper. It is associated with the distobuccal cuspule where it crosses the occlusal margin
1529 but becomes imperceptible at about mid-crown. The lingual face is unremarkable.

1530 The root was still forming at the time of death and only a sliver is preserved
1531 around the cervix. The root canal is packed with sediment.

1532 This is the probable antimere of U.W. 101-334. The two teeth are virtually
1533 identical morphologically and in their state of wear. The teeth were also excavated within
1534 centimeters of each other.

1535

1536 U.W. 101-334: RP⁴ (Fig. 18C; Table 1) The crown is unworn, with neither occlusal nor
1537 interproximal wear (stage 1). The occlusal profile is nearly symmetrical, with similarly
1538 sized cusps and the apex of the Pa offset slightly mesial to the Pr. Though both are dull,
1539 the MMR is narrower than the DMR, which is wide and rounded. Like other *H. naledi*
1540 P⁴s, the crown features two ridges on the face of the Pa and neither connects to the apex
1541 of the cusp. On the buccal face, the mesiobuccal groove is barely detectable even at the
1542 occlusal margin, while the distobuccal groove is wider and deeper. It is associated with a
1543 weak distobuccal cuspule where it crosses the occlusal margin but becomes imperceptible
1544 at about mid-crown. The lingual face is unremarkable.

1545 The roots are abraded across their surfaces and broken apically. Though the roots
1546 are broken, this specimen is obviously multirooted, with a rounded lingual root separated

1547 from the buccal roots. Buccally, a cleft is present in the center of the buccal root mass,
1548 which may indicate two distinct buccal root apices. In buccal view, the maximum height
1549 of the preserved root is 2.0 mm, while, in lingual view, the maximum root height is 4.0
1550 mm.

1551 This tooth is the proposed antimere of U.W. 101-333. They are virtually identical
1552 morphologically and in their state of wear.

1553

1554 U.W. 101-455: RP⁴ (Fig. 18D; Table 1) Reflecting its relatively unworn state, no IPF is
1555 present mesially and a small one (approximately 2.5 mm LaL by 1.8 mm OC) sits distally
1556 next to the Pa. The crown is minimally worn with small facets near the tip of the Pr and
1557 along the essential ridge of the Pa (stage 1). The Pa is slightly larger in area and ML
1558 longer than the Pr, giving the crown an asymmetrical profile in occlusal view. Though
1559 continuous, the lingual and buccal segments of the MMR are lower than the Pr and Pa
1560 essential crests. The segments slope from their origins to meet at angle on the mesial
1561 surface so that the low point of the MMR is mesial to the Pa. A groove-like Fa is limited
1562 to the Pa and merges with the MIg. It is bordered mesially by the MMR and distally by a
1563 hypertrophied ridge extending from the near the apex of the Pa. As with several *H. naledi*
1564 P⁴s, there are two ridges extending from the Pa towards the MIg and neither ridge
1565 precisely intersects the apex of the Pa. The distal of the two ridges is much narrower than
1566 the mesial ridge. A third ridge extends from near the junction of the distal crest of the Pa
1567 and the DMR and enters the space that might otherwise be occupied by the Fp, which is
1568 merely a pit at the distal end of the MIg. The DMR is indistinct. The Pr essential ridge is
1569 wide, and it terminates at the MIg. On the buccal face, the mesial groove is short and

1570 faint. The distobuccal groove is more distinct and extends to about two-thirds the crown
1571 height. It crosses the occlusal margin, becoming a shallow occlusal groove delineating an
1572 accessory ridge described above. The lingual face is featureless.

1573 In contrast to some other maxillary premolars in the assemblage, only a single
1574 root is present. The maximum preserved height of the broken and abraded root is
1575 approximately 7.0 mm in buccal view and 5.6 mm in lingual view. The root canal is
1576 exposed. On the buccal face, an invagination runs longitudinally along the root and subtle
1577 depressions run along the mesial and distal faces. The root is mostly compressed MD,
1578 with its major axis BL.

1579 This specimen is proposed as the antimere of U.W. 101-808. They are similar in
1580 occlusal and root morphology and the state of occlusal wear; however, their crown
1581 outlines are slightly different with the distolingual corner less abbreviated in U.W. 101-
1582 808.

1583

1584 U.W. 101-808: LP⁴ (Fig. 18E; Table 1) There is no mesial IPF and a small rounded distal
1585 IPF (2.7 mm BL by 1.8 mm OC). The crown is lightly worn with small facets on the Pa
1586 distal crest and on the mesial aspect of the Pr apex (stage 1). The Pr and Pa are sub-equal
1587 in height and the crown is only mildly asymmetric, with the lingual profile fairly straight
1588 and only slightly more tightly convex than the buccal. The apex of the Pr is mesial to that
1589 of the Pa. The MMR is low and rounded; and the buccal and lingual segments dip where
1590 they meet so that the MMR is v-shaped in mesial view. The Pr essential ridge is low and
1591 rounded and bordered mesially and distally by weak accessory ridges. The Pa is
1592 occlusally more complex: there is a distinct mesial ridge that starts narrow near the apex

1593 but widens quickly, flaring mesially and distally as it reaches the MIg. Distal to this ridge,
1594 there is a thin, sharp crest that that also widens about mid-crown (but less so) and merges
1595 with the mesial ridge at the MIg. As is common with the *H. naledi* maxillary premolars,
1596 neither of these crests is associated directly with the Pa apex. A third crest rises from near
1597 the junction of the distal Pa crest and DMR and is associated with a distinct occlusal
1598 elevation and occlusal and buccal grooves. The hypertrophied mesial Pa ridge forms the
1599 distal boarder of a fissure-like Fa that is limited to Pa and bordered mesially by the
1600 MMR. The DMR is not well-defined. No Fp is observed. The mesiobuccal and
1601 distobuccal grooves are wide and shallow and they fade away about one-third the crown
1602 height. A small pit, possibly hypoplastic, is observed about mid-crown on the buccal
1603 aspect.

1604 The root is abraded on all surfaces and broken irregularly so that the maximum
1605 preserved height is 7.0 mm buccally, while only 5.6 mm of the root remains lingually. In
1606 buccal view, a small cleft is visible running longitudinally along the root; however, given
1607 the state of preservation of the root, it is unclear if the apices would have diverged.

1608 This specimen is proposed as the antimere of U.W. 101-455. Articulation with
1609 U.W. 101-708 distally is reasonable as their IPFs are similar in size and shape and appear
1610 congruent.

1611

1612 U.W. 101-1362: LP⁴ (Fig. 19A; Table 1) Extensive chipping circumscribes the crown.
1613 Further damage is evident in the region of the mesial IPF, and recent damage removed a
1614 portion of the distal occlusal surface. Nearly the entire crown has been removed by wear
1615 and the pulp chamber is exposed. An enamel rim is primarily present buccally where it

1616 extends around the distobuccal corner and preserves a portion of the distal IPF.
1617 Additionally, a thin sliver of enamel still lines the lingual cervix (stage 7). The wear
1618 surface has a strong lingual slope, such that approximately 4.7 mm of the crown's height
1619 remains buccally but only a sliver, less than 0.5 mm in OC height, remains lingually.

1620 The tooth has two roots. The buccal root has moderate damage to its apex and the
1621 lingual root is nearly completely preserved. Both roots are covered in a thick layer of
1622 cementum. The lingual root is conical, longer, and more circular in cross section than the
1623 buccal root. The buccal root has two radicals separated by a moderate invagination
1624 running along its buccal surface. The μ CT scans reveal two distinct buccal root canals for
1625 nearly half the length of the root. The buccal roots are more individualized than apparent
1626 now because of the thick layer of cementum that has accumulated along the roots. The
1627 preserved height of the buccal root is 10.3 mm, while the lingual root is 10.9 mm.

1628 The distal IPF is a good fit for the mesial IPF of U.W. 101-796 (LM¹), which is
1629 argued to be associated with U.W. 101-528 (LM²) and U.W. 101-527 (LM³). If these
1630 proposed associations are correct, this would constitute a heavily worn set of maxillary
1631 postcanine teeth from a single individual. An association with the equally heavily worn
1632 teeth in the U.W. 101-361 mandible is also possible.

1633

1634 U.W. 101-1401: RP⁴ (Fig. 19B; Table 1) Enamel chipping is visible along the mesial and
1635 distal margins. Large mesial (5.6 mm BL by 2.2 mm OC) and distal (6.7 mm BL by 2.3
1636 mm OC) IPFs are present. The crown is worn, with a small dentine patch on the Pa apex
1637 and a larger pool at the Pr apex that extends to the mesial margin (stage 5). Very little
1638 surface topography remains beyond a remnant of the MIg. The mesiobuccal and

1639 distobuccal grooves are faint but detectable as shallow indentations. The lingual face is
1640 featureless.

1641 A portion of the buccal root face is broken away near its apex, where a notch is
1642 removed. While some *H. naledi* maxillary premolars have three distinct roots, in this
1643 specimen there is a single external root mass. This appearance results in part from a thick
1644 layer of cementum that obscures the contours of the underlying dentine but it is clear that
1645 the roots did not splay from one another. An examination of the μ CT scans show three
1646 distinct canals near the root apices with two tightly compressed buccal roots. Externally,
1647 two radicals are visible on the buccal face. The mesiobuccal root is BL broader than the
1648 distobuccal root. Both buccal roots are lingually inclined and, above the break, the
1649 mesiobuccal root deflects distally. The lingual root has a slight mesial inclination. All
1650 root components are separated by strong grooves. The nearly complete lingual root is
1651 13.0 mm tall. The preserved height of the mesiobuccal root is 9.5 mm and the distobuccal
1652 root is 8.8 mm tall.

1653 This specimen was excavated near U.W. 101-1402 (RP³), with which it has a
1654 good mesial articulation. It also has a good distal articulation with U.W. 101-1396 (RM¹).
1655 The LP⁴ U.W. 101-1561 is proposed as its antimere; though, U.W. 101-1401 is slightly
1656 less worn than U.W. 101-1561. Given the advanced state of wear of both specimens, it is
1657 difficult to confirm their status as antimeres.

1658

1659 U.W. 101-1561: LP⁴ (Fig. 19C; Table 1) There is enamel chipping along the mesial and
1660 distal margins. Large horizontally oriented IPFs are present mesially (4.9 mm BL by 2.1
1661 mm OC) and distally (7.6 mm BL by 2.6 mm OC). The occlusal surface is worn and

1662 preserves little detail. The moderately-sized dentine pools on the Pa and Pr are connected
1663 mesially by a narrow strait (stage 5). Shallow remnants of the mesiobuccal and
1664 distobuccal grooves are preserved. The lingual face is featureless.

1665 There are three distinct root components—two buccal and one lingual—with
1666 separate apices. They are tightly compressed into a single mass. The roots are abraded
1667 and the mesiobuccal and distobuccal roots are missing their apices, exposing the canals.
1668 The buccal roots are slightly distally inclined and run parallel to each other. They are
1669 more ovoid in cross section than the lingual root. The lingual root is also nearly vertical
1670 with a slight mesial inclination near its apex. The μ CT scans show that the buccal
1671 components are associated with separate root canals for about half their length, while the
1672 lingual root canal separates closer to the cervix. The preserved height of the nearly
1673 complete lingual root is 12.2 mm. The maximum height of the mesiobuccal root is 9.6
1674 mm and that of the distobuccal root is 7.5 mm.

1675 This specimen articulates mesially with the U.W. 101-1560 LP³. It also proposed
1676 as the antimere of U.W. 101-1401; though, their wear patterns are not identical.

1677

1678 *3.15. Permanent maxillary first molars*

1679 Eleven isolated M¹s and one present in the U.W. 101-1277 maxilla represent at
1680 least seven individuals. The sample includes a developing antimeric pair, U.W. 101-1305
1681 and U.W. 101-1688, which were nearing crown completion at death, through a range of
1682 wear stages, including a heavily worn specimen, U.W. 101-796, in which the steep
1683 bucco-lingual wear gradient had worn to the level of the pulp chamber. The specimens
1684 are all similar in morphology and size. Where detail can be assessed, all M¹s have four

1685 principal cusps and no supernumerary cusps. The Hy is relatively large and projects
1686 distolingually, giving the crown a rhomboidal occlusal outline. Carabelli's feature is
1687 evident mesiolingually as a faint obliquely oriented crest or small groove in some
1688 specimens. The Co is continuous. Buccal grooving is shallow; the lingual groove is
1689 narrow at the occlusal margin and widens as it reaches cervically.

1690

1691 U.W. 101-445: LM¹ (Fig. 20A; Table 1) A large ovoid mesial IPF (4.2 mm LaL by 2.9
1692 mm OC) is present. No distal IPF is detectable. Wear is present on all cusps, which
1693 removed details of occlusal ridging, and along the distal edge of the Co; however, no
1694 dentine is exposed (stage 1). There are four principal cusps and no supernumerary cusps.
1695 The Hy is relatively large and projects distolingually and the DMR—an extension of the
1696 Hy distal accessory lobe—is swollen, which rounds the distal profile and yields a
1697 rhomboidal occlusal outline. In size, the relative cusp sizes are $Pr > Me \geq Hy > Pa$. The
1698 mesial IPF has obscured the MMR, but a trace of the Fa remains as a small pit. A pit-like
1699 Fp is present between the Hy and Me; its size is reduced by the presence of a small distal
1700 tubercle. The Co is continuous. The buccal groove is a shallow depression throughout its
1701 course to the cervix. The lingual groove is deep and narrow near the occlusal margin and
1702 widens at mid-crown, becoming shallow as it approaches the cervix. A Carabelli's feature
1703 is evident mesiolingually as a faint obliquely oriented crest.

1704 Three roots, a mesiobuccal, distobuccal, and centrally placed lingual root, are
1705 evident. The lingual and mesiobuccal roots are broken near their apices, exposing their
1706 root canals, and are abraded along their outer surfaces. The distobuccal root broke away
1707 at the cervix (apparent in the μ CT scans) but has been refit to the crown, which is evident

1708 in Figure 20A. Approximately 11.0 mm of the distally tilting lingual root is preserved.
1709 The lingual root angles out over the lingual face; in cross section it is longest MD and
1710 compressed BL with a prominent groove running along its lingual surface and a subtler
1711 groove along its buccal surface. In buccal view, approximately 10.0 mm of the
1712 mesiobuccal root is preserved. The mesiobuccal root is longer BL and compressed MD in
1713 cross section, shallow depressions run along its mesial and distal faces, and it tilts slightly
1714 distally.

1715 This specimen is a possible antimere of U.W. 101-583. The teeth are similar
1716 morphologically and in their state of occlusal and interproximal wear. The teeth do differ
1717 slightly distally where U.W. 101-583 has a slight crest on the distal face that is absent in
1718 this specimen.

1719

1720 U.W. 101-525+1574: RM¹ (Fig. 20B; Table 1) This tooth comprises two pieces that were
1721 recovered and catalogued separately. U.W. 101-525 is a crown with most of the
1722 mesiobuccal and lingual roots remaining attached. A portion of refitting distobuccal root
1723 is catalogued as U.W. 101-1574. For clarity, we describe them together here.

1724 There are enamel chips missing along the mesiobuccal corner and just occlusal
1725 and buccal to the mesial IPF. Another chip is evident distobuccally. A large oval IPF (5.2
1726 mm BL by 2.0 mm OC) reaches the occlusal margin. A larger distal IPF (5.2 mm BL by
1727 3.6 mm OC) is also present and offset lingually. A large, mesially extended dentine pit is
1728 present on the Pr, and smaller dentine pits cover the apices of the Me and Hy (stage 3). In
1729 occlusal view, the crown outline is rhomboidal, with a mesiobuccally projecting Pa and a
1730 large, distolingually-projecting Hy. Interproximal wear creates a slightly concave mesial

1731 profile. Although worn, there is no indication of a C5 at the outer enamel surface (there is
1732 no dentine horn at the EDJ for a C5 either). A remnant of Carabelli's trait can be
1733 observed as a small groove on the mesiolingual aspect of the Pr that spills onto the worn
1734 occlusal surface. Occlusal and interproximal wear have obliterated the Fa and MMR.
1735 Distally, the Fp remains as a moderately-sized pit between the Hy and Me and bordered
1736 mesially by their distal margins and distally by a low rounded DMR. The Co is worn but
1737 thick and continuous; a continuous Co is confirmed with examination of the EDJ. A
1738 shallow buccal groove remains. The occlusal portion of a deep lingual groove can still be
1739 observed near the occlusal margin. This groove widens and becomes shallow as it reaches
1740 the cervix.

1741 Three roots are evident: a lingual root, a mesiobuccal root, and a distobuccal root.
1742 The roots are abraded, especially the mesial and distal aspects of the lingual root. The
1743 entire height (14.1 mm in lingual view) of the lingual root is preserved; however, the
1744 mesiobuccal root is broken off 8.8 mm from the cervix and the distobuccal root is broken
1745 off 4.1 mm from the cervix. A separate 8.4 mm fragment, catalogued as U.W. 101-1574
1746 (not illustrated in Figure 20), is broken at its apex but refits to the distobuccal root of
1747 U.W. 101-525. The lingual root is wider MD than BL, with shallow invaginations
1748 running along both the buccal and lingual faces. The root angles strongly to the lingual
1749 side. The buccal roots are close together and are wider BL in cross section. The mesial
1750 buccal root is broader than the distal near the cervix. Grooves run along the mesial and
1751 distal sides of the mesial buccal root. A slight groove sits on the mesial side of the distal
1752 buccal root as well.

1753 This specimen is a possible antimere of U.W. 101-1676. They are virtually
1754 identical in the occlusal wear pattern and in preserved morphology.
1755
1756 U.W. 101-583: RM¹ (Fig. 20C; Table 1) Enamel chips are missing along the buccal
1757 portion of the MMR and near the apex of the Me. There is a large ovoid mesial IPF (4.2
1758 mm BL by 3.2 mm OC), but no distal IPF. All four cusps are flattened by wear but no
1759 dentine is exposed (stage 2). The crown is rhomboidal in occlusal outline due to the
1760 relatively large, distolingually projecting Hy. The relative cusp sizes are $Pr > Hy > Me \geq$
1761 Pa. Part of the MMR has been removed by interproximal wear but what is preserved is
1762 thin and rounded. The Fa is a moderately-sized, buccolingually-, and slightly distally
1763 oriented groove bordered mesially by the MMR and distally by mesial extensions of the
1764 Pa and Pr. None of the cusps preserve accessory fissures or ridges. Though worn, the
1765 groove pattern suggests that the Co is continuous, which is confirmed by inspection of
1766 the EDJ. The buccal groove is very shallow and fades away mid-crown. The lingual
1767 groove is a deep fissure where it crosses the occlusal rim, then quickly becomes shallow
1768 and disappears at mid-crown. Carabelli's feature takes the form of a short obliquely
1769 oriented crest and associated pit restricted to the mesiolingual corner. The groove
1770 separating the Hy and Me opens into a small Fp that is formed by distal margins of the
1771 Me and Hy and a weak DMR. The distal face presents a v-shaped crest and groove just
1772 below the occlusal margin.

1773 There are three roots, a mesiobuccal, distobuccal, and vertically oriented lingual
1774 root. The root surfaces are cracked. The lingual root is broken just before its apex and
1775 measures 10.8 mm in height. The distobuccal root is broken at the cervix, while the

1776 mesiobuccal root is broken just before its apex. The distobuccal root is preserved as a
1777 separate fragment glued onto the fresh break (not apparent in the μ CT scans but visible in
1778 Figure 20C). The mesiobuccal root measures 9.6 mm in height and the distobuccal root
1779 9.4 mm. The lingual root has two distinct radicals and a complex cross-sectional shape.
1780 In apical view, it is L-shaped with a MD-oriented section along the lingual face and a
1781 LaL-oriented section along the distal face. The μ CT scans shows that the two portions
1782 share a single canal for most of their length. The lingual root tilts over the lingual margin
1783 of the crown and slightly distally as well. The mesiobuccal and distobuccal roots are
1784 compressed with their long axes BL. The distal root is broader BL than the mesial root.
1785 The buccal roots are more vertically oriented than the lingual root.

1786 This specimen is proposed as the antimere of U.W. 101-445. The teeth are similar
1787 morphologically and in their state of occlusal and interproximal wear. The U.W. 101-583
1788 specimen does feature grooving on the distal face of the crown and has a more well-
1789 defined Fa than U.W. 101-445.

1790

1791 U.W. 101-708: LM¹ (Fig. 20D; Table 1) The crown exhibits a large ovoid mesial IPF (4.2
1792 mm BL by 2.6 mm OC) and no distal IPF. Wear facets are present on all cusps; though,
1793 the occlusal topography is well preserved (stage 1). In occlusal outline, the crown is
1794 rhomboidal, with a strong distolingual projection of the Hy. The relative cusp sizes of the
1795 four cusps are Pr > Hy > Me \geq Pa. Any accessory ridges that were present have been
1796 obscured by wear, and the essential ridges are rounded and wide. Though worn, the Co
1797 appears to be continuous at the OES (a continuous Co is present at the EDJ). The faint
1798 groove-like Fa is barely preserved. The small Fp is bounded by a weak DMR. The buccal

1799 groove is shallow and becomes indistinct at mid-crown. The lingual groove is deep and
1800 forms a sharp cleft near the occlusal surface. This cleft becomes shallow about one-third
1801 the crown height and disappears at mid-crown. Carabelli's feature is expressed as a weak
1802 obliquely oriented crest confined to the mesiolingual corner of the Pr.

1803 There are three roots, a mesiobuccal, distobuccal, and lingual root. All roots have
1804 damaged apices that expose their canals. In cross section, the mesiobuccal root is an
1805 elongated figure-of-eight shape, with prominent grooves along its mesial and distal faces.
1806 It is BL broader than the distobuccal root. The mesiobuccal root tilts slightly distally and
1807 buccally. The distobuccal root is smaller in cross sectional area than the mesial, is more
1808 ovoid in cross section, and shows a stronger buccal tilt. The buccal roots are pressed
1809 together in buccal view. In cross section, the major axis of the labial root is MD and
1810 depressions run along the lingual and buccal faces, with the lingual face more deeply
1811 indented than the buccal. In buccal view, the mesial buccal root height is 10.2 mm, the
1812 distal buccal root is 9.3 mm, and in lingual view, the lingual root measures 11.2 mm in
1813 height.

1814 This specimen is a reasonable antimere of U.W. 101-999. The teeth are similar
1815 morphologically and in their state of occlusal and interproximal wear. An articulation
1816 mesially with U.W. 101-808 is reasonable.

1817

1818 U.W. 101-796: LM¹ (Fig. 20E; Table 1) Extensive wear and chipping have obliterated
1819 most of the crown. Enamel is preserved only on the buccal and distal aspects (stage 7–8).
1820 Both mesial and distal IPFs are present but not completely preserved, being reduced by
1821 occlusal wear. On the buccal aspect, about half the crown height is preserved. This

1822 contrasts with the extensive lingual wear, which has completely removed the enamel and
1823 some of the root and exposed a large portion of the pulp chamber. The worn lingual
1824 surface must extend beyond the original cervix of the crown. In mesial and distal views,
1825 the wear angle is steep. A trace of the weak buccal groove is observable.

1826 There are three roots: a mesiobuccal, distobuccal, and centrally placed lingual
1827 root. All roots are covered in a thick layer of cementum that has flaked off in places. Both
1828 buccal roots are missing their apices, though the root canals are not exposed. As
1829 measured from the buccal cervix, the mesiobuccal root is 10.1 mm tall and the
1830 distobuccal root is 10.0 mm tall. Each of the buccal roots is ovoid in cross section, with
1831 their major axes oriented BL. The major axis of the lingual root, in contrast, is oriented
1832 MD. The buccal roots project directly above the crown, while the lingual root splays
1833 lingually. The fully preserved lingual root measures 10.6 mm along its lingual face.

1834 The preserved distal IPF is a good match for the mesial IPF of U.W. 101-528
1835 (LM²), which is also heavily worn. U.W. 101-528 is arguably associated with U.W. 101-
1836 527 (LM³). The mesial IPF of this specimen is a good match for the preserved distal IPF
1837 of U.W. 101-1362 (LP⁴). If these proposed associations are correct, this would constitute
1838 a heavily worn set of maxillary postcanine teeth from a single individual. An association
1839 with the heavily worn teeth in the U.W. 101-361 mandible is also possible.

1840

1841 U.W. 101-999: RM¹ (Fig. 21A; Table 1 There is minor enamel chipping along the mesial
1842 margin. A large, ovoid mesial IPF (approximately 4.8 mm by 2.9 mm) is present. No
1843 distal IPF is visible. The lingual cusps are flattened by wear, but no dentine is exposed,
1844 and the occlusal topography is well preserved (stage 1). Four cusps are present and

1845 arranged in size as $Pr > Me \geq Hy > Pa$. The occlusal outline is rhomboidal due to the
1846 distolingual projection of the relatively large Hy. The Fa is restricted to the Pa and is
1847 continuous with the central groove. Wear has thinned the MMR so that, as preserved, it is
1848 low and narrow. The Fp is bounded mesially by Me and Hy occlusal ridges and distally
1849 by the DMR. The DMR is low, dipping well below the height of the Me and Hy occlusal
1850 ridges. The Co is continuous. The lingual groove forms a deep, narrow cleft near the
1851 occlusal margin, fades at mid-crown, and appears as a pit just above the cervix. The
1852 buccal groove is shallow, extending from the occlusal margin to the cervix. A small
1853 Carabelli's feature, restricted to the mesiolingual aspect of the Pr, is expressed as an
1854 oblique crest.

1855 All three roots are broken just prior to their apices and the root canals are
1856 exposed. The roots are abraded along their surfaces, especially the mesial and distal faces
1857 of the buccal roots and the lingual face of the lingual root. The lingual root is LaL
1858 compressed. It is an elongated figure-of-eight shaped in cross section as a result of buccal
1859 and lingual grooves running the length of the root. The lingual root deflects lingually and
1860 slightly distally. The two buccal roots are shorter than the lingual root and are more
1861 vertically oriented. The buccal roots are pressed together, but distinct, and run parallel to
1862 one another. Each buccal root is ovoid, being compressed MD. The mesiobuccal root is
1863 wider than the distobuccal root, has two distinct radicals, and is figure-of-eight in cross
1864 section. The narrower distobuccal root is ovoid in cross section. The lingual root is 11.2
1865 mm in height along the lingual aspect. The mesiobuccal root is 9.8 mm in height and the
1866 distobuccal root is 10.1 mm tall.

1867 This specimen is a possible antimere of U.W. 101-708. They are quite similar
1868 morphologically, in their wear status, in the size of their mesial IPFs, and lack of distal
1869 IPF.
1870
1871 U.W. 101-1305: LM¹ germ (Fig. 21B; Table 1) The nearly crown-complete germ shows
1872 no root development. The distal and mesiolingual cervical margins are slightly damaged.
1873 The crown outline is rhomboidal with a large distolingually projecting Hy. There are four
1874 cusps arranged in size as Pr > Me ≥ Pa > Hy. The Hy is tall and conical, with its apex
1875 subequal in height with those of the trigone. The essential ridges are well developed but
1876 not as well defined as the accessory ridges. The Pr and Pa have small, narrow mesial
1877 accessory ridges that meet, but do not join, at the central groove. These ridges form the
1878 distal border of a weak Fa. The Pr mesial accessory ridge presents as a small tubercle
1879 with a free apex (protoconule) and is adjacent to another small tubercle emanating from
1880 the MMR (mesial accessory tubercle). This ridge and tubercle pattern is unusual in the
1881 sample of maxillary molars. The Co is a continuous crest and composed of the distal
1882 accessory ridges of the Pr and Me. The wide Fp comprises a small pit and a BL-oriented
1883 groove mesial to the DMR. The DMR is low relative to the height of the Hy and Me and
1884 slopes cervically from its occlusal-most point adjacent to the Hy. The lingual groove is a
1885 deep, narrow cleft near the occlusal surface fading to a wider and shallower groove mid-
1886 crown and continuing to the cervix. The buccal groove is shallow throughout its course.
1887 Carabelli's feature is expressed as short horizontal shelf and associated pit restricted to
1888 the mesiolingual corner.

1889 This specimen is proposed as the antimere of U.W. 101-1688. The teeth are nearly
1890 identical in morphology and their developmental status. These teeth likely belong to the
1891 same individual as the U.W. 101-1400 mandible and its associated antimeres and other
1892 isolated maxillary teeth. More details on these associations are provided in the
1893 Discussion.

1894

1895 U.W. 101-1396: RM¹ (Fig. 21C; Table 1) Enamel chipping is evident along the mesial
1896 and distal margins occlusal to the IPFs. There is a large oblong mesial IPF (6.7 mm BL
1897 by 2.1 mm OC) and a large bean shaped distal IPF (7.1 mm BL by 3.9 mm OC). Most of
1898 the surface morphology has been removed by wear. Two coalesced dentine pools connect
1899 over the Pr and Pa, while smaller dentine patches are evident over the Hy and Me (stage
1900 5). The occlusal outline is a rounded, slightly tapered square that is slightly broader
1901 mesially than distally. The lingual groove is well preserved, especially its narrow and
1902 deep lingual and distal segments; it terminates distally in a moderate Fp. On the lingual
1903 aspect, it becomes shallow at mid-crown and continues to the cervix. The worn Co
1904 appears to be continuous; an examination of the μ CT scans shows that the Co is
1905 continuous at the EDJ. A shallow buccal groove is visible as an indentation at the
1906 occlusal surface.

1907 The three roots are missing their apices and are heavily abraded. The distobuccal
1908 root is broken near the crown cervix and refit to the crown. A notch of dentine is missing
1909 from the buccal side of the mesiobuccal root at about half its height. The buccal roots are
1910 ovoid in cross section, extend vertically from the crown, run parallel to each other, and
1911 are completely separated from one another. The mesiobuccal root is BL broader than the

1912 distobuccal root. The lingual root has two radicals separated by a shallow groove, which
1913 results in a slight figure-of-eight shape in cross section. It is BL compressed and tilts
1914 lingually. The maximum height of the mesiobuccal root is 9.8 mm buccally, and the
1915 maximum height of the distobuccal root is 9.4 mm along the buccal aspect. The
1916 maximum height of the lingual root is 11.1 mm on its lingual aspect.

1917 This specimen articulates mesially with U.W. 101-1401.

1918

1919 U.W. 101-1463: RM¹ (Fig. 21D; Table 1) Enamel chips are present along the mesial and
1920 distal margins. There is a large mesial IPF (5.4 mm BL by 2.0 mm OC) and a more
1921 circular distal IPF (4.8 mm BL by 3.5 mm OC). The crown is moderately worn, with
1922 small dentine patches exposed over the Pa and Hy and a larger dentine pool exposed over
1923 the Pr that extends mesially (stage 3). The crown has a rhomboidal occlusal outline due to
1924 a large, distolingually-projecting Hy. The relative cusp areas are $Pr > Hy > Pa \geq Me$.
1925 Occlusal wear has obscured details of the mesial crown; only two small fissures,
1926 presumed to be associated with the Fa, remain. The deeper Fp is preserved as a small pit.
1927 A Co is present. Remnants of the lingual and buccal grooves are preserved at the occlusal
1928 edge, and both become shallow depressions on their respective faces. A Carabelli's
1929 feature is absent.

1930 Two buccal roots and one lingual root are present, and a portion of the alveolar
1931 bone remains wedged between them. The buccal roots are both oval in cross section,
1932 being MD compressed. The mesial root is broader BL than the distal root. The buccal
1933 roots run parallel to each other and are pressed together, so that only a narrow, deep cleft
1934 separates them. Both roots are abraded and missing their apices. The maximum height of

1935 the mesiobuccal root is 12.2 mm. The distobuccal root is also broken near its apex,
1936 exposing the canal. The break angles distally so that the maximum height of the
1937 distobuccal root preserved along its mesial margin is 10.2 mm. The lingual root is broken
1938 near its apex, exposing the canal. It is also oval in cross section; however, it is
1939 compressed MD, with grooves along both the lingual and buccal faces, which gives it a
1940 shallow figure-of-eight shape in cross section. The lingual root is much broader distally
1941 than lingually. The lingual root has a strong lingual inclination and is broken near its
1942 apex, exposing the canal. In lingual view, the preserved maximum height of the root is
1943 12.4 mm.

1944 This specimen is the probable antimere of the U.W. 101-1277 LM¹. Their patterns
1945 and wear status, and even the pattern of enamel chips, are very similar. However, the
1946 determination is complicated by the lack of detailed occlusal morphology preserved on
1947 either specimen.

1948

1949 U.W. 101-1676: LM¹ (Fig. 21E; Table 1) Enamel chipping is visible along the mesial and
1950 distal margins. There are large mesial (5.5 mm BL by 2.2 mm OC) and distal (5.4 mm
1951 BL by 3.5 mm OC) IPFs. Dentine patches are exposed on all four cusps. The largest is a
1952 pool over the Pr that extends mesially (stage 3–4). The crown is rhomboidal in occlusal
1953 outline, with a large, distolingually projecting Hy. Most of the occlusal morphology has
1954 been removed by wear but remnants of the occlusal grooves remain between the Pa and
1955 Pr and between the Hy and Me. The Co, though worn, appears continuous. A remnant of
1956 Carabelli's trait can be observed as a small groove on the mesiolingual aspect of the Pr
1957 that spills onto the worn occlusal surface. Occlusal and interproximal wear have

1958 obliterated the Fa and MMR. Distally, a small remnant of the Fp remains. The preserved
1959 morphology does not suggest that accessory cusps were present. The buccal groove is
1960 shallow and the lingual groove is not well preserved.

1961 The roots are broken away and sediment adheres to the surface of the pulp cavity.
1962 In buccal view, a maximum of 2.5 mm of root are preserved below the cervix. A trace of
1963 the cleft between the mesial and distal buccal roots is visible.

1964 This specimen is proposed as the antimere of U.W. 101-525. It may articulate
1965 mesially with the U.W. 101-277 LP⁴. This proposition is reasonable because their
1966 reciprocal IPFs are a good match, and they have similar patterns of enamel chipping in
1967 the adjoining regions. It may also articulate distally with U.W. 101-1522. Their
1968 respective IPFs fit well, and their wear statuses are similar.

1969

1970 U.W. 101-1688: RM¹ germ (Fig. 21F; Table 1) This is the nearly crown-complete germ
1971 of the RM¹ with no root development. There is minor damage to the cervix distobuccally.
1972 The four primary cusps are present, and the crown is rhomboidal in outline due to the
1973 distolingually projecting Hy. The relative cusp sizes are Pr > Me ≥ Pa > Hy. The essential
1974 ridges of the Pa and Me are developed but those of the Pr and Hy are not well defined.
1975 The Pr has a weak mesial accessory ridge, and the Pa has a stronger one. They meet at the
1976 central groove but do not form an epicrista. The Me essential ridge becomes a wide
1977 triangle towards the occlusal basin. The Fa is weakly defined by the Pr and Pa mesial
1978 accessory ridges and continuous with the central groove. The DMR is low and forms the
1979 distal border of a small Fp. The lingual groove forms a narrow and deep cleft near the
1980 occlusal surface that becomes a shallow groove mid-crown as it continues to the cervix.

1981 The buccal groove is barely perceptible. Carabelli's feature takes the form of a faint,
1982 obliquely oriented ridge and associated pit that is restricted to the mesiolingual corner.

1983 This is the antimere of U.W. 101-1305. They are nearly identical in morphology
1984 and their state of development. As a result, this tooth is part of the set of teeth assigned to
1985 the subadult specimen that includes the U.W. 101-1400 mandible.

1986

1987 *3.16. Permanent maxillary second molars*

1988 Ten isolated M²s and one present in the U.W. 101-1277 maxilla, representing at
1989 least seven individuals, are known from the Dinaledi Chamber deposits. The M² sample
1990 includes an antimeric pair, U.W. 101-1063 and U.W. 101-1135, which were nearing
1991 crown completion, as well as other crowns with a range of wear stages. The sample
1992 includes a pair of heavily worn antimeres, U.W. 101-005 and U.W. 101-528, in which the
1993 steep bucco-lingual wear gradient had worn the crown to the level of the pulp chamber.

1994 The specimens are all similar in morphology and size. Where detail can be assessed, all
1995 M²s have four principal cusps and, except for U.W. 101-867, no supernumerary cusps.

1996 The Hy is relatively large and projects distolingually, giving the crown a rhomboidal
1997 occlusal outline. Carabelli's feature is either absent or weak in expression. In contrast to
1998 the M¹, except in U.W. 101-1006, the Co is not continuous. Buccal grooving is shallow;
1999 the lingual groove is narrow at the occlusal margin and widens as it reaches cervically.

2000

2001 U.W. 101-005: RM² (Fig. 22A; Table 1) The entire circumference of the tooth has
2002 undergone modification through chipping, which is especially extensive along the lingual
2003 and mesial occlusal margins. Other occlusal chips are present mesiobuccally and

2004 distobuccally. A portion of the mesial IPF remains, especially buccally, and it extends
2005 obliquely along the occlusal wear plane. Here, its maximum preserved dimension parallel
2006 to the occlusal surface is 4.2 mm and its maximum OC dimension is 1.5 mm. Occlusal
2007 wear obliterated the mesial IPF along its lingual extent. A large distal IPF (5.8 mm
2008 maximum BL breadth) is visible; though, occlusal wear and enamel chipping have
2009 reduced its lingual extent. The crown is severely worn and a large dentine pool spreads
2010 across all but a small portion of enamel between the Pa and Me and an enamel rim (<1.0
2011 mm on the lingual aspect) surrounding the crown (stage 6). The worn surface shows a
2012 strong BL slope, with approximately half of the crown's height remaining buccally and
2013 very little of its height remaining lingually.

2014 Three roots are present. Both buccal roots are broken and about two-thirds of their
2015 maximum height is preserved, while the lingual root is complete. The maximum
2016 preserved height of the mesiobuccal root is approximately 7.0 mm and the maximum
2017 preserved height of the distobuccal root is 8.2 mm. The height of the lingual root is 10.7
2018 mm. The external root surfaces are covered in cementum and evince some abrasion. In
2019 cross section, the buccal roots each have their major axis BL and minor axis MD. In
2020 contrast, the major axis of the lingual root is MD and the minor axis BL. The lingual root
2021 is invaginated along both buccal and lingual faces. The buccal roots extend vertically
2022 above the crown, while the lingual root is more strongly splayed.

2023 This tooth was recovered within centimeters of U.W. 101-006 (RM₃), another
2024 heavily worn molar. However, as U.W. 101-005 and -006 are from different arches,
2025 attribution to a single individual cannot be confirmed. The U.W. 101-528 LM² is a

2026 candidate antimere but this proposal is difficult to evaluate since both express advanced
2027 occlusal wear that has removed most morphological detail.
2028
2029 U.W. 101-505: LM² germ (Fig. 22B; Table 1) This is a nearly crown-complete germ
2030 (stage 1). The occlusal outline is rhomboidal, with a relatively large, distolingually
2031 projecting, Hy. There are four principal cusps arranged in size as Pr > Hy > Me ≥ Pa. The
2032 essential lobes lack distinct occlusal ridges and the occlusal surface lacks complexity.
2033 There are small pits on the apices of all four cusps and a small groove and ridge complex
2034 on the Pr near the central fovea; otherwise, there are no accessory features. The MMR is
2035 indistinct and lacks accessory tubercles. The groove-like, shallow Fa is confined to the Pa
2036 and defined distally by a weak Pa mesial accessory ridge. The Fp is a pit at the distal
2037 termination of the central groove. The essential ridges of the Pr and Me are separated by
2038 a deep groove and no Co is present. Carabelli's feature is absent. A deep lingual groove
2039 separates the Pr and Hy. It is a narrow cleft near the occlusal surface but becomes
2040 imperceptible near mid-crown. The buccal groove is a shallow v-shaped fossa near the
2041 occlusal edge, becoming a shallow groove that travels towards the cervix. Just before
2042 reaching the cervix, it becomes a short deep invagination.

2043 Given the ontogenetic status of this specimen, there was likely little-to-no root
2044 development on this crown. The surface of the pulp chamber is exposed and stained by
2045 sediment.

2046 Based upon morphological similarity and lack of occlusal wear, this specimen is
2047 proposed as the antimere of U.W. 101-593. The right M² of the pair does evince minimal
2048 root development.

2049

2050 U.W. 101-528: LM² (Fig. 22C; Table 1) The enamel rim is missing in an arc that extends
2051 from the distolingual corner, along the lingual side, around the mesiolingual corner, and
2052 to a point about halfway along the mesial edge of the tooth. When originally observed in
2053 2014, enamel extended to the middle of the lingual face, nearly to the groove between the
2054 Hy and Pa; the distolingual rim is missing as of 2015. Enamel chipping is present
2055 distally, especially along the lingual half, just above the IPF. Distally, a large centrally
2056 placed IPF (6.9 mm BL by 2.8 mm OC) is present. Mesially, the IPF (5.0 mm BL by 2.2
2057 mm OC) is evident where enamel is preserved. The crown is heavily worn, with a large
2058 dentine pool covering the lingual surface (stage 5). The wear surface is not planar, with
2059 the lingual moiety scooped out and the wear plane reaching its deepest point mesially.

2060 Three roots are present. The lingual root is damaged near its apex, especially
2061 along its mesial edge. Significant abrasion to the cementum covering the root is also
2062 evident lingually, especially concentrated near the cervix and extending to about half the
2063 root's length distally and lingually and across the entire mesial surface of the root. The
2064 cementum of the mesiobuccal root is abraded along its mesial and labial surfaces and the
2065 apex is broken away. The distobuccal root is also abraded along its distal surface and the
2066 apex damaged. Further, the apex of the distobuccal root is broken. The buccal roots
2067 extend directly above the crown, while the lingual root tilts over the crown. The
2068 mesiobuccal root is considerably broader than the distobuccal root; further, the
2069 mesiobuccal root is ovoid, while the distobuccal root is more circular in cross section.
2070 The lingual root is considerably larger in cross section than the buccal roots. A shallow
2071 groove runs along the lingual side and a deeper groove runs along the buccal side of the

2072 lingual root. The height of the mesiobuccal root, as measured from the buccal cervix, is
2073 10.3 mm; the distobuccal root is 9.3 mm in height from the buccal cervix; and the lingual
2074 root is 11.8 mm in height from the lingual cervix.

2075 The distal IPF is a good fit for the mesial facet of the U.W. 101-527 LM³. The
2076 mesial IPF is a reasonable match for the distal facet of the heavily worn U.W. 101-796
2077 LM¹, which is in turn argued to be associated with U.W. 101-1362 (LP⁴). Above, it was
2078 suggested that U.W. 101-527 may occlude with the M₃ in the U.W. 101-361 mandible.
2079 Thus, this specimen may occlude with the U.W. 101-361 as well. The U.W. 101-005
2080 RM² is a candidate antimere but this proposal is difficult to evaluate since both express
2081 advanced occlusal wear that has removed most morphological detail.

2082

2083 U.W. 101-593: RM² (Fig. 22D; Table 1) The crown is unworn (stage 1) and lacks IPFs.
2084 The relative sizes of the four primary cusps are Pr > Hy > Me ≥ Pa. The distal lobe of the
2085 Hy is hypertrophied and it is bordered by shallow depressions on either side, but this is
2086 not a true C5 and no distinct dentine horn is present at the EDJ. In occlusal outline, the
2087 crown is roughly rhomboidal due to the mesiobuccal projection of the Pa and the slight
2088 distolingual projection of the Hy. The swollen Hy distal accessory ridge gives a rounded
2089 outline to the distal border. However, the Hy is less projecting than in some other *H.*
2090 *naledi* maxillary molars since the distal lobe fills in the crown outline distally. The
2091 essential ridges are not well defined, except on the Me and Pa, where they are associated
2092 with accessory fissures. There is no continuous Co. There is a small, possibly
2093 hypoplastic, pit on the apex of the Me, and the Pr exhibits an unusual a small groove and
2094 ridge at its base. A mesial accessory ridge on the Pa defines the distal border of the Fa,

2095 which is a short mesiobuccal extension of the central groove. A thin MMR bounds the Fa
2096 mesially and is continuous from the mesial crests of the Pa and Pr. No Carabelli's feature
2097 is evident. The lingual groove is narrow and deep near the occlusal margin but fades
2098 away near mid-crown and reappears as a pit near the cervix. The buccal groove is very
2099 shallow throughout ending in a pit near the cervix.

2100 Though the roots were developing at death, very little of them remains and
2101 sediment fills the exposed pulp chamber.

2102 This tooth is the likely antimere of U.W. 101-505. They are nearly identical in
2103 morphology and developmental state.

2104

2105 U.W. 101-867: RM² (Fig. 22E; Table 1) A broad mesial IPF (approximately 6.0 mm BL
2106 by 3.4 mm OC) is centered near the occlusal margin, while the distal IPF is smaller
2107 (approximately 2.6 mm BL by 2.7 mm OC), offset lingually, and located at about half the
2108 crown height. Distinct wear facets are visible on the occlusal surface, but no dentine is
2109 exposed (stage 1). The occlusal outline is slightly rhomboidal due to the minor projection
2110 of the Hy distolingually and the stronger projection of the Pa mesiobuccally. Distally, the
2111 crown is worn, but the pattern of grooving suggests the presence of a small C5 or ridge
2112 extending from the DMR. In size, the cusps are approximately Pr > Hy > Pa ≥ Me. The
2113 region of the Fa and MMR is worn, but a remnant of the Fa is preserved as a slight
2114 groove mesial to the Pa. The Fp is preserved as pit adjacent to the C5. Though worn, the
2115 Co is not continuous on the outer enamel surface; this is confirmed at the enamel dentine
2116 junction as well. The buccal groove is quite shallow as it crosses the crown face; the
2117 lingual groove is a deep and narrow cleft in the occlusal half and then widens just below

2118 mid-crown to continue as a shallow indentation. The Carabelli's feature is expressed as a
2119 small crest and associated groove mesiolingually.

2120 A portion of alveolar bone remains wedged between the roots. The distobuccal
2121 (14.2 mm) and lingual (14.9 mm) roots are nearly complete; however, the mesiobuccal
2122 root (10.8 mm) is broken at about two-thirds its height. The buccal roots are pressed
2123 together and their mass tilts distally. The distobuccal root also leans over the crown face.
2124 In cross section, the buccal roots are both longer BL than they are MD, with the mesial
2125 root larger than the distal root in cross sectional area. The major axis of the lingual root is
2126 perpendicular to the buccal roots. There is a distinct invagination along its buccal face
2127 and a shallower depression along its lingual face, which gives it a shallow c-shape in
2128 cross section. The lingual root leans over the lingual face with a slight distal tilt,
2129 especially apically.

2130

2131 U.W. 101-1006: RM² (Fig. 23A; Table 1) The crown is unworn and lacks IPFs (stage 1).
2132 The crown has a slight distal taper, and the occlusal outline is rhomboidal due to the
2133 distolingual projection of the Hy. There are four principal cusps and a small distal cusp 5
2134 defined by weak grooves. In size, the relative cusp sizes are $Pr > Pa > Hy \geq Me$. The
2135 essential lobes of the main cusps are well broad but, apart from the Pa, not defined by
2136 distinct ridges. The Pa essential ridge is mesially offset and bifurcates near the apex into
2137 two thick ridges. The mesial-most ridge forms the distal border of the Fa. In addition,
2138 there are two faint distal accessory ridges on the Pa originating from the distal occlusal
2139 crest. The distal lobe of the Pr forms a crest that is constricted in the middle and then
2140 takes a mesial turn to merge with the mesial lobe of the Me to become the Co. The Me

2141 essential ridge defects distally and meets the Hy essential ridge. There are small
2142 hypoplastic pits at the tips of the Hy and Me. The Fa is restricted to the Pa and is
2143 continuous with the central fovea. The MMR is lower than the essential Pr and Pa ridges
2144 and rounded. It slopes to its most cervical point mesial to the Pa. The DMR is low and
2145 rounded and includes a small cusp rising from it. A small bifurcation of the Fp extends
2146 buccally up the Me. The lingual groove is deep and narrow. It forms a cleft near the
2147 occlusal margin, disappears about mid-crown and then reappears as a pit just above the
2148 cervix. The buccal groove is broad and shallow. Mesiolingually, there is a very small pit-
2149 like Carabelli's feature associated with a small, nearly vertically oriented, mesial crest.
2150 The roots have broken away from the crown. Given the lack of occlusal wear and IPFs,
2151 the roots were incompletely developed at death.

2152 This is a possible antimere of U.W. 101-1015. The two teeth are similar in
2153 morphology, wear status, absence of IPFs, and in size. Of note, U.W. 101-1015 does
2154 preserve a small portion of its roots. The two teeth differ in the morphology of the
2155 Carabelli's feature, which is absent on U.W. 101-1015 but present on U.W. 101-1006.
2156 They also differ in the morphology of the Co, which is discontinuous in U.W. 101-1015
2157 but continuous in U.W. 101-1006, and in the morphology of the DMR, where a distinct
2158 cusp sits near the Me on U.W. 101-1006 but is absent on U.W. 101-1015.

2159

2160 U.W. 101-1015: LM² (Fig. 23B; Table 1) The crown is unworn (stage 1). The relative
2161 cusp sizes are Pr > Pa > Hy ≥ Me. The crown tapers distally and is rhomboidal in outline
2162 due to the distolingual projection of the Hy. The essential lobes of the four primary cusps
2163 are well developed but lack strong ridges. The Pa mesial accessory crest is hypertrophied

2164 and forms the distal border of the Fa. The Pr has a distal accessory ridge that deflects
2165 mesially and terminates at the occlusal basin. There is no Co. The Fa is restricted to the
2166 Pa and is continuous with the central fovea. The rounded MMR is lower than the
2167 essential ridges of the Pr and Pa. The DMR is a low and rounded ridge bounding the pit-
2168 like Fp. The lingual groove is deep and narrow and forms a cleft near the occlusal
2169 margin, disappears about mid-crown, and then appears as a pit just above the cervix. The
2170 buccal groove is broad and shallow throughout its course. There is no Carabelli's feature
2171 visible.

2172 Most of the roots are broken away from the crown. About 2.5 mm of root remains
2173 lingually adjacent to the Pr, a maximum of 3.2 mm remains mesially in an irregularly
2174 broken surface, and 3.0 mm remains buccally adjacent to the Pa. Given the absence of
2175 occlusal wear and IPFs, the roots were likely incomplete at death.

2176 This specimen is a possible antimere of U.W. 101-1006. The two teeth differ in
2177 the morphology of the Carabelli's feature, which is absent on U.W. 101-1015 but present
2178 on U.W. 101-1006, in the morphology of the Co, which is discontinuous in U.W. 101-
2179 1015 but continuous in U.W. 101-1006, and in the morphology of the DMR, where a
2180 distinct swelling near the Me of U.W. 101-1006 is absent on U.W. 101-1015.

2181

2182 U.W. 101-1063: LM²? (Fig. 23C; Table 1) This is a developing tooth germ. The poorly
2183 mineralized enamel is covered with cracks. Especially deep cracks extend longitudinally
2184 around the margins of the tooth and the delicate cervix is broken in many places,
2185 especially mesiobuccally and mesiolingually. This fragile specimen was complete when

2186 it was first examined in 2014, scanned in 2015, and photographed in 2016. The specimen
2187 was broken some time in 2016 and is now repaired.

2188 Only the four primary cusps are present. The crown tapers somewhat distally and
2189 is rhomboidal in outline due to the projecting Hy. The Fa is expressed as a BL-elongated
2190 fissure that bordered distally by a weak epicrista connecting the mesial accessory crests
2191 of the Pr and Pa. The shallow Fp is bordered mesially by the essential ridges of the Me
2192 and Hy. The distal lobe of the Pr is hypertrophied, widening towards, and then
2193 terminating at, the central groove. As in other *H. naledi* M²s, but not M¹s, The Co is
2194 absent, which is confirmed by the examination of the EDJ morphology. The lingual
2195 groove is a narrow cleft, and the buccal groove is shallow. Crown damage precludes
2196 assessing Carabelli's trait expression.

2197 This specimen is the proposed antimere of U.W. 101-1135. They are identical in
2198 developmental status and similar in morphology. It is also likely associated with U.W.
2199 101-1002 based upon the similar degree of crown completeness.

2200

2201 U.W. 101-1135: RM²? (Fig. 23D; Table 1) This is a developing tooth germ. The poorly
2202 mineralized enamel is covered with cracks. A large flake of enamel on the mesiolingual
2203 corner has been refit to the crown. There are four primary cusps and a small distal
2204 accessory cusp (C5) arising from the DMR. The accessory cusp is associated with a small
2205 dentine horn at the EDJ. The crown tapers somewhat distally and is rhomboidal in outline
2206 due to the slight projection of the Hy. The MMR slopes to its most cervical extent
2207 adjacent to the Pa. The Fa is expressed as a BL-elongated fissure bordered distally by a
2208 weak epicrista connecting the mesial accessory crests of the Pr and Pa. The shallow Fp is

2209 bordered mesially by the essential ridges of the Me and Hy. The distal lobe of the Pr is
2210 hypertrophied, widening towards, and then terminating at, the central groove. As in other
2211 *H. naledi* M²s, but not M¹s, a Co is absent. The lingual groove is a narrow cleft, and the
2212 buccal groove is shallow. Crown damage precludes assessing Carabelli's trait expression.

2213 Based upon similarities in morphology and developmental status, this is the
2214 antimere of U.W. 101-1063. These antimeres are probably associated with the U.W. 101-
2215 1002 RM₂, which is at a similar state of crown development and mineralization.

2216

2217 U.W. 101-1522: LM² (Fig. 23E; Table 1) There is a large mesial IPF (4.9 mm BL by 3.5
2218 mm OC) and a smaller distal IPF (2.1 mm BL by 1.9 mm OC). Minor enamel chipping is
2219 present on the Me. Occlusal wear facets are present, but no dentine is exposed (stage 2).

2220 The occlusal outline is slightly rhomboidal. The relative cusp sizes of the four primary
2221 cusps are Pr > Me ≥ Pa ≥ Hy. The essential lobes are well developed but not associated

2222 with distinct crests. The MMR is only partially preserved. It forms the mesial border of a
2223 small Fa that is restricted to the Pa and is continuous with the central fovea. In mesial

2224 view, the MMR slopes from the Pr to reach its most cervical point mesial to the Pa. A

2225 small Fp is bordered mesially by Me and Hy occlusal crests. The Me has a doubled apex
2226 with a shallow groove separating each apex and continuing onto the buccal face. A Co is

2227 absent. There is a faint indentation associated with Carabelli's feature restricted to the

2228 mesiolingual aspect of the Pr. A shallow buccal groove terminates at the cervix. The

2229 lingual groove is a deep and narrow cleft near the occlusal margin that fades

2230 approximately mid-crown and then reappears as a pit above the cervix.

2231 A portion of alveolar bone remains between the mesial and distal buccal roots.
2232 The lingual root is broken at the apex, exposing the root canal, while the buccal roots are
2233 completely preserved. The buccal roots are MD compressed and ovoid in cross section.
2234 In buccal view, these roots are pressed together and tilt distally. The mesiobuccal root has
2235 a stronger apical distal tilt than the distobuccal root. In distal view, the buccal and lingual
2236 roots splay out from one another. The mesiobuccal root is 15.5 mm in height and the
2237 distobuccal root is 14.6 mm in height. The lingual root is invaginated buccally, giving it a
2238 c-shape cross section. The lingual root also apparently tilts distally, but its apex is broken.
2239 The maximum height of the lingual root is 12.1 mm.

2240 The distal IPF is very similar in size and shape to the mesial IPF of the U.W. 101-
2241 418C M³. Further, an articulation mesially with the U.W. 101-1676 M¹ is also reasonable
2242 based upon the morphology of their respective IPFs.

2243

2244 *3.17. Permanent maxillary third molars*

2245 Six isolated M³s represent at least four adults in the Dinaledi Chamber deposits.
2246 They present a consistent morphological pattern. While all M³s are squarer than the M¹s
2247 and M²s, the Hy still projects more distally than does the Me except in the specimens
2248 with the most pronounced C5s (i.e., U.W. 101-418C and U.W. 101-594). A
2249 supernumerary C5 is present on all specimens. In contrast to M¹s, no Co is present.
2250 Carabelli's feature is either weak or absent. Where preserved, the M³s all present a
2251 distinctive root morphology in comparison to the M¹s and M²s in the assemblage. The M³s
2252 possess three roots, of which the lingual root is the largest. The two buccal roots differ in
2253 size and orientation, with the larger and flatter mesial buccal root being vertically

2254 oriented and the much small and more circular distal buccal root having a strong buccal
2255 and distal cant.
2256
2257 U.W. 101-418C: LM³ (Fig. 24A; Table 1) A semicircular mesial IPF (3.3 mm BL by 2.8
2258 mm OC) is evident and offset lingual to the midpoint of the crown. No distal IPF is
2259 detectable. The cusp apices are unworn but there are small facets on the Pr essential
2260 ridge, Pa mesial accessory ridge, and Me essential ridge (stage 1). The crown outline is
2261 square with more or less parallel sides and slightly convex mesial and distal margins.
2262 There are five cusps evident, including a centrally placed C5. The relative cusp sizes are
2263 Pr > Pa > Me > Hy > C5 and the cusps are widely spaced. The flat MMR, a small Hy,
2264 and prominent C5 square off the crown to yield a roughly rectangular outline with a
2265 slight distolingual projection of the Hy and C5. The Hy and C5 are similar in size: both
2266 are remarkable in that they project to nearly the same height as the other cusps. The Fa is
2267 a centrally placed pit with buccal and lingual extensions. It is bordered distally by mesial
2268 accessory ridges of the Pr and Pa, which merge to form a mesial trigone crest. The MIg
2269 shallowly bisects this crest. The MMR forms a mesially extended shelf that features a
2270 small mesial accessory tubercle (sensu Scott and Irish, 2017). The essential ridge and
2271 distal accessory ridge of the Pr are well developed (the distal ridge more so than the
2272 essential ridge). The distal accessory ridge angles mesially as it reaches the MIg and
2273 meets the essential ridge. In contrast, the Pa lacks essential and distal accessory ridges.
2274 The Me essential lobe is well developed. It is separated from a short but distinct distal
2275 accessory ridge by a deep groove. This ridge merges with the C5 near the central fovea.
2276 There is a short Fp between the Hy and C5. The Me and Pr are separated by a deep

2277 groove; thus, no Co is present. The Carabelli's feature is evident as a very small pit and
2278 associated vertical groove. The lingual groove separating the Pr and Hy is deep and
2279 narrow, forming a cleft near the occlusal margin and then becoming a faint groove
2280 roughly one-third of the crown's height and disappearing as it reaches the cervix. The
2281 buccal groove is a shallow depression originating at the occlusal rim that becomes a short
2282 deep invagination near the cervix. The roots are broken off at the cervix and some
2283 sediment staining is evident in the pulp chamber.

2284 This specimen is the proposed antimere of U.W. 101-594. The crowns are not,
2285 however, identical in morphology, with the C5 relatively larger on U.W. 101-418C.
2286 Moreover, U.W. 101-418C may articulate with U.W. 101-1522, as they both have
2287 similarly shaped and small interproximal facets. The U.W. 101-1522 M² may articulate
2288 mesially with U.W. 101-1676, completing the set of left molars.

2289

2290 U.W. 101-527: LM³ (Fig. 24B; Table 1) Several enamel chips are missing from the
2291 mesiolingual and mesiobuccal corners, and around the buccal margin. A large mesial IPF
2292 (5.0 mm BL by 3.2 mm OC) is partially preserved on the Pa; the lingual extent is
2293 removed by occlusal wear. There is no distal IPF. Extensive wear has removed all
2294 occlusal features except for a portion of the groove between the Hy and Me, which
2295 indicates that a Co was not present. A large pool of dentine is exposed over the Pr (stage
2296 3). There is a strong mesiobuccal wear gradient, with the Pa representing the current
2297 topographical high point. The crown outline is trapezoidal, being BL broadest across the
2298 mesial cusps and tapering distally. The Hy is large and projects farther distally than does
2299 the Me. The lingual and buccal grooves are both indistinct.

2300 There are two buccal roots, one mesial and one distal, and a centrally placed
2301 lingual root. The lingual root is broken near its apex and its surface is abraded, especially
2302 mesially and to a lesser extent along the distal face. The preserved height of the lingual
2303 root is 10.9 mm. Both buccal roots are missing portions of their apices; though, the root
2304 canals are not exposed. The preserved height of the mesiobuccal root is 10.1 mm and the
2305 distobuccal is 7.7 mm. The major axis of the lingual root cross section is MD elongated
2306 with a shallow groove on its lingual side. The lingual root angles out over the crown face.
2307 The mesial buccal root is vertically oriented, and the distal buccal root has a stronger
2308 buccal and distal cant. The mesial buccal root is ovoid in cross section, while the distal
2309 buccal root is much smaller and more circular in cross section. Both buccal roots have
2310 their long axes BL. The strong asymmetry in size, shape, and orientation of the buccal
2311 roots is seen in other *H. naledi* M³s (i.e., U.W. 101-594, U.W. 101-1398A, U.W. 101-
2312 1471, and U.W. 102-001).

2313 The mesial IPF of this specimen articulates well with the distal facet of U.W. 101-
2314 528 (LM²), which is in turn arguably associated with U.W. 101-796 (LM¹) and U.W.
2315 101-1362 (LP⁴). If these proposed associations are correct, this would constitute a heavily
2316 worn set of maxillary postcanine teeth from a single individual. Further, occlusion of this
2317 tooth with the in situ M₃ in the U.W. 101-361 mandible is reasonable. This specimen and
2318 the U.W. 101-361 M₃ also show occlusal chipping in their corresponding regions.

2319

2320 U.W. 101-594: RM³ (Fig. 24C; Table 1) A large ovoid mesial IPF (5.2 mm BL by 5.3
2321 mm OC) is centered on the mesial face. There is no distal IPF. Small wear facets are
2322 present on all cusps but no dentine is exposed (stage 1). The crown is square in occlusal

2323 outline, owing to a large Me, a moderately sized, non-projecting Hy and a distinct C5.
2324 The relative cusp sizes are Pr > Pa > Me > Hy > C5. The essential ridges of the Pr and Hy
2325 are not well defined, whereas those on the Pa and Me are delineated on either side by
2326 distinct grooves. Accessory ridges are present on all four cusps. The Pa has well-
2327 developed mesial and distal accessory ridges; The Pr has a hypertrophied distal accessory
2328 ridge. The distal lobes of the Me and Hy are strong and that of the Hy forms a medium-
2329 sized C5. There is no Co. The Fa is BL-oriented groove that is expressed predominantly
2330 on the Pa and to a lesser extent on the Pr. The MMR is lower than the accessory ridges of
2331 the Pa and Pr and gently slopes from the Pr to reach its lowest point mesial to the Pa. The
2332 Carabelli's feature is a very small pit and vertically oriented furrow. The lingual groove
2333 is narrow and deep and fades at mid-crown where it intersects a weak horizontal shelf
2334 extending onto the Hy. The buccal groove is shallow throughout its course until it
2335 becomes a deep short fissure near the cervix.

2336 Portions of three roots are preserved: a lingual root, a distobuccal root, and a
2337 mesiobuccal root. A small bit of alveolar bone remains wedged between them. The
2338 lingual root is abraded mesially, buccally, and distally. The mesiobuccal root is also
2339 abraded mesially. The lingual and distobuccal roots are broken at half or more of their
2340 lengths, and the mesiobuccal root is broken at about a third of its length. All breaks
2341 expose the root canals, which are packed with sediment. In lingual view, the lingual root
2342 is 9.0 mm in height and, in buccal view, the mesiobuccal root is 8.8 mm in height along
2343 its distal margin and the distobuccal root is 9.0 mm in height. In cross section, the major
2344 axis of the lingual root is MD, and a prominent groove runs along its buccal face. As
2345 preserved, the lingual root begins to tilt distally and lingually just before the break. The

2346 distal tilt is especially evident when tracing the contour of the mesial edge of the root.
2347 The mesiobuccal root is very narrow MD and much broader BL. The distobuccal root is
2348 more circular in cross section than the mesiobuccal root. Both buccal roots tilt distally,
2349 with the distobuccal root more strongly inclined. The distobuccal root also angles
2350 strongly buccally. The asymmetry in the size, cross-sectional shape, and tilt seen in the
2351 buccal roots is consistent with the morphology of other *H. naledi* M³s (i.e., U.W. 101-
2352 527, U.W. 101-1398A, U.W. 101-1471, and U.W. 102-1) that preserve their roots.

2353 This is the proposed antimere of U.W. 101-418C. They are nearly identical in
2354 occlusal morphology, in the state of occlusal wear, and the development of the mesial
2355 IPFs.

2356

2357 U.W. 101-1269: LM³ (Fig. 24D; Table 1) An oval mesial IPF (4.7 mm BL by 2.4 mm
2358 OC) is present. No distal IPF is present. Each cusp is lightly polished by wear, but no
2359 dentine is exposed (stage 1). The crown outline is less rhomboidal than some maxillary
2360 molars in the sample and is rounded square, with the moderately sized Hy. The crown is
2361 BL broadest across the mesial cusps and tapers distally. In addition to the four principal
2362 cusps, the crown possesses a small C5. The relative cusp sizes are Pr > Pa > Hy ≥ Me >
2363 C5. The MMR is well developed, with the lingual and buccal components of the MMR
2364 sloping to meet at an angle with a faint groove at their junction in the midline. The
2365 fissure-like Fa is wide and continuous with the central groove. Its buccal branch is
2366 slightly shorter than its lingual segment. The Fa is bordered distally by a thin,
2367 discontinuous epicrista joining the mesial aspects of the Pr and Pa. The Co is interrupted

2368 by the central groove. A small pit-like Carabelli's feature sits on the mesiolingual aspect
2369 of the Pr.

2370 The tooth is three rooted; however, the distobuccal root broke off a few
2371 millimeters from the cervix. The mesiobuccal root is MD compressed with a depression
2372 separating two radicals along its distal face. Its apex curves distally. On the buccal aspect,
2373 the mesiobuccal root is 11.3 mm tall. The lingual root is robust, and MD compressed. It is
2374 c-shaped in cross section, especially apically, due to a strong invagination along the
2375 buccal face. The lingual root angles lingually and deflects distally. Its tip is broken just
2376 before its apex, exposing a small portion of the root canal. On the lingual aspect, the
2377 preserved height of the root is 11.3 mm.

2378 The mesial IPF of this specimen is proposed to match the distal IPF of the M² in
2379 the U.W. 101-1277 maxilla.

2380

2381 U.W. 101-1398A: RM³ (Fig. 24E; Table 1) An enamel chip is present along the distal
2382 margin. The crown has a very large, oval mesial IPF (6.9 mm BL by 4.2 mm OC), which
2383 reaches the occlusal surface and has no distal IPF. The occlusal surface is polished by
2384 wear but no dentine is exposed (stage 1–2). The occlusal outline is a rounded square with
2385 a convex distal margin. A cingular shelf crossing the lingual groove affects the lingual
2386 contour. There are four primary cusps. There was likely a C5; wear precludes its
2387 assessment at the outer enamel surface but a distinct dentine horn for it is present at the
2388 EDJ. The distal lobe of the Me is hypertrophied and divided from the essential lobe by a
2389 fissure. The expression of the MMR cannot be assessed due to IP wear. The Fa is
2390 preserved as a short groove still visible on the Pr. It appears to be divided from the central

2391 fovea by an epicrista joining the Pr and Pa (an epicrista is present at the enamel-dentine
2392 junction). Carabelli's feature is expressed as a v-shaped groove and associated weak
2393 shelf. The buccal groove is shallow.

2394 The crown has three roots: two buccal and one lingual. The distobuccal root is
2395 broken about mid-length and the mesiobuccal root is missing its apical third. The root
2396 surfaces are abraded. The lingual root is MD wide and comprises two components
2397 separated by a buccal invagination, which gives it a c-shape in cross section. The lingual
2398 root is distally inclined, especially along its mesial margin. The mesiobuccal root is MD
2399 compressed. At the cervix, the distobuccal root is more circular and smaller in cross
2400 section than the mesiobuccal root. It takes a strong buccal turn and slight distal
2401 inclination, which is quite different from the vertical orientation of the mesiobuccal root.
2402 The maximum height of the lingual root is 10.6 mm along its lingual aspect. The
2403 maximum height of the mesiobuccal root is 11.5 mm along its buccal aspect and the
2404 maximum height of the distobuccal root is 5.9 mm.

2405 This specimen is proposed as the antimere of U.W. 101-1471. Both specimens are
2406 likely M³s. Their diagnosis as M³s is based in part upon the morphology of their roots,
2407 which are better preserved on U.W. 101-1471 than U.W. 101-1398A. The distobuccal
2408 roots of these specimens are much smaller and more circular than the mesiobuccal roots
2409 and show a strong, and unusual, buccal and distal tilt. A similar heteromorphic root
2410 morphology is present in the U.W. 102-1 M³s (Hawks et al., 2017; L.D., personal
2411 observation), in contrast to the U.W. 102 M²s. Further, there is no distal interproximal
2412 facet present on either specimen. For comparison, the U.W. 101-1277 M², which is at a

2413 similar state of occlusal wear, has a distinct distal facet. In addition, the occlusal outline,
2414 which features a rounded Hy and divided Me, is matched in other proposed M³s.
2415
2416 U.W. 101-1471: LM³ (Fig. 24F; Table 1) There is an enamel chip on the Me apex. There
2417 is a large semicircular mesial IPF (5.8 mm BL by 3.4 mm OC) and no distal IPF. The
2418 cusps are flattened by occlusal wear, but no dentine is exposed (stage 2). The crown is
2419 somewhat rhomboidal in occlusal outline due to the distolingual projection of the
2420 relatively large Hy and a reduced Me. The four primary cusps have the following
2421 relationship: Pr > Hy ≥ Pa > Me. In addition, there is a small cuspule distal to the Me.
2422 The expression of the MMR and Fa is obscured by wear; however, it appears that the Fa
2423 is preserved as a small pit that was separated from the central fovea by a continuous
2424 epicrista connecting the Pr and Me. The lingual groove is a deep cleft at the occlusal
2425 margin but becomes shallow and broad below the occlusal surface. A small pit associated
2426 with Carabelli's feature is present on the mesiolingual aspect of the Pr. No crest extends
2427 distally from the Carabelli's feature; though, a subtle swelling of the cingulum is evident
2428 distal to the lingual groove. There is no buccal groove.

2429 The crown has two buccal roots and one lingual root. The lingual root apex is
2430 broken, exposing the root canal. The mesiobuccal root is also broken, exposing a tiny
2431 pinhole of the canal. The lingual root is large and angles distally. A prominent groove
2432 runs along its buccal face, giving it a c-shape in cross section. The mesiobuccal root is a
2433 MD-compressed oval. It is more plate-like than the distobuccal root, which is smaller and
2434 more circular in cross section. The mesiobuccal root angles slightly distally, while the

2435 distobuccal root angles distobuccally. The maximum height of the lingual root is 11.8
2436 mm. The mesiobuccal root is 11.0 mm tall and the distobuccal root is 8.5 mm tall.

2437 This specimen is proposed as the antimere of U.W. 101-1398A. The assessment
2438 of this tooth as an M³, and not M², is based on several features. The buccal roots of this
2439 specimen are strongly heteromorphic in cross sectional size, shape, and orientation. Such
2440 root asymmetry is not seen, for example, in the U.W. 101-1277 M², which is in situ in the
2441 maxilla. Further, *H. naledi* specimen U.W. 102-001, from the Lesedi chamber (Hawks et
2442 al., 2017), preserves all three maxillary molars bilaterally. The 102-001 M³s share with
2443 U.W. 101-1471 the distinctive buccal root heteromorphy (L.D., personal observation).
2444 The absence of a distal IPF is consistent with the identification of this tooth as an M³.
2445 Further, the occlusal outline, which features rounded Hy and reduced Me are matched in
2446 other proposed M³s.

2447

2448 3.18. *Permanent mandibular central incisors*

2449 Six isolated I₁s and those in the U.W. 101-1261 mandible represent at least four
2450 individuals. Morphologically, the teeth are simple in form. In labial and lingual views,
2451 the crown flares towards the incisal edge; the labial face is featureless and minimally
2452 convex at mid-crown; lingually, the marginal ridges are faint and bound a featureless
2453 lingual fossa.

2454

2455 U.W. 101-039: RI₁ (Fig. 25A; Table 1) Minor damage is evident to the labial and lingual
2456 cervical lines and enamel chipping is evident near the lingual margin of the mesial IPF.
2457 The mesial IPF (2.5 mm along its major axis) is teardrop shaped and located near the

2458 incisal edge. A much smaller distal IPF runs along the DMR below the incisal edge. The
2459 crown is worn with dentine exposed along the incisal edge and lingually along the mesial
2460 shoulder (stage 4). In labial and lingual views, the crown flares towards the incisal edge.
2461 The labial face is featureless and minimally convex at mid-crown. Lingually, the MMR
2462 and DMR are barely perceptible and defined by faint lingual grooves. The DMR is more
2463 visible than the MMR, which is obscured by incisal wear. The DMR is also stronger
2464 towards the incisal edge. There is no basal swelling.

2465 The root is abraded across its surface and slightly damaged just below the lingual
2466 cervix. The root is broken apically at an angle so that more of the labial height (9.4 mm)
2467 is preserved than the lingual. In cross section, the long axis of the root runs LaL. There is
2468 a wide and shallow depression running along the distal root face.

2469 This is the proposed antimere of the U.W. 101-601 LI₁. They are morphologically
2470 homogenous, their occlusal wear is similar, and their IPFs match.

2471 This specimen and U.W. 101-038 were both found on a rock and had been
2472 arranged by cavers prior to excavation (see area D in Figure 6B of Dirks et al., 2015).

2473

2474 U.W. 101-601: LI₁ (Fig. 25B; Table 1) The tooth is fragmented. One portion contains
2475 most of the crown, while the other contains the lingual cervix and root. The rejoined
2476 surfaces are not flush. Enamel chipping is evident in the region of the small mesial IPF,
2477 which is located very near the incisal edge. A larger distal IPF (2.3 mm IC by 1.3 mm
2478 LaL) is located at the incisal edge. Dentine is exposed along the incisal edge and the
2479 incisal aspect of the MMR (stage 3). The labial face is featureless and minimally convex
2480 at midcrown. Lingually, the MMR and DMR are barely defined by faint grooves that

2481 separate them from a featureless lingual fossa. The marginal ridges increase in
2482 topographical prominence as they approach the incisal edge; both are, however, worn on
2483 their lingual aspects near the incisal edge. Further, the MMR is truncated by the
2484 encroaching mesial IPF.

2485 The root is minimally abraded on its mesial side and the exposed root canal is
2486 packed with sediment. Labially, the preserved height of the root is approximately 9.3
2487 mm, accounting for the refit. In cross section, the root is broader LaL than MD and there
2488 is a subtle depression running along the distal side.

2489 This is proposed as the antimere of U.W. 101-039. Their wear is similar and their
2490 adjoining IPFs match in shape and the placement of enamel chipping.

2491

2492 U.W. 101-1005A: LI₁ (Fig. 25C; Table 1) An enamel chip is missing from the lingual
2493 margin of the distal IPF near the incisal edge. A large distal IPF (1.7 mm LaL by 3.2 mm
2494 IC) intersects the incisal edge. The similarly sized mesial IPF (1.7 mm LaL by 3.1 mm
2495 IC) also runs up to the incisal edge. A thin strip of dentine is exposed along most of the
2496 incisal edge (stage 2). The crown flares MD as it reaches the incisal edge; though, its
2497 maximum MD length is reduced by incisal and interproximal wear. The labial surface is
2498 featureless and minimally convex. The lingual surface is flat with faint marginal ridges.

2499 The root is abraded and broken just before the apex. In labial view, 11.4 mm of
2500 root is preserved. The root is MD compressed and deflects distally near its apex.

2501 Incisors U.W. 101-1005A (LI₁), U.W. 101-1005B (RI₁), and U.W. 101-1005C
2502 (RI₂) were excavated in contact with one another and are assigned a single accession
2503 number. Their morphology and interproximal facets are consistent with their attribution

2504 to a single individual. This is the antimere of U.W. 101-1005B to which its interproximal
2505 facet clearly articulates. It also articulates well with the U.W. 101-998 LI₂, which is also
2506 chipped along the adjoining IPF. This tooth is proposed to belong to the same individual
2507 as the U.W. 101-377/1014 mandibular specimens and their associated antimeres.

2508

2509 U.W. 101-1005B: RI₁ (Fig. 25D; Table 1) An enamel chip is missing from the lingual
2510 margin of the distal IPF near the incisal edge. A large distal IPF (2.6 mm LaL by 1.3 mm
2511 IC) intersects the incisal edge. The larger mesial IPF (1.7 mm LaL by 3.2 mm IC) also
2512 runs up to the incisal edge. A thin strip of dentine is exposed along the incisal edge (stage
2513 2). The crown flares as it reaches the incisal edge; though, its maximum MD length is
2514 reduced by wear. The labial surface is featureless and minimally convex. The lingual
2515 surface is flat with faint marginal ridges.

2516 The root is abraded and broken near the apex so that the root canal is exposed. In
2517 labial view, 10.3 mm of the root height is preserved. The root is MD compressed and
2518 deflects distally at its apex.

2519 This is the antimere of U.W. 101-1005A to which its interproximal facet clearly
2520 articulates. Incisors U.W. 101-1005A (LI₁), U.W. 101-1005B (RI₁), and U.W. 101-1005C
2521 (RI₂) were excavated in contact with one another and are assigned a single accession
2522 number. Their morphology and interproximal facets are consistent with their attribution
2523 to a single individual. This tooth is proposed to belong to the same individual as the U.W.
2524 101-377/1014 mandibular specimens and their associated antimeres.

2525

2526 U.W. 101-1132: LI₁ (Fig. 25E; Table 1) There is a small (0.9 mm LaL by 1.9 mm IC),
2527 slightly lingually offset, mesial IPF and no distal IPF. A thin strip of dentine is exposed in
2528 the central half of the incisal edge (stage 1). The incisal edge is straight and the mid-
2529 crown is minimally convex. The labial face is featureless. Lingually, there are trace
2530 marginal ridges that are primarily expressed near the incisal edge and quickly fade
2531 towards the cervix. The weak basal eminence is slightly offset mesially in incisal view.
2532 Linear hypoplasias are visible on the cervical quarter of the crown (for a discussion of
2533 hypoplasias on this specimen, see also Skinner, 2019).

2534 The root is abraded on all surfaces. Further, it is broken at about two-thirds of its
2535 height (8.8 mm in height in labial view), exposing the root canal. In cross section, the
2536 root is MD compressed.

2537 This tooth is the antimere of U.W. 101-1133. Both were excavated in anatomical
2538 contact and are identical in morphology and wear status. Further, the specimen articulates
2539 distally with U.W. 101-1131.

2540

2541 U.W. 101-1133: RI₁ (Fig. 25F; Table 1) There is an enamel chip along the incisal edge
2542 distally. A small mesial (1.1 mm by 1.9 mm) IPF is present, but one appears to be absent
2543 distally. A thin line of dentine is exposed in the center of the incisal surface edge (stage
2544 1). The labial face is featureless. It is minimally convex mid-crown with a straight incisal
2545 edge. Lingually, the weak basal eminence is offset mesially. There are faint marginal
2546 ridges that are expressed primarily near the incisal edge. Linear hypoplasias are visible on
2547 the cervical quarter of the crown (for a discussion of hypoplasias on this specimen, see
2548 also Skinner, 2019).

2549 The root is broken above its apex and abraded. The preserved length of the root is
2550 10.0 mm along the labial aspect. In cross section, the root is compressed MD.

2551 This is the antimere of U.W. 101-1132. The teeth were excavated in anatomical
2552 contact, they are identical in morphology, and their degree and pattern of wear matches.
2553 Further, the specimen articulates distally with U.W. 101-1075.

2554

2555 *3.19. Permanent mandibular lateral incisors*

2556 Five isolated I₂s are known from the Dinaledi Chamber deposits. A developing I₂
2557 was recovered from its exposed crypt in the U.W. 101-1400 mandible and the U.W. 101-
2558 1261 mandible preserves both I₂s in situ. Collectively, the I₂s represent at least five
2559 individuals. The incisal edge is straight, but the crown has moderate labial convexity at
2560 mid-crown. In labial view, the mesial corner sits slightly higher than the distal; the mesial
2561 shoulder is more perpendicular than the rounded distal shoulder. Weak marginal ridges
2562 bound a featureless lingual fossa. A developmental notch is present in the center of the
2563 incisal edge in those specimens that are unworn or relatively unworn.

2564

2565 U.W. 101-335: RI₂ (Fig. 26A; Table 1) The distal IPF (approximately 1.3 mm LaL by 2.5
2566 mm IC) is vertically oriented, while the mesial IPF (approximately 1.0 mm LaL by 1.5
2567 mm IC) is much smaller and placed very near the incisal edge. Dentine is exposed as a
2568 tiny speck in the center of the incisal edge and wear facets flatten the mesial and distal
2569 marginal ridges on the lingual face (stage 2). The incisal edge is straight, but the tooth has
2570 moderate labial convexity at mid-crown. The crown and root are also moderately convex
2571 in mesial and distal views. In labial view, the incisal margin is rounded with the mesial

2572 corner slightly higher and somewhat more perpendicular than the distal. Weak mesial and
2573 distal marginal ridges bound a shallow and featureless lingual fossa. The labial face is
2574 morphologically featureless, although there are several linear hypoplasias present in the
2575 cervical third (for a discussion of hypoplasias on this specimen, see also Skinner, 2019).

2576 The root surface is abraded along all faces and broken at the apex, which exposes
2577 the root canal. Its preserved labial height is 11.8 mm. The root is compressed MD and
2578 broader LaL in cross section. There are faint grooves on the mesial and distal aspects
2579 running the length of the root. The distal groove is deeper than the mesial.

2580 This specimen and U.W. 101-339 (RC₁) were recovered within centimeters of
2581 each other and their respective facets are potential matches.

2582

2583 U.W. 101-998: LL₂ (Fig. 26B; Table 1) Enamel chipping is present along the lingual
2584 margin of the mesial IPF. The mesial IPF (1.9 mm LaL by 3.0 mm IC) is teardrop shaped
2585 and located near the incisal edge. The distal IPF (2.0 mm LaL by 2.9 mm IC) is ovoid,
2586 concave, and located near the incisal edge. A thin strip of dentine is exposed in the center
2587 of the incisal edge (stage 2). Labially, the crown is minimally convex at midcrown. The
2588 labial face is featureless except for a minor distolabial depression. The marginal ridges
2589 are both low and rounded; as preserved, the DMR is stronger than the MMR. The lingual
2590 face is flat. Multiple linear hypoplasias are visible in the cervical third of the crown (for a
2591 discussion of hypoplasias on this specimen, see also Skinner, 2019).

2592 The root is missing its apex and is broken into two pieces that easily refit and are
2593 rejoined as of June 2018 (not evident in Figure 26B or scans). The root is abraded along
2594 most of its surface. When repaired, the root is 14.9 mm in height along the labial margin.

2595 The root is ovoid in cross section, being compressed MD. A wide, shallow depression
2596 runs along its distal aspect.

2597 This is the antimere of the U.W. 101-1005C RI₂. In addition, the mesial IPF is a
2598 good match for the distal IPF of the U.W. 101-1005A LI₁, which also evinces minor
2599 enamel chipping along its incisolabial aspect. Finally, the contact with the mesial IPF of
2600 the U.W. 101-1076 LC₁ is reasonable. If these associations are correct, then this
2601 specimen belongs to a nearly complete set of mandibular teeth that includes the U.W.
2602 101-377 mandible and other associated postcanine teeth.

2603

2604 U.W. 101-1005C: RI₂ (Fig. 26C; Table 1) The mesial IPF is close to the incisal edge (1.6
2605 mm LaL by 2.5 mm IC). The distal IPF is smaller (1.8 mm LaL by 3.8 mm IC), lingually
2606 oriented and comprised of two distinct planes. The incisal edge is minimally worn with a
2607 hairline strip of dentine exposed (stage 2). Incisal wear spills over onto the lingual
2608 surface. The crown flares towards the incisal edge, which is moderately convex. In incisal
2609 view, the labial face is minimally convex. It possesses a shallow vertical distal depression
2610 but is otherwise featureless. The lingual face is flat with faint marginal ridges. The DMR
2611 is associated with a slight distal projection that can be observed in both lingual and labial
2612 views. Multiple linear hypoplasias are visible in the cervical third of the crown (for a
2613 discussion of hypoplasias on this specimen, see also Skinner, 2019).

2614 The root is missing its apex and is abraded along most of its external surface. In
2615 labial view, the preserved height is 10.3 mm. The root is compressed MD, with a shallow
2616 depression running the length of the distal face.

2617 Incisors U.W. 101-1005A (LI₁), U.W. 101-1005B (RI₁), and U.W. 101-1005C
2618 (RI₂) were excavated in contact with one another and are assigned a single accession
2619 number. Their morphology and interproximal facets are consistent with their attribution
2620 to a single individual. The complexly shaped distal IPF of U.W. 101-1005C fits well with
2621 that of the mesial IPF of the U.W. 101-1014 RC₁; thus, this specimen is proposed to link
2622 these associated anterior teeth with those in situ in the U.W. 101-377 mandible and their
2623 associated antimeres.

2624

2625 U.W. 101-1075: RI₂ (Fig. 27A; Table 1) Labially, damage is evident to the distal portion
2626 of the cervical line. The crown evinces light incisal wear (stage 1). No IPFs are visible
2627 mesially or distally. Like other lightly or unworn *H. naledi* I₂s (e.g., U.W.101-1131 and
2628 U.W. 101-1400) and I₂s (i.e., U.W. 101-1588), a distinct developmental notch is present
2629 in the center of the incisal edge. In labial and lingual views, the mesial profile is vertical
2630 and the distal profile flares out with a rounded distal corner. The crown exhibits minimal
2631 labial convexity, with a straight incisal edge and a gently curved mid-crown. The labial
2632 face is featureless. Lingually, there is trace shoveling. The MMR and DMR are low and
2633 rounded, becoming stronger towards the incisal margin. There are multiple linear
2634 hypoplasias in the cervical third of the crown (for a discussion of hypoplasias on this
2635 specimen, see also Skinner, 2019).

2636 The root is abraded on all its external surfaces and is broken just before the apex.
2637 The preserved height of the root is 11.7 mm labially. The root is MD compressed with a
2638 shallow depression running the length of the distal facet.

2639 Based on shared morphology, size, and wear status, this is the proposed antimere
2640 of U.W. 101-1131. If this association is correct, then U.W. 101-1075 is also associated
2641 with the U.W. 101-886 RC₁, which is the antimere of the U.W. 101-1126 LC₁ and was
2642 excavated in anatomical contact with U.W. 101-1131. The association of U.W. 101-1075
2643 and U.W. 101-886 cannot be directly confirmed, however, because both specimens lack
2644 IPFs.

2645

2646 U.W. 101-1131: LI₂ (Fig. 27B; Table 1) The crown is lightly worn (stage 1) and no IPFs
2647 are present. The incisal edge is straight, and the mid-crown is minimally convex. The
2648 labial face is featureless. The lingual face presents trace marginal ridge development,
2649 primarily visible close to incisal edge and then fading quickly towards the cervix. The
2650 incisal edge is notched, similar to the lateral incisors in the maxilla (i.e., U.W. 101-1588)
2651 and mandible (i.e., U.W. 101-1075, and U.W. 101-1400). Faint linear hypoplasias are
2652 visible on the cervical third of the crown (for a discussion of hypoplasias on this
2653 specimen, see also Skinner, 2019).

2654 The root is broken, and its surface is abraded. Its preserved is 10.8 mm along the
2655 labial aspect. In cross section, the root is compressed MD, with a shallow depression
2656 running the length of the distal aspect.

2657 Based upon similarities in size, morphology, and wear status, this is proposed as
2658 the antimere of U.W. 101-1075. This specimen was excavated in anatomical position
2659 with the U.W. 101-1126 (LC₁), U.W. 101-1132 (LI₁), and U.W. 101-1133 (RI₁).

2660

2661 U.W. 101-1400: LI₂ germ (Fig. 27C) This is an incompletely formed crown recovered
2662 from the exposed crypt of the U.W. 101-1400 mandible. Few morphological details are
2663 evident, but faint marginal ridges are visible. As in unworn and lightly worn I₂s (i.e.,
2664 U.W. 101-1075 and U.W. 101-1131), a notch is present along the incisal edge.

2665

2666 3.20. *Permanent mandibular canines*

2667 Eight isolated mandibular canines have been recovered from the Dinaledi
2668 Chamber. Canines are also present in the U.W. 101-010, U.W. 101-377, and U.W. 101-
2669 1261 mandibles, and a developing C₁ is visible in its exposed crypt in the U.W. 101-1400
2670 mandible. Collectively, these canines represent a minimum of nine individuals if U.W.
2671 101-010 and U.W. 101-359 are antimeres. The *H. naledi* mandibular canines present a
2672 consistent suite of features. These include an asymmetrical crown in labial and lingual
2673 views, a mesially oriented apex, a high mesial shoulder, and a strongly sloping distal
2674 crest that ends in a low tubercle. The distal tubercle and adjacent lingual furrow are well
2675 defined. The crowns appear relatively tall compared to their small basal dimensions.

2676

2677 U.W. 101-245: RC₁ (Fig. 28A; Table 1) The crown is heavily damaged. Enamel from the
2678 labial face is almost entirely missing, leaving enamel distally and along the lingual face.
2679 Additionally, the cervical line is damaged across its preserved course. The crown is
2680 moderately worn. The apex is missing, leaving an elongated circular dentine patch and a
2681 wear facet that extends along the distal crest and onto the apex of the distal tubercle
2682 (stage 4). Despite the marked apical wear, there is no distal IPF. The original crown was
2683 asymmetrical with a mesially oriented apex, a high mesial shoulder, and a strongly

2684 sloping distal occlusal edge. The distal edge ends in a low distal tubercle. The distal
2685 tubercle and adjacent lingual furrow are well defined, as is common in all other *H. naledi*
2686 mandibular canines. The most cervical extent of the mesial lingual fossa is also preserved
2687 adjacent to the MMR, but its superior extent is removed by the break that detached the
2688 enamel from the crown. A trace of the distal labial groove defining the labial extent of the
2689 distal tubercle is also present. The lingual basal aspect is flat and the median lingual
2690 ridge, as preserved, is indistinct, flat, and broad.

2691 The root is broken near its apex, exposing the root canal. Additionally, abrasion is
2692 evident across the surface of the root. Measured from the inferred location of the labial
2693 cervix, the preserved root measures 14.1 mm in height. A subtle invagination runs along
2694 the mesial face.

2695

2696 U.W. 101-339: RC₁ (Fig. 28B; Table 1) There is a small and faint mesial IPF (1.2 mm
2697 LaL by 2.5 mm IC) near the apex of the mesial shoulder and along its lingual crest. No
2698 distal IPF is present. The crown apex is blunted by wear and the distal occlusal crest
2699 exhibits a shallow concave (J-shaped in labial view) facet that runs onto the apex of the
2700 distal tubercle. No dentine is exposed (stage 1). The crown is tall relative to its narrow
2701 base (Table 1). The occlusal edge is straight, but the mid-crown is moderately convex.
2702 The crown is minimally convex in mesial and distal views. In labial view, the crown is
2703 asymmetrical with an apex that is slightly offset distal to the MD midpoint. The mesial
2704 occlusal crest is short, convex, and situated more apically than the distal. The distal crest
2705 is longer and more vertically oriented and terminates at a distal tubercle. There are faint
2706 mesial and distal vertical grooves on the labial face. The distal labial groove is better

2707 defined than the mesial, but it is rather indistinct compared to the deep distal groove on
2708 the lingual face. Adjacent to the distolingual groove is a shallow triangular-shaped fossa
2709 bounded mesially by a weak median lingual ridge. There is a shallow mesiolingual fossa
2710 between the median lingual ridge and a moderately-developed MMR. The median lingual
2711 ridge bifurcates as it travels apically, with one branch extending towards the apex and the
2712 other towards the mesial occlusal crest. A pair of linear hypoplasias is observed on the
2713 cervical third of the labial face and fainter hypoplasias are also evident lingually.

2714 The root is abraded externally and broken at approximately half of its height,
2715 exposing the sediment packed root canal. In cross section, the root is broader LaL than
2716 MD. There is a faint invagination running along the root mesially. The preserved height
2717 of the root is 7.1 mm labially and 9.4 mm lingually.

2718 This tooth is the potential antimere of U.W. 101-985. They are similar in size and
2719 morphology, and both have a pair of prominent linear hypoplasias in their cervical
2720 regions. They do differ in the degree of occlusal wear. A wear facet runs along the distal
2721 crest of U.W. 101-339 but is absent on U.W. 101-985. There is also a small mesial IPF on
2722 U.W. 101-339 that is not apparent on U.W. 101-985. This could indicate a more
2723 advanced eruption status for U.W. 101-339 than U.W. 101-985. This specimen and U.W.
2724 101-335 (RI₂) were recovered within centimeters of each other and their respective facets
2725 are potential matches.

2726

2727 U.W. 101-359: LC₁ (Fig. 28C; Table 1) Occlusal wear is extensive, having removed all
2728 but a thin sliver of enamel (approximately 4.3 mm in length and 1.4 mm in height)
2729 mesiolabially (stage 7). The dentinal surface was functional given its polished

2730 appearance. The pulp chamber is exposed occlusally, and the margins are polished and
2731 rounded. The root is covered in cementum, which is extensively cracked. The maximum
2732 dimensions as preserved at the occlusal surface are 6.8 mm by 7.2 mm and the maximum
2733 length of the remaining root, which is damaged at the root apex, and crown is 16.6 mm.

2734 Specimens U.W. 101-357 to U.W. 101-359 were recovered from fragments and
2735 sediments associated with the U.W.101-361 mandible and are consistent with belonging
2736 to a single individual. This specimen evinces comparable wear to that of the U.W. 101-
2737 010 RC₁; that said, the absence of detailed crown morphology limits the inference that
2738 they represent antimeres.

2739

2740 U.W. 101-886: RC₁ (Fig. 28D; Table 1) The crown is unworn (stage 1). The labial crown
2741 face is minimally convex at midcrown. In labial and lingual views, it is tall relative to its
2742 narrow base (Table 1) and asymmetrical, with the apex situated distal to the MD
2743 midpoint. The convex mesial edge is shorter and higher than the longer, straighter and
2744 more vertically oriented distal edge. The distal edge terminates in a tubercle, which is
2745 associated with a short, faint distal groove on the labial face and a deeper fossa on the
2746 lingual face. A shallow and faint mesial labial groove runs nearly the entire crown height.
2747 The median lingual ridge is weakly developed. It is wide and flat near the base of the
2748 lingual fossa and becomes thinner, but more distinct, near the apex. The DMR is
2749 bordered by a groove and weak fossa. Linear hypoplasias are present in the cervical third
2750 of the crown (for a discussion of hypoplasias on this specimen, see also Skinner, 2019).

2751 The root is abraded and broken with only 4.8 mm remaining labially and 3.0 mm
2752 lingually. A shallow broad furrow is present on the mesial side of the root, and, in cross
2753 section, it is ovoid and slightly broader LaL than MD.

2754 Given the absence of occlusal or interproximal wear, but the presence of some
2755 root development, this tooth was likely unerupted at death and the root incompletely
2756 formed. Based upon shared morphology, its unworn state, and similarities in placement
2757 and presence of hypoplastic defects, U.W. 101-1126 and U.W. 101-886 are probable
2758 antimeres. The developmental defects are, however, more prominent on the lingual
2759 surface of U.W. 101-886 than on U.W. 101-1126. As U.W. 101-1126 was excavated in
2760 near anatomical contact with the U.W. 101-1131, U.W. 101-1132, and U.W. 101-1133
2761 mandibular incisors, then, if their status as antimeres is correct, U.W. 101-886, along
2762 with U.W. 101-1075, would form a complete set of anterior mandibular teeth.

2763

2764 U.W. 101-985: LC₁ (Fig. 29A; Table 1) Apart from minor damage to the cervical region
2765 distolabially, the crown is complete. Neither mesial nor distal IPFs are present. A very
2766 small facet blunted the apex (stage 1). In labial and lingual views, the crown is tall
2767 relative to its narrow base (Table 1), and is asymmetrical, with the apex situated distal to
2768 the MD midpoint. The mesial edge is short and convex, while the distal edge is longer,
2769 straighter, and more vertically oriented. The mesial shoulder is high, while the distal
2770 shoulder, which comprises a small tubercle, is much lower. This tubercle is associated
2771 with a subtle distal labial groove and a deeper lingual groove. A faint mesiolabial groove
2772 runs the length of the crown. The labial face is moderately convex at mid-crown; though,
2773 the occlusal edge is straight. The crown and root are moderately convex. A weak median

2774 lingual ridge extends to the crown apex and is bordered on either side by shallow mesial
2775 and distal fossae. A faint accessory ridge runs parallel to the MMR. Multiple linear
2776 hypoplasias are present on the cervical third of the labial face (for a discussion of
2777 hypoplasias on this specimen, see also Skinner, 2019).

2778 The root is broken in a radial manner so that more of the root is preserved
2779 lingually and mesially than labially and distally. Lingually, the maximum remaining
2780 height is 10.0 mm, while labially the preserved root height is 2.5 mm. The root is ovoid
2781 in cross section, being MD compressed.

2782 This is a potential antimere of U.W. 101-339. They are similar in size and
2783 morphology, and both have a pair of prominent linear hypoplasias in their cervical
2784 regions. They do differ in the degree of occlusal wear. A wear facet runs along the distal
2785 crest of U.W. 101-339, while one is absent on U.W. 101-985. Further, there is a small
2786 mesial IPF on U.W. 101-339, while one is not apparent on U.W. 101-985. This could
2787 indicate a more advanced eruption status for U.W. 101-339 than U.W. 101-985 regardless
2788 of their status as antimeres.

2789

2790 U.W. 101-1076: LC₁ (Fig. 29B; Table 1) A large mesial IPF (2.1 mm LaL by 2.5 mm
2791 OC) sits high on the mesial shoulder and a small distal IPF (1.8 mm LaL by 1.6 mm OC)
2792 is placed at the apex of the tubercle. There is a long concave wear facet along the distal
2793 crest and a smaller facet dulls the mesial crest as well (stage 1). The crown is tall relative
2794 to its narrow base. In labial and lingual views, the apex sits slightly distal to the MD
2795 midpoint. The mesial crest is short and convex, and the mesial shoulder sits high on the
2796 crown, while the distal crest is more vertically oriented and terminates at a distinct

2797 tubercle that sits low on the crown. A wide but shallow distal labial groove and shallow
2798 mesial groove are associated with the distal tubercle. The faint median lingual ridge that
2799 fades at mid-crown and reappears just below the crown apex. There is a shallow
2800 mesiolingual fossa between the median lingual ridge and the MMR and a well-developed
2801 fossa between the distal tubercle and the median lingual ridge that widens and becomes
2802 shallower towards the distal margin. A linear hypoplasia crosses the lingual crown near
2803 the cervix, while labially there are several linear and pit hypoplastic defects visible in the
2804 cervical third of the crown (for a discussion of hypoplasias on this specimen, see also
2805 Skinner, 2019).

2806 The root is broken and abraded across most of its preserved surface. It measures
2807 7.8 mm labially. The root is ovoid in cross section and MD compressed.

2808 This is the probable antimere of the canine in the U.W. 101-377+1014 mandible.
2809 The crowns are similar in morphology and wear status. Further, this specimen articulates
2810 well with the U.W. 101-998 LI₂ and with the U.W. 101-889 LP₃. As such, this specimen
2811 is proposed to be associated with a nearly complete set of mandibular teeth that also
2812 features those in situ in the U.W. 101-377/1014 mandible.

2813

2814 U.W. 101-1126: LC₁ (Fig. 29C; Table 1) The crown is unworn (stage 1); further, IPFs are
2815 not detectable mesially or distally. In labial and lingual views, the crown is tall relative to
2816 its narrow base (Table 1) and asymmetrical, with the apex situated distal to the MD
2817 midpoint. The convex mesial crest is shorter and higher than the longer, straighter and
2818 more vertically oriented distal crest. The distal crest terminates in a tubercle that is
2819 associated with a short, faint distal groove on the labial face. A shallow and faint mesial

2820 labial groove runs nearly the entire crown height. The median lingual ridge is faint,
2821 except near the apex, where it is low and dull. The adjacent mesial and distal fossae are
2822 each broad and shallow. The distal tubercle is bordered lingually by a deep groove and
2823 weak fossa. Multiple hypoplastic defects are visible on the labial and lingual faces. Pit-
2824 like defects are also evident in the cervical third of the labial face as well (for a
2825 discussion of hypoplasias on this specimen, see also Skinner, 2019).

2826 The root surface is abraded and broken so that only 4.6 mm remains below the
2827 cervix labially. The preserved root is ovoid in cross section, being more MD compressed.

2828 This is the proposed antimere of U.W. 101-886. Both are similar in morphology
2829 and wear status. Their pattern of hypoplastic defects is also similar; although, the lingual
2830 hypoplasias are more prominent on the left canine. This specimen was excavated in
2831 anatomical contact with U.W. 101-1131 (LI₂), U.W. 101-1132 (LI₁), and U.W. 101-1133
2832 (RI₁). As an antimere of U.W. 101-1131, this set of anterior teeth would also include
2833 U.W. 101-1075 (RI₂).

2834

2835 U.W. 101-1610: RC₁ germ (Fig. 29D; Table 1) The crown is developing. The mesial
2836 shoulder is visible and high on the crown. The distal margin is nearly vertical, and no
2837 distal shoulder is apparent, giving the crown an asymmetric shape. The mesial crest is
2838 convex, while the distal crest is nearly vertical. There is a shallow mesiolabial and no
2839 distolabial groove. Lingually, the median ridge is wide and low. There is a weak mesial
2840 fossa between the median ridge and MMR that becomes a groove adjacent to the ridge.
2841 The distal fossa is barely perceptible.

2842 This specimen is proposed as the antimere of the U.W. 101-1400 LC₁ germ that is
2843 still in its crypt and is associated with the U.W. 101-544B and U.W. 101-1548 maxillary
2844 canine germs. Each is at approximately the same developmental status.

2845

2846 3.21. *Permanent mandibular third premolars*

2847 Seven isolated P₃s have been recovered from the Dinaledi Chamber deposits.
2848 Other P₃s are found in situ in the U.W. 101-001, U.W. 101-010, U.W. 101-377, and U.W.
2849 101-1261 mandibles. Collectively, these teeth represent at least eight individuals. The *H.*
2850 *naledi* P₃s are ‘molarized’; they are fully bicuspid, with the Med and Prd separated by a
2851 longitudinal groove, and have a broad talonid. The MMR is continuous between the
2852 mesial crests of the Med and Prd. The buccal grooves are shallow and fade at midcrown.
2853 Two roots are present, with the distal root BL-broader than the smaller and more circular
2854 mesiobuccal root. The roots share a common canal at the cervix but separate apically.

2855

2856 U.W. 101-144: LP₃ (Fig. 30A; Table 1) Distally, a circular IPF (2.8 mm LaL by 3.0 mm
2857 OC) is present and slightly offset buccally. No mesial IPF is evident. The crown is
2858 minimally worn: there are small wear facets, but no dentine visible on the mesial Prd
2859 crest extending to the apex of the Prd, along the Prd distal accessory crest, and along the
2860 talonid (stage 1). The crown possesses two well developed cusps and a broad talonid. The
2861 Med is high with a free apex. It stands directly across from the Prd and is separated from
2862 it by a well-defined MIg. The Med is smaller in area and slightly lower in height than the
2863 Prd but occupies a significant portion of the mesial crown area. The essential ridges of
2864 the Prd and Med are low and rounded. The Prd also has a narrow mesial accessory ridge

2865 that extends towards the MIg and defines the distal border of the Fa. A thin MMR forms
2866 the mesial border of the Fa and takes the form of a continuous rim connecting the Med
2867 and Prd; it is low relative to the cusp apices. The Fa is a narrow BL-oriented groove
2868 continuous with the MIg. The buccal branch of the Fa is longer than the lingual branch.
2869 The MIg bifurcates distally into a transverse groove that separates the Prd and Med from
2870 a well-developed talonid. This fissure spills onto the buccal face to form a shallow
2871 distobuccal groove, which fades out before mid-crown, and onto the lingual aspect to
2872 form a weak furrow. A weak mesiobuccal groove is also present; like the distobuccal
2873 groove, it fades out before mid-crown. Distally, the polished talonid slopes up from the
2874 transverse groove to the distal border of the crown where the worn DMR is not detectable
2875 as a topographically distinct feature.

2876 Two roots are present, and a small fragment of alveolar bone remains wedged
2877 between them. Both roots are abraded on their exposed surfaces and the canals are
2878 packed with sediment. The distal root is larger and BL-broader than the mesiobuccal root.
2879 Their configuration conforms to the 2R: D+MB pattern of Wood et al. (1988). The roots
2880 share a common canal at the cervix but become individualized just above where they are
2881 broken. Buccally, the maximum preserved height of the mesiobuccal root is 7.7 mm and
2882 that of the distal root is 7.9 mm.

2883 Based upon similarities in morphology, the state of occlusal wear (i.e., presence
2884 of a small wear facet on the buccal aspect of the mesial Prd crest), and the presence of a
2885 distal IPF, but lack of a mesial IPF, this specimen is proposed as the antimere of U.W.
2886 101-506. They do differ slightly in the morphology of the Fa, with U.W. 101-506 lacking
2887 the accessory ridge defining the Fa distally; they are otherwise similar.

2888

2889 U.W. 101-298: RP₃ (Fig. 30B; Table 1) IPFs are absent. The crown is nearly unworn,
2890 with only a small wear facet visible on the buccal aspect of the mesial Prd crest near the
2891 cusp apex (stage 1). Two principal cusps are evident and separated by a well-defined
2892 Mlg. The Med is slightly smaller than the Prd in area but nearly equal to it in height and
2893 their cusp apices are aligned transversely. The MMR is not well defined; rather than
2894 being a continuous horizontally oriented structure, the buccal and lingual segments are
2895 short and thin and separated by a narrow groove. The two segments of the MMR dip
2896 towards the cervix to form a v-shaped contour when viewed mesially. The Fa is a pit
2897 contiguous with the Mlg and defined distally by subtle accessory ridges extending from
2898 the mesial crests of the Prd and Med. The talonid slopes up from the transverse groove,
2899 which extends completely between the distal Prd and Med crests without evident
2900 bifurcation. A small distolingual cusplet and larger distobuccal cusplet are present, with
2901 the distobuccal cusplet the more topographically prominent. A distinct DMR hardly
2902 exists as a crest discrete from the planar surface of the talonid. Instead, in distal view, the
2903 occlusal extent of the distal talonid slopes from the distobuccal cusplet to reach its most
2904 cervical extent lingually. The mesiobuccal groove is absent and the distobuccal groove is
2905 faint; the distobuccal groove extends about a third of the way down the buccal face
2906 before it fades away. No lingual grooves are present. The root(s), which were likely
2907 developing at the time of death, are broken away at the cervix and sediment fills in the
2908 exposed pulp cavity.

2909 U.W. 101-298 is morphologically similar to U.W. 101-1565, which may suggest
2910 that they are antimeres. However, U.W. 101-1565 has a distal IPF, which is lacking in

2911 U.W. 101-298, and more advanced occlusal wear. Such wear asymmetry is not
2912 unexpected for an individual, but it is possible that U.W. 101-298 represents a slightly
2913 younger individual.

2914

2915 U.W. 101-358: LP₃ (Fig. 30C; Table 1) Distally, a portion of the IPF (approximately 4.0
2916 mm LaL) is preserved and offset to the lingual side. Mesially, a small portion of an IPF is
2917 also preserved on the lingual side. The occlusal enamel is worn away, leaving only a thin
2918 rim. The rim is incomplete mesially and mesiolingually where two large antemortem
2919 enamel chips have been removed (stage 6+). The exposed dentine is polished from wear.
2920 The wear surface dips cervically from lingual to buccal and the outline of the pulp
2921 chamber is visible.

2922 A larger plate-like root sits distally and a smaller, more elliptical, root is situated
2923 mesiobuccally. The roots are covered in a thick layer of cementum and abrasions are
2924 evident on many surfaces of the roots. An examination of the μ CT scans shows that the
2925 thick layer of cementum partially fills in the space between the mesial and distal roots,
2926 which are more clearly individuated when only the dentine is considered. The apex of the
2927 distal root is broken away and at least half of the height of the mesiobuccal root is
2928 missing. In buccal view, the maximum preserved height of the mesial root is 5.5 mm, and
2929 the distal root is 9.7 mm.

2930 Given the advanced occlusal wear, the tooth's assignment as an LP₃ is based on
2931 the morphology of its roots. All well-preserved Dinaledi P_{4s} in the assemblage with two
2932 roots have roots that are similar in cross sectional area. Only unequivocal P_{3s} express two

2933 roots, one plate-like and distal and one rounded and mesiobuccal, which is the pattern
2934 observed in this specimen.

2935 Along with U.W. 101-357 (LP₄) and U.W. 101-359 (LC₁), this specimen was
2936 recovered from fragments and sediments associated with the U.W.101-361 mandible and
2937 its in situ left molars. These spatially associated specimens express advanced occlusal
2938 wear, are from the left side, and are consistent with belonging to a single biological
2939 individual.

2940

2941 U.W. 101-506: RP₃ (Fig. 30D; Table 1) The distal IPF (2.9 mm by 2.3 mm) is offset
2942 buccally with its major axis obliquely oriented. No mesial IPF is evident. The crown is
2943 minimally worn, with only small facets present on the mesial and distal Prd crests (stage
2944 1). There are two principal cusps separated by a well-developed MIg. The Med is smaller
2945 in area and slightly lower than the Prd. The cusp apices are nearly aligned transversely.
2946 The MMR sits low on the occlusal surface and is continuous between the mesial crests of
2947 the Med and Prd. These crests and the MMR enclose a small basin-like Fa that extends
2948 from the MIg. Faint accessory ridges emanate from the mesial Med crest and extend into
2949 the Fa. A deep transverse groove separates the trigonid and talonid portions of the crown.
2950 This fissure bifurcates before its lingual termination. The DMR is not an entity distinct
2951 from the sloping surface of the talonid. The buccal face possesses a weak mesiobuccal
2952 groove and a deeper distobuccal groove, which extends about a third of the way down the
2953 buccal face before becoming imperceptible. The distobuccal groove crosses the occlusal
2954 rim as a weak indentation that defines a small distobuccal cuspule. There are no lingual
2955 grooves.

2956 Portions of two broken roots, with exposed canals, are preserved. A plate-like
2957 distal root sits below the talonid, while a smaller elliptical root is placed beneath the
2958 mesiobuccal corner, thus conforming to the 2R: D+MB pattern of Wood et al. (1988). In
2959 buccal view, the preserved height of the mesiobuccal root is 8.2 mm, while the maximum
2960 preserved height of the distal root is 6.0 mm. The mesiobuccal root is abraded along its
2961 mesial and lingual faces and the distal root has patches of abrasion along its distal face.

2962 This is a possible antimere of U.W. 101-144. They differ slightly in the
2963 morphology of the Fa, with U.W. 101-144 having a mesial accessory Prd ridge extending
2964 into the Fa but are otherwise similar in crown and root morphology. They are similar in
2965 wear status, as both have distal IPFs and no mesial IPF, and both have only small wear
2966 facets on the buccal aspect of the MPC. However, U.W. 101-144 also exhibits polishing
2967 on the talonid.

2968

2969 U.W. 101-800: RP₃ (Fig. 31A; Table 1) Minor chipping is present along the occlusal
2970 surface of the distal margin. There is a large ovoid distal IPF (4.4 mm BL by 2.2 mm
2971 OC); however, despite the advanced wear, no mesial IPF is evident. Details of the
2972 occlusal morphology have been removed by wear and moderate dentine patches are
2973 exposed over the cusp apices (stage 4–5). The Prd dentine patch is larger than that of the
2974 Med. A trace of the Fa is present as a small pit distal to the worn MMR, which is set low
2975 on the occlusal surface. Additionally, a short lingual portion of the transverse groove
2976 remains. Only trace expression of the mesiobuccal and distobuccal grooves are present,
2977 while the lingual face is featureless.

2978 Two roots are completely preserved, with a portion of alveolar bone remaining
2979 between them, and are covered in a cracked layer of cementum. There is a wide distal
2980 root and a smaller mesiobuccal root, which conforms to the 2R: D+MB configuration
2981 (Wood et al., 1988). In cross section, both roots are broader BL and compressed MD.
2982 Wide and shallow grooves run along the mesial face of the mesiobuccal root and along
2983 the distal face of the distal root. The roots are more widely spaced lingually than
2984 buccally. In buccal view, the mesiobuccal root is 14.5 mm tall and the distal root is 14.9
2985 mm tall.

2986

2987 U.W. 101-889: LP₃ (Fig. 31B; Table 1) Enamel chips are evident in the occlusal surface
2988 just above the distal IPF. Mesially, a small IPF (approximately 1.7 mm BL by 1.6 mm
2989 OC) is present in the center of the crown's height. The distal IPF is larger (approximately
2990 3.5 mm BL by 2.2 mm OC) and centered BL. The crown is minimally worn, with wear
2991 facets evident along the mesial and distal Prd crests and along the buccal portion of the
2992 talonid (stage 1). The crown is fully bicuspid with the Prd and Med separated by a well-
2993 defined MIg and the Med only slightly smaller in area than the Prd. The Med is less worn
2994 than the Prd and its preserved height nearly equals that of the Prd. The MMR is
2995 continuous, and the Fa parallels it to run from mesiobuccal to distolingual. The branch of
2996 the Fa lingual to the MIg is broader than the portion buccal to the MIg. The deepest point
2997 of the Fa is also offset lingual to the MIg. A minor accessory ridge originating from the
2998 mesial Prd crest helps to define the distal extent of the Fa. The essential ridges are nearly
2999 nonexistent. The talonid is flat and, though the area is worn, the DMR is not elevated as a
3000 crest distinct from the planar surface of the talonid. A local topographic high

3001 distobuccally suggests the presence of a cusplet. The mesiobuccal and distobuccal
3002 grooves are faint and both become imperceptible at mid-crown. The lingual face lacks
3003 grooves.

3004 The preserved roots are abraded on their external surfaces and broken at about
3005 half their maximum height. In lingual view, the mesial root is 6.8 mm in height and the
3006 distal root is 7.7 mm in height. Though broken, the configuration of the preserved roots
3007 suggests a smaller mesiobuccal root and a larger, broader distal root that are separated for
3008 at least part of their lengths, especially lingually. At the height where broken, the mesial
3009 and distal roots are joined into a single canal but likely would have separated nearer their
3010 apices. In buccal view, a cleft is apparent running longitudinally; here, the portion mesial
3011 to the cleft is broader than the section distal to it. In lingual view, the roots are more
3012 clearly separated. The preserved distal root is clearly compressed MD and broader BL.
3013 And, in mesial view, a buccal cant to the mesiobuccal root is evident.

3014 Based upon morphological similarities of the crown and root, this is the proposed
3015 antimeres of the P₃ in the U.W. 101-1014/377 mandible. If they are antimeres, wear
3016 asymmetry is evident. A wear facet along the U.W. 101-889 mesial Prd crest is absent on
3017 U.W. 101-377. Further, this specimen articulates reasonably well with the U.W. 101-
3018 1076 mandibular canine, which is consistent with the hypothesis that these isolated teeth
3019 belong to the same biological individual as U.W. 101-377/1014.

3020

3021 U.W. 101-1565: LP₃ (Fig. 31C; Table 1) There is a moderately-size distal IPF (3.1 mm
3022 BL by 3.2 mm OC) and no mesial IPF. Wear facets are visible on the Prd near the apex
3023 and along the Prd crests, especially along the buccal aspect of the mesial Prd crest (stage

3024 1). The crown is fully bicuspid and a deep MIg separates the smaller and slightly shorter
3025 Med from the broader and taller Prd. The Med sits only slightly mesial to the Prd. The
3026 MMR is low and narrow, set low on the occlusal surface, continuous from the mesial
3027 crests of the Med and Prd, and encloses a small Fa that appears as a narrow BL-oriented
3028 groove paralleling the MMR and bounded distally by mesial accessory ridges extending
3029 from the cusps. The essential ridges are not well defined. The talonid is planar and slopes
3030 up to the DMR, which is not detectable as a distinct feature, except for a short segment
3031 distolingually near the distal Med crest. The talonid is delineated from the trigonid by a
3032 deep transverse groove, which extends buccally to define a small distobuccal cuspule.
3033 This cuspule is associated with a short, shallow distobuccal groove that fades before mid-
3034 crown. The mesiobuccal groove is faint and only visible close to the occlusal rim. The
3035 distal buccal groove is shallow and extends about halfway down the buccal face before it
3036 becomes imperceptible. The lingual face is featureless.

3037 The root(s) is broken near the cervix and sediment fills in the exposed canal. The
3038 maximum preserved root height, 3.6 mm, is preserved distolingually.

3039 This specimen is morphologically similar to U.W. 101-298 and is proposed as its
3040 antimere. However, U.W. 101-298 lacks the distal IPF that is evident on U.W. 101-1565.
3041 Though such asymmetry in eruption is not unexpected, alternatively, U.W. 101-1565 may
3042 represent a slightly more ontogenetically advanced individual.

3043

3044 3.22. *Permanent mandibular fourth premolars*

3045 Three isolated P_{4s} and those found in situ in the U.W. 101-001, U.W. 101-377,
3046 and U.W. 101-1261 mandibles collectively represent at least four individuals in the

3047 Dinaledi Chamber deposits. The P₄s are all similar and subtly differ from the P₃s in
3048 crown and root morphology. Like the P₃s, the P₄ crowns are bicuspid, with the two cusps
3049 separated by a longitudinal groove, and the talonid is relatively broad. In contrast to the
3050 P₃s, the P₄s tend to be MD shorter and more rounded in occlusal profile. The morphology
3051 of the roots is not well represented in the isolated specimens but, where preserved, they
3052 tend to depart from the P₃s. The U.W. 101-887 P₄ is single rooted, while U.W. 101-383 is
3053 multirooted, with a mesial root that is more plate-like than observed in the P₃s.

3054

3055 U.W. 101-184: LP₄ (Fig. 32A; Table 1) The crown is unworn and no IPFs are detectable
3056 (stage 1). The crown is noticeably BL broadest across the cusp apices and its rounded
3057 profile tapers distally. The Prd and Med are separated by a well-defined MIg. The Med is
3058 smaller in area than, but equal in height to, the Prd. The cusp apices are nearly aligned
3059 transversely, with the Med set slightly mesial to the Prd. The MMR is limited to a small
3060 area just mesial to a pit-like Fa; the buccal and lingual MMR segments are separated by a
3061 narrow groove. The Prd possesses three occlusal ridges that are very similar in
3062 expression, with the essential ridge the narrowest and sharpest of the three. The distal
3063 accessory ridge is thicker, and rounder and it terminates at the MIg. The essential ridge of
3064 the Med is not well delineated from the rest of the cusp. The Med has a thin distal
3065 accessory crest that originates mid-cusp and terminates at the MIg. The MIg is deep and
3066 runs from the mesial border to the transverse groove that separates the Prd and Med from
3067 the talonid. The transverse groove extends the width of the crown spilling over to the
3068 buccal and lingual faces. Both buccally and lingually, this groove bifurcates to form
3069 small distobuccal and distolingual cusplets. The distobuccal cusplet is larger and better

3070 defined by deeper grooves than is the distolingual cusplet and it is separated from the
3071 mass of the Prd by the extension of the transverse groove. The surface of the talonid
3072 slopes up distally from the transverse groove but the DMR is indistinct. There is no
3073 mesiobuccal groove and the distobuccal groove is shallow and becomes imperceptible at
3074 mid-crown. There is no mesiolingual groove but a small and shallow distolingual groove
3075 is evident adjacent to the distolingual cusplet.

3076 Given the absence of occlusal and interproximal wear, the crown was likely
3077 erupting at the time of death and the roots were incompletely developed. As preserved,
3078 the root(s) are broken just inferior to the cervix so that a maximum of 4.3 mm of root
3079 extends below the crown mesially and 3.2 mm extends below the cervix buccally.
3080 Sediment fills the exposed root canal. A single root canal is exposed, but clefts are
3081 present along the buccal and lingual faces of the root mass.

3082 This specimen is a reasonable antimere of U.W. 101-383. They are
3083 morphologically similar, and both lack occlusal and interproximal wear. This specimen
3084 does bear some similarities to P_{3s} in the assemblage but differs in the relative height of
3085 the Med, the placement of the Med mesial to the Prd, and in the presence of a discernible
3086 distobuccal cusp, which is absent in the unequivocal P_{3s}. It also differs from P_{3s} in the
3087 absence of a mesiobuccal groove, and in the crown outline, which is rounded and tapers
3088 distally.

3089

3090 U.W. 101-383: RP₄ (Fig. 32B; Table 1) The crown is unworn, but the Prd apex is
3091 damaged, reducing its height (stage 1). The bulk of the Med, and its apex, are situated
3092 slightly mesial to the Prd. The Prd is larger in area, but the Med is slightly higher as

3093 preserved. The Fa is a pit extending to a short BL-oriented groove situated between the
3094 MMR and the Prd mesial accessory ridge. Its deepest point is in the crown center at the
3095 intersection with Mlg. The MMR is low and rounded, with its buccal and lingual
3096 segments meeting at an angle at the center of the crown. In mesial view, the MMR is
3097 lower than the mesial accessory ridges. The Med lacks a distinct essential ridge, while the
3098 essential ridge of the Prd is equal in width to, but slightly lower in relief than, the mesial
3099 and distal accessory ridges. The Med also has a distal accessory ridge, but it is shorter
3100 and thinner than that of the Prd. The talonid is separated from the trigonid by a deep
3101 transverse groove that is divided into lingual, distal, and buccal components. The buccal
3102 component comprises a small distobuccal cusplet bounded mesially and distally by
3103 occlusal grooves that extend over onto the buccal face. The mesial groove becomes the
3104 distobuccal groove, which fades about half the distance to the cervix. The distal groove
3105 terminates shortly after crossing the occlusal rim. The distal portion of the talonid is not
3106 well defined, but it does possess a ridge and associated furrows that terminate at the
3107 transverse groove. The lingual portion of the talonid takes the form of a small, but
3108 palpable, distolingual cusplet that is not defined by occlusal grooves. There is no distinct
3109 DMR. The lingual face is featureless. In addition to the distobuccal groove, a shallower
3110 mesiobuccal groove is also visible on the buccal face but it does not cross the occlusal
3111 rim.

3112 From photos taken shortly after excavation when still covered in the sediment, the
3113 roots were more complete and it appears that this specimen is multi-rooted, with plate-
3114 like mesial and distal roots. As it exists at the time of description, the root is almost
3115 entirely broken away at the cervix, with the largest remaining portions present mesially

3116 and buccally. From the mesial cervix, the maximum preserved root height is
3117 approximately 5.0 mm and from the buccal cervix the maximum height is 4.2 mm. An
3118 associated, but detached, 5.4 mm root fragment fits cleanly onto the distal side.
3119 Additional undescribed root fragments are also associated with this specimen.

3120 This specimen is a reasonable antimere of U.W. 101-184. They are similar in
3121 crown morphology and in their absence of occlusal and interproximal wear.

3122

3123 U.W. 101-887: LP₄ (Fig. 32C; Table 1) IPFs are centered mesially (3.5 mm BL by 2.3
3124 mm OC) and offset lingually (3.8 mm BL by 2.1 mm OC) on the distal face. Occlusal
3125 wear is minimal, with a small wear facet visible along the buccal aspect of the mesial Prd
3126 crest (stage 1). The Med is smaller in area but nearly equal in height to the Prd. The apex
3127 of the Med is placed slightly mesial to that of the Prd and a well-defined MIg separates
3128 the cusps. The MMR is low, but continuous, between the mesial crests of the Med and
3129 Prd and encloses a small Fa. The Fa appears as a groove situated mostly mesiobuccally,
3130 with a fainter extension lingually, and its deepest point is in the center of the crown's BL
3131 axis. A rounded accessory ridge running from the mesial Prd crest is matched by a
3132 swelling on the mesial aspect of the Med and these ridges bound the Fa distally. The Med
3133 and Prd have weakly expressed essential ridges. The talonid is broad, with shallow
3134 grooves radiating up the DMR, which is only slightly topographically distinct from the
3135 sloping surface of the talonid. A faint distobuccal cusplet pokes up from the DMR. The
3136 mesiobuccal groove is shallow and becomes imperceptible approximately one third of the
3137 way down the crown face. The distobuccal groove is also shallow, though deeper than the

3138 mesial, and becomes indistinct about a third of the way down the crown face. The lingual
3139 face is featureless.

3140 The root is abraded across its external surface and broken so that approximately
3141 8.4 mm of its height is preserved buccally. Though broken, the root was apparently
3142 singular and is MD longer along the lingual margin than along its buccal margin, which
3143 gives the root a rounded triangular shape in cross section.

3144 The mesial facet of U.W. 101-887 is reasonably congruent with the distal IPF of
3145 U.W. 101-889. Further, the RP₄ of U.W. 101-377 is proposed as the antimeres of this
3146 specimen. The teeth are nearly identical in occlusal morphology, their state of occlusal
3147 wear, and in the morphology of their roots. The hypothesis that U.W. 101-887 and U.W.
3148 101-889 belong to the same individual is also reasonable, as both are proposed to have
3149 antimeres in the U.W. 101-377 mandible.

3150

3151 *3.23. Permanent mandibular first molars*

3152 Eight isolated M₁s are known from the Dinaledi Chamber. Additionally, a
3153 developing M₁ crown was recovered from its exposed crypt in the U.W. 101-1400
3154 mandible and the U.W. 101-001, U.W. 101-377, and U.W. 101-1261 mandibles retain
3155 M₁s. Collectively, these teeth represent a minimum of eight individuals. The M₁s present
3156 a consistent morphology. The five principal cusps are present, the Fa is not bounded
3157 distally by a midtrigonid crest, supernumerary cusps are absent, the mesial buccal groove
3158 is a cleft at the occlusal margin, and the distal buccal groove is shallow. The protostylid is
3159 either absent or a faint crest restricted to the mesiolingual corner of the crown. The two
3160 roots are plate-like.

3161

3162 U.W. 101-285: RM₁ (Fig. 33A; Table 1) Mesially, a large bean shaped IPF (3.0 mm OC
3163 by approximately 5.0 mm BL) is present. Distally, no IPF is detectable. Wear facets are
3164 visible on all five cusps and most occlusal ridging has been removed through wear;
3165 though, dentine is only exposed as a small pinpoint at the tip of the Prd (stage 2). The
3166 crown is a rounded rectangle with the talonid and trigonid nearly equal in breadth. The
3167 large mesial IPF has made the mesial margin concave, while the lingual profile is nearly
3168 straight, and the buccal profile is bilobed as the result of a deep mesiobuccal groove. The
3169 large Hld forms a rounded distobuccal contour. Only the five primary cusps are present,
3170 and their relative sizes are Hyd > Prd > Med > Hld ≥ End. The crown has a Y-5 fissure
3171 pattern, with the Med and Hyd in contact. The central groove is contiguous with the Fa,
3172 which is manifest only as a short groove limited to the Med. The apparent size of the
3173 MMR is reduced by the encroachment of the large mesial IPF. The distal aspects of the
3174 Hyd and Hld form a continuous crest that borders a fovea-like cleft on the distobuccal
3175 aspect of the crown. The DMR is short and worn on its buccal extent. A faint protostylid
3176 is restricted to the mesiobuccal corner where it is angled obliquely and distally and then
3177 turns towards the cervix disappearing at approximately mid-crown well before
3178 intersecting the mesiobuccal groove. The mesiobuccal groove is deep and narrow near
3179 the occlusal surface and at mid-crown becomes wider and shallower while continuing to
3180 the cervix. A shallow distobuccal groove terminates nearer the occlusal surface. The
3181 distolingual groove is only a faint depression occlusally, while the mesiolingual groove,
3182 which is placed slightly distal to the mesiobuccal groove, is a broad shallow depression
3183 near the occlusal margin.

3184 The roots are broken so that a maximum of 2.0 mm remains on the mesiobuccal
3185 side. Sediment stains the broken surface and fills in the exposed pulp chamber.

3186 This specimen is proposed as the antimere of U.W. 101-582 to which it is
3187 comparable in size, morphology, and its stage of occlusal and interproximal wear. The
3188 two crowns due differ slightly in the configuration of the distobuccal groove, which
3189 terminates at a pit in U.W. 101-582 but continues as a shallow groove in U.W. 101-285.

3190

3191 U.W. 101-297: RM₁ (Fig. 33B; Table 1) Enamel chipping is evident along the DMR
3192 above the distal IPF and on the buccal side of the Hyd. IPFs are present mesially (5.0 mm
3193 BL by 2.8 mm OC) and distally (5.2 mm BL by 3.2 mm OC). Moderate sized patches of
3194 dentine are exposed over each of the five principal cusps (stage 4). The talonid is slightly
3195 wider than the trigonid and the crown outline is roughly rectangular. Significant
3196 interproximal wear resulted in concave mesial and straight distal profiles. The crown has
3197 a Y-5 fissure pattern, with a substantial portion of the Med and Hyd in contact and a well-
3198 developed Hld; there is no evidence from the preserved topography or the pattern of
3199 grooves to suggest the presence of a C6 and a C7 is absent. Much of the occlusal
3200 topography is removed by wear, but a faint remnant of the Fa remains as pit mesiobuccal
3201 to the Med and just distal to the worn MMR. A weakly expressed protostylid presents as
3202 a shallow depression and indistinct crest limited to the mesiobuccal aspect of the Prd. The
3203 crest likely had its origin at the MMR, from which it is angled distocervically. The
3204 mesiobuccal groove is deep and cleft-like near the occlusal margin; it becomes wider and
3205 shallower as it extends to the cervix. The distobuccal groove is shallower and disappears
3206 approximately one third of the way down the crown face. The lingual grove is situated

3207 slightly distal to the mesiobuccal groove; it is shallow and becomes imperceptible at mid-
3208 crown.

3209 The mesial root is nearly completely preserved except for the apex of the buccal
3210 radical. The distal root is broken away at the cervix so that less than 1.0 mm of its height
3211 remains. The exposed break is stained by matrix. The mesial root measures 14.3 mm in
3212 height buccally and 15.8 mm lingually. Its maximum BL breadth, approximately at mid-
3213 root, is 11.1 mm. In mesial view, the mesial root is vertically oriented, while in buccal
3214 and lingual view it has a subtle distal tilt, especially apically. The circular buccal and
3215 lingual canals of the mesial root are joined by a thin isthmus for about two-thirds of their
3216 length until the isthmus closes and the root canals become individuated, giving the root a
3217 dumbbell shape in cross section. Externally, broad gutters extend the length of the mesial
3218 and distal faces.

3219 This specimen is similar morphologically and in its state of wear to its proposed
3220 antimere, U.W. 101-905.

3221

3222 U.W. 101-582: LM₁ (Fig. 33C; Table 1) A large mesial IPF (5.7 mm BL by 3.5 mm OC)
3223 extends to the occlusal margin. There is no distal IPF. Wear facets are evident on all five
3224 cusps and has removed most of the detail of occlusal ridging (stage 2) and the mesial face
3225 is concave as a result of interproximal wear. In occlusal view, the crown is roughly
3226 rectangular in outline, with the centrally placed Hld forming the rounded distal contour.
3227 The talonid and trigonid are nearly equally broad BL. The crown has a Y-5 fissure
3228 pattern, with a substantial portion of the Med and Hyd in contact and a well-developed
3229 Hld. The relative cusp sizes are Hyd > Prd > Med > Hld ≥ End. The deep central groove

3230 is contiguous with the Fa as it curves around mesial to the Med. There is no evidence of a
3231 buccal branch of the Fa. The mesial IPF has mostly removed the MMR. The partially
3232 preserved DMR is low and rounded. The protostylid takes the form of a faint but palpable
3233 obliquely oriented ridge that is restricted to the mesiolingual corner of the Prd. It ends at
3234 approximately mid-crown and is independent of the mesiobuccal groove. The
3235 mesiobuccal groove is a deep, narrow cleft that widens at mid-crown and then deepens
3236 again near the cervix. The distobuccal groove is broader than the mesiobuccal groove and
3237 is restricted to the occlusal third of the crown where it terminates in a pit created by a
3238 short cingular crest passing between the End and Hld. The mesiolingual groove, which is
3239 placed slightly distal to the mesiobuccal groove, is a faint depression near the occlusal
3240 margin. The distolingual groove is a faint depression near the occlusal rim.

3241 Plate-like mesial and distal roots are present. The vertically oriented mesial root is
3242 broken at the apices of the lingual and buccal radicals. A broad central gutter runs along
3243 the mesial root. As preserved, the lingual side of the mesial root is 12.1 mm in height,
3244 while the buccal side is 9.9 mm in height. The maximum breadth of the mesial root is
3245 11.4 mm. The buccally angled distal root is a broad oval and with a single canal exposed
3246 by a break near its apex. As preserved, the buccal side of the distal root is 10.0 mm in
3247 height and the lingual side is 10.6 mm. The maximum breadth of the distal root is
3248 approximately 9.0 mm. Further details of root morphology are provided by the μ CT-
3249 based analysis of Kupczik et al. (2019).

3250 Based upon similarities in morphology and the state of occlusal and interproximal
3251 wear, this is proposed as the antimere of U.W. 101-285. The two crowns do differ
3252 subtly in the configuration of their distobuccal grooves.

3253

3254 U.W. 101-809: LM₁ (Fig. 33D; Table 1) Enamel chipping is evident along the mesial and
3255 distal margins and on the Hyd near the cusp apex. There is a large, deeply excavated,
3256 mesial IPF (5.0 mm BL by 3.5 mm OC) that extends to the occlusal surface and a faint
3257 distal IPF. Wear facets are evident on all principal cusps and a small dentine pit is
3258 exposed on the Prd apex (stage 2). The lingual crown is not indented by a lingual groove,
3259 the trigonid and talonid are nearly equally broad BL so that the crown does not taper until
3260 it reaches the distally rounded Hld. Five principal cusps are oriented in a Y-5 fissure
3261 pattern, with a substantial portion of the Med and Hyd in contact. The relative cusp sizes
3262 are Hyd > Prd > Med > Hld > End. Wear has flattened the essential ridges and removed
3263 any accessory ridges that may have been present. However, a Med distal accessory ridge
3264 can be inferred from a weak occlusal groove. This accessory ridge is likely not associated
3265 with a C7 as a similar configuration is evident in the unerupted U.W. 101-1400 and U.W.
3266 101-1689 M_{1s} (Figs. 34C and 34D) where the ridge rises to meet a postmetaconulid along
3267 the distal metaconid crest. Wear precludes assessment of the MMR, but the lingual extent
3268 of a fissure-like Fa remains and is contiguous with the deep central groove. A small Fp is
3269 formed between the DMR and the End distal lobe. The protostylid is a moderate oblique
3270 crest limited to the mesiobuccal crown face that disappears before reaching the
3271 mesiobuccal groove. The mesiobuccal groove crosses the occlusal edge as a deep and
3272 narrow cleft, becomes shallow about mid-crown, and then deepens again just above the
3273 cervix. The distobuccal groove is also deep and narrow near the occlusal edge but
3274 disappears at mid-crown. The mesiolingual groove is distal to the mesiobuccal groove. It

3275 crosses the occlusal margin as a narrow and shallow groove, fading at mid-crown. The
3276 distal lingual groove is a wide, shallow indentation restricted to the occlusal margin.

3277 The crown has plate-like mesial and distal roots with a small portion of alveolar
3278 bone wedged between them. The roots are abraded and broken near the apices. In buccal
3279 view, the preserved mesial root height is 10.5 mm, while in buccal view the maximum
3280 preserved height of the distal root is 9.1 mm. In mesial view, the maximum breadth of the
3281 mesial root is 10.5 mm and in distal view the maximum breadth of the distal root is 8.2
3282 mm. Both roots have a slight distal deflection. The mesial root is dumbbell shaped in
3283 cross section with wide shallow depressions running along the mesial and distal faces.
3284 The distal root is a broad oval in cross section and is narrower than the mesial root. The
3285 distal root is offset slightly buccal to the crown.

3286 Based on similarities in morphology and the state of occlusal wear, this is a
3287 reasonable antimere of the RM₁ preserved in the U.W. 101-377/1014 mandible. The
3288 small distal IPF of this specimen is also congruent with the mesial facet of U.W. 101-789.
3289 This mesial IPF of this specimen also fits well with the distal IPF of U.W. 101-887. The
3290 association of U.W. 101-789, -809, and -887 is also reasonable because each is
3291 hypothesized to have an antimere in the U.W. 101-377 mandible. This specimen and
3292 U.W. 101-814, both LM₁s, are nearly identical in their degree of occlusal wear, with
3293 U.W. 101-809 possessing a distal IPF, which is lacking in U.W. 101-814. These
3294 specimens, of similar ontogenetic status, illustrate the difficulty in associating isolated
3295 teeth based on expected patterns of occlusal wear.

3296

3297 U.W. 101-814: LM₁ (Fig. 33E; Table 1) Chipping is present on the End apex and along
3298 the mesial margin. There is a large, convex mesial IPF (5.5 mm BL by 3.3 mm OC) that
3299 extends to the occlusal surface. There is no distal IPF. Wear facets are evident on all
3300 cusps and a small dentine pit is exposed on the Prd apex (stage 2). The crown outline has
3301 a straight lingual profile, a bi-lobed buccal profile, and a concave mesial margin. The
3302 large Hld sits just buccal to the center of the tooth's axis and forms the rounded distal
3303 profile. The crown has five well developed cusps arranged in a Y-5 fissure pattern, with a
3304 substantial portion of the Med and Hyd in contact. The relative cusp sizes are Hyd > Prd
3305 \geq Med > End \geq Hld. The talonid is wider than the trigonid. Wear has flattened the
3306 essential ridges and removed any accessory ridges that may have been present. Wear
3307 precludes assessment of the MMR, but the lingual extent of a fissure-like Fa remains and
3308 is contiguous with the deep central groove and limited to the mesial Med. It is bordered
3309 distally by Prd and Med ridges. The Fp is partially obscured by wear, but is a short
3310 fissure bordered distally by a broad and rounded DMR that sits low on the crown. There
3311 is no indication of a protostylid. The mesiobuccal groove crosses the occlusal edge as a
3312 deep and narrow cleft, becomes shallow about mid-crown and then deepens again just
3313 above the cervix. The distobuccal groove is also a deep cleft near the occlusal surface;
3314 however, it terminates as a pit and small shelf about one third of the way down the crown
3315 face. The mesiolingual groove is distal to the mesiobuccal groove. It is narrow and
3316 shallow before it fades away about mid-crown. The distolingual groove is a faint
3317 depression near the occlusal margin.

3318 The crown has plate-like mesial and distal roots with a small portion of alveolar
3319 bone wedged between. Both roots are broken near their apices; additionally, there is

3320 significant abrasion on all but the mesial root surfaces. In buccal view, the preserved
3321 mesial root measures 10.1 mm and the distal root 9.2 mm in height. The maximum
3322 breadth of the mesial root is 9.4 mm, and the maximum breadth of the distal root is just
3323 below the cervix and is 7.9 mm. The mesial root is vertically oriented, and dumbbell
3324 shaped in cross section, with wide, shallow depressions running along the mesial and
3325 distal faces. The distal root is more figure-of-eight shaped in cross section because it does
3326 not pinch in as extensively as the mesial root does. The distal root angles slightly
3327 buccally relative to the mesial root.

3328

3329 U.W. 101-905 + U.W. 101-294: LM₁ crown and associated root (Fig. 34A; Table 1)

3330 Enamel chipping lines the crown distally. Another, especially large chip is present on the
3331 occlusal margin distolingually, where it extends onto the crown face. Occlusally, a crack
3332 runs from the mesiolingual corner and passes through the dentinal exposures at the Med,
3333 Prd, Hyd, and Hld to terminate at the large distolingual enamel chip. The crack does not
3334 displace enamel or distort the morphology of the crown. Interproximal wear excavated
3335 deeply into the mesial margin, creating a concave facet, and the distal contour is also
3336 squared off by interproximal wear. Pools of uncoalesced dentine are exposed over the
3337 Prd, Med, and Hyd, and a very small pit is present on the Hld (stage 4). The preserved
3338 occlusal profile is roughly rectangular, with the Hld centrally placed in the crown's axis.
3339 The crown is slightly broader BL across the distal cusps than across the mesial. The
3340 crown has a Y-5 fissure pattern, with a substantial portion of the Med and Hyd in contact,
3341 and a well-developed Hld. The Fa and Fp are mostly obliterated by wear, with only the
3342 slightest remnant of the Fa remaining mesiobuccal to the Med apex. A weak protostylid

3343 is evident mesiobuccally as a faint crest. A remnant of the cleft of the mesiobuccal
3344 groove sits near the occlusal margin and then it opens up immediately and continues to
3345 the cervix as a broader indentation. The distobuccal groove is also deep at the preserved
3346 occlusal margin; though, it terminates at mid-crown. The lingual groove is set slightly
3347 distal to the mesiobuccal groove and is a shallow indentation across its entire preserved
3348 course.

3349 The roots are broken away near the cervix. The associated mesial root, recovered
3350 separately and catalogued as U.W. 101-294, is preserved as a detached fragment (not
3351 figured). The root has distinct rounded canals buccally and lingually that are connected
3352 by a narrow chamber stretching between them. A broad gutter is present along the mesial
3353 surface of the root. When refit, in buccal view the preserved root is 12.7 mm in height.
3354 The maximum breadth of the root is approximately 10.9 mm.

3355 Based upon similarities in crown morphology and wear state, this is a reasonable
3356 antimere for U.W. 101-297.

3357

3358 U.W. 101-1287B: RM₁ (Fig. 34B; Table 1) Enamel chipping is evident along the mesial
3359 and distal margins. The mesial IPF is large and concave (6.0 mm LaL by 2.7 mm OC),
3360 while the distal IPF is larger (7.3 mm LaL by 3.8 mm OC) and flattened the distolingual
3361 face. Both IPFs reach the occlusal edges. Large pools of dentine are exposed over each of
3362 the five principal cusps, with some coalescence between those of the Med and Prd (stage
3363 4). The crown has a rectangular profile modified by interproximal wear. The buccal
3364 profile is bilobed while the lingual profile is smooth. The talonid is wider than the
3365 trigonid. Very little occlusal morphology remains. The mesiobuccal groove is preserved

3366 as a deep, narrow cleft at the occlusal margin that becomes wider and slightly shallower
3367 as it reaches the cervix. The distobuccal and lingual grooves remain as shallow features
3368 near the occlusal margin.

3369 A portion of alveolus remains between the mesial and distal roots. The roots are
3370 complete, but their surfaces are abraded. The mesial root is wide and plate-like with two
3371 distinct radicals that bifurcate into separate apices. A shallow and broad depression runs
3372 between the rounded buccal and lingual root margins. The distal root also has two
3373 radicals, although they are less distinct. It is a broad oval in cross section. The mesial and
3374 distal roots deflect distally, running parallel to each other. In buccal view, the maximum
3375 height of the mesial root is 13.8 mm and that of the distal root measured buccally is 12.0
3376 mm.

3377 This tooth fits into the M₁ alveolus preserved in the U.W. 101-1142 mandible.
3378 Further, the distal IPF of U.W. 101-1287B perfectly matches the mesial IPF of the U.W.
3379 101-1142 M₂. This specimen is incorrectly published as U.W. 101-1304 in Berger et al.
3380 (2015: Supplemental File 1) and in the analysis of Odes et al. (2018). Despite sharing an
3381 accession number based on the spatial proximity of their recovery, this specimen and
3382 U.W. 101-1287A (LdC¹) cannot represent the same biological individual, as U.W. 101-
3383 1287B belongs to an individual with a completely erupted and worn permanent dentition,
3384 while U.W. 101-1287A represents a young subadult with light wear on its deciduous
3385 canines.

3386

3387 U.W. 101-1400: LM₁ germ (Fig. 34C; Table 1): This is a nearly complete crown with no
3388 trace of root development. The crown was in situ in its exposed crypt in the U.W. 101-

3389 1400 mandible at the time of excavation. In occlusal view, the crown is roughly
3390 pentagonal, with a straight lingual profile and bi-lobed buccal profile. The talonid is
3391 slightly wider than the trigonid. The crown has a Y-5 fissure pattern, with a substantial
3392 portion of the Med and Hyd in contact, and a well-developed Hld. The relative cusp sizes
3393 are Med > Hyd > Prd > End > Hld. The Hld is placed near the center of the crown's BL
3394 axis and forms the rounded distal contour. The essential lobes are well-developed but not
3395 associated with well-defined ridges. The Hy essential ridge widens mid-cusp, expanding
3396 into a triangular feature before it terminates. The End essential ridge bifurcates before
3397 reaching the occlusal basin. The distal accessory ridge of the Med is well developed,
3398 resulting in an incipient postmetaconulid. The MMR is lower than the essential ridges of
3399 the Pr and Med and its buccal and lingual components form a v-shape where they meet
3400 mesial to the Med. A small Fa is bordered mesially by the MMR and distally by weak
3401 mesial accessory ridges of the Prd and Med. The accessory ridges meet at the Mlg but do
3402 not form a mesial trigonid crest. A moderately sized Fp is bordered distally by the DMR
3403 and mesially by the occlusal ridges on the Hld and End. The protostylid is a faint,
3404 obliquely oriented crest on the mesiobuccal aspect of the Prd that terminates well before
3405 the mesiobuccal groove. The mesiobuccal groove is a narrow and deep cleft at the
3406 occlusal margin that becomes shallow at mid-crown and then deepens again just above
3407 the cervix. The distobuccal groove is deep and narrow and slightly shorter than the
3408 mesiobuccal groove. The lingual groove is situated distal to the mesiobuccal groove. It is
3409 very shallow and fades away at mid-crown.

3410 Based on shared morphology and developmental status, this is the antimere of
3411 U.W. 101-1689.

3412

3413 U.W. 101-1689: RM₁ germ (Fig. 34D; Table 1) The crown is nearly complete and there is
3414 no trace of root development. There is minor damage to the cervix distolingually. In
3415 occlusal view, the crown is roughly pentagonal with a straight lingual profile and bi-
3416 lobed buccal profile. The crown has a Y-5 fissure pattern, with a substantial portion of
3417 the Med and Hyd in contact, and a well-developed Hld, which is offset slightly buccal to
3418 mid-crown. The relative cusp sizes are Med > Prd = Hyd > End > Hld. The MMR is low
3419 and comprises a small cuspule that is delineated by shallow mesial grooves. It forms the
3420 mesial border of a short, groove-like Fa, which is bound distally by weak Prd and Med
3421 mesial accessory ridges. The Prd also has a distal accessory ridge. The Med essential
3422 crest is well defined near the apex and widens into a triangular feature towards the
3423 occlusal basin. The distal lobe of the Med is well developed. The Hyd terminates in a
3424 tubercle-like ridge at the occlusal basin. The essential ridge of the End is moderately
3425 developed. The groove-like Fp is bounded distally by a bipartite DMR and mesially by
3426 the Hld and End occlusal ridges. The protostylid is a faint oblique ridge confined to the
3427 mesiobuccal aspect of the Prd. Both the mesiobuccal and distobuccal grooves are deep
3428 and narrow clefts near the occlusal margin. The distobuccal groove fades at mid-crown,
3429 while the mesiobuccal groove continues to the cervix as a shallow groove. The lingual
3430 groove is deep and narrow at the occlusal margin but quickly becomes shallow on the
3431 lingual face. It is distal to the mesiobuccal groove. This is the antimere of the LM₁
3432 preserved in its crypt in the U.W. 101-1400 mandible.

3433

3434 *3.24. Permanent mandibular second molars*

3435 Six isolated M₂s and those present in the U.W. 101-001, U.W. 101-361, U.W.
3436 101-377, U.W. 101-1142, and U.W. 101-1261 mandibles represent at least nine
3437 individuals. The M₂ crown is rectangular in occlusal outline, with straight mesial and
3438 lingual margins, mildly bi-lobed buccal profile, and a rounded distal profile with a large
3439 Hld offset slightly buccal to the center of crown. The five principal cusps are present with
3440 a Y-5 fissure pattern. The occlusal surface is simple: supernumerary cusps are absent,
3441 essential ridges are not well defined, and the protostylid is either absent or a weak crest
3442 restricted to the mesiobuccal corner of the crown.

3443

3444 U.W. 101-145: LM₂ (Fig. 35A; Table 1) No wear facets are visible on the occlusal
3445 surface (stage 1) and IPFs are not present mesially and distally. Thus, it is likely
3446 unerupted, or at least not in functional occlusion, at the time of death. There are small
3447 developmental pits at the Hyd and End apices. Aside from minor damage at the cervical
3448 line lingually and distobuccally, the crown is complete. The crown is roughly rectangular
3449 in occlusal profile, with straight mesial and lingual margins, mildly bi-lobed buccal
3450 profile, and a rounded distal profile with a large Hld offset slightly buccal to the center of
3451 crown. Only the five principal cusps are present, and the crown has a Y-5 fissure pattern.
3452 A substantial portion of the Med and Hyd are in contact and the Hld is relatively large.
3453 The relative cusp proportions are Med > Prd ≥ Hyd > End > Hld. The essential ridges are
3454 not well defined, being thick and rounded. Those of the Prd and Med do not join to form
3455 any type of trigonid crest. The Prd and End each have a faint mesial accessory ridge. On
3456 the Prd, this ridge is separated from the essential ridge by a groove. The Med and Hyd
3457 each have a faint distal accessory ridge. The MMR is low and rounded and bordered

3458 distally by a small Fa that is continuous with the MIg. The Fa is short and BL-oriented
3459 and positioned between the Prd mesial accessory ridge and the bulbous Med essential
3460 ridge, with a slight topographical divide separating the shorter buccal arm from the longer
3461 lingual arm. The buccal groove forms a deep v-shaped cleft occlusally that becomes
3462 shallow at mid-crown as it continues to the cervix. The distobuccal groove is a distinct,
3463 yet shallower, groove rather than a cleft; it becomes imperceptible at mid-crown. There is
3464 only a faint suggestion of the protostylid, and it is limited to the mesiolingual aspect. It
3465 begins as a barely perceptible vertically oriented swelling that then curves distally to
3466 become indistinct under the Prd apex. The lingual groove sits slightly distal to the buccal
3467 groove, is shallow across its course, and fades at mid-crown. The developing roots are
3468 broken off so that only a small sliver remains buccally.

3469 Based on shared morphology and degree of occlusal wear, this is proposed as the
3470 antimere of U.W. 101-507.

3471

3472 U.W. 101-284: LM₂ (Fig. 35B; Table 1) Enamel chips are present along the marginal
3473 ridges and at the apex of the End. A large mesial IPF (5.5 mm BL by 3.4 mm OC) is
3474 centered on the crown and extends to the occlusal margin. The distal IPF (4.0 mm BL by
3475 3.2 mm OC) is distobuccally oriented and does not extend to the occlusal margin. Wear
3476 facets are visible on the occlusal surface, but no dentine is exposed (stage 1). In occlusal
3477 view, the width of the talonid and trigonid are approximately equal. The profile is a
3478 rounded rectangle, with a nearly straight lingual profile and bilobed buccal profile. The
3479 mesial margin is concave as the result of interproximal wear and distal interproximal
3480 wear squared off the once projecting Hld. The crown has a Y-5 fissure pattern, with a

3481 substantial portion of the Med and Hyd in contact and a well-developed Hld. No
3482 accessory cusps are observed. In relative size, the cusps are Hyd > Prd > Med > End >
3483 Hld. The MMR is set low, and its apparent size has been reduced by the mesial IPF and
3484 occlusal wear. The essential ridges, and nearly all accessory ridges that may have been
3485 present, have been removed by occlusal wear. The exception is the Prd mesial accessory
3486 ridge, which defines the distal border of a short branch of the Fa, and its associated
3487 groove. The Fa is not well defined and is mostly manifest as an extension of the central
3488 groove as it curves around the Med. A deep central groove separates the Prd and Med and
3489 no middle-trigonid crest was present. The protostylid is limited to the mesiolingual aspect
3490 of the Prd. It appears as a faint, but palpable, swelling that begins near the MMR as a
3491 vertically oriented crest and then traverses obliquely to become indistinct under the Prd
3492 apex. The mesiobuccal groove is deep at the occlusal surface and then becomes shallow
3493 at mid-crown as it travels to the cervix. The distobuccal groove is much shallower and
3494 fades at mid-crown. The lingual groove is set slightly distal to the mesiobuccal groove
3495 and is a shallow indentation at the occlusal surface.

3496 The roots are broken away near the cervix. The break is angled so that almost
3497 nothing of the roots remains below the lingual side, but approximately 3.3 mm of the
3498 mesial root and 3.2 mm of the distal root are preserved buccally. The broken surface is
3499 stained by matrix, suggesting that the break was ancient.

3500

3501 U.W. 101-507: RM₂ (Fig. 35C; Table 1) This is an unworn crown (stage 1). In occlusal
3502 view, the crown is roughly rectangular in profile with trigonid and talonid equal in width
3503 and a rounded distal profile formed by the projecting Hld. The crown has a Y-5 fissure

3504 pattern, with a substantial portion of the Med and Hyd in contact and a well-developed
3505 Hld. The relative cusp sizes are Med > Prd \geq Hyd > End > Hld. The mesial occlusal
3506 ridges of the Prd and Med join to form a thick rounded MMR that defines the mesial
3507 border of a groove-like Fa. The Fa is mostly limited to the Prd but extends a short
3508 distance lingually onto the Med. The Med essential ridge deflects sharply distally to form
3509 a deflecting wrinkle, but it does contact the End. The Med has a faint distal accessory
3510 ridge and the End presents a thin, short mesial accessory ridge. Otherwise, the occlusal
3511 surface is relatively simple. The DMR is a poorly defined, short crest that bounds a small
3512 groove-like Fp. A very faint, but palpable, vertical mesial groove is present on the
3513 mesiolingual corner of the Prd. The mesiobuccal groove is deep and narrow; it becomes
3514 shallower at mid-crown and then deeper again as it reaches the cervix. The distobuccal
3515 groove is shallower and becomes imperceptible about one-third of the crown height. The
3516 lingual groove is much shallower than the buccal grooves and is located slightly distal to
3517 the mesiobuccal groove. It fades at mid-crown.

3518 The roots are mostly broken away at the cervix and the pulp chamber is filled
3519 with sediment. The tooth was likely unerupted at death and the roots minimally
3520 developed. What remains of the roots are small extensions below the buccal cusps.

3521 This is the proposed antimere of U.W. 101-145. Their morphology is virtually
3522 identical, as is their developmental status, lack of IPFs, and lack of occlusal wear.

3523

3524 U.W. 101-655: RM₂ germ, likely RM₂ (Fig. 35D; Table 1) The occlusal surface is
3525 complete but only about one-third of the crown height has been attained. In occlusal
3526 view, the crown is a rounded rectangle with the talonid wider than the trigonid and the

3527 Hld offset buccal to the midline. The crown has five primary cusps arranged in a Y-5
3528 fissure pattern, with a substantial portion of the Med and Hyd in contact, and a well-
3529 developed Hld. The protostylid is evident on the mesiolingual aspect of the Prd as a small
3530 depression and associated oblique shelf. The developing MMR is much lower than the
3531 essential crests of the Prd and Med, and lowest just mesial to the Prd. It projects as a shelf
3532 with accessory tubercles. This shelf is associated with a v-shaped cleft on the
3533 mesiolingual aspect of the Med. The Fa is manifest as a BL-oriented groove that extends
3534 buccally and lingually from the central groove. On the Prd portion, a faint mesial
3535 accessory ridge borders it distally. The essential lobes of all cusps are well developed,
3536 although sharp ridges do not define them. A weak middle-trigonid crest, which is
3537 bisected by the central groove, joins the Prd and Med. The portion of the mesiobuccal
3538 groove that is preserved forms a shallow cleft and wide weak groove. The distobuccal
3539 groove is shallow but lacks the cleft. No lingual grooves are observed.

3540 The identification of the tooth as a permanent molar is based on the crown
3541 dimensions. It is likely an M₂ given the morphology of the Fa. Often in *H. naledi* M_{1s},
3542 the Fa is restricted to the region mesial to the Med, while on M_{2s} the Fa passes mesial to
3543 the Prd as well. Further, in *H. naledi* M_{1s}, the Hld tends to be more centrally placed,
3544 while in M_{2s} it is placed more buccally. This is unlikely to be an M₃, which tends to taper
3545 distally with a wider trigonid and narrower talonid.

3546

3547 U.W. 101-789: LM₂ (Fig. 35E; Table 1) An IPF (approximately 3.0 mm by 2.4 mm OC)
3548 is found mesially, but no IPF is detectable distally. Occlusal wear facets are limited to the
3549 Prd and Med on or close to their cusp apices (stage 1). In occlusal view, the crown has a

3550 straight lingual profile, straight mesial profile, bi-lobed buccal profile, and convex distal
3551 profile related to a large, Hld. The talonid is slightly wider than the trigonid. There are
3552 five well-developed primary cusps arranged in a Y-5 fissure pattern, with a substantial
3553 portion of the Med and Hyd in contact, and the relative cusp sizes are Med > Prd > End \geq
3554 Hyd > Hld. The essential lobes are not defined by sharp ridges. Accessory ridges can be
3555 observed on the Hyd (distal) and End (mesial). A deflecting wrinkle is present on the
3556 Med. The MMR is lower than the essential crests of the Prd and Med, with its lingual
3557 portion lower than the buccal portion. A fissure-like Fa is positioned mesial to the Med
3558 and is contiguous with the central groove. Buccally, a topographically discrete section of
3559 the Fa is bounded by a small accessory tubercle extending from the MMR and the
3560 essential ridge of the Pr. A shallow, but wide, Fp is bordered distally by a low and
3561 rounded DMR. A deep mesiobuccal groove forms a cleft between the Prd and Hyd; it
3562 becomes shallow at mid-crown and deepens again just above to the cervix. The
3563 distobuccal groove is wider and shallower, fading away about mid-crown. The lingual
3564 groove is distal to the mesiobuccal groove and does not cross onto the lingual face. The
3565 protostylid is a faint, obliquely oriented swelling limited to the mesiolingual aspect of the
3566 Prd.

3567 The roots are fragmented and some of the larger fragments have been refit to the
3568 crown. Many of the smaller fragments are pressed into the pulp chamber where they
3569 remain. The surfaces of the roots are abraded. A maximum of 6.1 mm of root remains
3570 mesially, 4.3 mm remains distolingually, 5.3 mm remains mesiolingually, and the roots
3571 are entirely broken away buccally.

3572 This specimen is proposed as the antimere of the RM₂ in situ in the U.W. 101-
3573 377/1014 mandible. They are virtually identical in morphology and their state of
3574 eruption. Both have a small IPF mesially and lack one distally. The mesial IPF of this
3575 specimen is also a possible match for the small distal IPF of the U.W. 101-809 LM₁.

3576

3577 U.W. 101-1002: RM₂? germ (Fig. 35F; Table 1) The crown is incompletely formed and
3578 poorly mineralized. The occlusal surface is covered in cracks that developed post-
3579 depositionally. In occlusal view, the lingual profile is straight, the buccal profile slightly
3580 bi-lobed, and the distal profile has a buccal projection. The crown has a Y-5 fissure
3581 pattern, with a substantial portion of the Med and Hyd in contact, and a well-developed
3582 Hld. There is no evidence of supernumerary cusps. The MMR is low and indistinct. The
3583 weak, fissure-like Fa is primarily expressed on the Med but extends slightly onto the Prd.
3584 The wide Fp is bordered mesially by occlusal ridges of the Hld and End and distally by
3585 the DMR. The protostylid is limited to the mesiolingual aspect of the Prd. It is a faint
3586 oblique swelling that terminates mid-way to the buccal groove. The mesiobuccal groove
3587 is a deep and narrow cleft near the occlusal surface that continues to mid-crown where
3588 crown development ended. The distobuccal groove is much shallower.

3589 The identification as an M₂ is based on the morphology of the Fa, which extends
3590 buccally onto the Prd and on the position of the Hld, which is offset buccally. In most of
3591 the Dinaledi M₁s, the Fa does not extend buccally to the Prd. The state of development of
3592 this specimen matches that of a pair of proposed antimeric maxillary molars, U.W. 101-
3593 1063 and U.W. 101-1135, and they are suggested to represent the same individual as
3594 U.W. 101-1002.

3595

3596 *3.25. Permanent mandibular third molars*

3597 Two isolated M₃s and those present in the U.W. 101-001, U.W. 101-361, U.W.
3598 101-1142, and U.W. 101-1261 mandibles collectively represent at least five individuals
3599 in the Dinaledi Chamber sample. The M₃ crown has five principal cusps arranged in a Y-
3600 5 pattern and the Hld is relatively large. Supernumerary cusps are absent and, with the
3601 notable exception of U.W. 101-1261, the protostylid is faint. The crown is BL broadest
3602 across the trigonid and tapers across the talonid. The M₃ roots present a consistent pattern
3603 as well. The mesial root is plate-like, while the distal root is more elliptical in cross
3604 section. The distal root tapers strongly along the lingual side, especially apically, which
3605 gives the root a buccal tilt in distal view. The mesial root has two distinct apices
3606 separated by a notch. The tapering of the distal root and the indentation between the
3607 mesial root radicals would have accommodated the passage of the mandibular canal.

3608

3609 U.W. 101-006: RM₃ (Fig. 36A; Table 1) A large enamel chip is evident along the
3610 occlusal margin mesiobuccally and other small chips dot the occlusal surface at the
3611 lingual margin, distally adjacent to the End, and in the area between the End and Hld. A
3612 large IPF is evident mesially with its full height preserved lingually (2.6 mm maximum
3613 OC by 6.6 mm maximum BL breadth); though, occlusal wear eliminated a portion of its
3614 buccal portion. A large dentine pool covers the buccal crown, and all but the distobuccal
3615 portion of the distal margin and the mesiobuccal portion of the mesial margin are worn
3616 away (stage 5). The wear plane is strongly angled distobuccally such that none of the
3617 crown is preserved above the distobuccal root.

3618 Very little morphological information can be gleaned from this worn crown. The
3619 crown is flattened mesially by interproximal wear, has a mildly convex lingual profile,
3620 and a convex distal profile with the distal-most point offset buccally, suggesting the
3621 presence of an expansive Hld. The crown is broadest across the mesial cusps and tapers
3622 distally. The buccal crown profile is substantially altered by occlusal wear and enamel
3623 chipping. Although no dentine is exposed on the Med and End, neither cusp retains any
3624 morphological information. However, the preserved Med is much higher than the End.
3625 The occlusal surface, though worn, preserves a hint of the groove separating the Med and
3626 End, together with a small pit just mesial to it. There is a slight suggestion of another
3627 fissure separating the Hld from the End.

3628 A portion of the mandibular alveolus remains wedged between the mesial and
3629 distal roots. The roots are minimally abraded, with only the tip of the mesiobuccal radical
3630 broken, and the exposed surfaces are covered with cementum. The mesial root is plate-
3631 like, while the distal root is more elliptical in cross section. The distal root has a fairly
3632 straight buccal profile but tapers strongly along the lingual side, especially in the apical
3633 quarter of its height, which, in distal view, gives the root a buccal tilt. The mesial root has
3634 two distinct apices, with the buccal one slightly shorter than the lingual. The tapering of
3635 the distal root and the separation of the mesial root radicals would have accommodated
3636 the passage of the mandibular canal. The maximum height of the mesial root buccally is
3637 11.6 mm, while along the lingual radical it is 13.9 mm. The distal root is 11.8 mm in
3638 height. All root measurements approximate their full heights.

3639 This tooth was recovered within centimeters of U.W. 101-005 (RM²), another
3640 heavily worn molar. However, as U.W. 101-005 and -006 are from different arches,
3641 attribution to a single individual cannot be confirmed.

3642

3643 U.W. 101-516: LM₃ (Fig. 36B; Table 1) There are chips of enamel missing from the
3644 mesiobuccal corner just occlusal to the mesial IPF, along the occlusal extent of the mesial
3645 IPF, and along the occlusal rim on either side of the lingual groove. The large mesial IPF
3646 (5.9 mm BL by 2.7 mm OC) extends to the occlusal surface. There is no distal IPF. Wear
3647 flattened much of the occlusal topography and small round dentine pits are exposed on
3648 the Prd and Hyd (stage 3). In occlusal view, the crown is rectangular with a worn concave
3649 mesial profile, mildly bi-lobed buccal profile, straight lingual profile, and convex distal
3650 profile related to a large, buccally offset Hld. The crown is BL broadest across the
3651 trigonid and slightly tapers across the talonid. The mesial IPF and occlusal wear have
3652 obscured expression of the Fa and MMR. Although worn, the Y-5 groove pattern can still
3653 be identified. Judging from this preserved groove pattern, C6 and C7 are absent (an
3654 examination of the EDJ confirms the absence of dentine horns for C6 and C7). The
3655 mesiobuccal groove is a deep v-shaped cleft where it crosses the occlusal surface. It
3656 becomes shallower on the buccal surface about mid-crown and then deepens near the
3657 cervix. The distobuccal groove is faint, fading away before mid-crown. The lingual
3658 groove is offset distal to the mesiobuccal groove. It is a slight indentation at the occlusal
3659 surface and becomes a faint groove on the buccal face extending to the cervix.

3660 A portion of alveolar bone remains wedged between the roots. The tips of the
3661 roots are damaged. The distal, lingual, and buccal surfaces of the distal root are abraded,

3662 as are the labial and lingual surfaces of the lingual root. The mesial root is plate-like, with
3663 two distinct buccal and lingual radicals that become independent root apices. In buccal
3664 view, the mesial root is 11.8 mm in height and the distal root is 11.5 mm. The distal root
3665 is more circular in cross section, notably tapers in its cervical half, is strongly canted
3666 buccally, and has a slight notch near the apex of its lingual margin. The tapering, notch,
3667 and cant of the distal root, along with the bifurcation of the mesial root apices, would
3668 have permitted passage of the mandibular canal (Kupczik et al., 2019).

3669 Based upon the morphology and occlusal wear similarity, this is proposed as the
3670 antimere of the M₃ preserved in the U.W. 101-001 mandible (for comparisons of the root
3671 morphology of these proposed antimeres, see also Kupczik et al., 2019).

3672

3673 *3.26. Crown and root fragments*

3674 U.W. 101-293: C₁? (Fig. 37A; Table 1) This is the root of an anterior tooth lacking a
3675 crown. The preserved occlusal surface is polished, and the pulp canal is exposed. No
3676 enamel remains around the circumference of the crown (stage 8). The advanced wear,
3677 combined with the heavy accumulation of cementum along the root and tertiary dentine
3678 in the pulp canal, indicates that this tooth is from an ontogenetically advanced individual
3679 (it is of comparable, or more advanced wear, to the U.W. 101-010 mandibular canine, for
3680 example). The contours of the root throughout are hard to discern because the root is
3681 covered in a thick layer of cementum that has flaked away in some places. The root is
3682 roughly circular in cross section and somewhat flattened along what is inferred to be the
3683 distal side. The apex of the root is damaged, where a large cementum flake is missing,
3684 and the maximum length of root along the inferred mesial edge is 15.0 mm. The circular

3685 cross-sectional shape of the root is inconsistent with incisors in the Dinaledi sample and
3686 is most like those of mandibular canine roots.

3687

3688 U.W. 101-357: mesial root of LM₁ or LP₄? (not figured; Table 1) This plate-like root
3689 preserves a thin sliver of enamel on either its mesial or distal side. The preserved occlusal
3690 surface was a functional surface with polished dentine. A broad shallow depression is
3691 present on one side. Minor damage occurs just below the occlusal surface on the grooved
3692 side. The maximum height of the preserved root is 13.5 mm, and its maximum BL width
3693 is 10.3 mm just below the preserved occlusal surface.

3694 Specimens U.W. 101-357, U.W. 101-358, and U.W. 101-359 were recovered
3695 from fragments and sediments associated with the U.W.101-361 mandible and are
3696 consistent with belonging to a single individual.

3697

3698 U.W. 101-388: Root fragment (Fig. 37B; Table 1) This broken root fragment, 13.6 mm in
3699 length, is circular in cross section and curved along its longitudinal axis. The root is
3700 broken near the cervix and is also damaged near its apex. This root is from an older
3701 individual. A thick layer of cementum covers the root, and it is flaked off the external
3702 surface. Further, the μ CT scans reveal that the root canal is nearly filled in with tertiary
3703 dentine. The shape, size, and the curvature of the root do not match canines, which are
3704 larger, or incisors, which are much more elliptical. This is possibly a root from a
3705 maxillary molar. If so, the closest matches in the Dinaledi assemblage are distobuccal
3706 roots of maxillary molars.

3707

3708 U.W. 101-589: M₂ root (Fig. 37C; Table 1) This is a heavily worn molar crown fragment
3709 and root. Based on the relative degree of occlusal wear and comparison with the U.W.
3710 101-602 RM₁, this specimen is possibly an RM₁. The tooth is preserved in two fragments
3711 that poorly rejoin. The larger fragment preserves what is interpreted as the mesial root
3712 with a small piece of enamel remaining occlusally. An enamel chip is evident on the
3713 preserved occlusal surface. The root is covered throughout in a thick layer of cementum.
3714 The second fragment includes a piece of enamel, a portion of dentine from the occlusal
3715 surface, and a small bit of the root. Approximately one half of an IPF that extends to the
3716 occlusal surface is present on this fragment. The smaller fragment refits poorly with the
3717 larger. When they are refit, it is evident that the IPF continues onto the enamel fragment
3718 that remains attached to the root. The break between the fragments appears recent.

3719 The mesial face of the root is flat, while a slight invagination runs along the distal
3720 face. The buccal apex of the root is shorter than the lingual apex. Such asymmetry is
3721 present in other mandibular molar roots. The maximum height of the root is 12.4 mm,
3722 and the maximum breadth is 9.3 mm.

3723

3724 U.W. 101-602: RM₂? (Fig. 37D; Table 1) This is a portion of heavily worn crown and
3725 associated root. The root appears to be the mesial root of a mandibular molar, which
3726 would make this a fragment of a right molar and the associated lingual rim. Occlusally,
3727 there is a portion of enamel along the inferred mesiolingual corner; the occlusal surface
3728 here features several antemortem chips. The remaining occlusal surface is polished
3729 dentine (stage 7–8) that shows a steep wear gradient with no enamel remaining mesially
3730 or buccally and approximately 3.4 mm of enamel remaining lingually. In fact, the wear

3731 surface buccally is likely well below the original cervix of the crown. Enamel chipping is
3732 evident on the preserved occlusal surface.

3733 The root is plate-like and damaged along the apex of its inferred mesial and
3734 lingual surfaces. The root is coated in a thick layer of cracked cementum. In mesial view,
3735 from the center of the BL axis of the tooth, the remaining root height is 11.9 mm and,
3736 below the preserved enamel rim it is 12.7 mm, and its maximum BL breadth is 10.5 mm.
3737 The inferred buccal profile of the root is nearly vertical, while the lingual profile is
3738 curved, and matches the profile of mesial roots of mandibular molars.

3739

3740 U.W. 101-652: Developing cusp (Fig. 38; Table 1) This specimen is a single cusp of a
3741 postcanine tooth germ. Crests extend mesially and distally, while the developing essential
3742 ridge is faint. What is interpreted as the mesial crest is longer than the preserved section
3743 of distal occlusal rim. A faint swelling can be seen on the longer crest. Whether this
3744 represents a permanent or deciduous tooth is undetermined; however, in preserved
3745 occlusal detail (i.e., faint essential ridge, longer mesial than distal crest, faint swelling on
3746 mesial crest) this specimen resembles the developing End on U.W. 101-655. Both
3747 specimens have similarly thin enamel as well.

3748

3749 U.W. 101-653: Incisor root? (Fig. 39A; Table 1) This is a single conical root that is ovoid
3750 in cross section. Its cross-sectional size and shape are consistent with attribution to an
3751 incisor. The thick cementum covering the root is flaking off. The occlusal surface is
3752 heavily worn, and all enamel has been removed except for the tiniest portion lingually
3753 (stage 7). The preserved maximum root height is 15.6 mm. Though the crown is likely

3754 worn past the contours of the original cervix, the preserved maximum LaL width of the
3755 root near the cervix is 5.6 mm and the maximum MD length is 4.5 mm.

3756

3757 U.W. 101-654: LM₇ root (Fig. 39B; Table 1) This specimen is a single plate-like root
3758 with functional wear surface that slopes steeply downward toward the inferred buccal
3759 side. No enamel is preserved. Given the extent of exposed dentine, the thick layer of
3760 cementum evident along the external surface of the root, and the buildup of tertiary
3761 dentine in the root canals, which is evident on the μ CT scans, this specimen must belong
3762 to an individual of advanced age (stage 8). There is moderate abrasion to the root surface
3763 near its apex. The maximum preserved height of the root in inferred buccal view is 11.9
3764 mm and its breadth just below the deepest extent of the worn surface is 8.4 mm. The
3765 shape and size of the root are consistent with mesial roots of mandibular molars.

3766 In the degree of occlusal wear and the profile of the root, it bears a strong
3767 resemblance to U.W. 101-589. There is no other evidence, however, to link these
3768 specimens.

3769

3770 U.W. 101-680: Lingual root of maxillary molar? (not figured) A single root with an
3771 invagination on one side. It resembles the lingual root of a maxillary molar.

3772

3773 U.W. 101-686: anterior tooth root? (Fig. 39C; Table 1) This specimen is an unidentified
3774 anterior tooth root lacking enamel and with a polished functional surface. The preserved
3775 root is short and circular in cross section. The root is damaged near the occlusal edge,
3776 where a portion of the root is flaked off. Additionally, opposite that damage, a linear

3777 portion of the root is missing along nearly the entire length of the root. The apex of the
3778 root is preserved, which gives a maximum height of 13.4 mm and a maximum diameter
3779 near the surface of 6.0 mm.

3780

3781 U.W. 101-864: crown and root fragment (Fig. 39D; Table 1) This is a tooth fragment
3782 preserving a small ring of enamel and a portion of a root. Polished dentine and the lack of
3783 occlusal enamel indicate that this is a heavily worn tooth. The total height of the fragment
3784 from occlusal surface to the tip of the broken root is approximately 15.4 mm. The thick
3785 layer of cementum covering the external root surface further indicates the advanced age
3786 of the individual.

3787

3788 U.W. 101-1398B: I²? root (Not figured; Table 1) This is a heavily worn root. It is covered
3789 in cementum, which is cracked and pitted over the entire surface. The root apex is broken
3790 away. The enamel is completely worn away, and the dentine exposed on the surface is
3791 polished by wear, suggesting the tooth was functional at death. The pulp chamber is
3792 exposed by wear and damaged postmortem. The root strongly curves just before its apex;
3793 the apparent curvature is accentuated by a thick layer of cementum. The root is elliptical
3794 in cross section and not as rounded in roots of the canines; thus, this most likely comes
3795 from an incisor. The maximum preserved height of the root is 16.2 mm, which is much
3796 longer than the measurable distobuccal roots of maxillary molars, which precludes this
3797 specimen from belonging to a postcanine tooth.

3798

3799 U.W. 101-1605: LM²? (Not figured; Table 1) A developing tooth germ in fragments, in
3800 which the enamel surface is fractured.

3801

3802 *3.27. Maxilla with teeth*

3803 U.W. 101-1277: LI¹–LM² (Fig. 40; Table 1) This set of teeth is associated with the U.W.
3804 101-1261 mandibular dentition.

3805 LI¹: Damage to the alveolus is evident labially, exposing approximately 6.0 mm
3806 of the root. The incisal wear plane slopes lingually, with a greater portion of dentine
3807 exposed along the MMR than along the DMR (stage 4–5). The labial face is featureless.
3808 Lingually, incisal wear removed most of the marginal ridges so that what remains are
3809 subtle swellings at the incisal edge. There is no hint of a median lingual ridge.

3810 LI²: Damage to the alveolus exposes approximately 3.1 mm of the root labially.
3811 The incisal wear plane slopes lingually and exposes more dentine along the MMR than
3812 along the DMR (stage 4). The remaining labial face is minimally convex. On the labial
3813 face, there is a circular depression of unknown etiology at approximately mid-crown.
3814 Linear hypoplasias are evident in the cervical third of the crown. Although worn, the
3815 MMR and DMR are still evident and were likely moderate in expression. As preserved,
3816 the DMR is broader than the MMR. The weak lingual basal eminence is offset mesially.
3817 The lingual fossa is moderately convex with a pit near the basal eminence.

3818 LC¹: There is some damage to the labial alveolus that exposes 2.7 mm of the root.
3819 The crown is worn, with a large dentine patch exposed over the apex (stage 3). There is a
3820 large, lingually angled facet along the distal crest. At this stage of wear, it appears that
3821 the wear facet along the distal crest is like that typically seen on the lingual face of the *H*.

3822 *naledi* maxillary canines (i.e., U.W. 101-337, U.W. 101-412, U.W. 101-501, U.W. 101-
3823 706, and U.W. 101-908). The occlusal and distal facets meet at an angle just distal to the
3824 crown apex. Labially, there are faint mesial and distal grooves running along the crown.
3825 Lingually, there is a broad median lingual ridge between a narrow mesial lingual groove
3826 and a broader and shallower distal fossa. The MMR is strong near the occlusal edge and
3827 then blends into the basal of the crown. Linear hypoplastic defects cross the labial face
3828 near the cervix.

3829 LP³: There is minor damage to the alveolus lingually. Enamel chips are present on
3830 the mesiolingual and buccolingual corners of the Pr. The occlusal topography is flattened
3831 by wear and a small dentine patch is exposed over the Pr apex (stage 2–3). The crown
3832 profile is slightly asymmetric in occlusal view with a more tightly convex lingual than
3833 buccal margin. The Mlg deflects buccally to form a short fissure-like Fa. The
3834 mesiobuccal and distobuccal grooves are shallow and disappear at mid-crown. The
3835 lingual face is featureless.

3836 The external topography of the alveolar bone suggests the presence of multiple
3837 buccal roots, which is confirmed by examination of the μ CT scans. Three roots are
3838 present: two buccal and one lingual. The three roots have separate canals for much of
3839 their lengths; though, the buccal roots are not widely splayed apart.

3840 LP⁴: The occlusal surface is polished by wear and there is a tiny dentine pit
3841 exposed over the Pr (stage 2). The crown is ovoid in occlusal view with the cusps
3842 approximately equal in size. The Pa is slightly MD longer than the Pr. Though worn, the
3843 Pa retains two occlusal ridges, each likely emanating from either side of the apex, as in
3844 less worn *H. naledi* P⁴s. The Fa is a short groove confined to the Pa. The Fp is a

3845 bifurcation of the MIg with a short lingual branch and longer buccal branch. It is
3846 associated with a shallow distal buccal groove. A shallow mesiobuccal groove is also
3847 evident. They are more prominent than on the P³ of this individual. The lingual crown is
3848 featureless.

3849 The μ CT scans were investigated to compare the root morphologies of the in situ
3850 P³ and P⁴. Like the P³, the P⁴ is three rooted, with two buccal roots and one lingual root.
3851 The root canals are separated for most of their lengths and the radicals of the buccal roots
3852 are also completely separated for most of their lengths.

3853 LM¹: The alveolus surrounding the buccal roots is mostly missing and no alveolar
3854 bone remains distally or superiorly. Lingually, alveolar bone covering the root exists as a
3855 separate fragment refit to the maxilla. The cervical portion of the roots remains exposed.
3856 Enamel chipping exists along the mesial margin above the IPF. Dentine is exposed over
3857 the Pr, Hy, and Pa. The dentine pool over the Pr is large and deep (stage 3–4). Details of
3858 the occlusal morphology are obscured by wear, but the four principal cusps and most of
3859 the fissure pattern are preserved. The occlusal outline is rhomboidal due to the
3860 distolingual projection of the Hy. The expression of the MMR and Fa cannot be assessed.
3861 A remnant of the Fp remains as a pit between the Me and Hy. The Co was probably
3862 continuous, based on what is preserved, and the DMR retains its distinction. Portions of
3863 the buccal and lingual grooves are preserved, with the lingual deeper than the buccal.
3864 Wear precludes assessment of Carabelli's feature.

3865 The two buccal roots are separated by a deep invagination, especially lingually.
3866 They are pressed together and run parallel to each other and perpendicular to the crown.
3867 The mesiobuccal root measures 10.7 mm and distobuccal root 10.5 mm. The buccal roots

3868 are MD compressed and ovoid in cross section. The lingual root is the largest in cross
3869 sectional area. It is MD elongated with clefts running along its buccal and lingual faces,
3870 which gives the root a figure-of-eight shape in cross section. The lingual root has a sharp
3871 lingual inclination.

3872 The U.W. 101-1463 RM¹ is a possible antimere to this tooth. They are very
3873 similar in their preserved morphology, wear status, and even the pattern of enamel
3874 chipping. However, given their lack of occlusal detail, this hypothesis is difficult to
3875 evaluate.

3876 LM²: Enamel chipping is evident along the worn mesial margin. The mesial IPF is
3877 obscured by the M¹. Distally, an IPF (4.9 mm by 2.4 mm) is present in the cervical half.
3878 The occlusal surface is smoothed by wear, but no dentine is exposed (stage 1). The four
3879 primary cusps are well developed, and a possible C5 may be present (wear precludes
3880 being certain) along the DMR. In occlusal view, the crown is rhomboidal with a
3881 distolingually projecting Hy. The relative cusp sizes are Pr > Hy > Pa > Me. The MMR
3882 and Fa cannot be assessed. Though worn, the Co appears to have been continuous. The
3883 Fp remains as a small, but deep pit between the Me and Hy. The lingual groove is deep
3884 and narrow at the occlusal margin, becoming shallow mid-crown and reappearing as a pit
3885 near the cervix. The buccal groove is wider and shallower, and it extends to the cervix.
3886 There is no indication of Carabelli's feature.

3887 A portion of alveolar bone remains wedged between the roots. There are three
3888 roots: two buccal and one lingual. The buccal roots run parallel to each other but are
3889 more widely spaced, longer, and larger in cross sectional area than those of the adjacent
3890 M¹. Both roots are distally inclined, but the mesiobuccal root apex has a strong distal

3891 deflection, while that of the distobuccal root deflects buccally. The mesiobuccal root is
3892 slightly taller (13.2 mm) than the distobuccal root (11.6 mm) along their buccal faces.
3893 The mesiobuccal root has a bifurcated apex and is more elliptical in cross section than the
3894 distobuccal root. The lingual root is the tallest of the three (13.0 mm). It possesses two
3895 distinct radicals separated by a shallow groove, giving it a figure-of-eight shape in cross
3896 section. It has a strong lingual and a slight distal inclination. The distobuccal and lingual
3897 roots are broken at their apices.

3898 This tooth likely articulates with U.W. 101-1269 (LM³) distally.

3899

3900 *3.28. Teeth in mandibles*

3901 U.W. 101-001+U.W. 101-850: RP₃-M₃ (Fig. 41; Table 1) The U.W. 101-001 partial
3902 corpus contains RP₄-RM₃ in situ. An RP₃ with a portion of adhering mandibular corpus
3903 surrounding its roots, recovered separately and catalogued as U.W. 101-850, is now refit
3904 to the mandible. The morphology and preservation of the mandible are described in Laird
3905 et al. (2017).

3906 RP₃: Part of the lateral portion of the inferior mandibular corpus, approximately
3907 10.0 mm in height, remains attached to the RP₃ roots. The mandibular fragment extends
3908 superiorly along the mesial root of the P₃ and exposes the RC₁ alveolus mesially. Here,
3909 the maximum height of the alveolar fragment is approximately 15.7 mm. Lingually,
3910 alveolar bone surrounds only the mesial root, leaving the distal root free from adhering
3911 bone.

3912 Enamel chipping is present along the occlusal surface of the DMR and adjacent to
3913 similar damage on the P₄. Occlusal to the mesial IPF, chipping is also evident along the

3914 MMR. Mesially, a large IPF (approximately 4.4 mm BL by 2.0 mm OC) is evident. Both
3915 the Prd and Med are blunted by wear and dentine is exposed at the Prd apex (stage 4). A
3916 trace of the MIg remains evident, indicating that the crown is fully bicuspid and that the
3917 Med is topographically distinct from the Prd; though, as is evident in less worn *H. naledi*
3918 P_{3s}, it would have been slightly smaller than the Prd in area. Much of the topography of
3919 the mesial crown is flattened by wear; however, a small centrally placed BL-oriented
3920 groove remains as evidence of the Fa. Though much of its extent is worn away, the
3921 transverse groove curves around a worn Med distal accessory ridge, with only a short
3922 segment of the groove remaining buccal to the MIg. The distal occlusal surface is worn to
3923 such an extent that a DMR is not detectable as a feature rising above the talonid. No trace
3924 of a mesiobuccal groove remains and only a hint of a shallow distobuccal groove is
3925 evident at the occlusal rim. No grooves are visible on the lingual face.

3926 Two roots are largely visible and preserved in their entireties. Buccally,
3927 approximately 10.5 mm of the mesial root is exposed, mesially about 5.6 mm of the root
3928 is exposed, and lingually about 4.8 mm of the root is exposed. In buccal view, about 9.1
3929 mm of the distal root is exposed, while 13.4 mm is exposed in lingual view. Cementum
3930 has flaked off the exposed root surfaces. An examination of the μ CT scans shows that the
3931 roots become individualized with separate canals at approximately one-third of their
3932 distance below the cervix. The distal root itself has two identifiable canals, one buccal
3933 and one lingual, throughout much of its length. The distal root is BL-broader and larger
3934 in cross sectional area than the mesiobuccal, which conforms to the 2R: D+MB pattern of
3935 Wood et al. (1988).

3936 RP₄: Along the MMR and occlusal to the mesial IPF, several enamel chips are
3937 present and another chip is visible in the mesiolingual corner adjacent to the Med.
3938 Distally, especially distobuccally, smaller enamel chips are evident along the DMR as
3939 well. A large interproximal carious lesion, largely confined to the root but extending
3940 superiorly onto the distal crown, runs parallel to the cervix. This lesion also affects the
3941 mesial aspect of the adjacent M₁ and is visible in the lateral and buccal views of the
3942 specimen in Figure 41. Examination of μ CT scans shows significant demineralization of
3943 the enamel and adjacent dentine, with sediment filling in the demineralized hollow (see
3944 Towle et al. (2021) for a systematic assessment of caries in *H. naledi*). Very little
3945 occlusal detail remains, as a large dentine pool obliterates most of the buccal crown
3946 moiety, leaving a buccal rim of enamel less than 2.0 mm in breadth. The dentine pool
3947 widens distally and reaches its greatest BL breadth along the distal margin. A small
3948 dentine pit is evident at the Med apex as well (stage 5). Occlusally, the only morphology
3949 that remains is a small remnant of the lingual arm of the transverse groove. Yet, it is clear
3950 that the Med was high — likely subequal in height to the Prd. No trace of the
3951 mesiobuccal and distobuccal grooves remains and the lingual face is featureless..

3952 The bone delimiting the alveolar margin is preserved with minimal damage:
3953 approximately 2.9 mm of the RP₄ root is visible buccally and less than 1.5 mm of the root
3954 is visible lingually. Buccally, a shallow groove is evident along the root; however,
3955 separate radicals are not visible at this level. The μ CT scans show deep lingual and
3956 buccal invaginations and that the mesial and distal root canals separate at about half the
3957 roots' heights and bifurcate into separate external mesial and distal radicals near the root
3958 apices.

3959 RM₁: A large carious lesion is present on the mesial aspect of the root and crown.
3960 The lesion runs the width of the root and affects the mesial margin of the Prd. Mesially,
3961 demineralization associated with the caries is evident to the naked eye and is easily seen
3962 in Figure 41. Examination of the μ CT scans shows that demineralization extends down
3963 the face of the mesial root (see Towle et al. (2021) for a systematic assessment of caries
3964 in *H. naledi*). Buccally, the crown is damaged just above the distal root. Here, a notch of
3965 enamel extending nearly to the cervix has broken from the crown. Distobuccally, enamel
3966 chipping is evident occlusally. Additional chipping is present in the mesiolingual corner
3967 and mesiobuccally. Further, the enamel rim is incomplete from near the center of the
3968 mesial IPF towards the buccal margin where the crown begins to turn distally. The
3969 preserved break is sharp and the adjacent dentine is recently damaged, suggesting that it
3970 may be postmortem; however, the missing enamel is in the region of an interproximal
3971 caries that likely weakened the enamel and contributed to the break. The crown is heavily
3972 worn: the buccal cusps are obliterated, and tertiary dentine fills in the pulp canals at the
3973 occlusal surface. Only a thin rim of enamel is preserved along the buccal and distal
3974 aspects. Wear flattened the lingual cusps and large dentine pits cover the Med and End as
3975 well (stage 5). The occlusal wear along the buccal half of the crown is not planar, having
3976 excavated nearly to the pulp chamber near the center of the occlusal surface.

3977 Although the occlusal fissures are all but obliterated by wear, it is evident from
3978 the crown shape and cusp orientations that at least five cusps were originally present.
3979 Lingually, the Med is higher than the End; though, the extent of their dentine exposure is
3980 similar. Occlusally, the only remnant of surface morphology preserved is a weak groove
3981 separating the Med and End. This groove extends onto the lingual surface. A remnant of

3982 a deep buccal groove is evident; though, the buccal crown is worn nearly down to the
3983 cervical line.

3984 The alveolus of the mandible is broken away irregularly around the roots,
3985 exposing more of the roots buccally than lingually. Buccally, approximately 7.0 mm of
3986 the mesial root and 7.5 mm of the distal root are exposed. Lingually, the alveolus is
3987 largely undamaged, and less than 2.0 mm of the mesial root is visible. The buccal
3988 surfaces of both roots are covered with cementum and are abraded. The lingual root
3989 surfaces are less abraded than apparent on the buccal side. The broader mesial root is
3990 oriented vertically below the crown, while the smaller distal root cants buccally. Further
3991 details of root and pulp chamber morphology are presented in Kupzcik et al. (2019).

3992 RM₂: Buccally, a large enamel chip is evident at the occlusal margin of the
3993 mesiobuccal groove, essentially on the face of the Hyd and reaching nearly to the cervix,
3994 and a smaller chip is present distobuccally adjacent to the Hld. Smaller enamel chips line
3995 the occlusal margins of both IPFs and sit lingually adjacent to End. The chip at the buccal
3996 groove is the largest and reaches nearly to the cervix, while the others are confined to the
3997 occlusal surface. The buccal contour has been altered by a large enamel chip at the
3998 occlusal surface. Enamel chipping has also altered the morphology of the mesiobuccal
3999 and distobuccal grooves. The crown is moderately worn, with large uncoalesced dentine
4000 patches over each buccal cusp and a tiny dentine pit on the End apex (stage 4). The Med
4001 is the highest of the preserved cusps, with a steep wear plane sloping buccally. Occlusal
4002 wear has removed most of the surface morphology, but remnants of the occlusal fissures
4003 remain. The crown has a Y-5 fissure pattern, with a substantial portion of the Med and
4004 Hyd in contact, and a well-developed Hld. The central groove is deep, while the

4005 remaining grooves separating Prd from Hyd, Med from End, and End from Hld are
4006 weaker. Although somewhat obscured by the large enamel chip at the buccal groove, in
4007 occlusal view the buccal profile was mildly bi-lobed, while the lingual profile is
4008 straighter. No trace of a protostylid is detectable. Though interproximal wear reduced the
4009 MD length of all the molars, the M₂ is larger in area than the M₁.

4010 Alveolar bone is broken irregularly along the buccal side, exposing small portions
4011 of the mesial and distal roots. Damage to the alveolar bone is greatest along the distal
4012 root, where approximately 2.0 mm of the root is exposed. Along the mesial root,
4013 approximately 2.0 mm of the root is exposed. The root surfaces are well preserved, with
4014 only minor abrasion evident. Further details of root and pulp morphology are presented in
4015 Kupzcik et al. (2019).

4016 RM₃: There are two small enamel chips along the DMR and others at the apices
4017 of the End and Med. Interproximal wear excavated into the mesial margin of the crown.
4018 The crown is mildly worn and much of the cuspal relief has been reduced. Only small
4019 dentine pits are exposed on the Prd and Hyd and the principal fissure pattern is preserved
4020 (stage 2). The Med apex represents the high point of the occlusal surface. The five
4021 principal cusps are present and oriented in a Y-fissure pattern. Cusp 7 is absent and there
4022 is no suggestion of a C6 from the preserved occlusal fissure pattern. In size, the cusps are
4023 ordered as Med = Prd > Hyd > Hld > End. The crown is BL-broadest across the mesial
4024 cusps and tapers distally so that the Hld is placed just buccal to the center of the crown.
4025 The Hld itself projects quite far distally. The central groove separating the Prd and Med is
4026 deep and curves around the mesial aspect of the Med to form a small Fa. The MMR and
4027 DMR are each worn away as distinct topographical features. The mesiolingual face is

4028 smooth, but a faint indentation represents a weakly expressed protostylid. The
4029 mesiobuccal groove is deep and forms a cleft near the occlusal margin. It is oriented
4030 somewhat mesially. The distobuccal groove is barely perceptible and fades away at mid-
4031 crown. The lingual groove is faint but continues to the cervix. The M₃ is the largest molar
4032 in the sequence. The alveolar bone is undamaged, and the roots are not exposed either
4033 buccally or lingually; details of root and pulp morphology are presented in Kupzcik et al.
4034 (2019).

4035

4036 U.W. 101-010: RC₁-RP₃ (Fig. 42; Table 1) A portion of the right mandibular corpus
4037 holds the heavily worn crowns and roots of the canine and P₃. The morphology of the
4038 mandible is described in Laird et al. (2017).

4039 RC₁: Nearly the entire crown has been removed by wear, with only a thin rim of
4040 enamel remaining distolabially (stage 7), and the pulp cavity is exposed at the surface.
4041 What is likely postmortem chipping is present mesially and labially; though, it seems that
4042 enamel would not have remained in that area. Polishing on the dentinal surface indicates
4043 that the tooth was in use at the time of death. The wear surface dips strongly towards the
4044 cervix mesially and lingually.

4045 The surface of the exposed root is covered in cementum, which is extensively
4046 cracked. The root is roughly circular in cross section, with its LaL breadth slightly
4047 exceeding its MD length. Labially, 15.6 mm of root are exposed below the worn occlusal
4048 surface and the apex of the root is hidden in the alveolus.

4049 This specimen is of comparable wear to that of the U.W. 101-359 LC₁; though,
4050 the absence of any remaining detailed crown morphology limits the inference that these
4051 specimens represent antimeres.

4052 RP₃: Enamel chipping is evident along the occlusal margin above the buccal
4053 aspect of the distal IPF (5.4 mm BL by 2.1 mm OC). A mesial IPF is also evident, but its
4054 shape is obscured by contact with the distal surface of the canine. The crown is
4055 significantly worn; only an enamel ring circumscribes the crown and a small amount of
4056 enamel remains on the distolingual corner (stage 6–7). As a result of the extensive wear,
4057 little occlusal detail remains. A short segment of the lingual arm of the transverse groove
4058 remains distal to the metaconid. The distance from that remaining groove to the distal
4059 crown, combined with the profile of the crown, suggests an expanded talonid comparable
4060 to less worn Dinaledi P_{3s}. Abrasion to the alveolar bone exposes two roots:
4061 approximately 6.5 mm of the mesial root and 3.0 mm of the distal root are visible. The
4062 presence of two roots is confirmed through inspection of the μ CT scans. The mesiobuccal
4063 root is the smaller of the two, with the distal root BL-expanded. The roots share a
4064 common canal at the cervix but are individuated for more than half their heights. The
4065 distal root itself has two distinct canals throughout much of its course. Thus, the roots
4066 correspond to the 2R: MB +D configuration of Wood et al. (1988).

4067

4068 U.W. 101-361: root fragment, LM₂–LM₃ (Fig. 43; Table 1) This specimen preserves
4069 much of a left mandibular corpus with LM₂ and LM₃ in place. The mandible is broken
4070 lateral to the symphysis and along the alveoli of the postcanine dentition. The break plane
4071 slopes inferiorly from the posterior molars. Thus, the M₃ alveolus is preserved intact and

4072 the distal root of the M₂ sits in its alveolus, while the mesial root of the M₂ is exposed.
4073 Lingually, the mandible is damaged along the M₂ alveolar margin, exposing both the
4074 mesial and distal roots. The morphology of the mandible is described in Laird et al.
4075 (2017). As elaborated upon in the Discussion, a mandibular condyle, U.W. 101-196, is
4076 refit to the corpus and articulates with the DH3 cranium (Berger et al., 2015).

4077 Specimens U.W. 101-357 to U.W. 101-359 were recovered from fragments and
4078 sediments associated with this specimen. These specimens express advanced occlusal
4079 wear and are from the left side and likely belong to a single biological individual.

4080

4081 Associated Root: LP₄? (not figured): This is a single ovoid root with a groove
4082 running along one side and a small piece of enamel adhering to the surface. The
4083 preserved occlusal surface was a functional surface with polished dentine. There is some
4084 abrasion apparent on the root near the enamel remnant and there is substantial damage to
4085 the side of the root opposite the enamel. The maximum height of the root is 13.9 mm and
4086 its maximum width is 7.1 mm.

4087 LM₂: A prominent BL crack at mid-crown, effectively in the space between the
4088 mesial and distal roots, splits the tooth into mesial and distal portions. The entire enamel
4089 cap is removed by wear (stage 8). Much of the exposed dentine is polished, and the center
4090 of the occlusal basin is extensively scooped out by wear. The high point of the occlusal
4091 surface is the mesiolingual corner, while the wear plane dips so that the low points are the
4092 mesiobuccal and distobuccal corners.

4093 The mesial root is exposed, while the distal root is obscured from view by
4094 alveolar bone. The exposed mesial root is covered in a thick layer of cementum. On the

4095 mesiolingual corner of the mesial root, a notch is apparent near the occlusal margin. The
4096 contours of the notch are rounded, and it appears that it formed after the enamel cap was
4097 removed during life and the occlusal surface contour continued to wear into the exposed
4098 dentine. The maximum breadth of the mesial root is 10.9 mm. Further details on the
4099 morphology of the in-situ roots are found in Kupczik et al. (2019).

4100 LM₃: There is a large, wide mesial IPF present; its OC height has been reduced
4101 buccally by extensive occlusal wear. The crown is extensively chipped around the
4102 occlusal margin. A flake is missing in the lingual groove, another is evident extending
4103 mesially from the mesiobuccal groove, and multiple chips are present in the mesiolingual
4104 corner. A deep dentine pool extends from the Hyd to the Prd. The pool is narrowest
4105 distally and broadens over the Prd. The entire Prd, nearly down to the cervix, has been
4106 removed by wear. The Hyd has a large but shallower pool of dentine over its apex. Small
4107 pits of dentine are also exposed over the Hld and Med (stage 5). Little occlusal detail is
4108 preserved. The crown is broadest across the mesial cusps and tapers distally. The buccal
4109 margin of the tooth is straighter than the lingual margin, so that the most distal point is
4110 just buccal to the midpoint of the crown. The roots are not visible externally; however,
4111 their morphology is described in Kupczik et al. (2019).

4112

4113 U.W. 101-377+U.W. 101-1014: RC₁–RM₂ (Fig. 44; Table 1) U.W. 101-377 is a partial
4114 mandibular corpus of a sub-adult that contains RP₃–RM₂. The mandible is described in
4115 Laird et al. (2017). Details on root formation and dental eruption sequence are in Cofran
4116 and Walker (2017). The mandibular fragment also includes the distal portion of the right
4117 canine alveolus. An isolated RC₁, recovered separately and catalogued as U.W. 101-

4118 1014, is now refit to the U.W. 101-377 mandible. The canine is described here with the
4119 remainder of the U.W. 101-377 dentition.

4120 The teeth found in the mandible all have proposed antimeres. Further, a complete
4121 set of incisors (U.W. 101-998, -1005A, -1005B, and -1005C) likely belongs to this
4122 individual as well. If these proposed associations are correct, they represent one of the
4123 most complete mandibular dentitions of *H. naledi*.

4124 RC₁: A large oblong IPF (2.5 mm IC by 2.3 mm LaL) is situated high on the
4125 mesial shoulder. A distal IPF is also evident, though its true extent is obscured by the P₃.
4126 Wear blunted the mesial crest near the apex, while wear along the distal crest is more
4127 extensive and created a J-shaped contour in labial view (stage 1). The crown appears tall
4128 in height relative to its narrow basal size (Table 1). The crown is asymmetric, with the
4129 apex placed distal to the MD midpoint. The mesial crest is short and convex, while the
4130 distal crest, which is partially obscured by contact with the mesial face of the P₃, is longer
4131 and more vertically oriented. The distal crest terminates at a tubercle that sits more
4132 cervically than the mesial shoulder. The labial grooves are both shallow and indistinct.
4133 Lingually, a few minor ridges run from a flat and indistinct median lingual ridge towards
4134 the mesial crest; otherwise, the lingual fossa is featureless. The MMR is low and rounded
4135 and the DMR is barely present, in part because the distal IPF eats into the DMR. Linear
4136 hypoplasias are evident in the lower third of the labial crown and near the lingual cervix.

4137 The mandibular corpus in the region of the canine alveolus is broken labially and
4138 lingually, exposing a portion of the root in these regions. The root is entirely exposed in
4139 mesial view, where it measures 13.8 mm in height from the tip of the embrasure at the
4140 cervix. Abrasions are evident to the mesial, labial, and lingual sides of the root and the

4141 distal side is now obscured from view by refitting. As judged from μ CT scans, the apex
4142 of the root is open (see also Cofran and Walker, 2017).

4143 This specimen is the probable antimere of U.W. 101-1076. The two canines are
4144 similar morphologically, in wear, in the position, size, and shape of the IPF, and in the
4145 position and type of hypoplasias on their labial faces. Further, this specimen reasonably
4146 articulates with the U.W. 101-1005C RI₂.

4147 RP₃: The crown is lightly worn, with an elongated facet along the distal Prd crest
4148 that runs onto the buccal aspect of a distobuccal cuspsule (stage 1). The Prd and Med are
4149 well developed and separated by a well-defined, uninterrupted MIg. The Med area is
4150 slightly smaller than the Prd and its cusp apex is sub-equal in height. The Fa is a BL-
4151 oriented groove with extensions both lingual and buccal to the MIg. It is bounded distally
4152 by mesial accessory ridges of the Prd and Med. The Prd mesial accessory ridge is more
4153 prominent than the one extending from the Med. The MMR forms a continuous rim
4154 extending from the Med to the Prd. In mesial view, it dips slightly at the MIg and is lower
4155 than the mesial Prd and Med accessory crests. The Prd and Med essential ridges are
4156 strongly developed, although not sharply defined. The talonid is polished; however, a
4157 small cusplet, defined by buccal and occlusal grooves and a less distinct, but well
4158 developed, distolingual portion, is palpable distobuccally. Though wear removed some
4159 relief in the distal aspect of the talonid, the DMR is not detectable topographically as a
4160 feature distinct from the planar surface of the talonid. The mesiobuccal groove is faint
4161 and does not continue onto the occlusal rim, whereas the distobuccal groove is deeper at
4162 the occlusal rim. Both become imperceptible about a third of the way down the buccal
4163 face. Faint linear hypoplastic defects are apparent near the cervix on the buccal face. In

4164 lingual view, the trigonid portion of the crown is much higher than the talonid portion.

4165 The lingual face is featureless.

4166 The crown and roots are in situ in the mandible, with approximately 2.4 mm of
4167 the root mass exposed in buccal view. Examination of the μ CT scans shows that two
4168 roots are present and conform to the 2R: MB + D pattern of Wood et al. (1988). In
4169 contrast to some other *H. naledi* P₃s, the mesiobuccal and distal roots do not become
4170 completely individualized until near their apices; in fact, their root canals are connected
4171 by an isthmus throughout most of their lengths.

4172 Based upon similarities in morphology and the state of occlusal wear, this tooth is
4173 the antimere of the U.W. 101-889 LP₃.

4174 RP₄: Wear is minimal, with a minor facet on the Prd apex and no dentine
4175 exposure (stage 1). The Med and Prd are separated by a well-defined MIg. The Med is
4176 slightly smaller in area than the Prd, but equal in height. The apex of the Med sits well
4177 mesial to that of the Prd. The MMR is low and continuous and encloses a shallow Fa,
4178 which is a short and shallow groove with its deepest point where it meets the MIg. It is
4179 bordered distally by the mesial accessory crests of the Prd and Med. The Med mesial
4180 accessory crest is rounded and originates from the cusp apex, while the Prd mesial
4181 accessory crest is better defined and originates as an extension of the mesial lobe. The
4182 essential ridges of the Prd and Med are well developed, rather broad, and not very
4183 distinct. The talonid is defined mesially by a deep transverse groove. Mesial to this
4184 groove, the Prd and Med possess distinct distal accessory ridges. Shallow indentations
4185 radiate distally from the transverse groove and the DMR is not distinct from the talonid.
4186 The buccal face is indented by shallow mesial and distal grooves, with the distal groove

4187 better defined than the mesial. Both extend about a third of the way down the face before
4188 becoming indistinct. There is no mesiolingual groove and but a faint and shallow
4189 distolingual indentation near the occlusal margin.

4190 Very little of the root is visible; though, an inspection of the μ CT scans shows
4191 that this specimen has a single root that is round in cross section.

4192 Based upon similarities in occlusal and root morphology and occlusal wear state,
4193 this is the proposed antimere of U.W. 101-887.

4194 RM₁: Wear facets are evident on all cusps and a very small dentine pit is present
4195 on the Prd apex (stage 2). In occlusal view, the crown is nearly equally BL-broad across
4196 the trigonid and the talonid and the crown outline is roughly rectangular. The large Hld
4197 projects distally, forming the rounded distobuccal profile, and the buccal profile is deeply
4198 indented by the buccal grooves. Substantial interproximal wear resulted in a concave
4199 mesial contour. The crown has a Y-5 fissure pattern, with a substantial portion of the
4200 Med and Hyd in contact. The relative cusp sizes are Hyd > Prd > Med > Hld > End. Most
4201 of the MMR has been removed by interstitial wear; what remains is low and thin. The
4202 remnant of a small, pit-like Fa remains visible with a portion of it extending lingually
4203 onto the Med. The Fp is little more than a pit at the termination of the central groove and
4204 bordered mesially by weak distal accessory ridges of the End and Hld. The protostylid is
4205 limited to the mesiobuccal portion of the Prd and takes the form of a faint, but palpable,
4206 oblique crest that terminates mesial to the mesiobuccal groove. This groove is deep,
4207 forming a narrow cleft near the occlusal margin and broadening at mid-crown into a
4208 shallower groove that continues to the cervix. The distobuccal groove is partially
4209 obscured by matrix, but it was evidently shallower and shorter than the mesiobuccal

4210 groove, fading away shortly after crossing the occlusal margin. The main lingual groove
4211 is placed slightly distal to the mesiobuccal groove. While deep at the occlusal margin it
4212 quickly becomes shallower and disappears at mid-crown. The distolingual groove is little
4213 more than an indentation near the occlusal margin.

4214 Approximately 4.5 mm of the mesial buccal root is exposed by a break in the
4215 alveolar margin; though, little can be discerned of its morphology. Details of its
4216 morphology are provided by Kupczik et al. (2019) based upon an analysis of μ CT based
4217 data.

4218 Based upon similarities in morphology and wear state, this is a reasonable
4219 antimer of the U.W. 101-809 LM₁.

4220 RM₂: A mesial IPF is present but, consistent with the developmental status of the
4221 individual, there is no distal IPF. The tooth was erupting at death (Cofran and Walker,
4222 2017); however, a small wear facet is visible on the mesial to the Prd apex (stage 1). In
4223 occlusal view, the crown is roughly rectangular in profile, with a slightly wider talonid
4224 than trigonid. The lingual and mesial profiles are more-or-less straight, the buccal profile
4225 mildly bi-lobed, and distal profile convex because of a large Hld placed slightly buccal of
4226 center. The crown has a Y-5 fissure pattern, with a substantial portion of the Med and
4227 Hyd in contact. The relative cusp sizes are Med > Prd > End \geq Hyd > Hld. The cusps do
4228 not possess well-defined essential ridges. The weak Med essential ridge travels towards
4229 the Mlg and then deflects distally to meet the Hyd (deflecting wrinkle). It also possesses a
4230 thin, but well-defined distal accessory ridge that takes the form of a small cuspule in
4231 lingual view. Although not a 'true' cusp 7 as defined by the ASUDAS, Skinner et al
4232 (2008: 179) have referred to this as "Metaconulid-type on the distal shoulder of the

4233 Med.” The End has a mesial accessory ridge that is independent of the cusp apex and
4234 meets the essential lobe near the occlusal basin. The MMR is not well defined and is
4235 lower than the essential lobes of the Prd and Med in mesial view. The majority of the
4236 groove-like Fa is situated mesial to the Med with a slight buccal extension onto the Prd
4237 (this is slightly different than the configuration seen on its proposed antimere). A
4238 moderate but shallow Fp is formed by grooves separating the End and Hld essential lobes
4239 from their distal accessory lobes, which comprise an indistinct DMR. The mesiobuccal
4240 groove is quite deep and narrow occlusally and becomes shallower and wider as it
4241 continues to the cervix. The distobuccal groove is much wider but shallower occlusally
4242 and is imperceptible by mid-crown. The mesiolingual groove is absent and the
4243 distolingual groove is a shallow triangular depression near the occlusal margin. The
4244 protostylid is evident as the faintest of swellings confined to the mesiobuccal aspect of
4245 the Prd. It begins as a vertically oriented crest that curves around distally to become
4246 indistinct half the distance to the mesiobuccal groove.

4247 Matrix adheres to the crown mesially, along the buccal grooves, distally, and
4248 around the base lingually. The distal root is exposed in lingual and distal views. The
4249 distal root appears to be broken apically. In distal view, approximately 3.2 mm of root are
4250 exposed. Examination of the μ CT scans indicates that the mesial root, which is preserved
4251 fully in situ, was open at death (see also Cofran and Walker, 2017).

4252 Although not identical (the configuration of the Fa is slightly different), based
4253 upon morphological similarities and shared ontogenetic status, this is proposed as the
4254 antimere of U.W. 101-789.

4255

4256 U.W. 101-1142: RM₂–RM₃ (Fig. 45; Table 1) A fragment of mandibular corpus and
4257 ramus preserves M₂ and M₃ in situ. Portions of the alveoli for the M₁ mesial and distal
4258 roots are also present. An isolated RM₁, U.W. 101-1287B, fits into the preserved alveoli
4259 and its distal IPF is a match for the mesial IPF of the U.W. 101-1142 RM₂. The
4260 morphology of the mandible is described in Laird et al. (2017) and its neoplastic
4261 pathology is discussed in Odes et al. (2018).

4262 RM₂: Enamel chips are present along the mesial and distal margins, above the
4263 respective IPFs. A large mesial IPF (7.4 mm BL by 3.5 mm OC) extends to the occlusal
4264 margin. The entire crown is smoothed by wear and small dentine pits are exposed on the
4265 Pr, Hy, and Hld (stage 2). Although worn, the crown retains its Y-5 fissure pattern, with a
4266 substantial portion of the Med and Hyd in contact. The occlusal topography of the crown
4267 is worn down; though, the Hyd appears relatively large. In fact, an investigation of the
4268 EDJ shows that two distinct, and nearly equally large, dentine horns are present
4269 distobuccally. Thus, this specimen likely would have expressed a C6 that is nearly the
4270 same size as the Hyd. No other M₂ in the current sample has a similar configuration
4271 distobuccally; however, a similar configuration is present at the EDJ of the M₃ of this
4272 individual. In occlusal view, the crown is roughly rectangular and with a slightly broader
4273 talonid than trigonid. The lingual profile is straight, while the buccal profile is mildly bi-
4274 lobed. The MMR and Fa are flattened by occlusal wear and obscured by interproximal
4275 wear. Mesiobuccally, trace expression of the protostylid is visible. The mesiobuccal
4276 groove is narrow and deep near where it crosses the occlusal margin; it fades at mid-
4277 crown and then appears again just above the cervix. The distobuccal groove is shallow at

4278 the occlusal surface. Buccally, the alveolus is damaged, exposing approximately 3.5 mm
4279 of the mesial and distal roots. The lingual alveolar margin is undamaged.

4280 RM₃: Enamel chipping is present along the mesial margin above the IPF, along
4281 the distolingual margin, and on the End apex. The crown is polished by wear, but no
4282 dentine is exposed (stage 1). The M₃ is larger in area than the M₂. In occlusal view, the
4283 lingual profile is mildly convex, the buccal profile is slightly bi-lobed, and the distal
4284 contour is convex with its distal-most point slightly buccal to midline. The talonid is
4285 wider than the trigonid and the crown is broadest at mid-crown before tapering distally.
4286 The crown has a Y-5 fissure pattern, with a substantial portion of the Med and Hyd in
4287 contact, and a well-developed Hld. The relative cusp sizes are Prd > Hyd > Med > Hld ≥
4288 End. Some definition of the Prd essential ridge remains. Lingually, there are swellings on
4289 the mesial End crest, distal End crest, and distal Med crest. None are associated with
4290 grooving on the lingual face that suggests distinct, individualized cusps in the unworn
4291 state. The apparent area of the of Hld is quite large. Though the presence of a C6 is not
4292 evident at the outer enamel surface due to occlusal wear, an investigation of the EDJ
4293 surface show that two distinct dentine horns are present distobuccally, which indicates
4294 the likely presence of C6 that is nearly equal in size to the Hld. Another dentine horn is
4295 present distolingually; above that dentine horn at the outer enamel surface is an enamel
4296 chip that obscures the occlusal topography of the region. The expression of the MMR is
4297 obscured by wear, but a hint of the Fa groove can be seen passing mesial to the Med. The
4298 Fp remains as a small pit at the termination of the groove between the End and Hld. A
4299 weak protostylid is expressed as an oblique crest restricted to the mesiolingual corner of
4300 the Prd. The buccal grooves are both broad and shallow. Though the mesiobuccal groove

4301 is more distinct than the distal, both lack the narrow cleft at the occlusal surface observed
4302 in many other *H. naledi* molars. There is no detectable lingual groove.

4303

4304 U.W. 101-1261: complete mandibular dentition (Fig. 46; Table 1) The specimen was
4305 recovered in numerous fragments that were initially assigned separate accession numbers
4306 (Laird et al., 2017: Table 2); upon refitting, a single accession number, U.W. 101-1261, is
4307 now assigned to the mandible and all the teeth. Damage to the alveolar bone is minor, but
4308 present throughout: the LM₁ alveolus is damaged, exposing a portion of the LM₁ distal
4309 root; the LP₃ alveolus is damaged, exposing most of the mesial root and a portion of the
4310 distal root; the area around the left canine is damaged, exposing a portion of its root; the
4311 labial alveolus across the incisal region is damaged; a portion of the right canine root is
4312 exposed; there is a clean break between RM₁ and RM₂ that exposes the distal root of the
4313 RM₁ and the mesial root of the RM₂; damage is evident to the lingual and distal alveolar
4314 margin near the LM₃; and the mesial root of the LM₁ is exposed. The morphology of the
4315 mandible is described in Laird et al. (2017). The U.W. 101-1261 dentition is associated
4316 with the U.W. 101-1277 partial maxillary dentition, its possible antimere RM¹ U.W. 101-
4317 1463, and the U.W. 101-1269 LM³.

4318 Left and Right I₁: Both I₁ roots are exposed labially for approximately 7.0 mm. At
4319 the point of exposure, the roots and crowns of the incisors broke cleanly from the
4320 mandible and have been refit.

4321 The central incisors are worn, with wide dentine exposure along their incisal
4322 edges and enamel rims intact (stage 4–5). The incisal wear plane angles lingually, slightly
4323 more so distally than mesially. On both crowns, the labial face is featureless and more-or-

4324 less flat. The lingual surface is flat, and the base is offset mesially. Marginal ridges were
4325 probably present, but wear precludes assessing their expression. There is no median
4326 lingual ridge.

4327 Left and Right I₂: The RI₂ and LI₂ alveoli are damaged on the labial side. The LI₂
4328 broke away with the central incisors. The RI₂ is apparently unbroken but became
4329 dislodged from its alveolus when the break to the incisors occurred. Lingually, the alveoli
4330 are also slightly damaged.

4331 The crowns are worn, with wide dentine exposure across their incisal edges and
4332 intact enamel rim (stage 4–5). The wear plane is angled lingually, more so along the
4333 MMR than along the DMR. Labially, the crowns are featureless, with hypoplastic defects
4334 evident in the cervical third. Lingually, the mesial margin of the tooth is straighter than
4335 the distal, which is convex near the incisal edge. The lingual surface is flat and marginal
4336 ridge development has been mostly removed by wear.

4337 Left and Right C₁: There is damage to both the left and right canine alveoli that
4338 exposes approximately 6.2 mm of the left root and approximately 2.6 mm of the right
4339 root. There is less damage to the lingual alveoli.

4340 Both crowns are similarly worn. Exposed dentine extends from the mesial crest,
4341 across the apex, and terminates at or before the distal tubercle (stage 4). The wear surface
4342 is not planar, and, in labial view, there are distinct mesial to the distal wear facets that
4343 meet at the apex. Wear obscures some of the crown contours; however, it is apparent that
4344 the teeth show the typical *H. naledi* canine feature set. For example, the mesial shoulder
4345 sits higher than the distal shoulder and a faint distal labial groove is detectable adjacent to
4346 a small distal tubercle. Lingually, the MMR is strongest near the occlusal edge, while the

4347 DMR, if present, is worn away. The wide median lingual ridge barely rises above the
4348 lingual fossa. There is a very narrow groove adjacent to the MMR and a deeper, but
4349 narrow, groove adjacent to the DMR. Multiple linear hypoplasias are evident in the lower
4350 third of the crown.

4351 Left and Right P₃: The alveolus of the RP₃ is mostly undamaged but that of the
4352 LP₃ is heavily damaged, exposing most of both roots in buccal view and large portion of
4353 the distal root in lingual view.

4354 For both crowns, enamel chips are present along the distal margin above the IPF.
4355 Occlusal wear is slightly more advanced on the LP₃ than the RP₃. For the LP₃, dentine is
4356 exposed over the Prd apex, and a smaller pit is exposed over the Med apex (stage 2). The
4357 RP₃ only has dentine exposed on the Prd; as a result, its Med retains more topographical
4358 relief than that of the LP₃. The P₃s are fully bicuspid and much of the course of the MIg
4359 can be detected on the RP₃. Most of the detail of the Fa is worn away; though, in each
4360 case, the groove appears to curve slightly to the lingual side around the Med. Details of
4361 talonid morphology are better preserved on the RP₃; for both, the transverse fissure
4362 bifurcates slightly at its lingual end. Both P₃s possess faint mesiobuccal and distobuccal
4363 grooves. The mesiobuccal groove is shallower than the distal and does not extend as far
4364 down the crown. For the more worn LP₃, only the faintest trace of the distobuccal groove
4365 remains. The lingual face is featureless.

4366 The root morphology can be determined from the more exposed LP₃ roots. On the
4367 buccal aspect, there is a clear separation between the mesial and distal root canals. On the
4368 lingual aspect, the distal root appears broader than the mesial, which is offset buccally
4369 relative to the distal root. Examination of μ CT confirms that both P₃s are two rooted and

4370 that the mesial and distal roots are completely individualized just below the crown and
4371 conform to the 2R: D+MB pattern (Wood et al., 1988) seen in the other *H. naledi* P_{3s}.

4372 Left and Right P₄: The alveolus is nearly complete for the LP₄, while that of the
4373 RP₄ is minimally damaged along the lingual edge. Both crowns exhibit enamel chipping
4374 on the distal margin. The damage is more apparent for the RP₄, where a large enamel chip
4375 is missing just above the distal IPF. Minor enamel chipping is also evident above the
4376 mesial IPF. For the LP₄, a smaller chip is missing from the distal margin just above the
4377 IPF, and a second, smaller, chip is evident buccally. Small dentine patches are exposed
4378 over the Prd of both P_{4s} (stage 3). The RP₄ occlusal topography is better preserved than
4379 the LP₄. Both crowns are fully bicuspid with a well-defined MIg. A thin, high crest
4380 interrupts the MIg and connects the mesial aspects of the Prd and Med, defining the Fa
4381 distally. The Med is smaller in area than and its apex sits slightly mesial to that of the
4382 Prd. For both crowns, the MMR is worn, and the Fa is preserved as a small pit at the
4383 mesial termination of the MIg. For the LP₄, very little is preserved of the buccal or lingual
4384 extensions of the transverse groove. For the RP₄, the fissure has a small lingual
4385 bifurcation; additionally, there a small deflection evident distobuccally where the groove
4386 and MIg meet, which probably reflects an accessory ridge extending from the Prd as is
4387 common on other *H. naledi* premolars. For both P_{4s}, the mesiobuccal and distobuccal
4388 grooves are faint. The lingual aspects of both crowns are featureless.

4389 Examination of the μ CT scans of the roots embedded in the mandible show that
4390 left and right teeth differ slightly in their root configuration. Both have distinct mesial
4391 and distal root canals for most of the roots' courses. However, the mesial and distal roots
4392 of the RP₄ are externally connected for much of their length with a very deep invagination

4393 evident buccally and a shallower one lingually. For the LP₄, the mesial and distal roots
4394 are completely individualized for nearly half of their lengths. For the RP₄, the distal root
4395 is MD compressed, while the mesial root is obliquely oriented and runs from mesiobuccal
4396 to distolingual. For the LP₄, the major axes of both roots are parallel and approximately
4397 BL-oriented with the mesial root offset more to the buccal side than the more centrally
4398 placed distal root.

4399 Left and Right M₁: The alveolus of the left tooth is undamaged. In contrast,
4400 damage is extensive to the alveolus of the right tooth where an ancient break cleanly
4401 separated the mandibular corpus between the first and second molars. As preserved,
4402 about 2.0 mm of the mesial RM₁ root is exposed buccally and approximately 10.3 mm of
4403 its distal root is exposed buccally. Additionally, a portion of the distal face of the distal
4404 root is also visible in the region of damage.

4405 Both M₁s exhibit chipping to the distal margin above the IPF. On both crowns,
4406 concave dentine pools are exposed over the Prd, Hyd and Hld apices (stage 4). The LM₁
4407 is slightly more worn than the RM₁. Both crowns are a rounded rectangle in occlusal
4408 view, with a concavely worn mesial margin and a flattened distal margin. The lingual
4409 margin is more-or-less straight, and the buccal margin is gently bi-lobed. Both crowns
4410 have five primary cusps and no accessory cusps. Although worn, the crowns retain a Y-5
4411 fissure pattern, with a substantial portion of the Med and Hyd in contact and a well-
4412 developed Hld. The talonid is slightly wider than the trigonid in both crowns. For each,
4413 the Fa and MMR are worn, but a trace of the Fa is preserved as a short lingually-deflected
4414 extension of the central groove. A remnant of the mesiobuccal groove is preserved as a
4415 narrow and deep cleft near the occlusal margin that becomes shallow at mid-crown and

4416 deepens again just above the cervix. The distobuccal and lingual grooves are shallow at
4417 the occlusal margin and fade away mid-crown. There is no indication of a protostylid
4418 preserved.

4419 Left and Right M₂: The RM₂ has enamel chipping along the mesial margin of the
4420 Med and just above the IPF. The LM₂ is only obviously chipped along the MMR. Both
4421 crowns have moderate occlusal wear, which has flattened the cusps but no dentine is
4422 exposed (stage 2). The M₂s are larger than the M₁s in area but smaller than the M₃s. The
4423 crown is pentagonal in occlusal profile, with straight mesial and lingual profiles, mildly
4424 bi-lobed buccal profile, and relatively large Hld rounding the distal profile. In both M₂s,
4425 the talonid is wider than the trigonid. Both crowns have five principal cusps arranged in a
4426 Y-5 fissure pattern, with a substantial portion of the Med and Hyd in contact, and a well-
4427 developed Hld. The relative cusp areas are Hyd > Med ≥ End ≥ Prd > Hld. The pattern of
4428 grooves is better preserved on the right crown; though, there are no traces of
4429 supernumerary cusps for either. For each crown, the Fa is small and primarily a slight
4430 buccal extension of the central groove. Most of the MMR is obliterated by interproximal
4431 wear so that its expression cannot be assessed. The mesiobuccal groove is a narrow and
4432 deep cleft near the occlusal margin that becomes shallow at mid-crown. The distobuccal
4433 groove and lingual groove are both faint indentations in the crown face that disappear at
4434 mid-crown. Neither tooth presents any indication of a protostylid.

4435 Left and Right M₃: There is slight damage to the lingual and distobuccal alveolus
4436 of the LM₃. The distobuccal damage represents a clean break between the corpus and the
4437 ramus of the mandible. The apices of the Prd, Hyd and Hld are blunted by occlusal wear
4438 and a wear facet is visible along the mesial aspect of the Med, but no dentine is exposed.

4439 The lingual cusps remain mostly unworn (stage 1). The crown has five primary cusps
4440 arranged in a Y-5 fissure pattern, with a substantial portion of the Med and Hyd in
4441 contact, and a well-developed Hld. There are no accessory cusps. Relative cusp sizes are
4442 Med > Prd > Hyd > End > Hld (a large protostylid is included in the relative Prd area).
4443 The trigonid is wider than the talonid and the crown tapers distally. The wide and
4444 rounded MMR is lower than the essential crests of the Prd and Med. The fissure-like Fa
4445 appears as a lingual extension of the central groove, with a separate buccal section
4446 bounded distally by a small accessory Prd crest. The essential ridges of the primary cusps
4447 are not well defined. There are accessory ridges visible, especially on the RM₃ distally on
4448 the Med and mesially on the End. The End accessory ridge is slightly more prominent
4449 than the Med. The Fp is a slight distolingual extension of the central groove and is better
4450 expressed on the RM₃ than the LM₃. The mesiobuccal groove is a deep, narrow cleft near
4451 the occlusal margin that becomes shallow at mid-crown, and the distobuccal groove is a
4452 faint indentation that disappears mid-crown. The lingual grooves are faint indentations.
4453 Both crowns have a large protostylid; they are, in fact, the most prominent in the current
4454 Dinaledi sample. The LM₃ protostylid is more pronounced than that on the RM₃. For the
4455 both, the protostylid begins as a mesiolingual crest and becomes a distinct shelf that
4456 angles sharply towards the mesiobuccal groove. On the RM₃, the crest merges with the
4457 crown just prior to the mesiobuccal groove, while on the LM₃ the crest stops just at the
4458 mesiobuccal groove and does not cross it. The LM₃ protostylid has a free apex, while the
4459 RM₃ lacks such an occlusal-ward projection.
4460

4461 U.W. 101-1400: LdC₁-LM₁ (Table 1) This subadult left hemimandible holds the crowns
4462 of the dC₁, dP₃, and dP₄. The germs of the developing LI₂ and LM₁ were recovered from
4463 their damaged crypts and are described above with the isolated teeth. The LC₁ germ is
4464 visible in its crypt, where it remains. Several isolated teeth are attributed to this individual
4465 as well (for details on dental development and eruption sequences, see also Cofran and
4466 Walker, 2017) and are iterated in the descriptions and in the Discussion.

4467

4468 LdC₁ (Fig. 47): Alveolar bone is primarily preserved distally. The tooth is glued
4469 onto the U.W. 101-1400 mandible. No mesial IPF is visible. Dentine is exposed at its
4470 apex (stage 1). In occlusal view, the crown is ovoid. In labial and lingual views, the
4471 crown is asymmetrical, with a short, high mesial shoulder and a long distal edge that
4472 terminates in a low distinct tubercle. The mesial border is moderately angled and convex,
4473 while the distal border is more steeply angled and slightly concave. The crown apex is
4474 slightly offset distally. On the lingual surface, there is a shallow mesial groove and a
4475 slightly deeper distal groove and ridge associated with a distal tubercle. A shallow furrow
4476 delineates the distal tubercle labially. The labial aspect is otherwise unremarkable. On the
4477 lingual aspect, a broad median ridge is bordered by a weak groove-like mesial fossa and a
4478 wider and deeper distal fossa. From the occlusal aspect, the slightly swollen basal
4479 eminence is distally oriented.

4480 The root is broken at its apex and approximately 8.0 mm of root remains visible
4481 labially. The root is nearly circular in cross-section and only slightly narrower BL than
4482 LaL. There is a shallow mesial groove running along its length.

4483 This tooth is proposed as the antimere of U.W. 101-1611.

4484 LdP₃ (Fig. 47): The crown exhibits minor wear on the mesial Prd crest, the buccal face of
4485 the End, the apex of the Hyd, and the apex of the Hld (stage 2). Enamel chipping is
4486 evident along the DMR. The occlusal outline is rectangular, being elongated MD and
4487 narrow BL. The crown is wider BL across the talonid than across the trigonid. The crown
4488 has a Y-5 fissure pattern, with a substantial portion of the Med and Hyd in contact, and a
4489 well-developed Hld; in size, they are arranged as Prd > Hyd > Med > End > Hld. The tip
4490 of the Prd is markedly mesial to that of the Med and it is internally placed, so much so
4491 that it lies nearly along the midline of the tooth. The groove-like Fa is bounded by a thick
4492 MMR mesially and a prominent mesial trigonid crest distally that is incompletely
4493 bisected by the central groove. Two cuspules (mesioconulid and premetaconulid) are
4494 evident along the MMR. Each cuspule, though worn, appears to have a free apex. The
4495 mesio Buccal groove is a narrow v-shaped furrow occlusally, which gives the crown a
4496 pinched in or 'waisted' appearance in occlusal profile. The crown lacks a distinct DMR
4497 and Fp; though, occlusal wear reduced the crown's height distally. On the buccal aspect
4498 of the crown, a faint vertical furrow is associated with the mesiolingual cuspule of the
4499 MMR.

4500 Damage to the alveolar bone exposes its mesial root along the entire labial extent.

4501 9.1 mm of the mesial root are evident, which is approximately the full height of the root.

4502 This is proposed as the antimere of U.W. 101-1685.

4503 LdP₄ (Fig. 47): The occlusal surface is lightly worn, with a small wear facet visible along
4504 the mesial Prd crest (stage 1). The occlusal outline is rectangular, being MD elongated
4505 and BL narrow, and broader across the talonid than the trigonid. Five cusps are present
4506 and have the following size relationships: Hyd > Med ≥ Prd > End > Hld. The MMR is

4507 thick and comprises three small tubercles (premetaconulid, mesioconulid and
4508 preprotoconulid) defined by shallow grooves on both the occlusal and mesial surfaces.
4509 The Prd and Med each have prominent mesial accessory crests, which meet to form a
4510 thick mesial trigonid crest that divides the Fa into two transverse grooves. Occlusal
4511 complexity is present as a triplet of small ridges on the Hyd and an incipient post-
4512 metaconulid associated with a shallow vertical furrow mesial to the buccal groove. Very
4513 faint accessory ridges are present on the End and Hyd. The components of the DMR
4514 originating from the Hld and End meet at an angle and delineate a groove-like Fp. The
4515 mesio Buccal groove is deep, forms a wide v-shaped fovea near the occlusal edge, and
4516 terminates at approximately mid-crown.

4517 This specimen is the antimere of U.W. 101-1686.

4518 LC₁ germ (not figured): The developing crown is visible in its crypt within the
4519 mandible. The description is based upon the morphology evident in the μ CT images.
4520 Labially, the apex is offset distal to the MD midpoint. The mesial margin is convex and
4521 terminates at the mesial shoulder. A slight mesial labial groove runs adjacent to the
4522 mesial crest. The distal crest is vertically oriented. A distal shoulder is not yet formed;
4523 thus, this specimen would have had an asymmetric placement of the shoulders as seen in
4524 other *H. naledi* mandibular canines. Lingually, the median lingual ridge is offset distally
4525 relative to MD midpoint. It is indistinct and rounded and reaches its greatest relief near
4526 the apex. The mesial and distal lingual fossae are each broad and shallow, with the mesial
4527 fossa deepening and narrowing adjacent to the MMR. The mesial fossa is broader than
4528 the distal fossa.

4529 This germ is the proposed antimere of U.W. 101-1610.

4530

4531 **4. Discussion**

4532 *4.1. Significant associations*

4533 There are several sets of antimeres and metamerer that are proposed for the
4534 known Dinaledi Chamber teeth and enumerated above. Correctly associating isolated
4535 teeth has implications for reconstructing the taphonomic history of the fossils in the
4536 Dinaledi chamber and will inform assessments of the demography of the sample. As well,
4537 associating isolated teeth will permit a fuller evaluation of dental proportions, dental
4538 development, and metameric variation. Though a cautious approach is taken in proposing
4539 such associations, there are nine associations for which many isolated teeth and/or teeth
4540 in jaws can be associated. The justifications for associating these specimens are discussed
4541 in more detail and listed in Table 2. Not all antimeres identified in the main text are
4542 repeated below; we restrict the following discussion to those cases where multiple teeth
4543 can be associated with some certainty. We refer to each set of teeth as Association 1 –
4544 Association 9; however, we do not intend to imply that each set of teeth represents a
4545 distinct biological individual. Further research may reveal that some associations (e.g.,
4546 Associations 3 and 4) represent the same individual. We arrange the associations below
4547 in ontogenetic order from youngest to oldest.

4548

4549 Association 1 (infant) The U.W. 101-1400 mandible holds the crowns of the Ld_c, LdP₃,
4550 and LdP₄ and the germs of the developing LI₂ and LM₁ were recovered from their
4551 damaged crypts. Further, the developing crown of the permanent left canine is visible on

4552 the μ CT scans. The LM₁ is nearly crown complete, while the permanent canine is only
4553 approximately half crown complete.

4554 Based upon morphological similarity, the proposed right antimeres of the U.W.
4555 101-1400 teeth are: U.W. 101-1611 (Rd_c), U.W. 101-1685 (RdP₃), U.W. 101-1686
4556 (RdP₄), U.W. 101-1610 (RC₁ germ), and U.W. 101-1689 (RM₁ germ). These antimeres
4557 were all recovered from a single excavation block, block 1477, that also contains
4558 undescribed subadult cranial fragments (J.H., personal observation). Specimen U.W. 101-
4559 1612 (RdI₂) was also found in block 1477 and is provisionally associated with this
4560 individual. Consistent with that attribution is the lack of a distal IPF on U.W. 101-1612
4561 and a mesial IPF on U.W. 101-1611.

4562 Associating isolated maxillary and mandibular teeth must be approached with
4563 caution in a commingled assemblage; however, a reasonable case can be made that
4564 several isolated maxillary teeth are associated with this individual. Also recovered from
4565 block 1477 are an RdP⁴, U.W. 101-1687, and an RM¹ germ, U.W. 101-1688. The RM¹
4566 germ is nearly crown-complete and matches the developmental status of the U.W. 101-
4567 1400 and U.W. 101-1689 mandibular molars. An isolated LM¹ germ, U.W. 101-1305, is
4568 the proposed antimeres of U.W. 101-1688. These M¹s are nearly identical in morphology
4569 and developmental status. Assigning the U.W. 101-1687 RdP⁴ to the same biological
4570 individual cannot be certain, but its spatial association with the subadult material and the
4571 degree of its macrowear are consistent with that observed in the U.W. 101-1400
4572 mandibular deciduous molars. The antimeres of the RdP⁴ is proposed to be U.W. 101-
4573 1376, which was excavated within centimeters of an LdP³, U.W. 101-1377. Both U.W.
4574 101-1376 and U.W. 101-1377 lack adjoining IPFs, which is consistent with their

4575 attribution to the same individual. Further, a pair of maxillary deciduous canines (U.W.
4576 101-728 and U.W. 101-1287A) is provisionally assigned to this individual. Their status
4577 as antimeres is proposed on morphological grounds. Their association with the other
4578 maxillary teeth assigned to this individual is consistent with the absence of IPFs between
4579 adjacent teeth and the degree of macrowear on the deciduous mandibular canine in the
4580 U.W. 101-1400 mandible and its antimere. Rounding out the deciduous teeth assigned to
4581 this individual are a pair of antimeric dI^1 s (U.W. 101-544C and U.W. 101-1331), an LdI^2
4582 (U.W. 101-1304), and a pair of permanent maxillary canine germs (U.W. 101-544B and
4583 U.W. 101-1548). The status of the dI^1 s as antimeres is proposed on morphological
4584 grounds and the congruency of their mesial IPF. The status of the permanent maxillary
4585 canine germs, U.W. 101-544B and U.W. 101-1548, as antimeres is based on their
4586 morphology and developmental stages. Their developmental status matches that of the
4587 canine germ found in its crypt in the U.W. 101-1400 mandible. Finally, two developing
4588 antimeric M^2 s, U.W. 101-1063 and U.W. 101-1135, and a developing M_2 , U.W. 101-
4589 1002, may belong to this individual as well. Their association is tentative but consistent
4590 with their developmental status.

4591 If these proposed associations are correct, then all deciduous tooth classes, except
4592 for the mandibular deciduous central incisor, are represented for this individual. Further,
4593 all four nearly crown-complete $M1$ s are represented and so are all four permanent canine
4594 germs, which are approximately half crown complete.

4595

4596 Association 2 (sub-adult) The U.W. 101-377 mandible contains the crowns of RP_3 – RM_2
4597 in their alveoli and an isolated canine, U.W. 101-1014, is refit to this specimen. The roots

4598 of the canine and M₂ are open, indicating that these teeth were erupting at the time of
4599 death (Cofran et al., 2017). The U.W. 101-377 mandible is described as a ‘late juvenile’
4600 in Bolter et al. (2020). Based on morphological details and stage of occlusal wear, each of
4601 the U.W. 101-377/1014 teeth have proposed antimeres on the left side. From mesial to
4602 distal, these are U.W. 101-1076 (LC₁), U.W. 101-889 (LP₃), U.W. 101-887 (LP₄), U.W.
4603 101-809 (LM₁), and U.W. 101-789 (LM₂). The assignment of the isolated left teeth to the
4604 same individual is consistent with the shapes and sizes of their IPFs. An RI₂, U.W. 101-
4605 998, has a complexly shaped distal IPF that is perfectly congruent with the mesial IPF of
4606 the U.W. 101-1014 RC₁ and likely belongs to this individual as well. Importantly, U.W.
4607 101-998 has a proposed antimere, U.W. 101-1005C, which is part of a set of spatially
4608 associated mandibular incisors (U.W. 101-1005A, U.W. 101-1005B, and U.W. 101-
4609 1005C). The assignment of these anterior teeth to this individual completes the left and
4610 right dental arcades (to the M₂) for an individual that died while the M₂s and C₁s were
4611 erupting. There are only two isolated M₃s in the current Dinaledi assemblage (i.e., U.W.
4612 101-006 and U.W. 101-516) and both have mesial IPFs and occlusal wear, which
4613 indicates that neither belong to this individual.

4614

4615 Association 3 (sub-adult/young adult): As indicated by their morphological similarity and
4616 the shapes of their adjoining IPFs, a complete set of lightly worn maxillary incisors and
4617 canines from a single individual may be formed by U.W. 101-706 (LC¹), U.W. 101-932
4618 (LI²), U.W. 101-931 (LI¹), U.W. 101-1012 (RI¹), U.W. 101-709 (RI²), and U.W. 101-816
4619 (RC¹). Relating these specimens to postcanine teeth cannot be certain because the canines
4620 lack distal IPFs and there are several lightly worn P³s in the assemblage that lack mesial

4621 IPFs (i.e., U.W. 101-182, U.W. 101-729, U.W.101-786, and U.W.101-1107). There are
4622 clearly several individuals of similar late sub-adult/young adult ontogenetic status in the
4623 assemblage.

4624

4625 Association 4 (subadult/young adult) An associated set of lightly worn mandibular
4626 anterior teeth, U.W. 101-1126 (LC₁), U.W. 101-1131 (LI₂), U.W. 101-1132 (LI₁), U.W.
4627 101-1133 (RI₁), U.W. 101-1075 (RI₂), and U.W. 101-886 (RC₁) is suggested to belong to
4628 a single individual. This proposal is based on morphological grounds and the congruency
4629 of IPFs. Four of the teeth, U.W. 101-1126, U.W. 101-1131, U.W. 101-1132, and U.W.
4630 101-1333 were excavated in anatomical contact, making their association certain. Both
4631 canines attributed to this individual lack distal IPFs, which complicates attempts to link
4632 this set of teeth to the postcanine dentition. There are two sets of proposed antimeric P_{3s}
4633 (U.W. 101-298/1565 and U.W. 101-144/506), which are both lightly worn and lack
4634 mesial IPFs. As with the lightly worn maxillary teeth in Association 3 discussed above,
4635 there are clearly several individuals of comparable late sub-adult/young adult ontogenetic
4636 status in the assemblage.

4637

4638 Association 5 (adult) A set of maxillary left postcanine teeth extending from LP⁴–LM³
4639 for a single individual is arguably formed by U.W. 101-277 (LP⁴), U.W. 101-1676
4640 (LM¹), U.W. 101-1522 (LM²), and U.W. 101-418C (LM³). These associations are
4641 tentative and supported by the shapes and sizes of the respective IPFs. Though not
4642 confirmatory, especially given the high frequency of enamel chipping in the assemblage,
4643 patterns of interproximal enamel chipping are consistent with these attributions. Based on

4644 morphological similarity, U.W. 101-525 (RM¹) and U.W. 101-594 (RM³) may be
4645 antimeres of U.W. 101-1676 (LM¹) and U.W. 101-418C (LM³), respectively.

4646

4647 Association 6 (adult) A set of moderately worn adult maxillary teeth formed by U.W.
4648 101-1403 (RC¹), U.W. 101-1402 (RP³), U.W. 101-1401 (RP⁴), and U.W. 101-1396
4649 (RM¹) are proposed to be associated. Supporting this inference, the RC¹ through RP⁴
4650 were excavated in anatomical contact. A comparably worn set of left teeth, U.W. 101-
4651 1556 (LC¹), U.W. 101-1560 (LP³), and U.W. 101-1561 (LP⁴) are also derived from a
4652 single individual. An LI², U.W. 101-1684, is arguably associated with U.W. 101-1556
4653 based upon the shape and size of their adjoining IPFs and their degree of macrowear. The
4654 IPFs of the left canine through P⁴ are perfectly congruent with one another. Given their
4655 stage of wear, it is difficult to confirm that the left and right teeth are antimeres, but their
4656 size, premolar root morphology, and patterns of macrowear are consistent with this
4657 assessment. Unfortunately, U.W. 101-1403 lacks a crown, which complicates attempts to
4658 confirm that it is the antimeres of U.W. 101-1556.

4659

4660 Association 7 (adult) A complete mandibular dentition, U.W. 101-1261, is associated
4661 with a left maxilla, U.W. 101-1277, that contains the crowns of LI¹–LM² in their alveoli.
4662 The maxillary and mandibular teeth occlude perfectly. The mesial IPF of an isolated
4663 LM³, U.W. 101-1269, is congruent with the distal IPF of the U.W. 101-1277 M². Further,
4664 an isolated RM¹, U.W. 101-1463, is provisionally assigned to this individual. Its
4665 inclusion is not certain but its status as an antimeres of the U.W. 101-1277 M¹ is

4666 consistent with its morphology and state of macrowear. These teeth belong to the
4667 holotype (DH1) of *H. naledi* (Berger et al., 2015).
4668
4669 Association 8 (older adult) Specimens U.W. 101-357 (mesial root of LM₁), U.W. 101-
4670 358 (LP₃), U.W. 101-359 (LC₁), and U.W. 101-361 (LP₄–LM₃ in situ) were recovered in
4671 close spatial proximity. These left teeth all express advanced occlusal wear. A fragment
4672 of mandibular condyle (U.W. 101-196) is refit to the U.W. 101-361 mandible and
4673 articulates with the mandibular fossa of the DH3 partial cranium (Berger et al., 2015).
4674 There are many other heavily worn mandibular teeth in the assemblage (e.g., U.W. 101-
4675 010 and U.W. 101-006) that are candidates to belong to this individual; however, there
4676 are currently no conclusive grounds to argue for their association.

4677
4678 Association 9 (older adult) The U.W. 101-1362 (LP⁴), U.W. 101-796 (LM¹), U.W. 101-
4679 528 (LM²), and U.W. 101-527 (LM³) teeth form a metameric series from an adult
4680 showing advanced dental wear. Though it is difficult to evaluate given their wear stage,
4681 U.W. 101-005 (RM²) is a possible antimere of U.W. 101-528. The degree of occlusal
4682 wear on this set of teeth is comparable to that of the U.W.101-361 (i.e., DH3) individual
4683 described above. While it is tempting to link these two sets of teeth together in a single
4684 individual, there is currently no confirmatory evidence to do so.

4685

4686 *4.2. The Dinaledi dental feature set*

4687 Tooth size and relative size: In size, the Dinaledi incisors and canines are smaller on
4688 average (Table 1) than those of species of *Australopithecus* and *Paranthropus*, and only

4689 overlap with the smallest-toothed specimens of early *Homo* (e.g., the I² MD for KNM-ER
4690 1813 and OH 39); however, few early *Homo* specimens, except KNM-WT 60000
4691 (Leakey et al., 2012), match the exceptionally small Dinaledi incisor breadths (Berger et
4692 al., 2015; Hawks et al., 2018). The *H. naledi* C₁ MD length also falls below species of
4693 *Australopithecus*, *H. habilis*, and early *H. erectus* (Hawks et al., 2018). The Dinaledi
4694 postcanine teeth are smaller than species of *Australopithecus* and *Paranthropus* and fall
4695 toward the lower end of the size range of early *Homo* species (Berger et al., 2015; Hawks
4696 et al., 2018). For *H. rudolfensis*, only the Koobi Fora specimens KNM-ER 60000 and
4697 KNM-ER 62000, which are among the smallest teeth of that species yet discovered
4698 (Leakey et al., 2012), are similar in size, and they lie either above the *H. naledi* range or
4699 just within its upper limits (Berger et al., 2015; Hawks et al., 2018). While not well
4700 represented, the postcanine teeth of the South African teeth previously attributed to early
4701 *Homo* (e.g., SK 15, SK 18a, SK 27, SKX 257/258, SKW 3114, DNH 39, DNH 62, DNH
4702 67, DNH 70, Stw 19, Stw 53, Stw 80, SE 255, SE 1508) are also typically larger; though,
4703 the status of most of these teeth as *Homo* has been challenged (Zanolli et al., 2022),
4704 leaving few definitive South African early *Homo* specimens with which to compare *H.*
4705 *naledi* tooth size. Like the crowns, *H. naledi* mandibular molar roots are also smaller than
4706 those of species of *Paranthropus*, *Australopithecus*, and most early *Homo* specimens
4707 (Kupczik et al., 2019). *Homo naledi* is likely derived relative to species of
4708 *Australopithecus* and early *Homo*, and possibly convergent with species of *Paranthropus*,
4709 in having small anterior teeth. It is also likely derived relative to species of
4710 *Australopithecus*, *Paranthropus*, and early *Homo* in having smaller postcanine crowns
4711 and roots.

4712 Three Dinaledi mandibles (U.W. 101-001, U.W. 101-1142 + 1287B, and U.W.
4713 101-1261) preserve M_1 – M_3 , making their dental associations definitive (Figs. 41, 45, and
4714 46); two others (U.W. 101-361, U.W. 101-377) preserve partial sequences (Figs. 43 and
4715 44). In all cases, the molar size gradient is $M_3 > M_2 > M_1$. This gradient is typical of
4716 species of *Australopithecus* and *Paranthropus* and observed for some *H. habilis* (e.g., OH
4717 13), but not all (e.g., OH 16), for *H. rudolfensis* (e.g., KNM-ER 60000), and for some
4718 early *H. erectus* (e.g., KNM-ER 992, KNM-BK 8518), but not others (e.g., KNM-BK 67;
4719 Wood and Abbott, 1983; Wood and van Noten, 1986; Wood, 1991). The gradient is
4720 variable among Dmanisi *H. erectus*, with some having reduced M_3 s and an $M_1 > M_2 >$
4721 M_3 pattern, while D2600 evinces an $M_3 > M_2 > M_1$ gradient (Martinón-Torres et al.,
4722 2008). Among relevant South African specimens, molar proportions can only be judged
4723 directly for SK 15; its M_3 and M_2 are nearly the same MD length but the M_3 is narrower
4724 BL (Robinson, 1956), yielding an $M_2 > M_3 > M_1$ gradient. The SK 45 M_2 is larger than
4725 the M_1 and, based on the size of the M_3 alveolus, Robinson (1956) argued that, like SK
4726 15, the M_3 would have been smaller than the M_2 . Unfortunately, molar size cannot be
4727 determined accurately for Stw 80; though, its M_2 is clearly larger than its M_1 . For LD
4728 350-1, the most ancient fossil of *Homo*, the M_3 is slightly smaller than the M_2 (Villmoare
4729 et al., 2015). Middle and Late Pleistocene *Homo* tend to have reduced M_3 s and a derived
4730 $M_1 > M_2 > M_3$ or $M_2 > M_3 > M_1$ size gradient. *Homo naledi* relative molar size may be
4731 plesiomorphic for genus *Homo*, but LD-350 hints that M_3 reduction was already present
4732 in some *Homo* specimens near the base of the genus; therefore, the relatively large M_3
4733 could be a feature evolved convergently with species of *Australopithecus* and
4734 *Paranthropus*.

4735

4736 Mandibular canine morphology Despite their small size, the *H. naledi* C₁s share much of
4737 their crown shape and cingular morphology with species of *Australopithecus* and most
4738 specimens of early *Homo*. From the crown apex, the mesial crest is short and convex,
4739 while the distal is tall and vertical and terminates at a distal cuspule (Figs. 28 and 29).
4740 Robinson (1956: 46) described the distal cuspule on the canines of *A. africanus* when he
4741 wrote: “on the distal side of the crown there is a distinct small cusplet approximately
4742 half-way down the crown. This is formed by the remnants of the cingulum.” Martínón-
4743 Torres et al. (2008) noted the presence of this feature on the C₁s of Dmanisi *H. erectus*,
4744 where they referred to it as an ‘accessory distal cuspule.’ Our inspection of original
4745 fossils show that is present on KNM-ER 992, KNM-ER 60000, and KNM-ER 3734 (the
4746 crown of this specimen is worn in the region of interest, but the remaining lingual and
4747 labial topography suggest its presence; L.D., personal observation). Among early *H.*
4748 *erectus* specimens, the cingulum of KNM-WT 15000 is weakly developed and departs
4749 from this general condition. Among fossils purported to represent South African early
4750 *Homo*, a distal cuspule is present on Stw 80 (Kuman and Clarke, 2000). In contrast, in
4751 Middle and Late Pleistocene *Homo* the C₁ cingulum may be prominent (e.g., *Homo*
4752 *antecessor*, *Homo heidelbergensis*, Zhoukoudian *H. erectus*; Bermudez de Castro et al.,
4753 1999; Carbonelli et al., 2005; see Weidenreich 1937: plate VI and Weidenreich, 1943:
4754 Figure 282), but it rarely forms a topographically distinct prominence. Our examination
4755 of Krapina *Homo neanderthalensis* and extant *Homo sapiens* reveal little in the way of a
4756 cingulum and no trace of a distal tubercle. Thus, we consider the presence of the distal

4757 tubercle on the *H. naledi* C_{1S} to be a symplesiomorphy shared with species of
4758 *Australopithecus* and most specimens of early *Homo*.

4759

4760 Morphology of the permanent and deciduous premolars Both the Dinaledi dP³ and dP₃
4761 are molariform. For the dP³ (Fig. 4), there is no hint of distal cusp reduction seen in
4762 Neandertals and *H. sapiens* (Bailey et al., 2019). For the dP₃ (Fig. 8), all five principal
4763 cusps are well developed, the talonid is BL broader than the trigonid, and the Fa is
4764 enclosed by the MMR (Bailey et al., 2019; Brophy et al., 2021). In general terms, the dP₃
4765 of early species of *Australopithecus* (i.e., *Australopithecus anamensis* and
4766 *Australopithecus afarensis*) is comparatively primitive and the crown is dominated by the
4767 Prd without a prominent MMR (e.g., Leakey et al., 1998; Kimbel and Delezene, 2009). A
4768 five-cusped dP₃ with enclosed Fa is observed in *A. africanus* and in species of
4769 *Paranthropus*, but the MMR is reduced in mid-Pleistocene and younger species of *Homo*
4770 and the distal cusps are relatively small (Bailey et al., 2019). In species of early *Homo*,
4771 dP₃s are not well documented. Two that have been attributed to *Homo erectus*, KNM-ER
4772 1507 and KNM-ER 820, have only three cusps and a relatively large Prd (Wood, 1991).
4773 Thus, if *A. africanus* and species of *Paranthropus* capture the expected primitive states
4774 for genus *Homo*, then *H. naledi* retains a plesiomorphic configuration of the dP₃; the
4775 other alternative is that *H. naledi* is convergent with the morphology seen in those taxa.

4776 The *H. naledi* P₃s are also molarized in crown form: the mesiolingual corner of
4777 the crown is filled out, the crown is symmetric in occlusal view, the Med is large and
4778 fully separated from the Prd by a longitudinal groove, the Med is nearly the same height
4779 as the Prd, and the talonid is relatively large (Fig. 8). In general terms, these features can

4780 be matched in species of *Australopithecus* and *Paranthropus*; though, at larger crown
4781 sizes. Early *Homo* specimens show a wide range of variation in P₃ crown morphology. At
4782 one extreme, KNM-ER 1802, which may represent *H. rudolfensis* (but see Leakey et al.,
4783 2012), is fully bicuspid and symmetrical about the mesiodistal axis in occlusal view
4784 (Wood, 1991). Though broken buccally, a similar configuration can be inferred for the
4785 isolated *Homo* sp. P₃ KNM-ER 2599. In contrast, in paradigmatic examples of *H. habilis*
4786 from Olduvai (i.e., OH 7, OH 13) and *H. erectus* (e.g., KNM-ER 820, KNM-ER 992), the
4787 Med tends to be smaller in height and area than the Prd (Wood, 1991; L.D., personal
4788 observation). The same is true of KNM-ER 62004, where the Med is barely
4789 topographically distinct from the Tc and probably true of the more worn KNM-ER 62000
4790 (L.D., personal observation), where dentine is exposed on the Prd, but the Tc and Med
4791 remain covered in enamel at the same topographic wear plane. In Olduvai *H. habilis*
4792 (e.g., OH 7) and some early *H. erectus* (e.g., KNM-ER 992, KNM-WT 15000), the Med
4793 is not a topographically distinct cusp at all; it is instead linked to the Prd by a continuous
4794 and elevated Tc (a ‘prominent triangular ridge’ to Brown and Walker, 1993) not divided
4795 from the Prd by a longitudinal groove. In some *H. habilis* (e.g., KNM-ER 1507) and
4796 likely *H. erectus* (e.g., SKX 21204), a longitudinal groove is present, but the Med is
4797 subequal in height and projected area to the Prd. In *H. habilis* and early *H. erectus*, the
4798 mesiolingual corner of the P₃ is often abbreviated, giving the crown an asymmetric shape
4799 (e.g., D211, KNM-ER 820, KNM-ER 992, OH 7; Wood, 1991). In these regards, the
4800 specimens of *H. erectus* and *H. habilis* presage the reduced Med of Middle and Late
4801 Pleistocene forms. Thus, the *H. naledi* P₃ crown lacks the occlusal simplification, relative
4802 to *A. africanus* and species of *Paranthropus*, seen in some early *Homo* specimens; KNM-

4803 ER 1802 and KNM-ER 2599 are exceptions. Despite these general resemblances, the
4804 KNM-ER 1802 P₃ enamel-dentine junction (EDJ) shape is not similar to *H. naledi*. In
4805 fact, P₃ EDJ shape clearly distinguishes *H. naledi* from all other hominin taxa (Davies et
4806 al., 2020). Further, Davies et al. (2020) noted that *H. naledi* is the only hominin to have a
4807 P₃ that is larger than the P₄ in centroid size; a notable exception is Stw 80, which is
4808 discussed above. Thus, if *A. africanus* and early *Homo* specimens KNM-ER 1802 and
4809 KNM-ER 2599 reflect the plesiomorphic condition for genus *Homo*, then *H. naledi* may
4810 retain a generally primitive P₃. Alternatively, its molarized morphology would be
4811 convergent with that of early *Homo* specimens like KNM-ER 1802.

4812 The Dinaledi P₃s are all multirooted (2R: MB + D; Wood et al., 1988; Figs. 30
4813 and 31). Some early *Homo* specimens express simple P₃ roots, with either a Tomes' or
4814 single root noted for most *H. erectus* and *H. habilis* specimens. The few multirooted
4815 examples are commonly attributed to *H. rudolfensis* (though not all have complex roots;
4816 Wood, 1991). Additionally, multirooted P₃s are seen in the enigmatic KNM-ER 1805,
4817 which may represent *H. habilis*, UR 501, and at least the D2600 specimen of Dmanisi *H.*
4818 *erectus* (Wood et al., 1988; Wood, 1991; Martínón-Torres et al., 2008; Lordkipanidze et
4819 al., 2013: Table S3B). In the small sample of South African P₃s from Swartkrans and
4820 Sterkfontein that have been attributed to early *Homo* (e.g., Robinson, 1953; Kuman and
4821 Clarke, 2000; Grine, 2005), none matches the morphology of *H. naledi*. Our inspection of
4822 the alveoli or exposed roots of SK 15, SK 18a, and Stw 80 show that they are all Tomes'
4823 in form. Zanolli et al. (2022) argue that SK 15 is not *Homo*, while the taxonomic status of
4824 Stw 80 is more ambiguous. Thus, there are very few southern African specimens of early
4825 *Homo* with which to compare *H. naledi*. *Homo naledi* P₃ roots, like the crown, are

4826 distinct relative to the condition typically observed in small-toothed *Homo* specimens of
4827 eastern and southern Africa. As with crown form, if the multirooted early *Homo*
4828 specimens represent the plesiomorphic condition for the genus, then *H. naledi* retains a
4829 primitive root morphology.

4830 *Homo naledi* P³s and P⁴s are occasionally three rooted, with two tightly
4831 compressed buccal roots paired with a lingual root (Figs. 16–19). Most early *Homo* P³s
4832 are two-rooted, with buccal and lingual roots (e.g., OH 65, A.L. 666-1, KNM-ER 1470,
4833 KNM-ER 1805, KNM-ER 1813, OH 13), though there are some examples of three-
4834 rooted (e.g., OH 24) and one-rooted individuals (e.g., OH 16; e.g., Kimbel et al., 1997;
4835 Clarke, 2012; Lordkipanidze et al., 2013: Table S3B). Most early *Homo* P⁴s are two- or
4836 three-rooted (e.g., Kimbel et al., 1997; Lordkipanidze et al., 2013: Table S3B). Thus,
4837 multirooted maxillary premolars in *H. naledi* are another candidate plesiomorphy shared
4838 with early *Homo* species; however, detailed comparisons of *H. naledi* premolar root form
4839 have yet to be conducted.

4840

4841 Nonmetric traits of the molars The consistent absence of mass additive traits, like
4842 prominent cingular features, distinguishes the Dinaledi molars from *Australopithecus*,
4843 *Paranthropus*, and many early *Homo* specimens. For example, all Dinaledi M¹s and M²s
4844 have weakly expressed (or absent) Carabelli's features that are isolated on the
4845 mesiolingual corner of the crown and not in contact with the lingual groove (Figs. 20–
4846 23). In species of *Australopithecus* and *Paranthropus*, more prominent expression states
4847 are observed (either a large depression or pit, a cusp, or a crest-like feature), and the
4848 Carabelli's feature may wrap around the lingual surface of the crown to contact, or cross,

4849 the lingual groove (Van Reenen and Reid, 1995). Swartkrans specimen SKX 3114, a
4850 possible early *Homo* tooth, exhibits a large prominent feature with two deep vertical
4851 furrows on the mesiolingual corner of the crown. SKX 268 and SE 255 (both argued not
4852 to be *Homo* by Zanolli et al., 2022) have distinct Carabelli's (Grine, 1989; L.D., personal
4853 observation). From eastern Africa, *H. rudolfensis* can exhibit complex Carabelli's
4854 morphology (e.g., KNM-ER 1590 M²; Wood, 1991;), while *H. habilis* and *H. erectus* can
4855 exhibit minimal or no expression at all (e.g., KNM-ER 1813, KNM-ER 3733; Wood,
4856 1991). For the mandibular molars, the Dinaledi protostylids are small, restricted to the
4857 mesiobuccal corner, and do not intersect or cross the buccal groove (Fig. 4). A wide
4858 range of molar protostylid expression is observed in fossil hominins. Hlusko (2004), for
4859 example, identified six forms on *Australopithecus* and *Paranthropus* molars and noted
4860 that in *Australopithecus* and *Paranthropus* the "protostylid is more centrally located on
4861 the buccal side of the crown with a stronger relationship to the buccal groove" (Hlusko,
4862 2004: 582). Importantly, the figured example in Hlusko (2004) of no protostylid
4863 expression (STW 309a) does possess a diagonal crest on the mesiolingual corner;
4864 however, she does not consider it to be part of the protostylid trait. The very faint sub-
4865 vertical depression on the mesiolingual corner of the Dinaledi Prd resembles this
4866 condition; Skinner et al. (2008, 2009) have argued that such features should be
4867 considered part of the protostylid complex. Many early *Homo* molars from eastern Africa
4868 and Dmanisi express the protostylid form where it is adjacent to or crosses the mesial
4869 buccal groove. The small Carabelli's feature and protostylid that are mesially restricted in
4870 the Dinaledi sample would appear to be derived relative to species of *Australopithecus*,
4871 *Paranthropus*, and most early *Homo* specimens.

4872 *Homo naledi* mandibular molars lack crenulation, secondary fissures, and defined
4873 supernumerary cusps, which are frequently observed on molars of species of
4874 *Australopithecus*, *Paranthropus*, and early *Homo*; thus, *H. naledi* mandibular molars
4875 appear occlusally simple in comparison. All Dinaledi M₁s lack a C6, and only one M₂,
4876 U.W. 101-1142, expresses a C6 (Fig. 45). A C6 is common in species of *Paranthropus*
4877 (Wood and Abbott, 1983; Wood, 1991) and noted in *A. afarensis* and *A. africanus* as well
4878 (Guatelli-Steinberg and Irish, 2005; Bailey and Wood, 2007). Large C7s are not observed
4879 in the Dinaledi M₁ and M₂ sample (Irish et al., 2018). Some Dinaledi M₁s do express a
4880 small postmetaconulid (Figs. 33 and 34). Though not ubiquitous, examples of
4881 individualized C7s can be found on M₁s and M₂s attributed to all early *Homo* species
4882 (e.g., KNM-ER 1802, KNM-ER 1507, KNM-WT 15000, KNM-ER 60000, D211, OH 7,
4883 LD 350; Wood and Abbott, 1983; Wood, 1991; Leakey et al., 2012; Villmoare et al.,
4884 2015), among the Omo and Turkana ‘nonrobust’ assemblage (e.g., KNM-ER 5431, Omo
4885 75-14) that may also represent early members of the genus (Wood, 1991; Suwa et al.,
4886 1996; Villmoare et al., 2015), and on DNH 67, a suggested early *Homo* M₁ from
4887 Drimolen (Moggi-Cecchi et al., 2009; but see Zanolli et al., 2022). The absence of a C7
4888 appears to be derived in *H. naledi* relative to species of early *Homo*; the absence of a C6
4889 is shared with most species of *Homo*.

4890

4891 Molar shape Dinaledi molar cuspal proportions are distinct from most Middle and Late
4892 Pleistocene *Homo* samples but resemble those in species of early *Homo*. For the Dinaledi
4893 sample, the M¹ and M² have a relatively large Hy and a ‘rhomboidal’ outline (e.g.,
4894 Kimbel et al., 1997). For the Dinaledi M₁, the distal cusps (End and H1d) are relatively

4895 large, and not reduced as is common in Middle and Late Pleistocene *Homo* (Zanolli,
4896 2013). Thus, the rhomboidal shape of the maxillary molars and the relative cuspal size
4897 the maxillary and mandibular molars would be plesiomorphies shared with basal species
4898 of the genus *Homo*; however, analyses the M₁ and M₂ EDJ shape easily distinguish *H.*
4899 *naledi* from all other hominin taxa (Skinner et al., 2016).

4900

4901 Morphological summary The Dinaledi fossils capture a dental feature set that is distinct
4902 from all other hominins. The Dinaledi canines are small, but express features typical of
4903 basal members of the genus. The permanent and deciduous P₃s have molarized crowns
4904 that are reminiscent of *A. africanus* and species of *Paranthropus*, but at a much smaller
4905 size. Many features of the *H. naledi* dentition are candidate plesiomorphies shared with
4906 basal species of the genus *Homo* (e.g., distally increasing mandibular molar size gradient,
4907 molarized dP₃ and P₃, multirooted maxillary and mandibular premolars, rhomboidal
4908 maxillary molar outline, distal cuspule on C₁). Other traits are candidate apomorphies of
4909 *H. naledi* relative to basal members of the genus (e.g., anterior tooth size reduction,
4910 postcanine tooth size reduction, C7 absence on mandibular molars, configuration of the
4911 protostylid, postcanine EDJ shape). Though much comparative work remains to be done,
4912 the morphology of the Dinaledi teeth provides strong support for the taxonomic diagnosis
4913 of *H. naledi*.

4914

4915 **5. Conclusion**

4916 Hominin fossils from the Dinaledi Chamber provide the first large single-site
4917 sample of Middle Pleistocene-aged dental remains from Africa. Though comparative

4918 analyses are just beginning, their abundance, excellent state of preservation, and
4919 completeness provide a detailed picture of the *H. naledi* dental feature set. The teeth are
4920 commingled and often found in isolation, but it is clear that numerous individuals, from
4921 infants to older adults, are represented in the dental assemblage. In fact, several
4922 significant associations are proposed, including two subadults that will provide insight
4923 into the life history and dental development of *H. naledi*. The Dinaledi teeth hold a
4924 wealth of information that is only beginning to be prospected for their potential. We
4925 expect that this sample will provide valuable insights into the paleobiology of *H. naledi*
4926 for years to come.

4927

4928 **Acknowledgements**

4929 We are indebted to Bernhard Zipfel and Sifelani Jirah for access to and assistance with
4930 the hominin collections at the Evolutionary Studies Institute at the University of the
4931 Witwatersrand. We also express our thanks to the staff of the Evolutionary Studies
4932 Institute, especially Wilma Lawrence and Sonia Sequeira, for help in organizing research
4933 trips. We are grateful to Kudakwashe Jakata for his assistance with tomographic
4934 scanning. The discovery, recovery and preparation of the material was funded by a Grant
4935 from the National Geographic Society and the Lyda Hill Foundation. Research was also
4936 supported by a workshop grant from the National Research Foundation of South Africa.
4937 We are grateful for a workshop grant (to L.K.D. and M.M.S.) from the Wenner-Gren
4938 Foundation that funded participation for many coauthors. L.K.D. thanks the Office of
4939 Research and Development at the University of Arkansas and the Connor Family Faculty
4940 Foundation for providing funding. J.K.B. thanks the LSU Council of Research Summer

4941 Stipend Grant for funding research on the material. Participation of M.M.S. supported by
4942 European Research Council (grant agreement No. 819960). We thank Tom Davies and
4943 William Plummer for helpful discussions and comparative images of tooth crown
4944 morphology and Mykolas Imbrasas for assistance with figure revision. We also thank the
4945 Editor-in-Chief, Clément Zanolli, the Associate Editor, and the reviewers of the
4946 manuscript for their thoughtful and thorough edits and, especially, for their patience.

4947

4948 **References**

- 4949 AlQahtani, S.J., Hector, M.P., Liversidge, H.M., 2010. Brief communication: The
4950 London atlas of human tooth development and eruption. *American Journal of*
4951 *Physical Anthropology* 142, 481–490.
- 4952 Bailey, S.E., Brophy, J.K., Moggi-Cecchi, J., Delezene, L.K., 2019. The deciduous
4953 dentition of *Homo naledi*. *Journal of Human Evolution* 136, 102655.
- 4954 Bailey, S.E., Hublin, J.J., 2013. What does it mean to be dentally “modern”? In: Scott,
4955 G. R., Irish, J.D. (Eds.), *Anthropological Perspectives on Tooth Morphology:*
4956 *Genetics, Evolution, Variation*. Cambridge University Press, Cambridge, pp. 222–
4957 249.
- 4958 Bailey, S. E., Wood, B. A., 2007. Trends in postcanine occlusal morphology within the
4959 hominin clade: the case of *Paranthropus*. In: Bailey, S.E., Hublin, J.-J. (Eds.),
4960 *Dental Perspectives on Human Evolution: State of the Art Research in Dental*
4961 *Anthropology*. Springer, Dordrecht, pp. 33–52.

4962 Berger, L.R., De Ruiter, D.J., Churchill, S.E., Schmid, P., Carlson, K.J., Dirks, P.H.,
4963 Kibii, J.M., 2010. *Australopithecus sediba*: A new species of *Homo*-like
4964 australopith from South Africa. *Science* 328, 195–204.

4965 Berger, L.R., Hawks, J., de Ruiter, D.J., Churchill, S.E., Schmid, P., Deleuzene, L.K.,
4966 Kivell, T.L., Garvin, H.M., Williams, S.A., DeSilva, J.M., Skinner, M.M.,
4967 Musiba, C.M., Cameron, N., Holliday, T.W., Harcourt-Smith, W., Ackermann,
4968 R.R., Bastir, M., Bogin, B., Bolter, D., Brophy, J., Cofran, Z.D., Congdon, K.A.,
4969 Deane, A.S., Dembo, M., Drapeau, M., Elliott, M.C., Feuerriegel, E.M., Garcia-
4970 Martinez, D., Green, D.J., Gurtov, A., Irish, J.D., Kruger, A., Laird, M.F., Marchi,
4971 D., Meyer, M.R., Nalla, S., Negash, E.W., Orr, C.M., Radovicic, D., Schroeder,
4972 L., Scott, J.E., Throckmorton, Z., Tocheri, M.W., VanSickle, C., Walker, C.S.,
4973 Wei, P., Zipfel, B., 2015. *Homo naledi*, a new species of the genus *Homo* from
4974 the Dinaledi Chamber, South Africa. *eLife* 4, e09560.

4975 Berger, L.R., Hawks, J., Dirks, P.H., Elliott, M., Roberts, E.M., 2017. *Homo naledi* and
4976 Pleistocene hominin evolution in subequatorial Africa. *eLife* 6, e24234.

4977 Berger, L.R., Keyser, A.W., Tobias, P.V., 1993. Gladysvale: First early hominid site
4978 discovered in South Africa since 1948. *American Journal of Physical*
4979 *Anthropology* 92, 107–111.

4980 Berger, L.R., Parkington, J.E., 1995. A new Pleistocene hominid-bearing locality at
4981 Hoedjiespunt, South Africa. *American Journal of Physical Anthropology* 98, 601–
4982 609.

4983 Bermúdez de Castro, J. M., Rosas A., Nicolás, M. E., 1999. Dental remains from
4984 Atapuerca–TD6 (Gran Dolina site, Burgos, Spain). *Journal of Human Evolution*
4985 37, 523–566.

4986 Berthaume, M.A., Delezene, L.K., Kupczik, K., 2018. Dental topography and the diet of
4987 *Homo naledi*. *Journal of Human Evolution* 118, 14–26.

4988 Bolter, D.R., Elliott, M.C., Hawks, J., Berger, LR., 2020. Immature remains and the first
4989 partial skeleton of a juvenile *Homo naledi*, a late Middle Pleistocene hominin
4990 from South Africa. *PloS One* 15, e0230440.

4991 Bolter, D. R., Hawks, J., Bogin, B., Cameron, N., 2018. Palaeodemographics of
4992 individuals in Dinaledi Chamber using dental remains. *South African Journal of*
4993 *Science* 114, 1–6.

4994 Brink, J.S., Herries, A., Moggi-Cecchi, J., Gowlett, J., Bousman, C.B., Hancox, J.P.,
4995 Grün, R., Eisenmann, V., Adams, J.W., Rossouw, L., 2012. First hominine
4996 remains from a ~1.0 million year old bone bed at Cornelia-Uitzoek, Free State
4997 Province, South Africa. *Journal of Human Evolution* 63, 527–535.

4998 Broom, R., 1938. The Pleistocene anthropoid apes of South Africa. *Nature* 142, 377–379.

4999 Broom, R., Robinson J.T., 1949. A new type of fossil man. *Nature* 164, 322–323.

5000 Brophy, J.K., Moggi-Cecchi, J., Matthews, G.J., Bailey, S.E., 2021. Comparative
5001 morphometric analyses of the deciduous molars of *Homo naledi* from the
5002 Dinaledi Chamber, South Africa. *American Journal of Physical Anthropology*
5003 174, 299–314.

5004 Brown, B., Walker, A., 1993. The dentition. In: Walker, A., Leakey, R. (Eds.), *The*
5005 *Nariokotome Homo erectus* Skeleton. Harvard University Press, Cambridge.

5006 Carbonell, E., Bermúdez de Castro, J. M., Arsuaga, J. L., Allue, E., Bastir, M., Benito,
5007 A., Cáceres, T., Canals, J., Díez, J. C., van der Made, J., Mosquera, M., Ollé, A.,
5008 Pérex-González, A., Rodríguez, J., Rodríguez, X. P., Rosas, A., Rosell, J., Sala,
5009 R., Vallverdú, J., Vergés, J. M., 2005. An Early Pleistocene hominin mandible
5010 from Atapuerca-TD6, Spain. *Proceedings of the National Academy of Sciences*
5011 USA 102, 5674–5678.

5012 Clarke, R.J., 1977a. The cranium of the Swartkrans hominid SK 847 and its relevance to
5013 human origins. Ph.D. Dissertation, University of the Witwatersrand.

5014 Clarke, R.J., 1977b. A juvenile cranium and some adult teeth of early *Homo* from
5015 Swartkrans, Transvaal. *South African Journal of Science* 73, 46–49.

5016 Clarke, R., 1985. Early Acheulean with *Homo habilis* at Sterkfontein. In: Tobias, P.V.
5017 (Ed.), *Hominid Evolution: Past, Present and Future*. Alan R. Liss, New York, pp.
5018 287–298.

5019 Clarke, R.J., 2012. A *Homo habilis* maxilla and other newly-discovered hominid fossils
5020 from Olduvai Gorge, Tanzania. *Journal of Human Evolution* 63, 418–428.

5021 Cofran, Z., Walker, C.S., 2017. Dental development in *Homo naledi*. *Biology Letters* 13,
5022 20170339.

5023 Curnoe, D., 2009. The mandible from Bed 3, Cave of Hearths. In: McNabb, J., Sinclair,
5024 A. (Eds.), *The Cave of Hearths: Makapan Middle Pleistocene Research Project:*
5025 *Field research by Anthony Sinclair and Patrick Quinney, 1996–2001.*
5026 Archaeopress, Oxford, pp. 138–149.

5027 Curnoe, D., Tobias, P.V., 2006. Description, new reconstruction, comparative anatomy,
5028 and classification of the Sterkfontein Stw 53 cranium, with discussions about the

5029 taxonomy of other southern African early *Homo* remains. *Journal of Human*
5030 *Evolution* 50, 36–77.

5031 Dart, R.A., 1925. *Australopithecus africanus*: The man-ape of South Africa. *Nature* 115,
5032 195–199.

5033 Davies, T.W., Deleuzene, L.K., Gunz, P., Hublin, J.-J., Berger, L.R., Gidna, A., Skinner,
5034 M.M., 2020. Distinct mandibular premolar crown morphology in *Homo naledi*
5035 and its implications for the evolution of *Homo* species in southern Africa.
5036 *Scientific Reports* 10, 13196.

5037 Davies, T.W., Deleuzene, L.K., Gunz, P., Hublin, J.-J., Skinner, M.M., 2019a.
5038 Endostructural morphology in hominoid mandibular third premolars: Geometric
5039 morphometric analysis of dentine crown shape. *Journal of Human Evolution* 133,
5040 198–213.

5041 Davies, T.W., Deleuzene, L.K., Gunz, P., Hublin, J.-J., Skinner, M.M., 2019b.
5042 Endostructural morphology in hominoid mandibular third premolars: Discrete
5043 traits at the enamel-dentine junction. *Journal of Human Evolution* 136, 102670

5044 Dembo, M., Radovčić, D., Garvin, H.M., Laird, M.F., Schroeder, L., Scott, J.E., Brophy,
5045 J., Ackermann, R.R., Musiba, C.M., de Ruiter, D.J., Mooers, A.Ø., 2016. The
5046 evolutionary relationships and age of *Homo naledi*: An assessment using dated
5047 Bayesian phylogenetic methods. *Journal of Human Evolution* 97, 17–26.

5048 Dirks, P.H., Berger, L.R., Roberts, E.M., Kramers, J.D., Hawks, J., Randolph-Quinney,
5049 P.S., Elliott, M., Musiba, C.M., Churchill, S.E., de Ruiter, D.J., Schmid, P., 2015.
5050 Geological and taphonomic context for the new hominin species *Homo naledi*
5051 from the Dinaledi Chamber, South Africa. *eLife* 4, e09561.

5052 Dirks, P.H., Roberts, E.M., Hilbert-Wolf, H., Kramers, J.D., Hawks, J., Dosseto, A.,
5053 Duval, M., Elliott, M., Evans, M., Grün, R. and Hellstrom, J., 2017. The age of
5054 *Homo naledi* and associated sediments in the Rising Star Cave, South Africa.
5055 eLife 6, e24231.

5056 Dreyer, T.F., 1935. A human skull from Florisbad, Orange Free State, with a note on the
5057 endocranial cast by C. U. Ariens Kappers. Proc. K. Ned. Akad. Wet. 38, 119–128.

5058 Elliott, M.C., Peixotto, B., Morris, H., Feuerriegel, E.M., Tucker, S., Hunter, R.,
5059 Ramalepa, M., Tsikoane, M., Roberts, E.M., Spandler, C. Hawks, J., 2018.
5060 Hominin material recovered from the base of the Chute in the Hill Antechamber,
5061 in the Dinaledi Chamber System of the Rising Star Cave. American Journal of
5062 Physical Anthropology 165, 76.

5063 Feuerriegel, E.M., Green, D.J., Walker, C.S., Schmid, P., Hawks, J., Berger, L.R.
5064 Churchill, S.E., 2017. The upper limb of *Homo naledi*. Journal of Human
5065 Evolution 104, 155–173.

5066 Garvin, H.M., Elliott, M.C., Delezene, L.K., Hawks, J., Churchill, S.E., Berger, L.R.,
5067 Holliday, T.W., 2017. Body size, brain size, and sexual dimorphism in *Homo*
5068 *naledi* from the Dinaledi Chamber. Journal of Human Evolution 111, 119–138.

5069 Grine, F.E., 1989. New hominid fossils from the Swartkrans Formation (1979–1986):
5070 Craniodental specimens. American Journal of Physical Anthropology 79, 409–
5071 449.

5072 Grine, F.E., 2005. Early *Homo* at Swartkrans, South Africa: A review of the evidence and
5073 an evaluation of recently proposed morphs. South African Journal of Science 101,
5074 43–52.

5075 Grine, F.E., 2016. The Late Quaternary hominins of Africa: The skeletal evidence from
5076 MIS 6–2. In: Jones, S.C., Stewart, B.A. (Eds.), Africa from MIS 6–2: Population
5077 Dynamics and Paleoenvironments. Springer, Dordrecht, pp. 323–381.

5078 Grine, F.E., Bailey, R.M., Harvati, K., Nathan, R.P., Morris, A.G., Henderson, G.M.,
5079 Ribot, I., Pike, A.W.G., 2007. Late Pleistocene skull from Hofmeyr, South Africa,
5080 and modern human origins. *Science* 315, 226–229.

5081 Grine, F.E., Gonzalvo, E., Rossouw, L., Holt, S., Black, W., Braga, J., 2021. Variation in
5082 Middle Stone Age mandibular molar enamel-dentine junction topography at
5083 Klasies River Main Site assessed by diffeomorphic surface matching. *Journal of*
5084 *Human Evolution* 161, 103079.

5085 Grine F.E., Jungers, W.L., Schultz, J., 1996. Phenetic affinities among early *Homo* crania
5086 from East and South Africa. *Journal of Human Evolution* 30, 189–225.

5087 Grine, F.E., Marean, C.W., Faith, J.T., Black, W., Mongle, C.S., Trinkaus, E., le Roux,
5088 S.G., du Plessis, A., 2017. Further human fossils from the Middle Stone Age
5089 deposits of Die Kelders Cave 1, Western Cape Province, South Africa. *Journal of*
5090 *Human Evolution* 109, 70–78.

5091 Grine, F.E., Smith, H.F., Heesy, C.P., Smith, E.J., 2009. Phenetic affinities of Plio-
5092 Pleistocene *Homo* fossils from South Africa: Molar cusp proportions. In: Grine,
5093 F.E., Fleagle, J.G., Leakey, R.E. (Eds.), *The First Humans—Origin and Early*
5094 *Evolution of the Genus Homo*. Springer, Dordrecht, pp. 49–62.

5095 Grine, F.E., Wurz, S., Marean, C.W., 2017. The Middle Stone Age human fossil record
5096 from Klasies River Main site. *Journal of Human Evolution* 103, 53–78.

5097 Grün, R., Brink, J.S., Spooner, N.A., Taylor, L., Stringer, C.B., Franciscus, R.G., Murray,
5098 A.S., 1996. Direct dating of Florisbad hominid. *Nature* 382, 500–501.

5099 Grün, R., Pike, A., McDermott, F., Eggins, S., Mortimer, G., Aubert, M., Kinsley, L.,
5100 Joannes-Boyau, R., Rumsey, M., Denys, C., Brink, J., 2020. Dating the skull from
5101 Broken Hill, Zambia, and its position in human evolution. *Nature* 580, 372–375.

5102 Guatelli-Steinberg, D., Irish, J. D., 2005. Brief Communication: Early hominin variability
5103 in first molar dental trait frequencies. *American Journal of Physical Anthropology*
5104 128, 477–484.

5105 Guatelli-Steinberg, D., O’Hara, M.C., Le Cabec, A., Delezene, L.K., Reid, D.J., Skinner,
5106 M.M., Berger, L.R., 2018. Patterns of lateral enamel growth in *Homo naledi* as
5107 assessed through perikymata distribution and number. *Journal of Human*
5108 *Evolution* 121, 40–54.

5109 Harcourt-Smith, W.E.H., Throckmorton, Z., Congdon, K.A., Zipfel, B., Deane, A.S.,
5110 Drapeau, M.S.M., Churchill, S.E., Berger, L.R., DeSilva, J.M., 2015. The foot of
5111 *Homo naledi*. *Nature Communications* 6, 8432.

5112 Harvati, K., Bauer, C.C., Grine, F.E., Benazzi, S., Ackermann, R.R., van Niekerk, K.L.,
5113 Henshilwood, C.S., 2015. A human deciduous molar from the Middle Stone Age
5114 (Howiesons Poort) of Klipdrift Shelter, South Africa. *Journal of Human Evolution*
5115 82, 190–196.

5116 Hawks, J., Elliott, M., Schmid, P., Churchill, S.E., de Ruiter, D.J., Roberts, E.M., Hilbert-
5117 Wolf, H., Garvin, H.M., Williams, S.A., Delezene, L.K., Feuerriegel, E.M.,
5118 Randolph-Quinney, P., Kivell, T.L., Laird, M.F., Tawane, G., DeSilva, J.M.,
5119 Bailey, S.E., Brophy, J.K., Meyer, M.R., Skinner, M.M., Tocheri, M.W.,

5120 VanSickle, C., Walker, C.S., Campbell, T.L., Kuhn, B., Kruger, A., Tucker, S.,
5121 Gurtov, A., Hlophe, N., Hunter, R., Morris, H., Peixotto, B., Ramalepa, M., van
5122 Rooyen, D., Tsikoane, M., Boshoff, P., Dirks, P.H.G.M., Berger, L.R., 2017. New
5123 fossil remains of *Homo naledi* from the Lesedi Chamber, South Africa. *eLife* 6,
5124 e24232.

5125 Herries, A.I.R., Martin, J.M., Leece, A.B., Adams, J.W., Boschian, G., Joannes-Boyau,
5126 R., Edwards, T.R., Mallett, T., Massey, J., Murszewski, A., Neubauer, S.,
5127 Pickering, R., Strait, D.S., Armstrong, B.J., Baker, S., Caruana, M.V., Denham,
5128 T., Hellstrom, J., Moggi-Cecchi, J., Mokobane, S., Penzo-Kajewski, P., Rovinsky,
5129 D.S., Schwartz, G.T., Stammers, R.C., Wilson, C., Woodhead, J., Menter, C.,
5130 2020. Contemporaneity of *Australopithecus*, *Paranthropus*, and early *Homo*
5131 *erectus* in South Africa. *Science* 368, eaaw7293.

5132 Hlusko, L.J., 2004. Protostylid variation in *Australopithecus*. *Journal of Human*
5133 *Evolution* 46, 579–594.

5134 Holloway, R.L., Hurst, S.D., Garvin, H.M., Schoenemann, P.T., Vanti, W.B., Berger,
5135 L.R., Hawks, J., 2018. Endocast morphology of *Homo naledi* from the Dinaledi
5136 Chamber, South Africa. *Proceedings of the National Academy of Sciences USA*
5137 115, 5738–5743.

5138 Hublin, J.J., Ben-Ncer, A., Bailey, S.E., Freidline, S.E., Neubauer, S., Skinner, M.M.,
5139 Bergmann, I., Le Cabec, A., Benazzi, S., Harvati, K., Gunz, P., 2017. New fossils
5140 from Jebel Irhoud, Morocco and the pan-African origin of *Homo sapiens*. *Nature*
5141 546, 289.

5142 Hughes, A.R., Tobias, P.V., 1977. A fossil skull probably of the genus *Homo* from
5143 Sterkfontein, Transvaal. *Nature* 265, 310–312.

5144 Irish, J.D., Bailey, S.B., Guatelli-Steinberg, D., Delezene, L.K., Berger, L.R., 2018.
5145 Ancient teeth, phenetic affinities, and African hominins: Another look at where
5146 *Homo naledi* fits in. *Journal of Human Evolution* 122, 108–123.

5147 Irish, J.D., Grabowski, M., 2021. Relative tooth size, Bayesian inference, and *Homo*
5148 *naledi*. *American Journal of Physical Anthropology* 176, 262–282.

5149 Irish, J.D., Guatelli-Steinberg, D., Legge, S.S., de Ruiter, D.J., Berger, L.R., 2013. Dental
5150 morphology and the phylogenetic “place” of *Australopithecus sediba*. *Science*
5151 340, 1233062.

5152 Johanson, D.C., White, T.D., Coppens, Y., 1978. A new species of the genus
5153 *Australopithecus* (Primates: Hominidae) from the Pliocene of eastern Africa.
5154 *Kirtlandia* 28, 1–14.

5155 Kimbel, W.H., 2009. The origin of *Homo*. In: Grine, F.E., Fleagle, J.G., Leakey, R.E.
5156 (Eds.), *The First Humans—Origin and early evolution of the genus Homo*.
5157 Springer, Dordrecht. 31–37.

5158 Kimbel, W.H., Delezene, L.K., 2009. “Lucy” redux: A review of research on
5159 *Australopithecus afarensis*. *American Journal of Physical Anthropology* 140, 2–
5160 48.

5161 Kimbel, W.H., Johanson, D.C., Rak, Y., 1997. Systematic assessment of a maxilla of
5162 *Homo* from Hadar, Ethiopia. *American Journal of Physical Anthropology* 103,
5163 235–262.

5164 Kivell, T.L., Deane, A.S., Tocheri, M.W., Orr, C.M., Schmid, P., Hawks, J., Berger, L.R.,
5165 Churchill, S.E., 2015. The hand of *Homo naledi*. Nature Communications 6,
5166 8431.

5167 Klein, R.G., Grine, F.E., 1993. Late Pleistocene human remains from the Sea Harvest
5168 site, Saldanha Bay, South Africa. South African Journal of Science 89, 145–152.

5169 Kruger, A., Randolph-Quinney, P., Elliott, M., 2016. Multimodal spatial mapping and
5170 visualization of Dinaledi Chamber and Rising Star Cave. South African Journal of
5171 Science 112, 1–11.

5172 Kuman, K., Clarke, R.J., 1986. Florisbad—New investigations at a Middle Stone Age
5173 hominid site in South Africa. Geoarchaeology 1, 103–125.

5174 Kuman, K., Clarke, R.J., 2000. Stratigraphy, artifact industries and hominid associations
5175 from Sterkfontein Member 5. Journal of Human Evolution 38, 827–847.

5176 Kupczik, K., Deleuzene, L.K., Skinner, M.M., 2019. Mandibular molar root and pulp
5177 cavity morphology in *Homo naledi* and other Plio-Pleistocene hominins. Journal
5178 of Human Evolution 130, 83–95.

5179 Laird, M.F., Schroeder, L., Garvin, H.M., Scott, J.E., Dembo, M., Radovčić, D., Musiba,
5180 C.M., Ackermann, R.R., Schmid, P., Hawks, J., Berger, L.R., 2017. The skull of
5181 *Homo naledi*. Journal of Human Evolution 104, 100–123.

5182 Leakey, L.S.B., 1959. A new fossil skull from Olduvai. Nature 184, 491–493.

5183 Leakey, M.G., Feibel, C.S., McDougall, I., Ward, C., Walker, A., 1998. New specimens
5184 and confirmation of an early age for *Australopithecus anamensis*. Nature 393, 62–
5185 66.

5186 Leakey, M.B., Spoor, F., Dean, M.C., Feibel, C.S., Anton, S.C., Kiarie, C., Leakey, L.N.,
5187 2012. New fossils from Koobi Fora in northern Kenya confirm taxonomic
5188 diversity in early *Homo*. *Nature* 488, 201–204.

5189 Leakey, L.S.B., Tobias, P.V., Napier, J.R., 1964. A new species of the genus *Homo* from
5190 Olduvai Gorge. *Nature* 202, 7–9.

5191 Lordkipanidze, D., Ponce de León, M.S., Margvelashvili, A., Rak, Y., Rightmire, G.P.,
5192 Vekua, A., Zollikofer, C.P., 2013. A complete skull from Dmanisi, Georgia, and
5193 the evolutionary biology of early *Homo*. *Science* 342, 326–331.

5194 Marchi, D., Walker, C.S., Wei, P., Holliday, T.W., Churchill, S.E., Berger, L.R., DeSilva,
5195 J.M., 2017. The thigh and leg of *Homo naledi*. *Journal of Human Evolution* 104,
5196 174–204.

5197 Marean, C.W., Nilssen, P.J., Brown, K., Jerardino, A. Stynder, D., 2004.
5198 Paleoanthropological investigations of Middle Stone Age sites at Pinnacle Point,
5199 Mossel Bay (South Africa): Archaeology and hominid remains from the 2000
5200 field season. *Paleoanthropology* 2004, 14–83.

5201 Martin, J.M., Leece, A.B., Neubauer, S., Baker, S.E., Mongle, C.S., Boschian, G.,
5202 Schwartz, G.T., Smith, A.L., Ledogar, J.A., Strait, D.S., Herries, A.I.R., 2021.
5203 Drimolen cranium DNH 155 documents microevolution in an early hominin
5204 species. *Nature Ecology and Evolution* 5, 38–45.

5205 Martín-Torres, M., de Castro, J. M. B., Gómez-Robles, A., Margvelashvili, A., Prado,
5206 L., Lordkipanidze, D., Vekua A., 2008. Dental remains from Dmanisi (Republic
5207 of Georgia): Morphological analysis and comparative study. *Journal of Human*
5208 *Evolution* 55, 249–273.

5209 Martín-Torres, M., de Castro, J.M.B., Gómez-Robles, A., Prado-Simón, L., Arsuaga, J.
5210 L., 2012. Morphological description and comparison of the dental remains from
5211 Atapuerca-Sima de los Huesos site (Spain). *Journal of Human Evolution* 62, 7–
5212 58.

5213 McNabb, J., 2009. The ESA stone tool assemblage from the Cave of Hearths, Beds 1–3.
5214 In: McNabb, J., Sinclair, A. (Eds.), *The Cave of Hearths: Makapan Middle*
5215 *Pleistocene Research Project: Field research by Anthony Sinclair and Patrick*
5216 *Quinney, 1996–2001*. Archaeopress, Oxford, pp. 76–104.

5217 Menter, C.G., Kuykendall, K.L., Keyser, A.W., Conroy, G.C., 1999. First record of
5218 hominid teeth from the Plio-Pleistocene site of Gondolin, South Africa. *Journal of*
5219 *Human Evolution* 37, 299–307.

5220 Moggi-Cecchi, J., Grine, F.E., Tobias, P.V., 2006. Early hominid dental remains from
5221 Members 4 and 5 of the Sterkfontein Formation (1966–1996 excavations):
5222 Catalogue, individual associations, morphological descriptions and initial metrical
5223 analysis. *Journal of Human Evolution* 50, 239–328.

5224 Moggi-Cecchi, J., Menter, C., Boccone, S., Keyser, A., 2010. Early hominin dental
5225 remains from the Plio-Pleistocene site of Drimolen, South Africa. *Journal of*
5226 *Human Evolution* 58, 374–405.

5227 Moggi-Cecchi, J., Tobias, P.V., Beynon, A.D., 1998. The mixed dentition and associated
5228 skull fragments of a juvenile fossil hominid from Sterkfontein, South Africa.
5229 *American Journal of Physical Anthropology* 106, 425–465.

5230 Niespolo, E.M., Sharp, W.D., Avery, G., Dawson, T. E., 2021. Early, intensive marine
5231 resource exploitation by Middle Stone Age humans at Ysterfontein 1 rockshelter,

5232 South Africa. Proceedings of the National Academy of Sciences USA 118,
5233 e2020042118.

5234 Odes, E.J., Delezene, L.K., Randolph-Quinney, P.S., Smilg, J.S., Augustine, T.N., Jakata,
5235 K., Berger, L.R., 2018. A case of benign osteogenic tumour in *Homo naledi*:
5236 Evidence for peripheral osteoma in the UW 101-1142 mandible. International
5237 Journal of Paleopathology 21, 47–55.

5238 Prabhat, A.M., Miller, C.M., Prang, T.C., Spear, J., Williams, S.A., DeSilva, J.M., 2021.
5239 Homoplasmy in the evolution of modern human-like joint proportions in
5240 *Australopithecus afarensis*. eLife 10, e65897.

5241 Rak, Y., Kimbel, W.H., Moggi-Cecchi, J., Lockwood, C.A., Menter, C., 2021. The DNH
5242 7 skull of *Australopithecus robustus* from Drimolen (Main Quarry), South Africa.
5243 Journal of Human Evolution 151, 102913.

5244 Reynolds, S.C., Clarke, R.J., Kuman, K.A., 2007. The view from the Lincoln Cave: Mid-
5245 to late Pleistocene fossil deposits from Sterkfontein hominid site, South Africa.
5246 Journal of Human Evolution 53, 260–271.

5247 Riga, A., Oxilia, G., Panetta, D., Salvadori, P.A., Benazzi, S., Wadley, L., Moggi-Cecchi,
5248 J., 2018. Human deciduous teeth from the Middle Stone Age layers of Sibudu
5249 Cave (South Africa). Journal of Anthropological Sciences 96, 75–87.

5250 Rightmire, G.P., 1978. Florisbad and human population succession in southern Africa.
5251 American Journal of Physical Anthropology 48, 475–486.

5252 Rightmire, G.P., 2008. *Homo* in the Middle Pleistocene: Hypodigms, variation, and
5253 species recognition. Evolutionary Anthropology 17, 8–21.

- 5254 Robbins, J.L., Dirks, H.G.M., Roberts, E.M., Kramer, J.D., Makhubela, T.V., Hilbert-
5255 Wolf, H.L., Elliott, M., Wiersma, J.P., Placzek, C.J., Evans, M., Berger, L.R.,
5256 2021. Providing context to the *Homo naledi* fossils: Constraints from flowstones
5257 on the age of sediment deposits in Rising Star Cave, South Africa. *Chemical*
5258 *Geology* 567, 120108.
- 5259 Robinson, J.T., 1953. *Telanthropus* and its phylogenetic significance. *American Journal*
5260 *of Physical Anthropology* 11, 445–501.
- 5261 Robinson, J.T., 1954. Prehominid dentition and hominid evolution. *Evolution* 8, 324–
5262 334.
- 5263 Robinson J.T., 1956. The Dentition of the Australopithecinae. Transvaal Museum
5264 Memoir 9. Transvaal Museum, Pretoria.
- 5265 Scott, R.S, Irish, J. D., 2017. Human Tooth Crown and Root Morphology: The Arizona
5266 State University Dental Anthropology System. Cambridge University Press,
5267 Cambridge.
- 5268 Scott, G.R., Turner, C.G., 1997. *Anthropology of Modern Human Teeth*. Cambridge
5269 University Press, Cambridge.
- 5270 Skinner, M.M., Lockey, A.L., Gunz, P., Hawks, J., Delezene, L.K., 2016. Enamel-dentine
5271 junction morphology and enamel thickness of the Dinaledi dental collection.
5272 *American Journal of Physical Anthropology* 159, 293.
- 5273 Skinner, M.M., Wood, B.A., Hublin, J.-J., 2009. Protostylid expression at the outer
5274 enamel surface and at the enamel-dentine junction of mandibular molars of
5275 *Paranthropus robustus* and *Australopithecus africanus*. *Journal of Human*
5276 *Evolution* 56, 76–85.

- 5277 Skinner, M.M., Wood, B.A., Boesch, C., Olejniczak, A.J., Rosas, A., Smith, T.S., Hublin,
5278 J.-J., 2008. Dental trait expression at the enamel-dentine junction of lower molars
5279 in extant and fossil hominoids. *Journal of Human Evolution* 54, 173–186.
- 5280 Skinner, M.F., 2019. Developmental stress in South African hominins: Comparison of
5281 recurrent enamel hypoplasias in *Australopithecus africanus* and *Homo naledi*.
5282 *South African Journal of Science* 115, 1–10.
- 5283 Smith, B.H., 1984. Patterns of molar wear in hunter-gatherers and agriculturalists.
5284 *American Journal of Physical Anthropology* 63, 39–56.
- 5285 Smith, T.M., Olejniczak, A.J., Tafforeau, P., Reid, D.J., Grine, F.E., Hublin, J.-J., 2006.
5286 Molar crown thickness, volume, and development in South African Middle Stone
5287 Age humans. *South African Journal of Science* 102, 513–517.
- 5288 Stynder, D.D., Moggi-Cecchi, J., Berger, L.R., Parkington, J.E., 2001. Human
5289 mandibular incisors from the late Middle Pleistocene locality of Hoedjiespunt 1,
5290 South Africa. *Journal of Human Evolution* 41, 369–383.
- 5291 Suwa, G., White, T. D., Howell, F. C., 1996. Mandibular postcanine dentition from the
5292 Shungura Formation, Ethiopia: crown morphology, taxonomic allocations, and
5293 Plio-Pleistocene hominid evolution. *American Journal of Physical Anthropology*
5294 101, 247–282.
- 5295 Tobias, P.V., 1965. New discoveries in Tanganyika: Their bearing on hominid evolution.
5296 *Current Anthropology* 6, 391–399.
- 5297 Tobias, P.V., 1971. Human skeletal remains from the Cave of Hearths, Makapansgat,
5298 Northern Transvaal. *American Journal of Physical Anthropology* 34, 335–367.

5299 Towle, I., Irish, J.D., De Groot, I., 2017. Behavioral inferences from the high levels of
5300 dental chipping in *Homo naledi*. *American Journal of Physical Anthropology* 164,
5301 184–192.

5302 Towle, I., Irish, J. D., Groot, I. D., Fernée, C., Loch, C., 2021. Dental caries in South
5303 African fossil hominins. *South African Journal of Science* 117, 1–8.

5304 Ungar, P.S., Berger, L.R., 2018. Brief communication: Dental microwear and diet of
5305 *Homo naledi*. *American Journal of Physical Anthropology* 166, 228–235.

5306 Van Reenen, J. F., and Reid, C., 1995. The Carabelli trait in early South African
5307 hominids: a morphological study. In: Moggi-Cecchi, J. (Ed.), *Aspects of Dental*
5308 *Biology: Palaeontology, Anthropology, and Evolution*. International Institute for
5309 the Study of Man, Florence, pp 291–298.

5310 VanSickle, C., Cofran, Z., García-Martínez, D., Williams, S.A., Churchill, S.E., Berger,
5311 L.R., Hawks, J., 2018. *Homo naledi* pelvic remains from the Dinaledi Chamber,
5312 South Africa. *Journal of Human Evolution* 125, 122–136.

5313 Vandermeersch, B., 1981. *Les Hommes Fossiles de Qafzeh (Israel)*. Cahiers de
5314 Paléontologie (Paléoanthropologie). Editions du CNRS, Paris.

5315 Villmoare, B., Kimbel, W.H., Seyoum, C., Campisano, C.J., DiMaggio, E.N., Rowan, J.,
5316 Braun, D.R., Arrowsmith, J.R., Reed, K.E., 2015. Early *Homo* at 2.8 Ma from
5317 Ledi-Geraru, Afar, Ethiopia. *Science* 347, 1352–1355.

5318 Weidenreich, F., 1943. The skull of *Sinanthropus pekinensis*: A comparative study on a
5319 primitive hominid skull. *Palaeontol. Sin. D* 10, 1–484.

5320 Weidenreich, F., 1937. The dentition of *Sinanthropus pekinensis*: A comparative
5321 odontography of the hominids. *Palaeontol. Sin. D* 1, 1–180.

5322 Will, M., El-Zaatari, S., Harvati, K., Conard, N.J., 2019. Human teeth from securely
5323 stratified Middle Stone Age contexts at Sibudu, South Africa. *Archaeological and*
5324 *Anthropological Sciences* 11, 3491 – 3501.

5325 Wood, B.A., 1991. *Koobi Fora Research Project, Vol. 4. Hominid Cranial Remains.*
5326 Clarendon Press, Oxford.

5327 Wood, B.A., Abbott, S.A., Uytterschaut, H., 1988. Analysis of the dental morphology of
5328 Plio-Pleistocene hominids. IV. Mandibular postcanine root morphology. *Journal*
5329 *of Anatomy* 156, 107–139.

5330 Wood, B.A., van Noten, F.L., 1986. Preliminary observations on the BK 8518 mandible
5331 from Baringo, Kenya. *American Journal of Physical Anthropology* 69, 117–127.

5332 Zanolli, C., 2013. Additional evidence for morpho-dimensional tooth crown variation in a
5333 new Indonesian *H. erectus* sample from the Sangiran Dome (Central Java). *PLoS*
5334 *One* 8, e67233.

5335 Zanolli, C., Davies, T.W., Joannes-Boyau, R., Beaudet, A., Bruxelles, L., de Beer, F.,
5336 Hoffman, J.H., Hublin, J.-J., Jakata, K., Kgasi, L., Kullmer, O., Macchiarelli, R.,
5337 Pan, L., Schrenk, F., Santos, F., Stratford, D., Tawane, M., Thackeray, F., Xing,
5338 S., Zipfel, B., Skinner, M.M., 2022. Dental data challenge the ubiquitous presence
5339 of *Homo* in the Cradle of Humankind. *Proceedings of the National Academy of*
5340 *Sciences USA* 119, e2111212119.

5341

5342 **FIGURE LEGENDS**

5343 **Figure 1.** Maxillary deciduous central incisors. For all teeth, from left to right, lingual,
5344 labial, mesial, and distal views: A) U.W. 101-544C (right dI¹); B) U.W. 101-1331 (left
5345 dI¹). Scale bar is 10 mm.

5346

5347 **Figure 2.** Maxillary deciduous lateral incisor. From left to right, lingual, labial, mesial,
5348 and distal views of U.W. 101-1304 (left dI²). Scale bar is 10 mm.

5349

5350 **Figure 3.** Maxillary deciduous canines. For all teeth, from left to right, lingual, labial,
5351 mesial, and distal views: A) U.W. 101-595 (left dC¹); B) U.W. 101-728 (right dC¹); C)
5352 U.W. 101-1287A (left dC¹). Scale bar is 10 mm.

5353

5354 **Figure 4.** Maxillary first deciduous molars. For all teeth, from left to right, occlusal,
5355 mesial, distal, buccal, and lingual views: A) U.W. 101-823 (right dP³); B) U.W. 101-1377
5356 (left dP³). Scale bar is 10 mm.

5357

5358 **Figure 5.** Maxillary second deciduous molars. For all teeth, from left to right, occlusal,
5359 mesial, distal, buccal, and lingual views: A) U.W. 101-384 (right dP⁴); B) U.W. 101-
5360 544A (right dP⁴); C) U.W. 101-1376 (left dP⁴); D) U.W. 101-1687 (right dP⁴). Scale bar
5361 is 10 mm.

5362

5363 **Figure 6.** Mandibular deciduous lateral incisor. From left to right, lingual, labial, mesial,
5364 and distal views of U.W. 101-1612 (right dI₂). Scale bar is 10 mm.

5365

5366 **Figure 7.** Mandibular deciduous canines. For all teeth, from left to right, lingual, labial,
5367 mesial, and distal views: A) U.W. 101-824 (left dC₁); B) U.W. 101-1571 (left dC₁); C)
5368 U.W. 101-1611 (right dC₁). Scale bar is 10 mm.

5369

5370 **Figure 8.** Mandibular first deciduous molar. From left to right, occlusal, mesial, distal,
5371 buccal, and lingual views of U.W. 101-1685 (right dP₃). Scale bar is 10 mm.

5372

5373 **Figure 9.** Mandibular second deciduous molar. From left to right, occlusal, mesial, distal,
5374 buccal, and lingual views of U.W. 101-1686 (right dP₄). Scale bar is 10 mm.

5375

5376 **Figure 10.** Maxillary central incisors. For all teeth, from left to right, lingual, labial,
5377 mesial, and distal views: A) U.W. 101-038 (right I¹); B) U.W. 101-591 (left I¹); C) U.W.
5378 101-931 (left I¹); D) U.W. 101-1012 (right I¹); E) U.W. 101-1558 (right I¹). Scale bar is
5379 10 mm.

5380

5381 **Figure 11.** Maxillary lateral incisors. For all teeth, from left to right, lingual, labial,
5382 mesial, and distal views: A) U.W. 101-073 (right I²); B) U.W. 101-417 (left I²); C) U.W.
5383 101-709 (right I²); D) U.W. 101-932 (left I²). Scale bar is 10 mm.

5384

5385 **Figure 12.** Maxillary lateral incisors. For all teeth, from left to right, lingual, labial,
5386 mesial, and distal views: A) U.W. 101-952 (left I²); B) U.W. 101-1588 (left I²); C) U.W.
5387 101-1684 (left I²). Scale bar is 10 mm.

5388

5389 **Figure 13.** Maxillary canines. For all teeth, from left to right, lingual, labial, mesial, and
5390 distal views: A) U.W. 101-337 (right C¹); B) U.W. 101-412 (left C¹); C) U.W. 101-501
5391 (left C¹); D) U.W. 101-544B (lingual and labial views only; right C¹). Scale bar is 10
5392 mm.

5393

5394 **Figure 14.** Maxillary canines. A) U.W. 101-706 (left C¹); B) U.W. 101-816 (right C¹); C)
5395 U.W. 101-908 (right C¹); D) U.W. 101-1403 (right C¹). Scale bar is 10 mm.

5396

5397 **Figure 15.** Maxillary canines. A) U.W. 101-1510 (right C¹); B) U.W. 101-1548 (lingual
5398 and labial views only; left C¹); C) U.W. 101-1556 (left C¹). Scale bar is 10 mm.

5399

5400 **Figures 16.** Maxillary third premolars. For all teeth, from left to right, occlusal, mesial,
5401 distal, buccal, and lingual views: A) U.W. 101-037 (right P³); B) U.W. 101-182 (right
5402 P³); C) U.W. 101-729 (right P³); E) U.W. 101-786 (left P³). Scale bar is 10 mm.

5403

5404 **Figure 17.** Maxillary third premolars. For all teeth, from left to right, occlusal, mesial,
5405 distal, buccal, and lingual views: A) U.W. 101-1004 (right P³); B) U.W. 101-1107 (left
5406 P³); C) U.W. 101-1402 (right P³); D) U.W. 101-1560 (left P³). Scale bar is 10 mm.

5407

5408 **Figure 18.** Maxillary fourth premolars. For all teeth, from left to right, occlusal, mesial,
5409 distal, buccal and lingual views: A) U.W. 101-277 (left P⁴); B) U.W. 101-333 (left P⁴ or

5410 left P³); C) U.W. 101-334 (right P⁴); D) U.W. 101-455 (right P⁴); E) U.W. 101-808 (left
5411 P⁴). Scale bar is 10 mm.

5412

5413 **Figure 19.** Maxillary fourth premolars. For all teeth, from left to right, occlusal, mesial,
5414 distal, buccal, and lingual views: A) U.W. 101-1362 (left P⁴); B) U.W. 101-1401 (right
5415 P⁴); C) U.W. 101-1561 (left P⁴). Scale bar is 10 mm.

5416

5417 **Figure 20.** Maxillary first molars. For all teeth, from left to right, occlusal, mesial, distal,
5418 buccal, and lingual views: A) U.W. 101-445 (left M¹); B) U.W. 101-525 (right M¹); C)
5419 U.W. 101-583 (right M¹); D) U.W. 101-708 (left M¹); E) U.W. 101-796 (left M¹). Scale
5420 bar is 10 mm.

5421

5422 **Figure 21.** Maxillary first molars. For all teeth, from left to right, occlusal, mesial, distal,
5423 buccal, and lingual views: A) U.W. 101-999 (right M¹); B) U.W. 101-1305 (left M¹); C)
5424 U.W. 101-1396 (right M¹); D) U.W. 101-1463 (right M¹); E) U.W. 101-1676 (left M¹); F)
5425 U.W. 101-1688 (right M¹). Scale bar is 10 mm.

5426

5427 **Figure 22.** Maxillary second molars. For all teeth, from left to right, occlusal, mesial,
5428 distal, buccal, and lingual views: A) U.W. 101-005 (right M²); B) U.W. 101-505 (left
5429 M²); C) U.W. 101-528 (left M²); D) U.W. 101-593 (right M²); E) U.W. 101-867 (right
5430 M²). Scale bar is 10 mm.

5431

5432 **Figure 23.** Maxillary second molars. For all teeth, from left to right, occlusal, mesial,
5433 distal, buccal, and lingual views: A) U.W. 101-1006 (right M²); B) U.W. 101-1015 (left
5434 M²); C) U.W. 101-1063 (left M²?); D) U.W. 101-1135 (right M²); E) U.W. 101-1522 (left
5435 M²). Scale bar is 10 mm.

5436

5437 **Figure 24.** Maxillary third molars. For all teeth, from left to right, occlusal, mesial, distal,
5438 buccal, and lingual views: A) U.W. 101-418C (left M³); B) U.W. 101-527 (left M³); C)
5439 U.W. 101-594 (right M³); D) U.W. 101-1269 (left M³); E) U.W. 101-1398A (right M³);
5440 F) U.W. 101-1471 (left M³). Scale bar is 10 mm.

5441

5442 **Figure 25.** Mandibular central incisors. For all teeth, from left to right, lingual, labial,
5443 mesial, and distal views: A) U.W. 101-039 (right I₁); B) U.W. 101-601 (left I₁); C) U.W.
5444 101-1005A (left I₁); D) U.W. 101-1005B (right I₁); E) U.W. 101-1132 (left I₁); F) U.W.
5445 101-1133 (right I₁). Scale bar is 10 mm.

5446

5447 **Figure 26.** Mandibular lateral incisors. For all teeth, from left to right, lingual, labial,
5448 mesial, and distal views: A) U.W. 101-335 (right I₂); B) U.W. 101-998 (left I₂); C) U.W.
5449 101-1005C (right I₂). Scale bar is 10 mm.

5450

5451 **Figure 27.** Mandibular lateral incisors. For all teeth, from left to right, lingual, labial,
5452 mesial, and distal views: A) U.W. 101-1075 (right I₂); B) U.W. 101-1131 (left I₂); C)
5453 U.W. 101-1400 (left I₂). Scale bar is 10 mm.

5454

5455 **Figure 28.** Mandibular canines. For all teeth, from left to right, lingual, labial, mesial,
5456 and distal views: A) U.W. 101-245 (right C₁); B) U.W. 101-339 (right C₁); C) U.W. 101-
5457 359 (left C₁); D) U.W. 101-886 (right C₁). Scale bar is 10 mm.

5458

5459 **Figure 29.** Mandibular canines. For all teeth, from left to right, lingual, labial, mesial,
5460 and distal views: A) U.W. 101-985 (left C₁); B) U.W. 101-1076 (left C₁); C) U.W. 101-
5461 1126 (left C₁); D) U.W. 101-1610 (right C₁). Scale bar is 10 mm.

5462

5463 **Figure 30.** Mandibular third premolars. For all teeth, from left to right, occlusal, mesial,
5464 distal, buccal, and lingual views: A) U.W. 101-144 (left P₃); B) U.W. 101-298 (right P₃);
5465 C) U.W. 101-358 (left P₃); D) U.W. 101-506 (right P₃). Scale bar is 10 mm.

5466

5467 **Figure 31.** Mandibular third premolars. For all teeth, from left to right, occlusal, mesial,
5468 distal, buccal, and lingual views: A) U.W. 101-800 (right P₃); B) U.W. 101-889 (left P₃);
5469 C) U.W. 101-1565 (left P₃). Scale bar is 10 mm.

5470

5471 **Figure 32.** Mandibular fourth premolars. For all teeth, from left to right, occlusal, mesial,
5472 distal, buccal, and lingual views: A) U.W. 101-184 (left P₄); B) U.W. 101-383 (right P₄);
5473 C) U.W. 101-887 (left P₄). Scale bar is 10 mm.

5474

5475 **Figure 33.** Mandibular first molars. For all teeth, from left to right, occlusal, mesial,
5476 distal, buccal, and lingual views: A) U.W. 101-285 (right M₁); B) U.W. 101-297 (right

5477 M₁); C) U.W. 101-582 (left M₁); D) U.W. 101-809 (left M₁); E) U.W. 101-814 (left M₁).

5478 Scale bar is 10 mm.

5479

5480 **Figure 34.** Mandibular first molars. For all teeth, from left to right, occlusal, mesial,

5481 distal, buccal, and lingual views: A) U.W. 101-905 (left M₁); B) U.W. 101-1287B (right

5482 M₁); C) U.W. 101-1400 (left M₁); D) U.W. 101-1689 (right M₁). Scale bar is 10 mm.

5483

5484 **Figure 35.** Mandibular second molars. For all teeth, from left to right, occlusal, mesial,

5485 distal, buccal and lingual views: A) U.W. 101-145 (left M₂); B) U.W. 101-284 (left M₂);

5486 C) U.W. 101-507 (right M₂); D) U.W. 101-655 (right M₂); E) U.W. 101-789 (left M₂); F)

5487 U.W. 101-1002 (right M₂). Scale bar is 10 mm.

5488

5489 **Figure 36.** Mandibular third molars. For all teeth, from left to right, occlusal, mesial,

5490 distal, buccal, and lingual views: A) U.W. 101-006 (right M₃); B) U.W. 101-516 (left

5491 M₃). Scale bar is 10 mm.

5492

5493 **Figure 37.** Root fragments. A) U.W. 101-293; B) U.W. 101-388; C) U.W. 101-589; D)

5494 U.W. 101-602. Scale bar is 10 mm.

5495

5496 **Figure 38.** Occlusal view of U.W. 101-652, cusp germ of postcanine tooth. Scale bar is

5497 10 mm.

5498

5499 **Figure 39.** Root fragments. A) U.W. 101-653; B) U.W. 101-654; C); U.W. 101-686; D)
5500 U.W. 101-864. Scale bar is 10 mm.

5501

5502 **Figure 40.** From left to right, lateral, anterior, and occlusal views of the U.W. 101-1277
5503 maxilla with dentition. Scale bar is 10 mm.

5504

5505 **Figure 41.** Clockwise from top left, buccal, lingual, and occlusal views of U.W. 101-001
5506 (right mandible fragment with P₄–M₃) and U.W. 101-850 (right P₃ with surrounding
5507 alveolar bone), which are refitted together. Scale bar is 10 mm.

5508

5509 **Figure 42.** Clockwise from top left, buccal, lingual, and occlusal views of U.W. 101-010
5510 (right mandible fragment with C₁–P₃). Scale bar is 10 mm.

5511

5512 **Figure 43.** From top to bottom: buccal, lingual, and occlusal views of U.W. 101-361 (left
5513 mandible fragment with M₂ and M₃). Scale bar is 10 mm.

5514

5515 **Figure 44.** Clockwise from top left: buccal, lingual, and occlusal views of U.W. 101-377
5516 (right mandible fragment with P₃–M₂) and U.W. 101-1014 (right C₁), which are refitted
5517 together. Scale bar is 10 mm.

5518

5519 **Figure 45.** Clockwise from top left, buccal, lingual, occlusal, and occlusal view of U.W.
5520 101-1142 (right mandible fragment with M₂ and M₃), with the U.W. 101-1287B M₁
5521 placed in its alveolus and without U.W. 101-1287B M₁. Scale bar is 10 mm.

5522

5523 **Figure 46.** Occlusal view of the U.W. 101-1261 complete mandible with dentition.

5524 Scale bar is 10 mm.

5525

5526 **Figure 47.** From left to right, buccal, lingual, and occlusal views of U.W. 101-1400

5527 (mandible fragment with dC₁-dP₄). Scale bar is 10 mm.

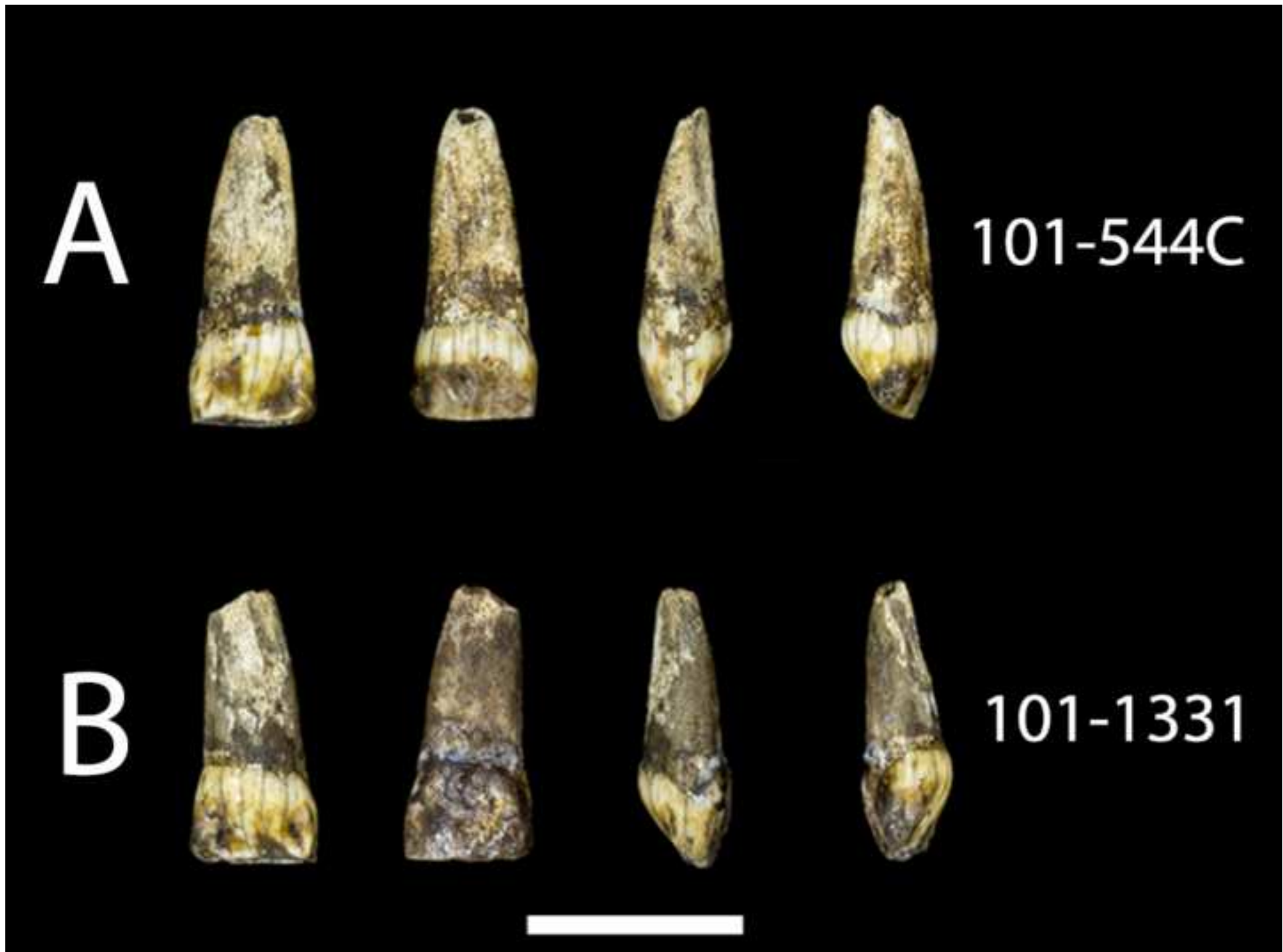




Figure 2_upper deciduous lateral incisor_color.tif

Figure 3_deciduous maxillary canines.tif

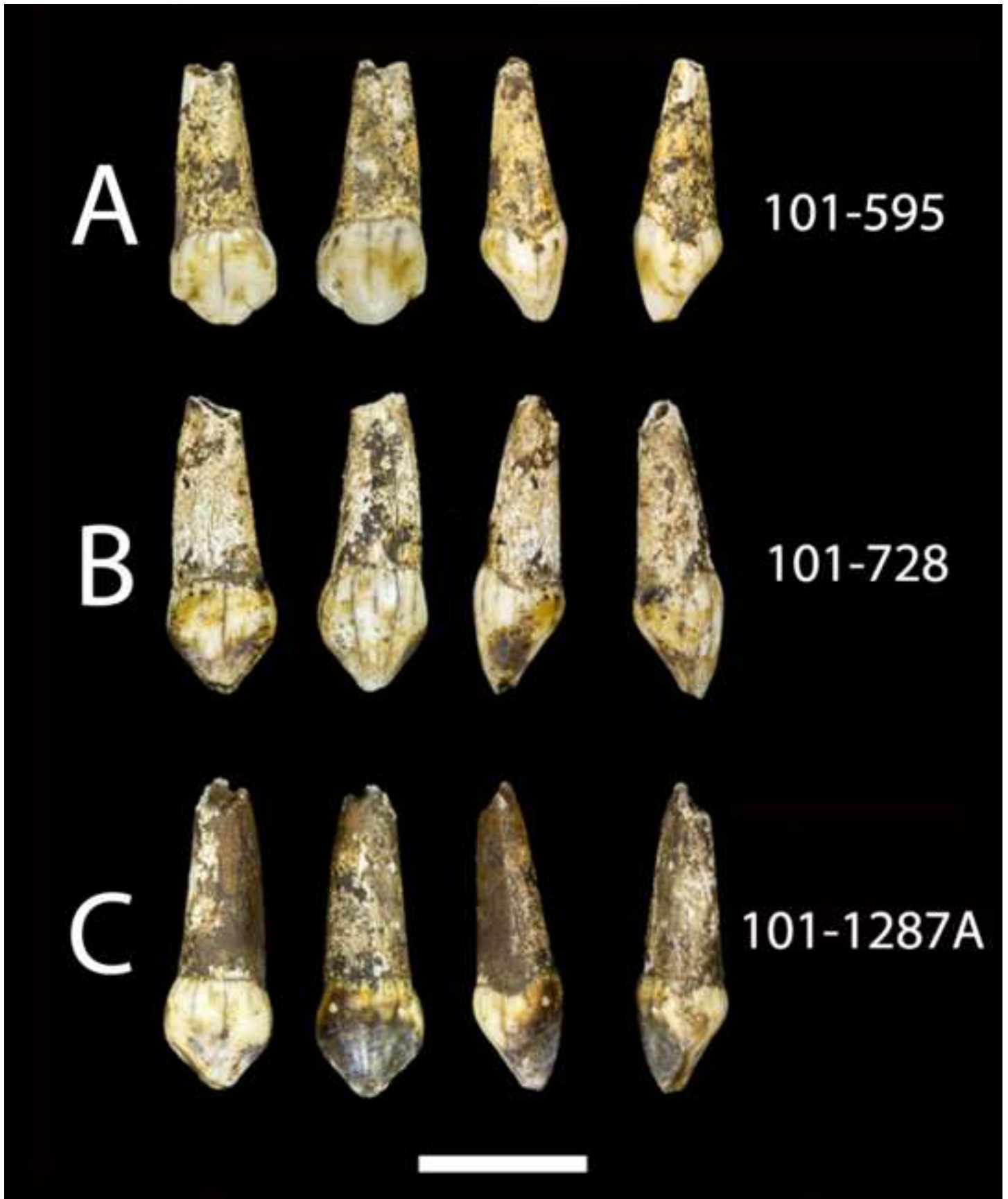




Figure 4_Upper dm1_color.tif

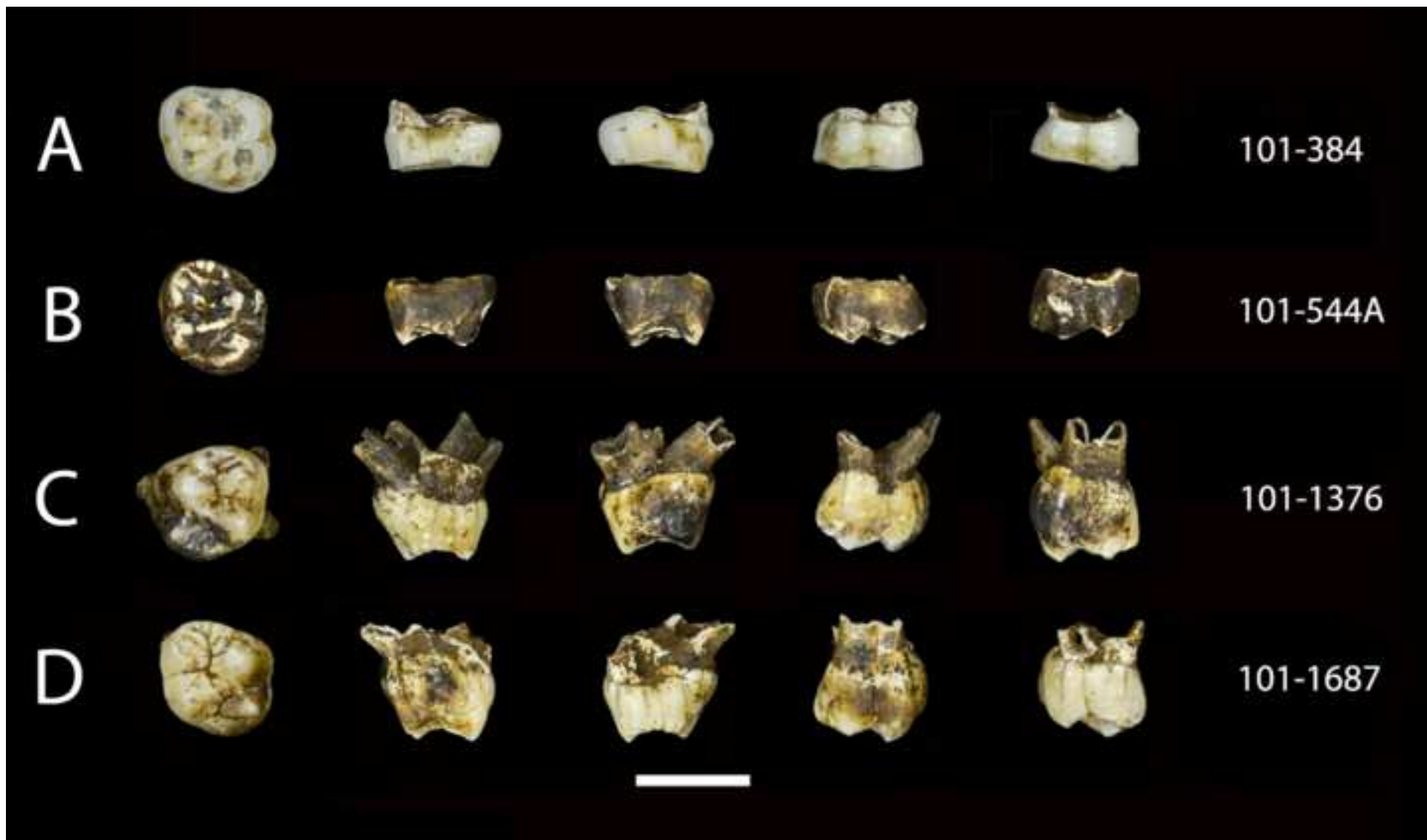




Figure 6_deciduous mandibular second incisors_color.tif

Figure 7_lower deciduous canines_color.tif

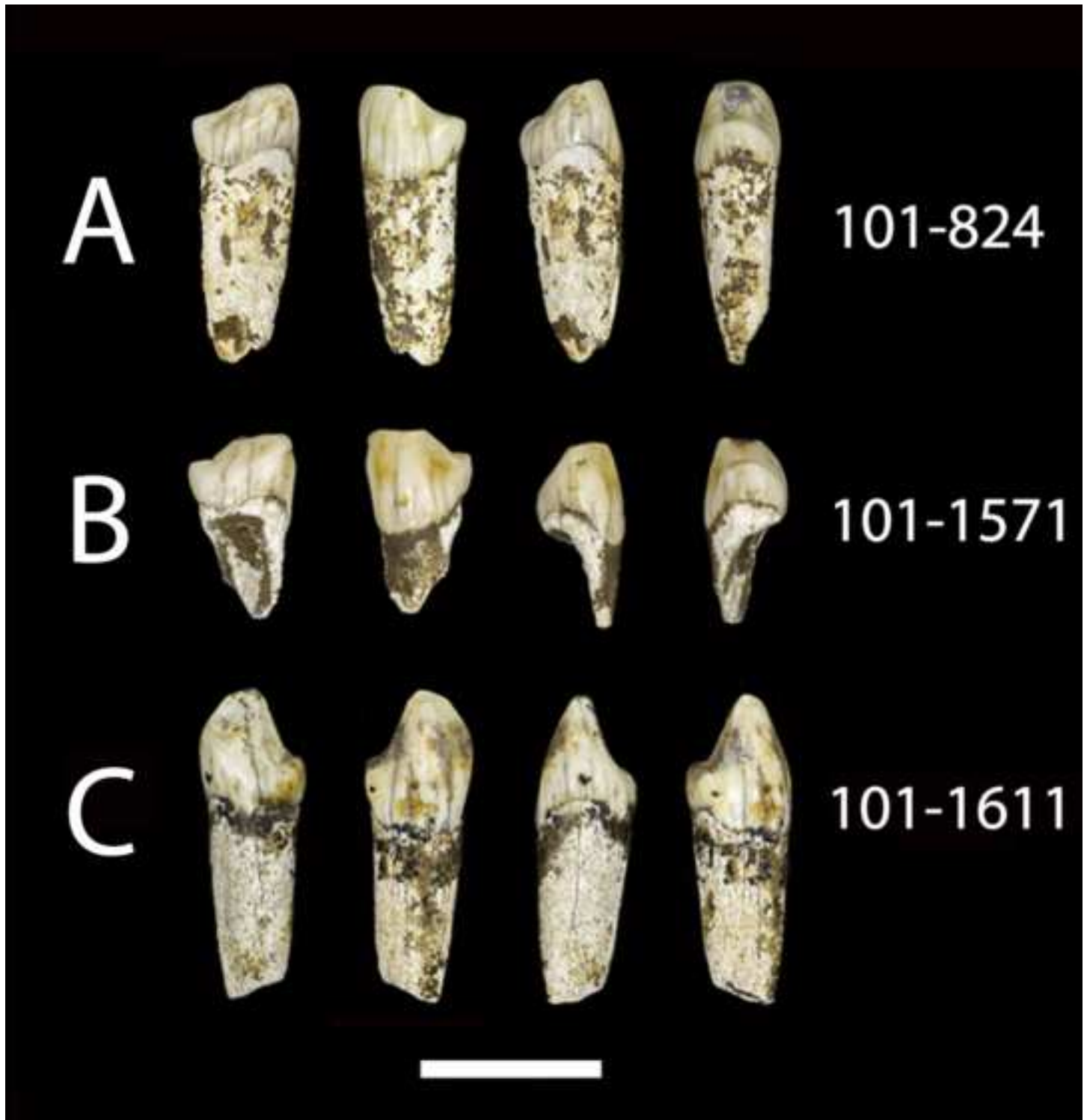
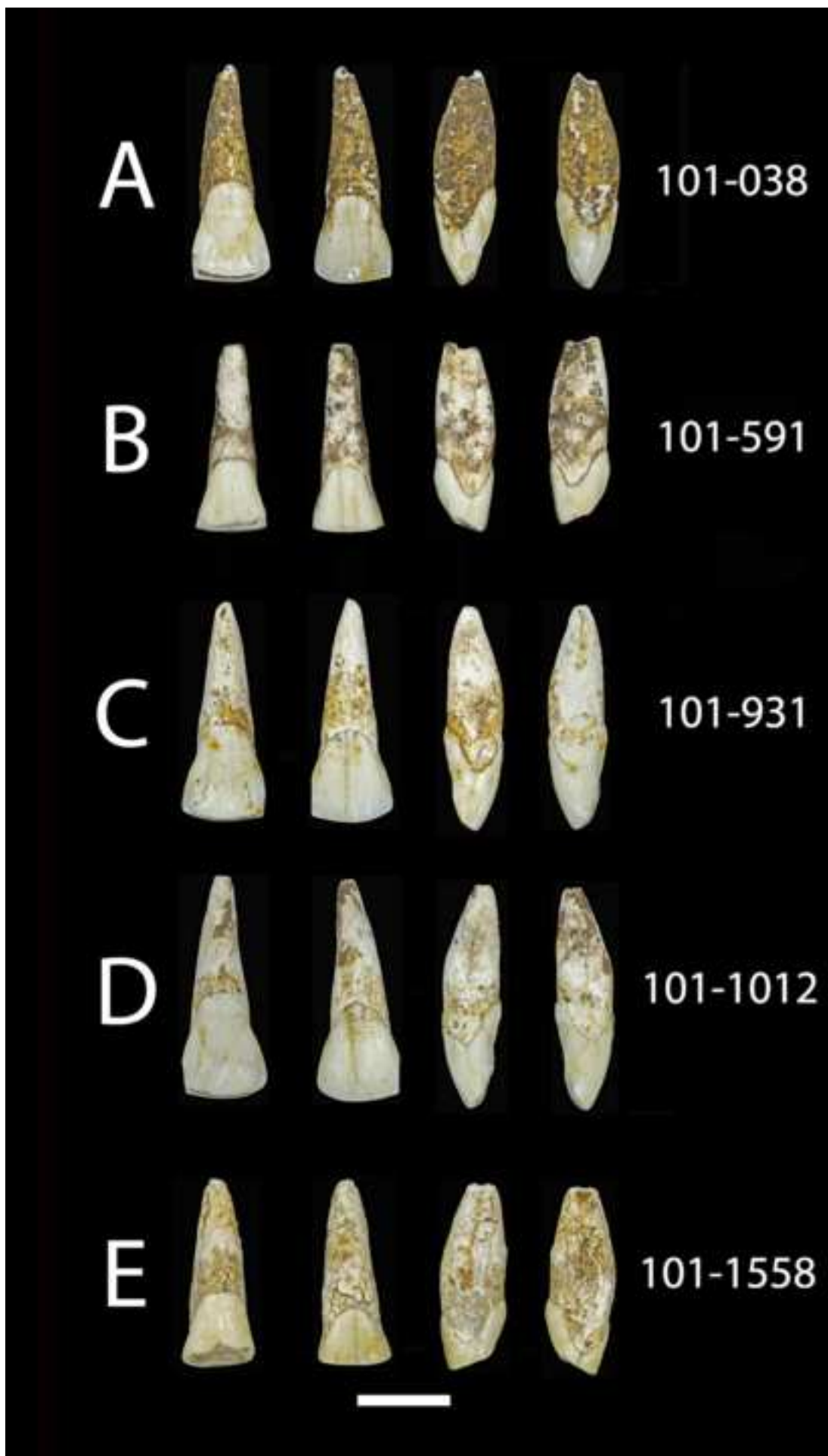


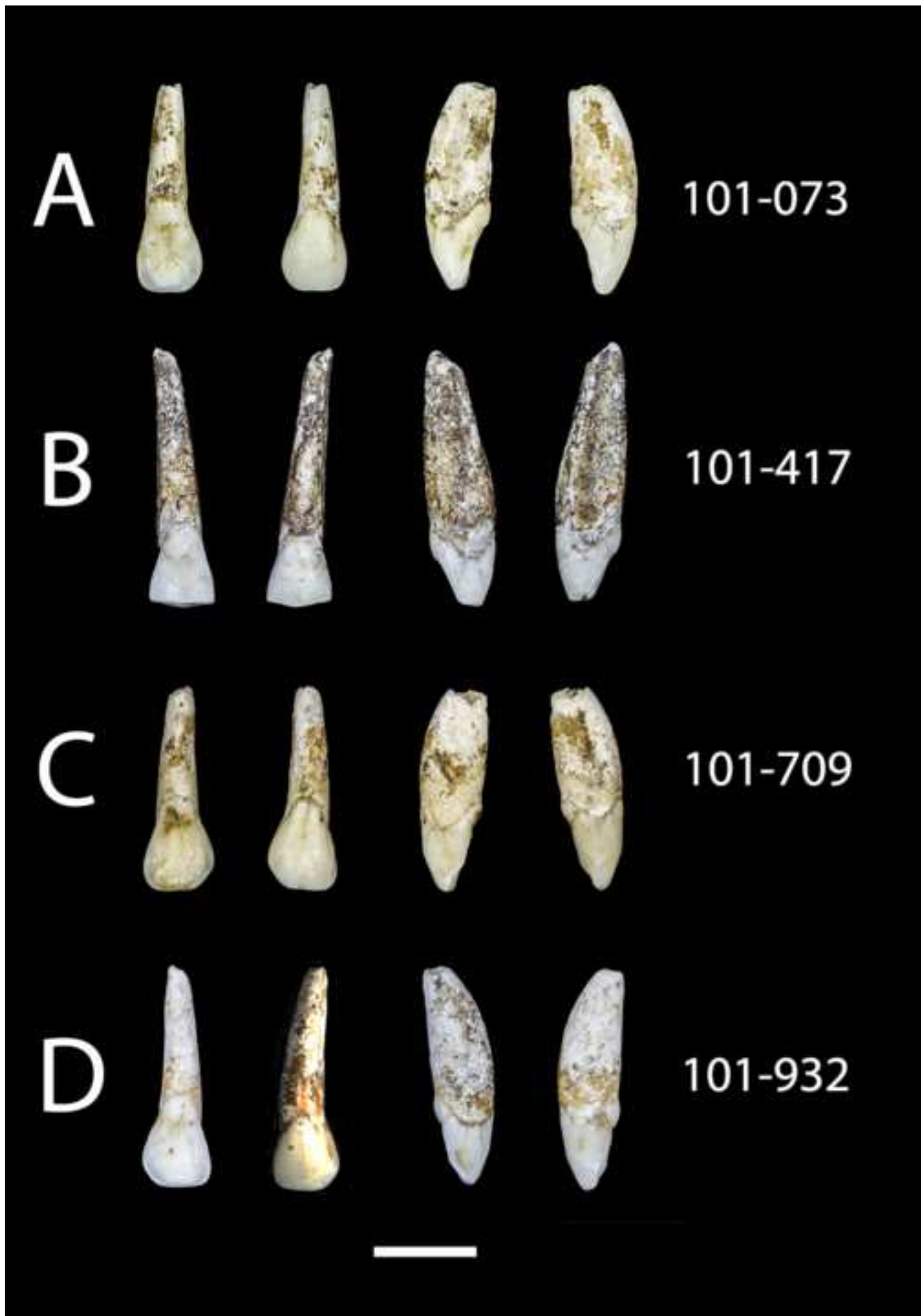


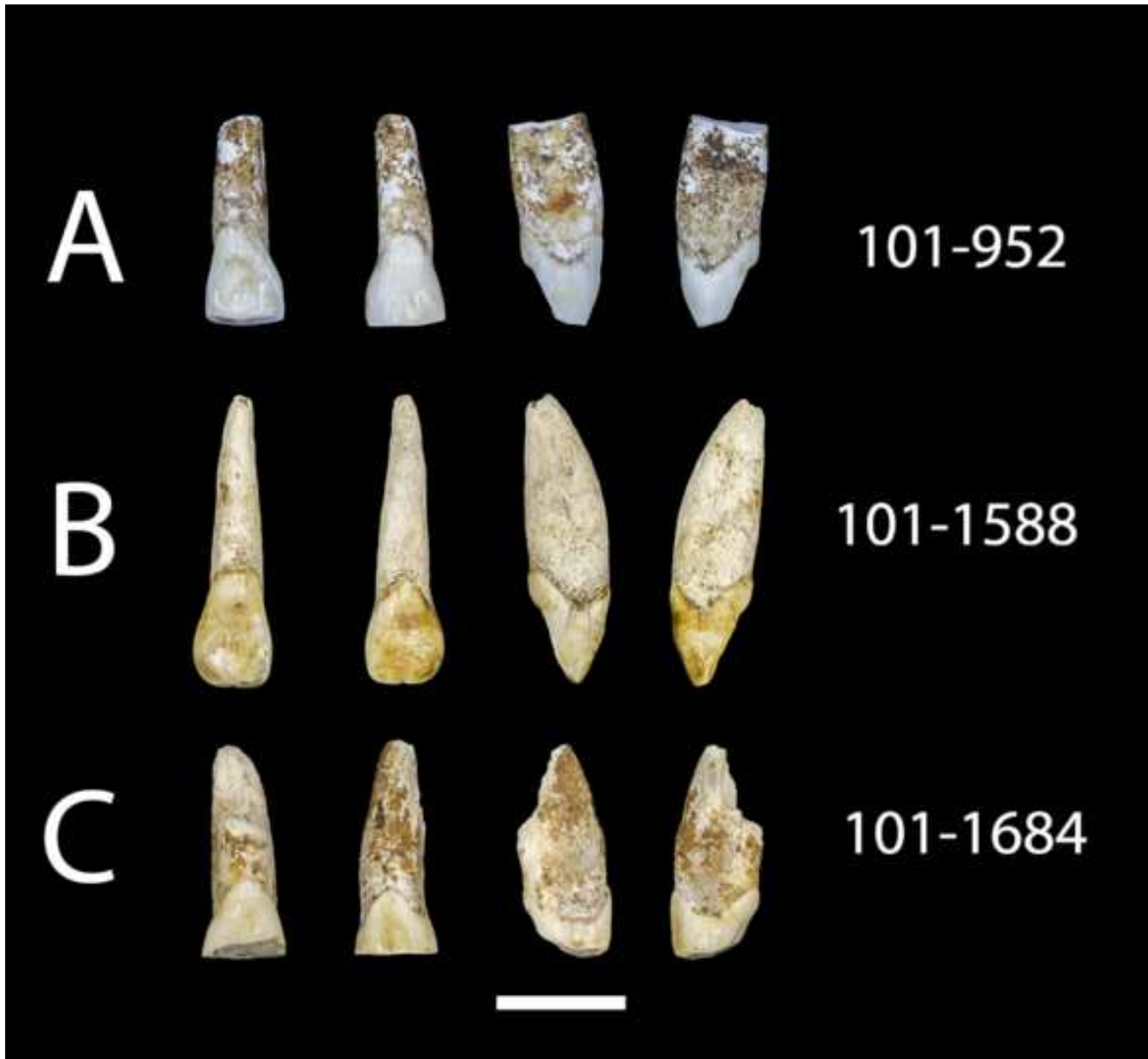
Figure 8_deciduous mandibular first molar_color.tif

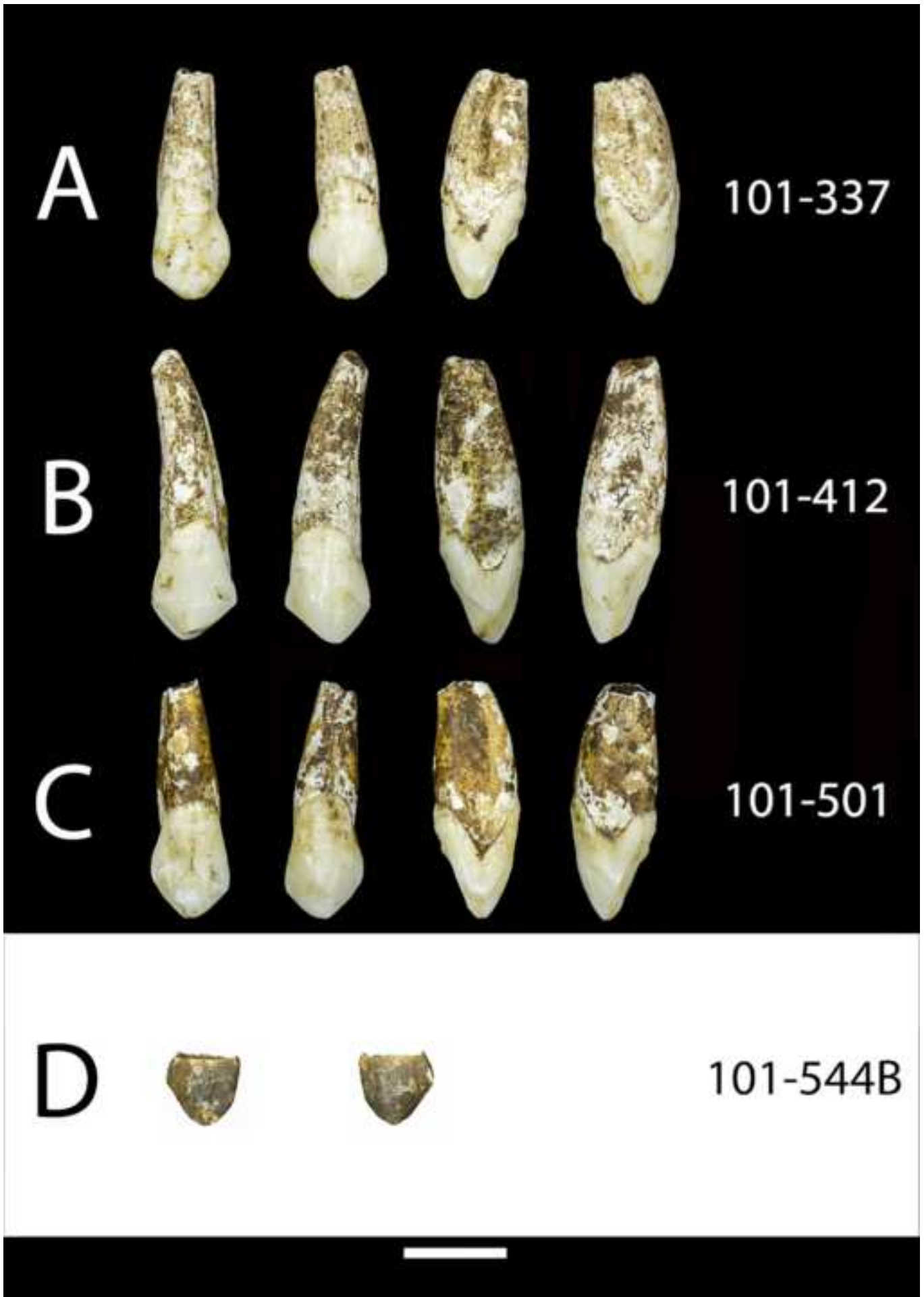


Figure 9_deciduous mandibular second molars_color.tif









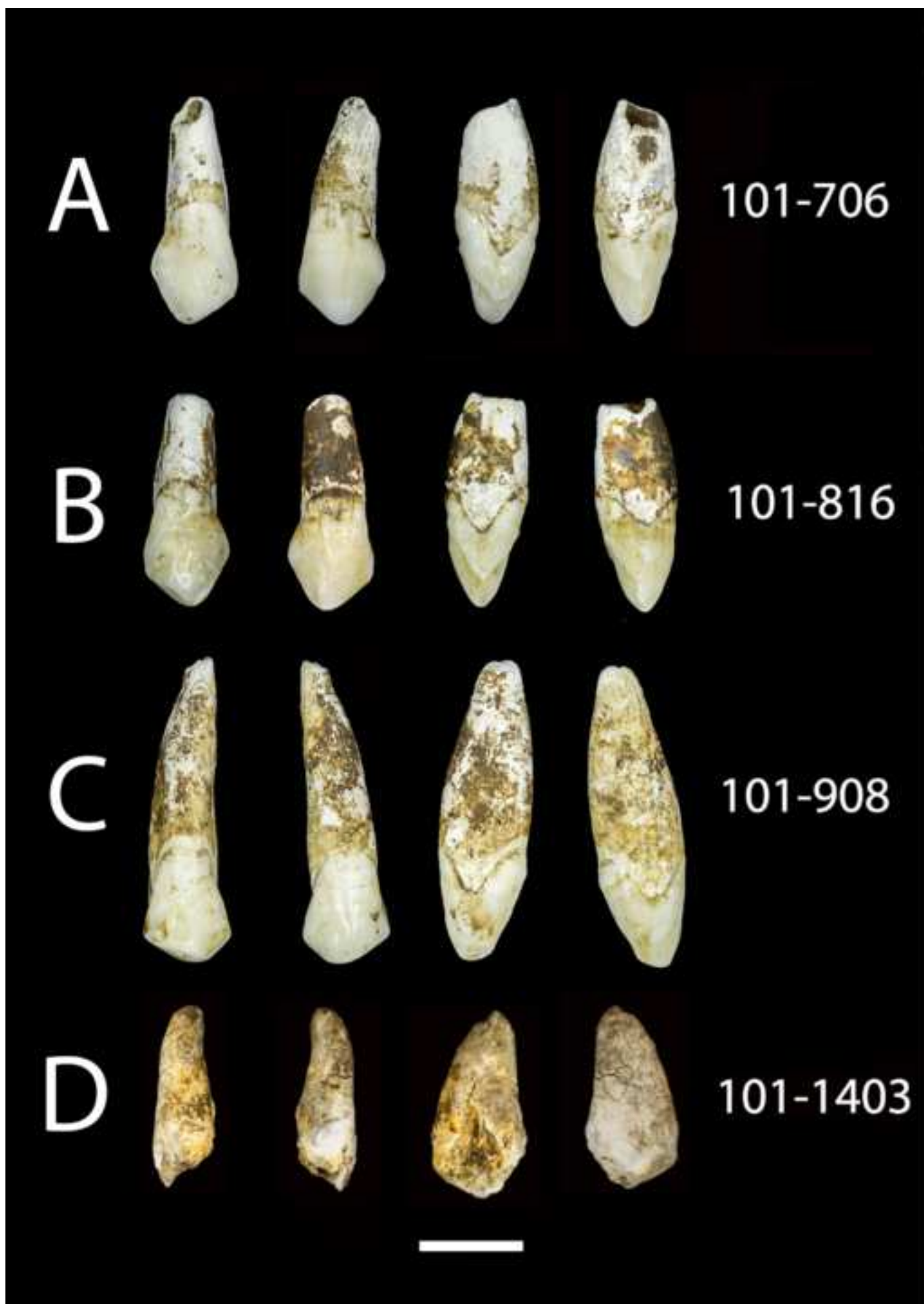
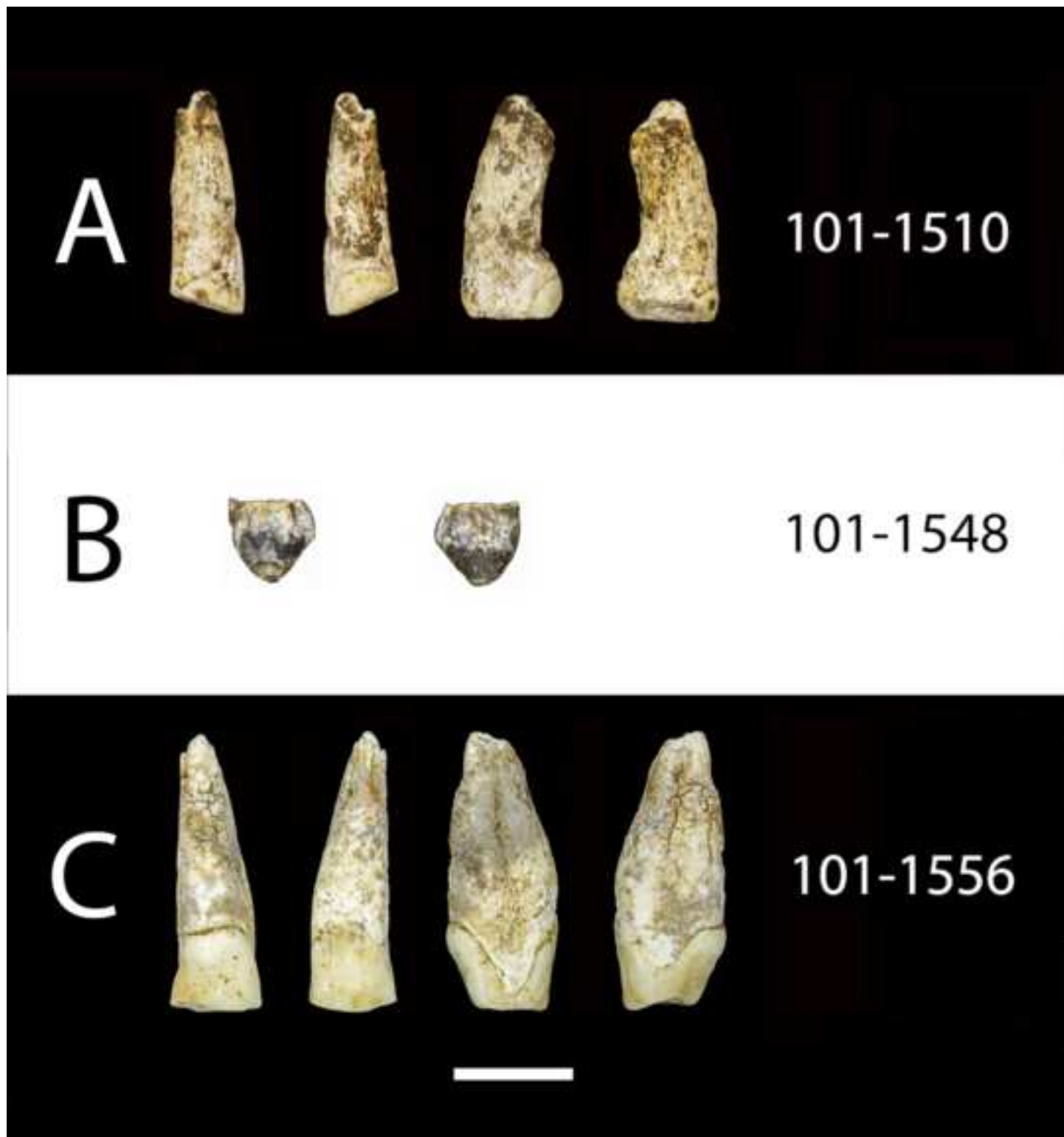
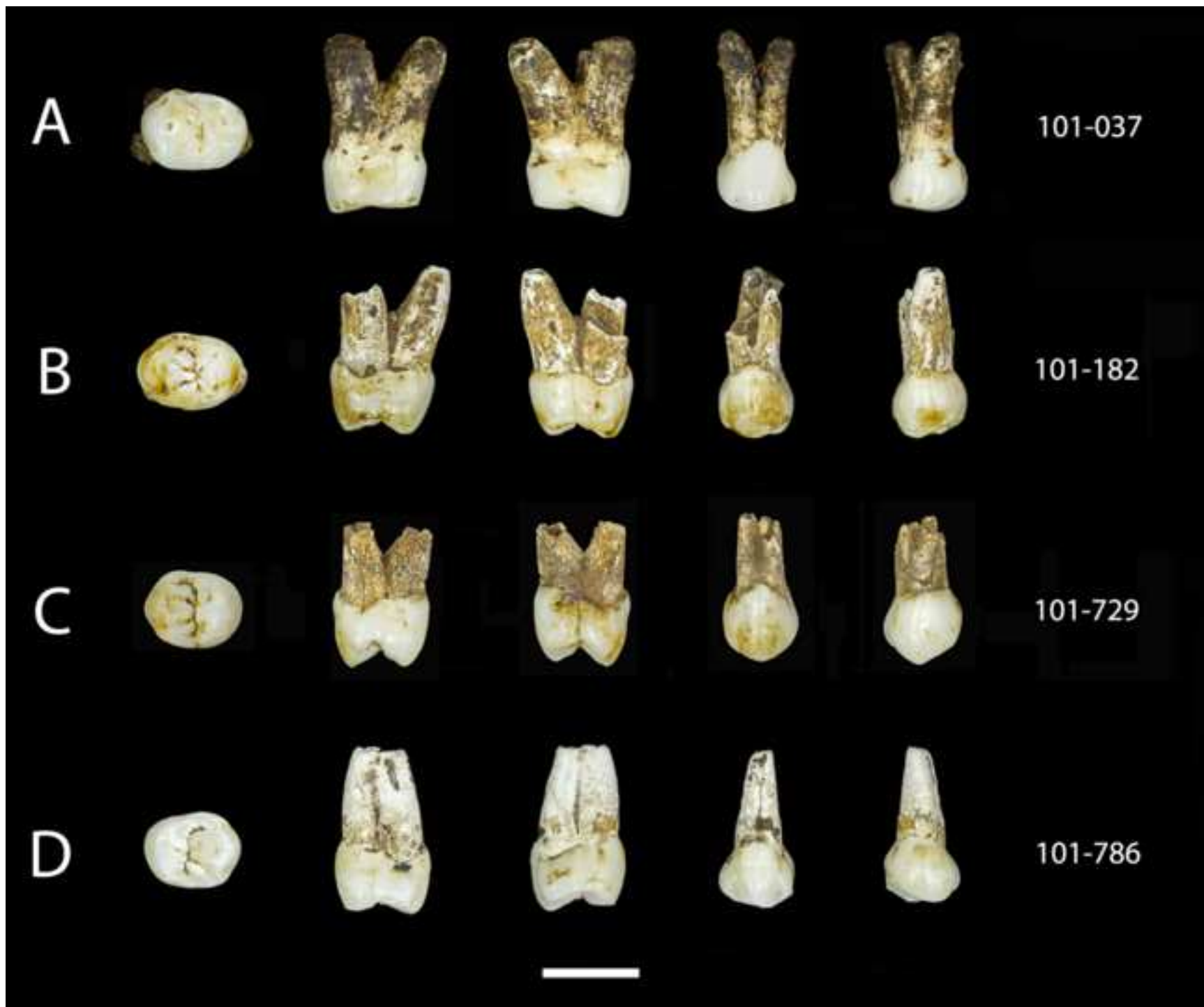


Figure 15_upper canines_part 3_color.tif





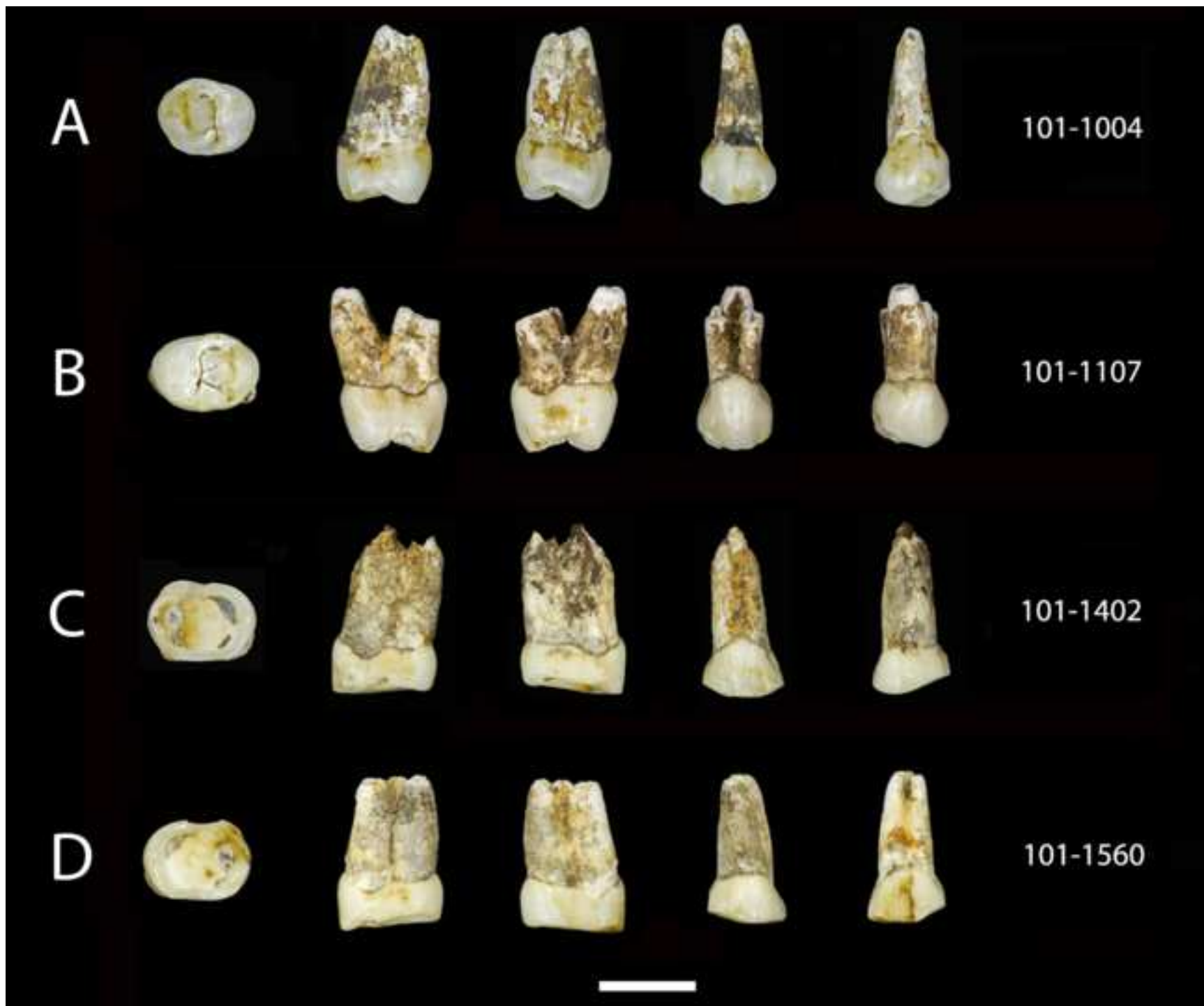
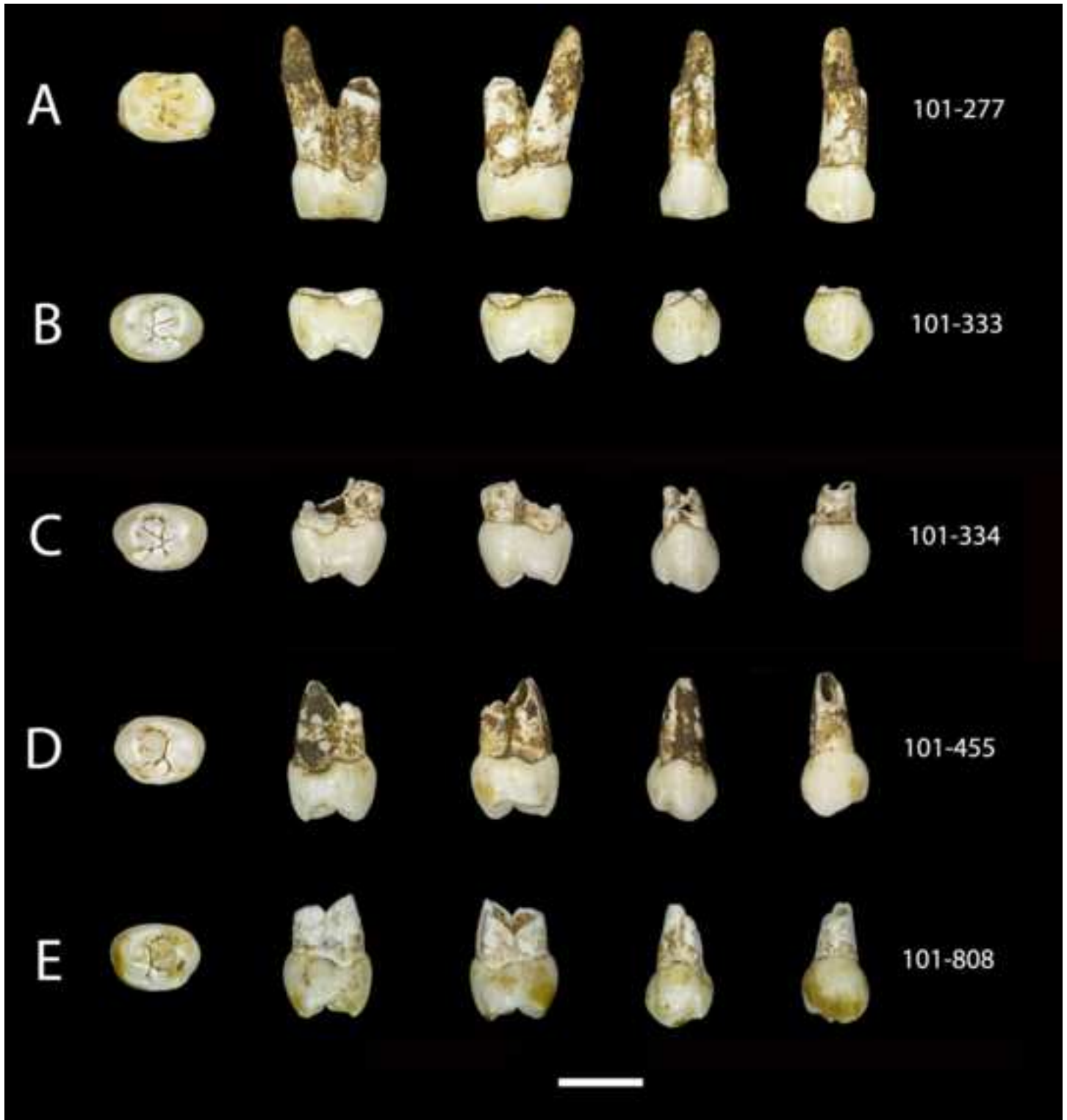


Figure 17_Upper p3_cont_color.tif

Figure 18_Upper p4s_color.tif



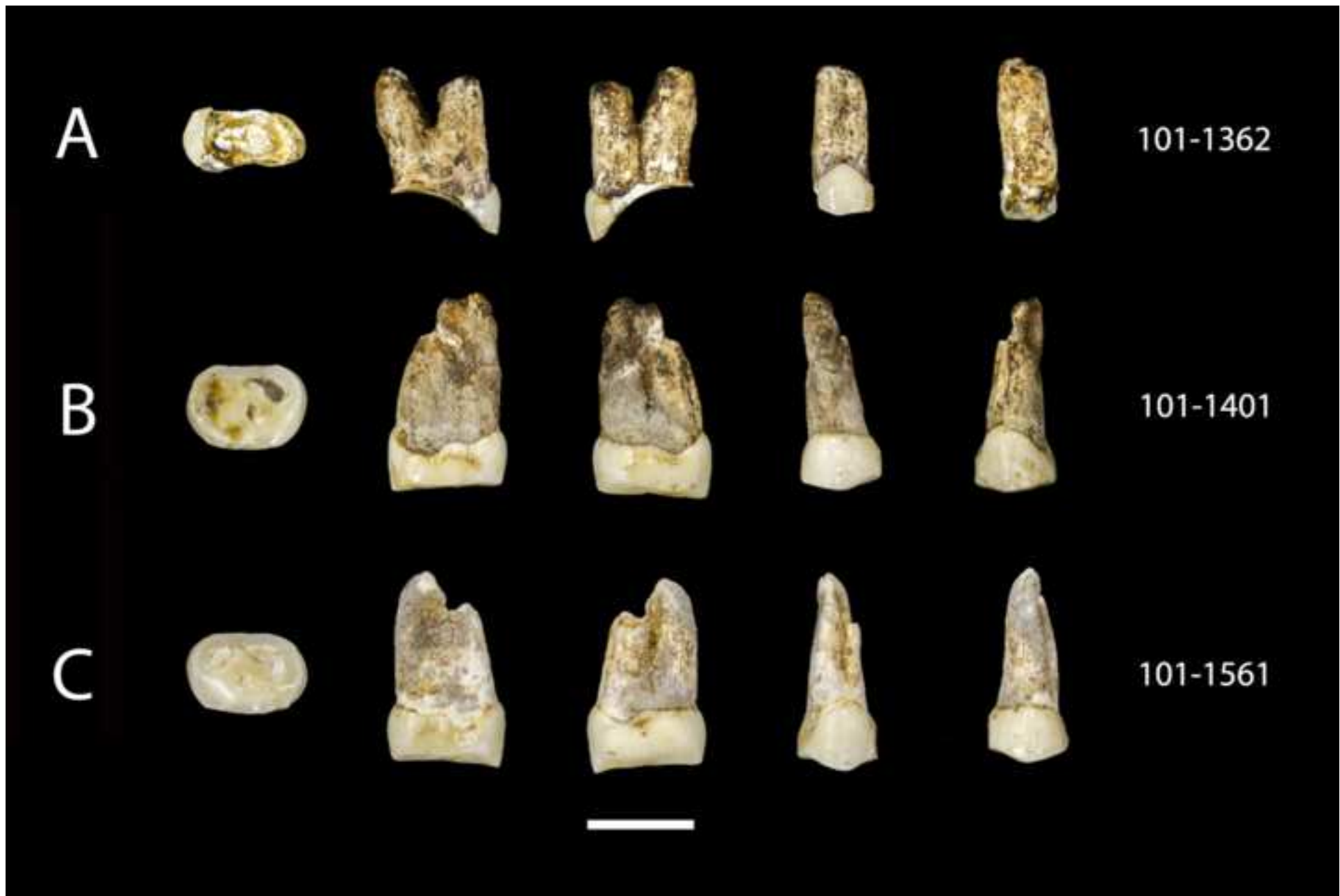


Figure 19_Upper p4s_continued_color.tif

Figure 20_upper M1_color.tif

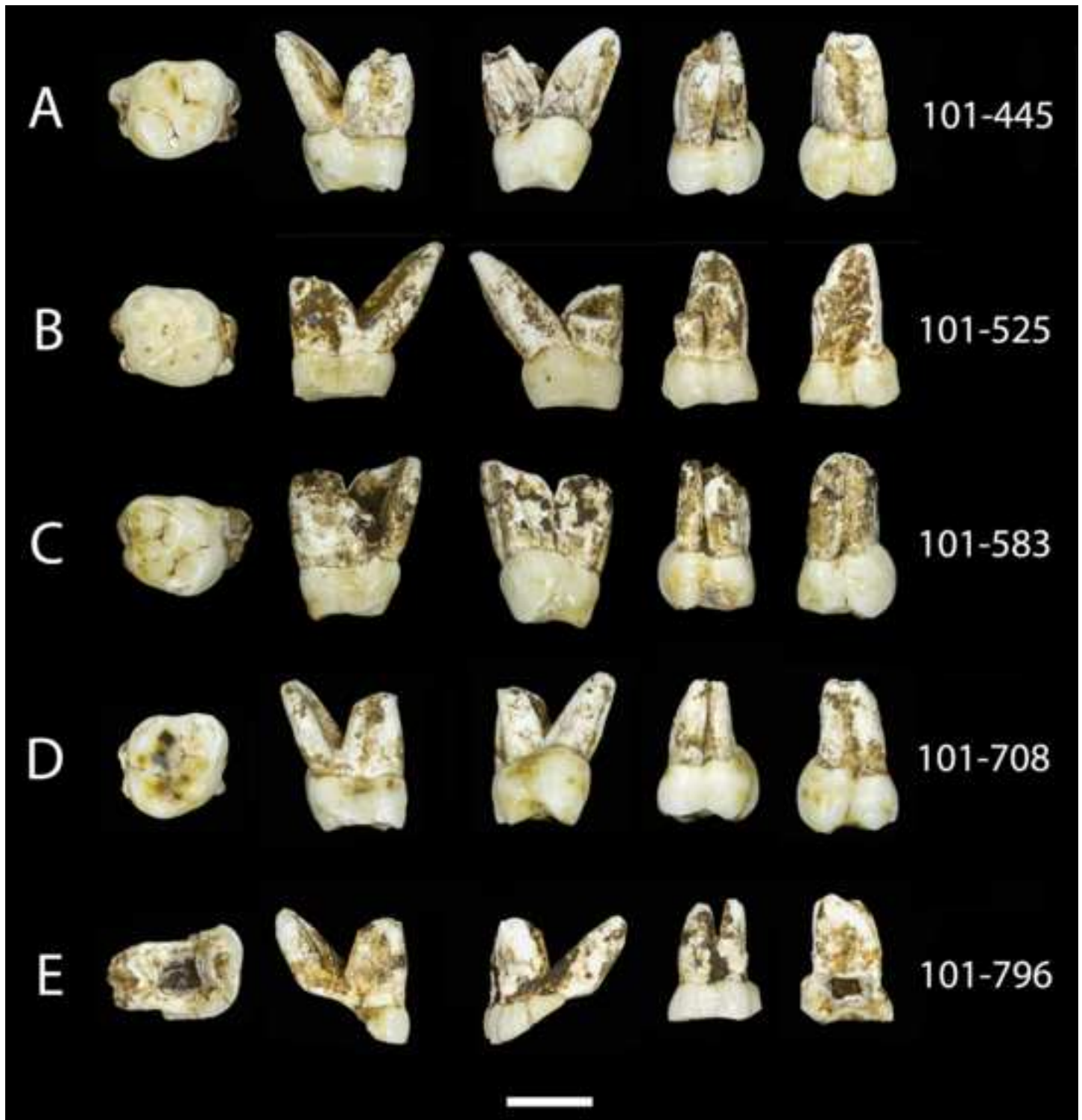


Figure 21_upper M1_cont_color.tif

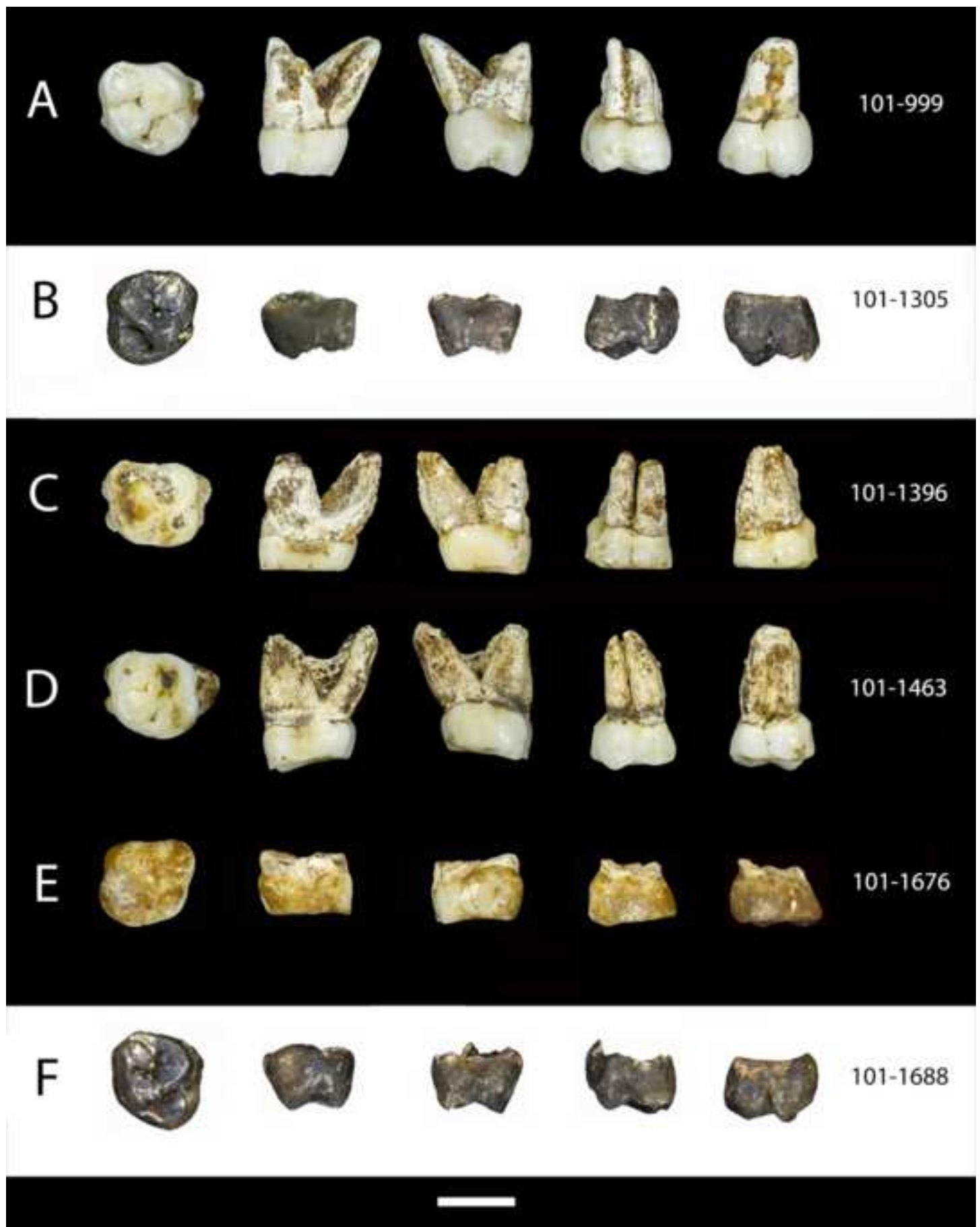


Figure 22_Maxillary M2_color.tif

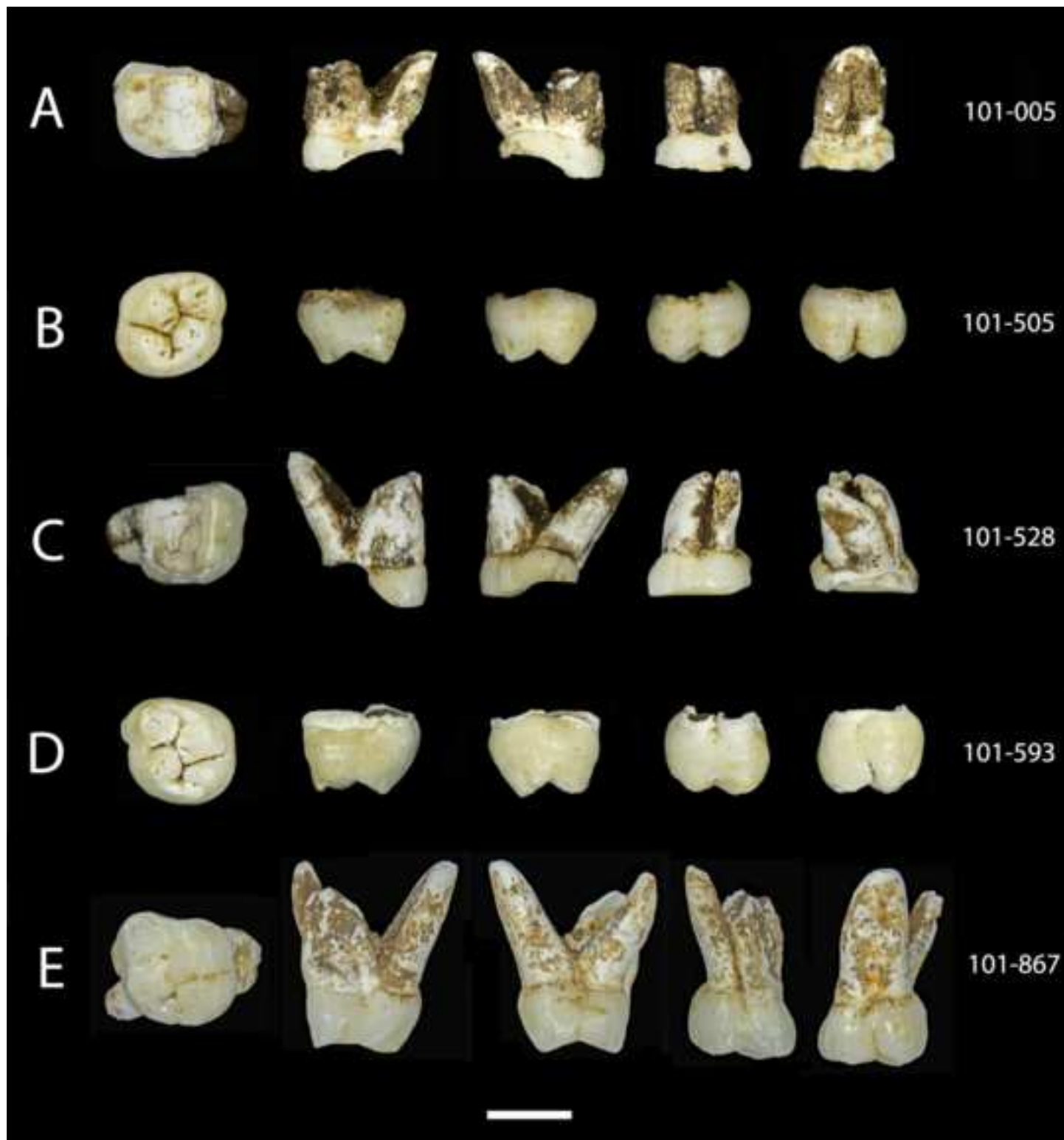


Figure 23_Maxillary M2_continued_color.tif

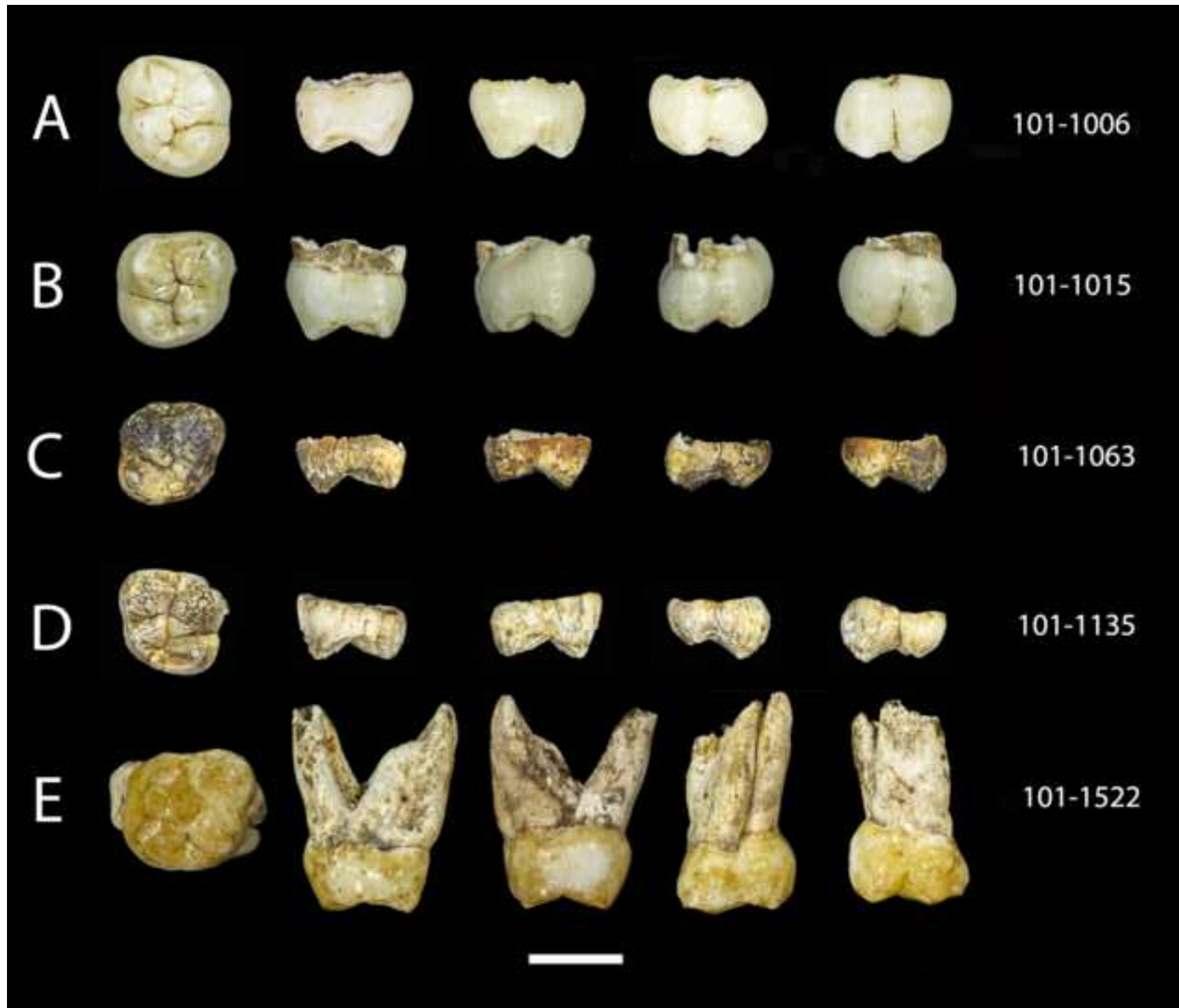
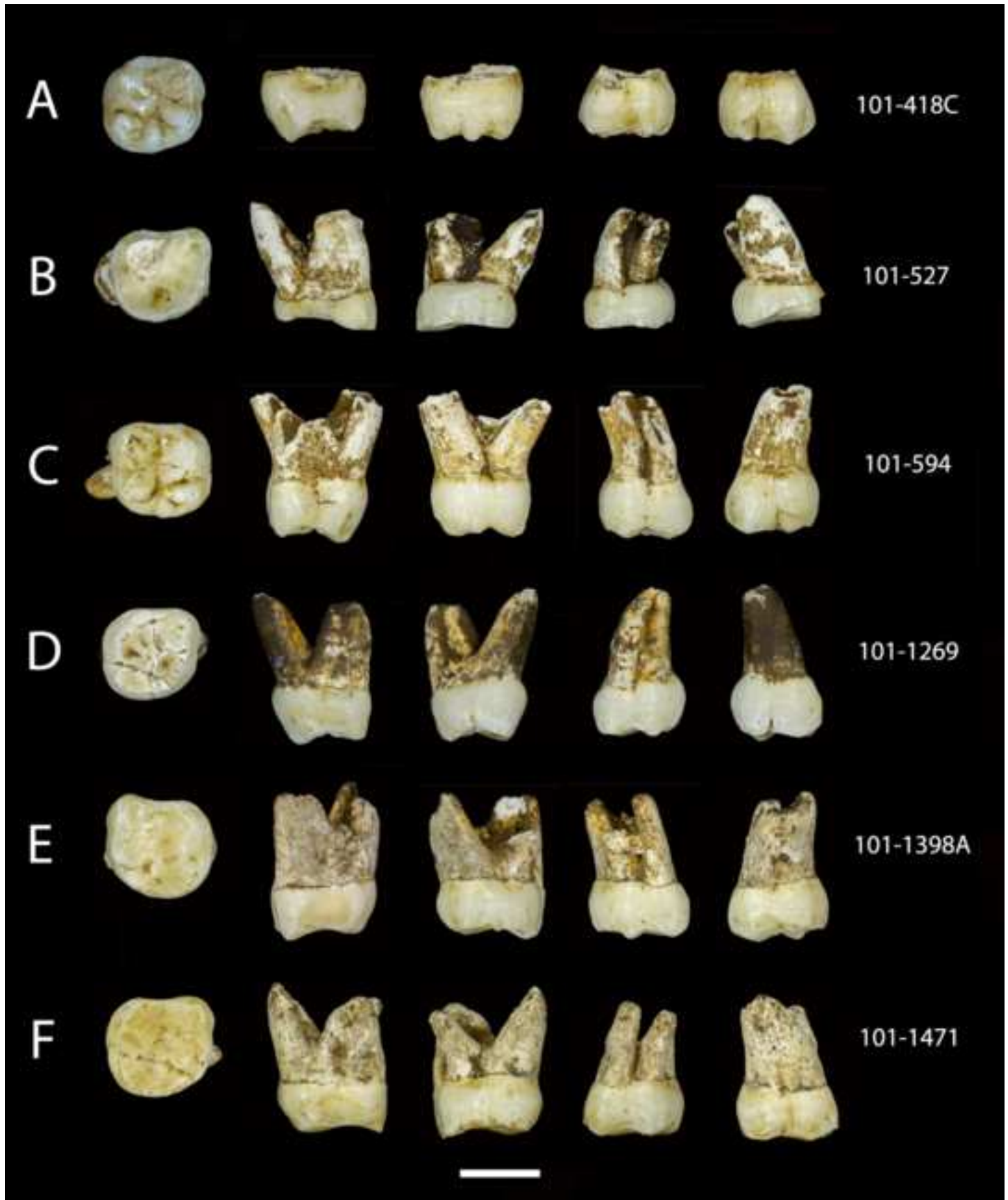


Figure 24_upper M3s_color.tif



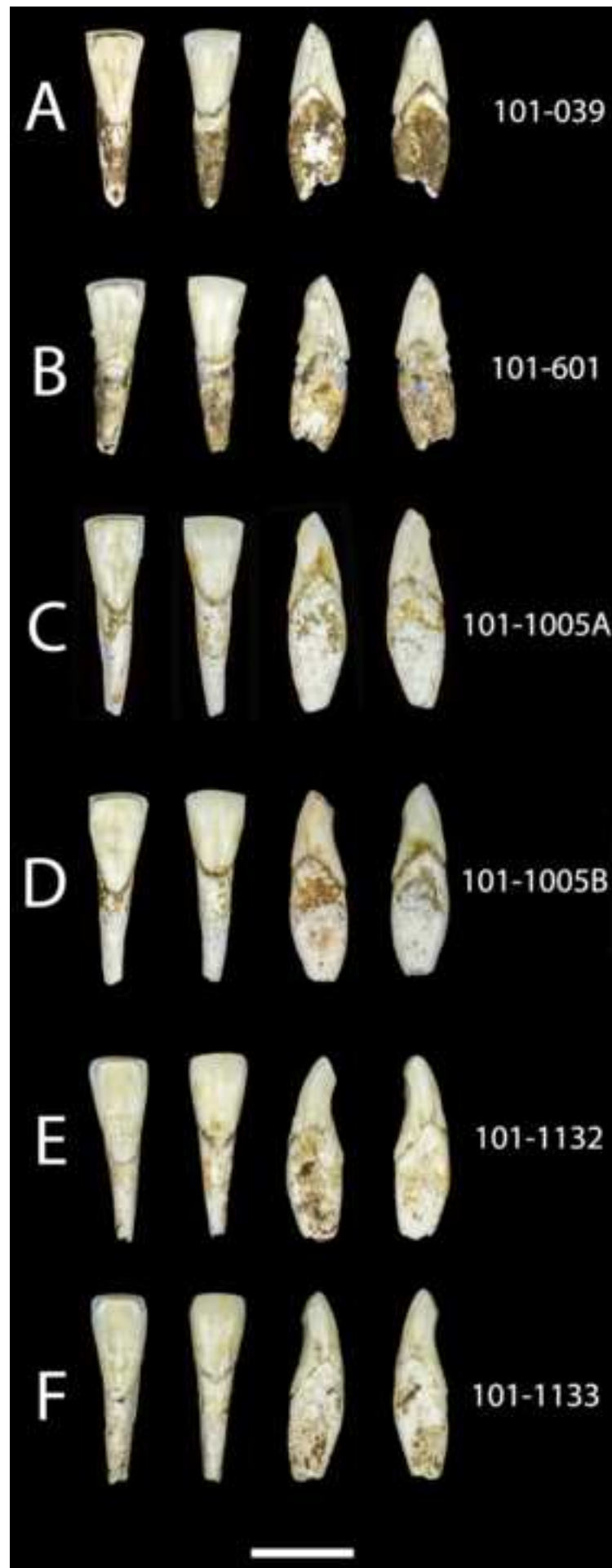


Figure 26_lower I2_color.tif

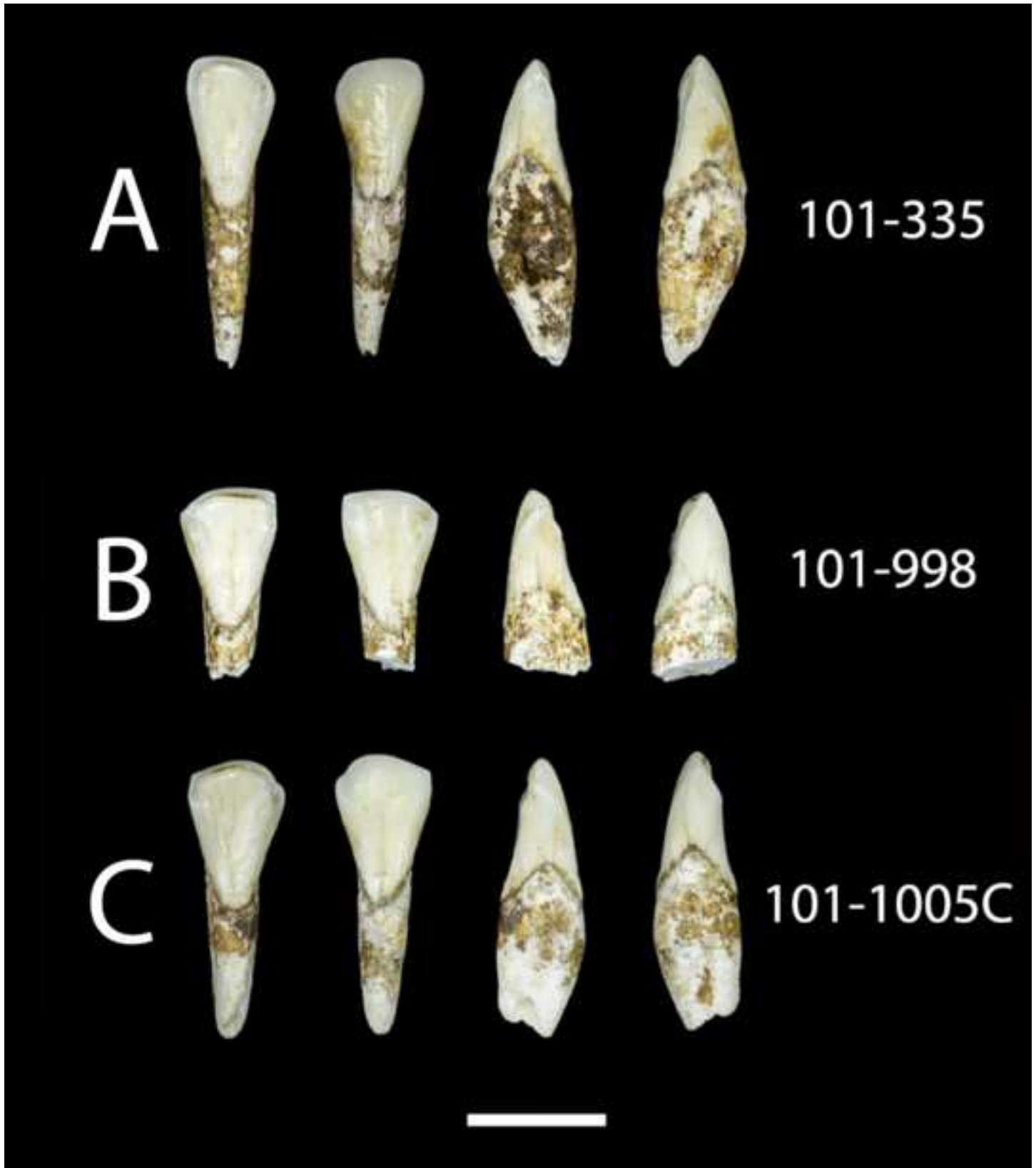
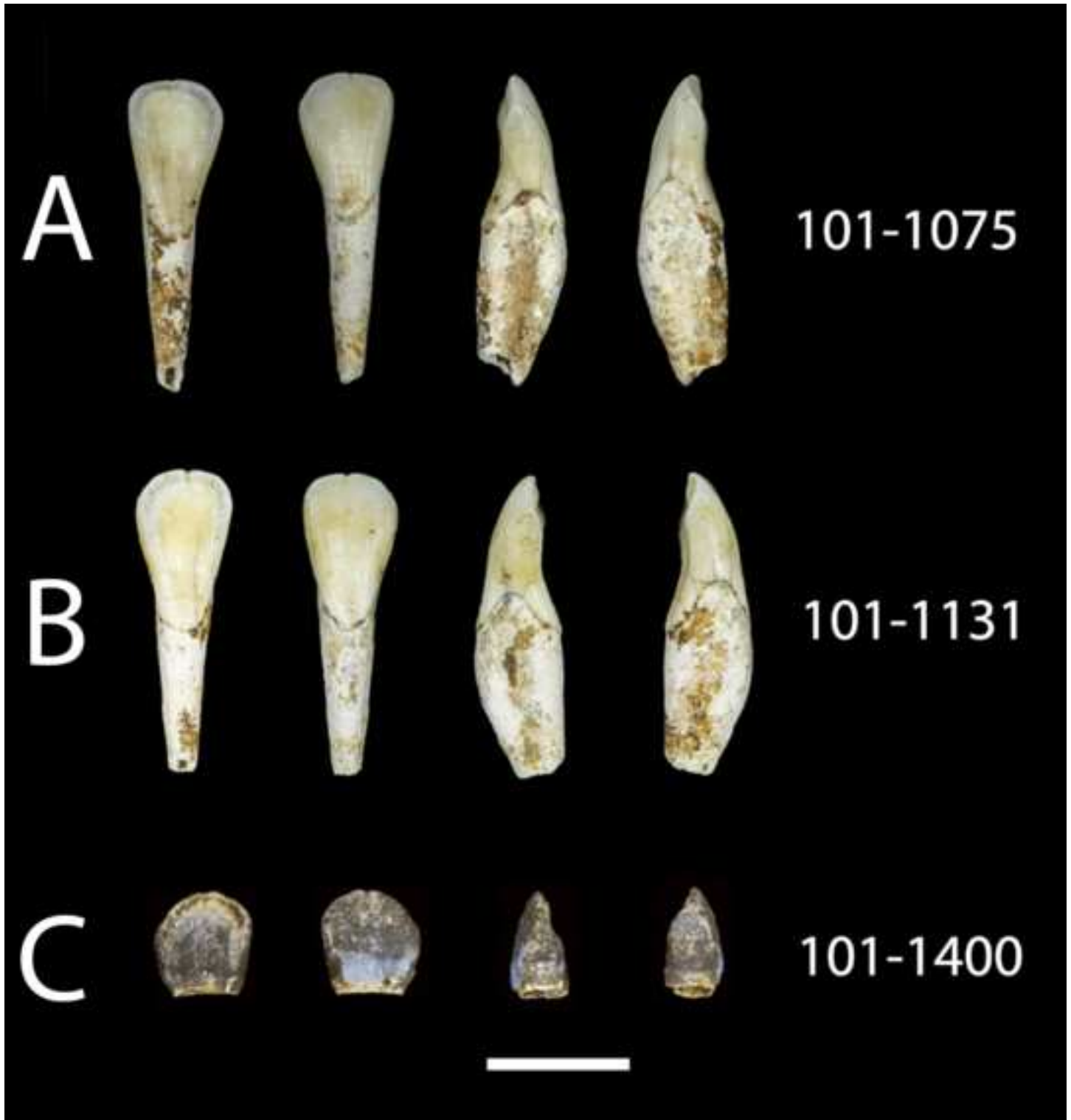


Figure 27_lower I2_cont_color.tif



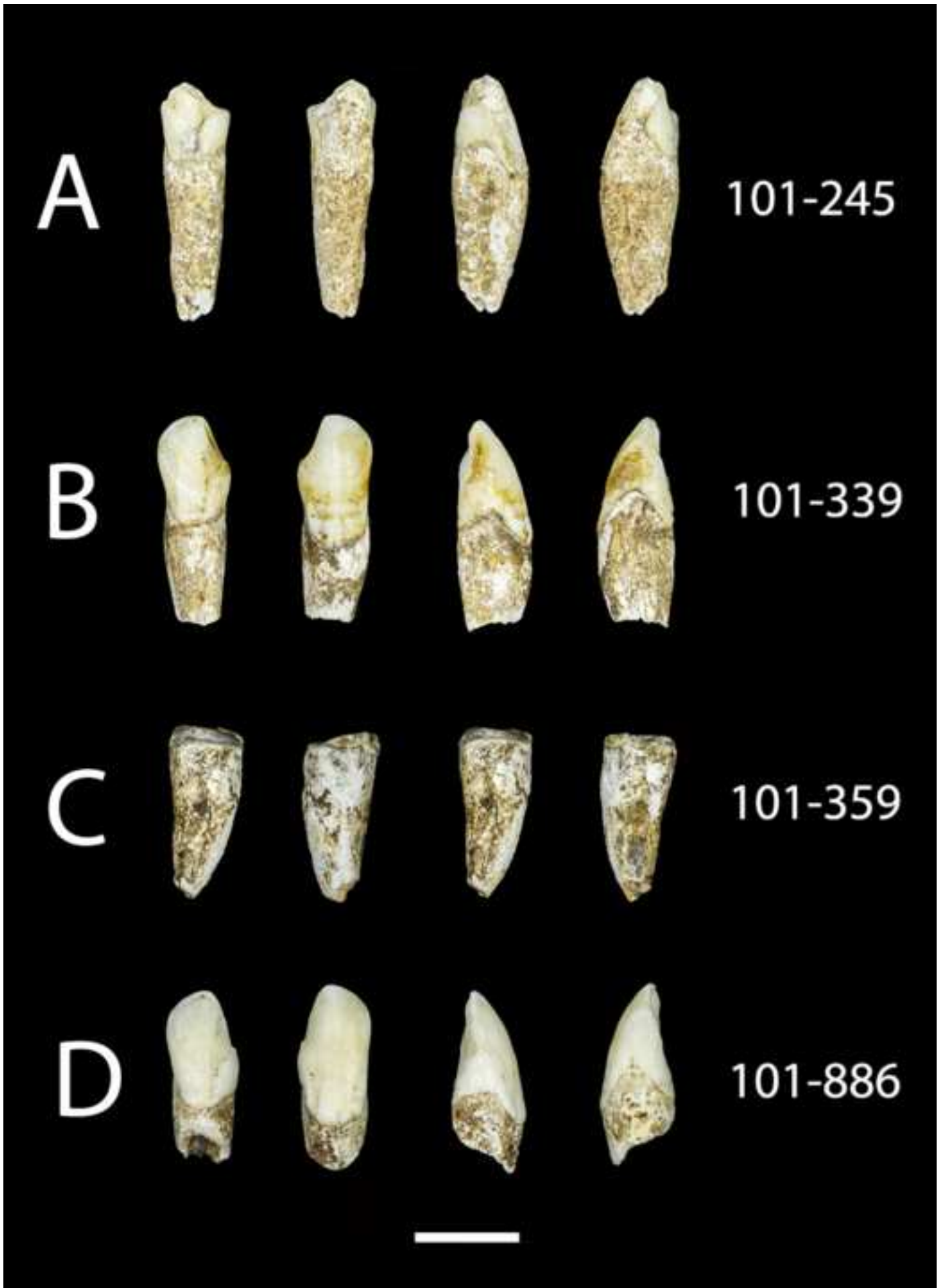


Figure 29_lower canines_cont_color.tif

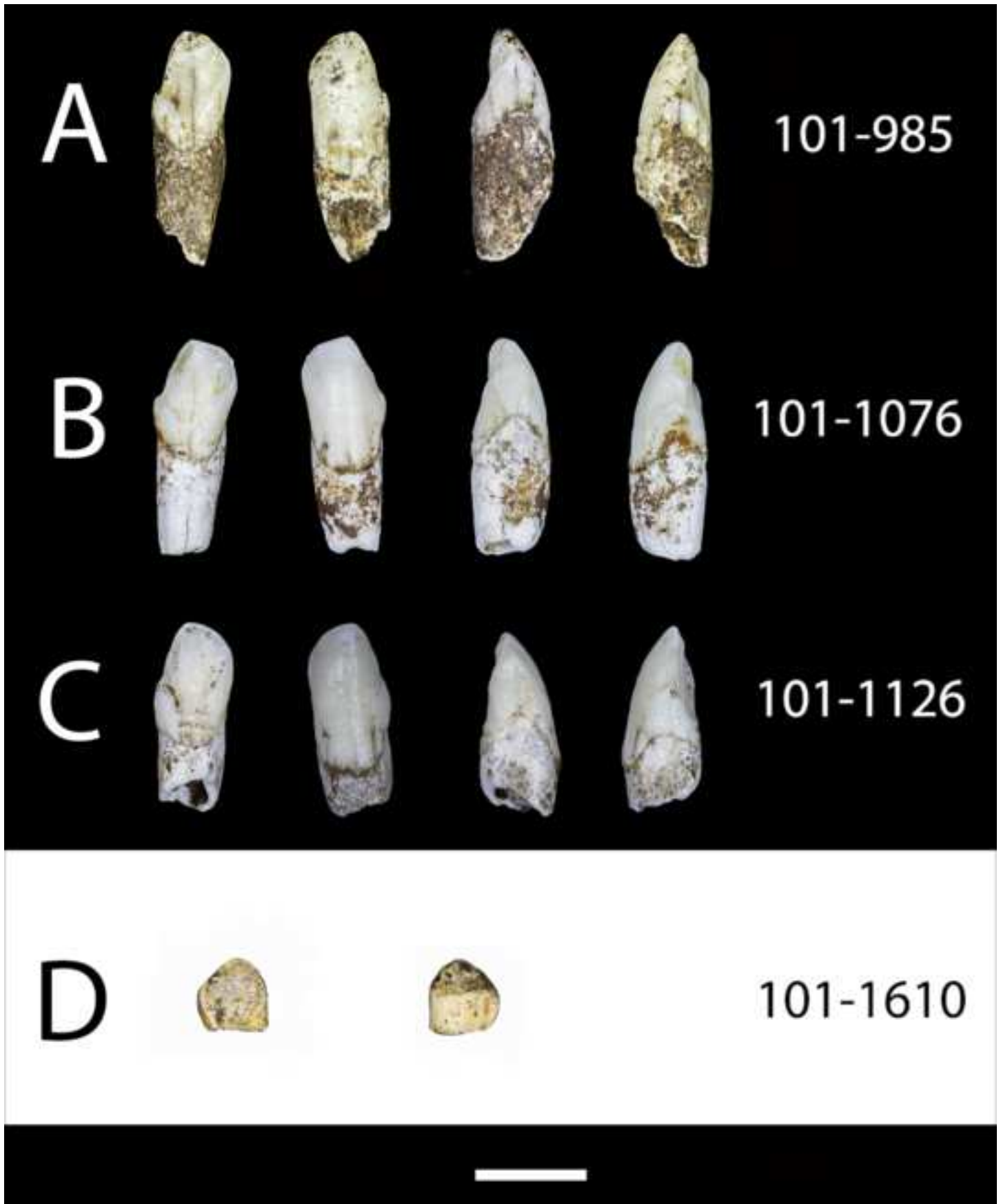
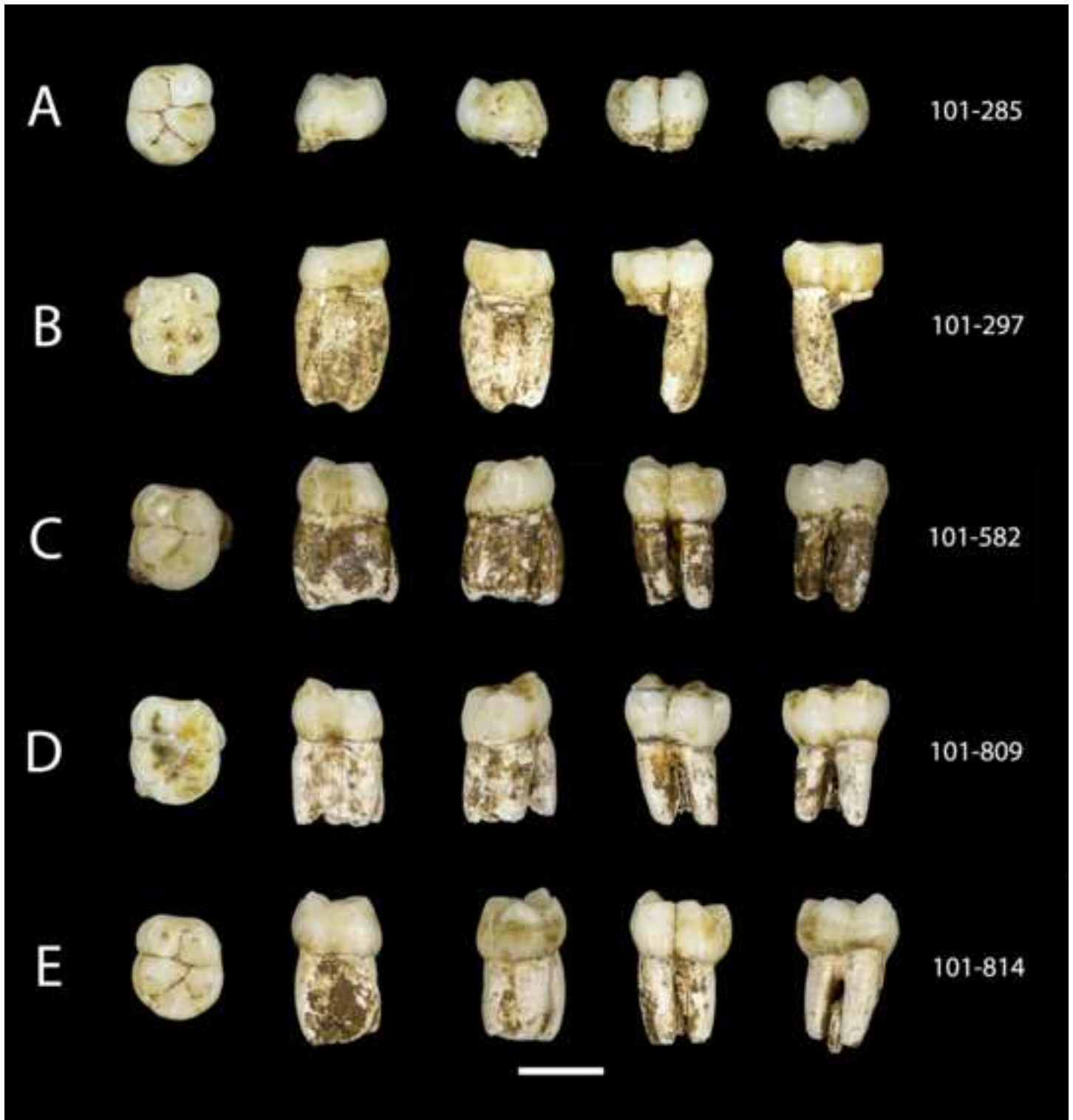








Figure 33_lower m1s_color.tif



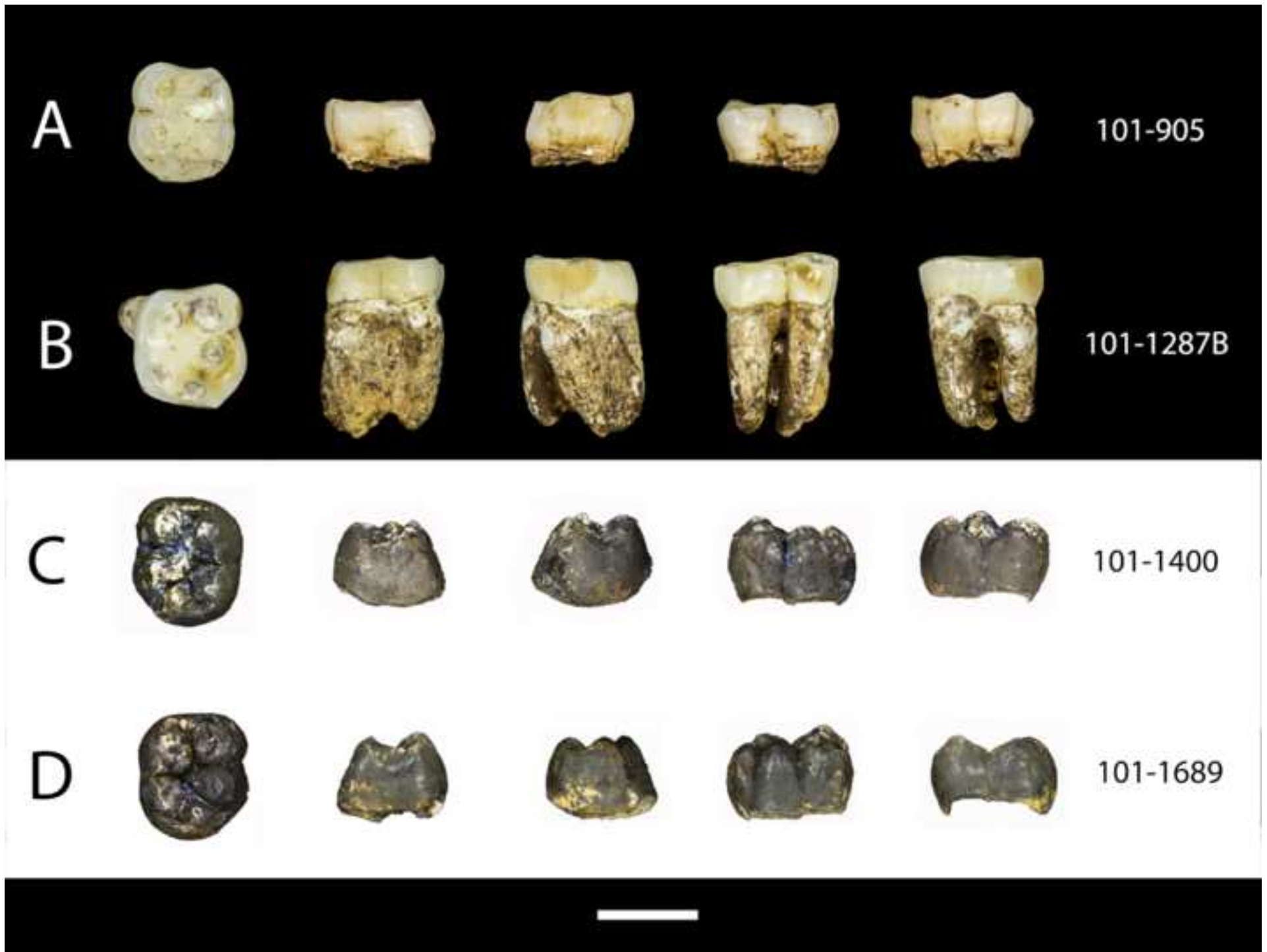


Figure 35_lower M2s_color.tif

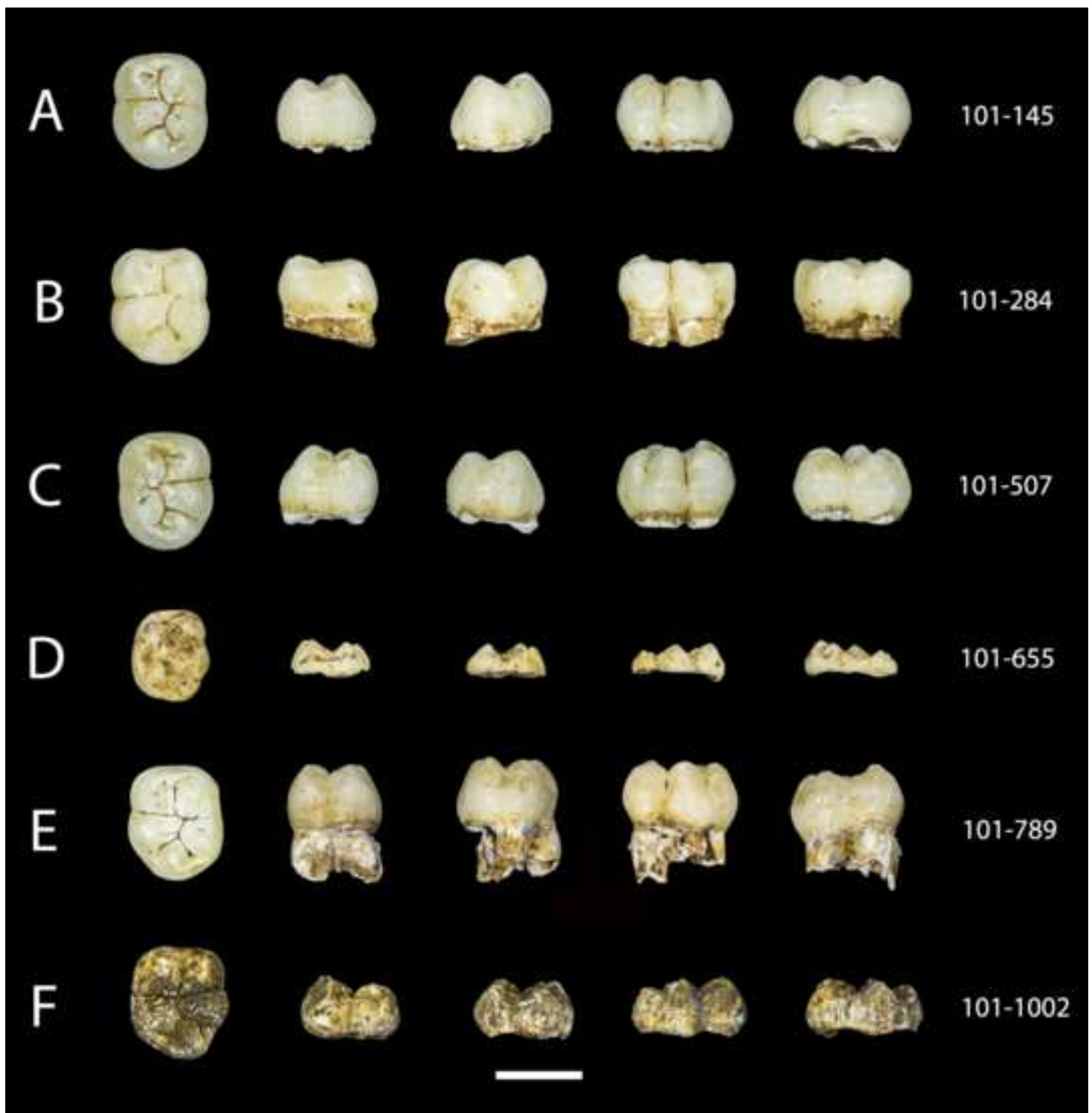




Figure 36_lower M3s_color.tif

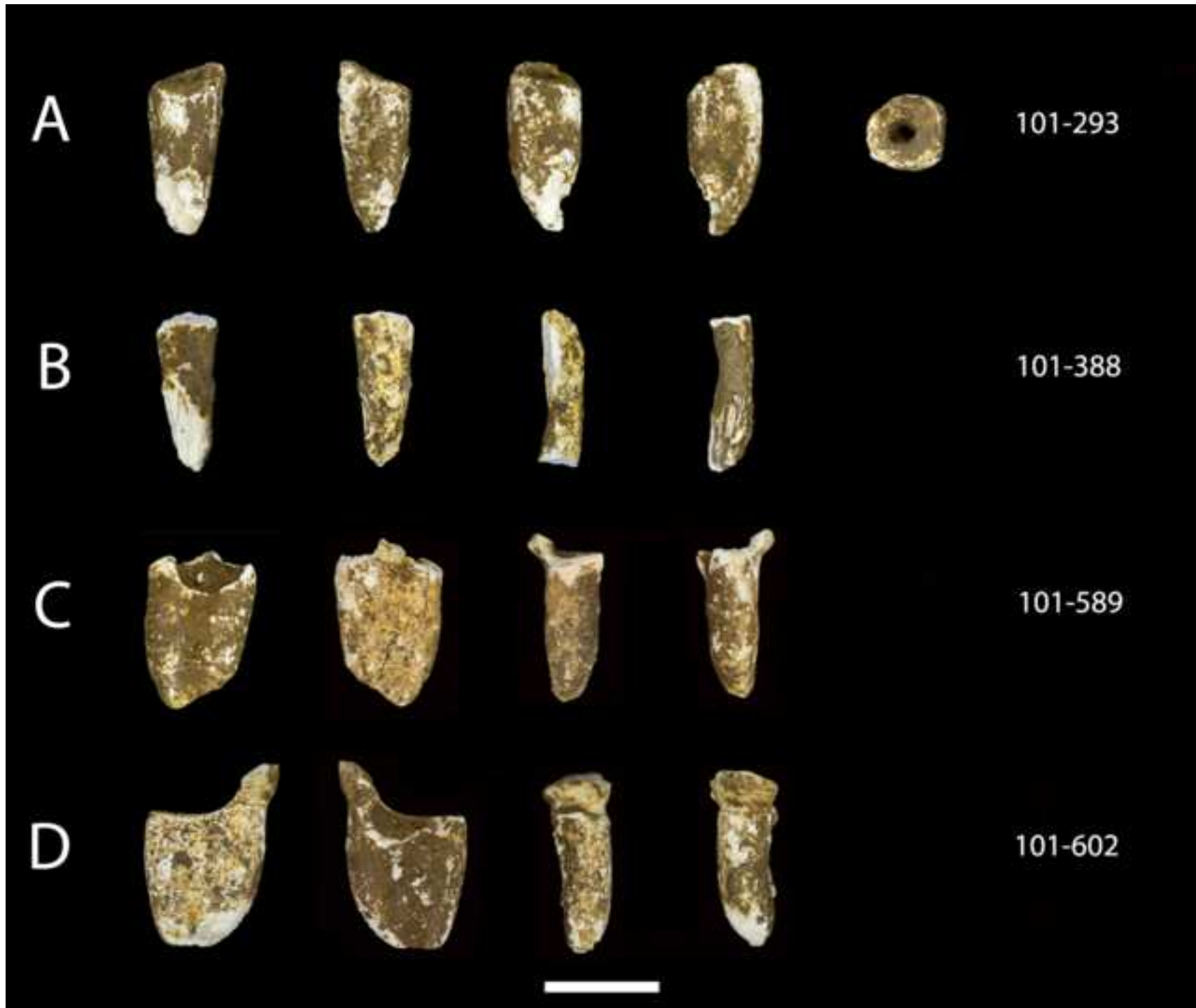


Figure 37_unknown.tif



Figure 38_developing cusp_color.tif





Figure 40_1277 maxilla_color.tif



Figure 41_UW 101_001_color.tif



Figure 42_010_mandible_color.tif

Figure 43_361 mandible_color.tif





Figure 44_377 mandible_color.tif



Figure 45_1142 mandible_color.tif

Figure 46_1261 mandible_color.tif





Figure 47_1400 mandible_color.tif

Table 1

Dental elements from the 2013–2015 excavations of the Dinaledi chamber. Mesiodistal (MD), buccolingual (BL), and labiolingual (LaL) measurements are reported in millimeters.

Specimen No.	Element	Figure	Basis for ID ^a	Wear stage ^b	MD (mm)	BL/LaL (mm)	Notes
U.W. 101-001	RP ₄ crown and roots	41	1	5	8.7	10.2	
	RM ₁ crown and roots	41	1	5	11.8		
	RM ₂ crown and roots	41	1	4	13.3	11.7	
	RM ₃ crown and roots	41	1	2	13.8	12.1	
U.W. 101-005	RM ² crown and roots	22A	3	6	(11.0) ^c	(12.2) ^c	Measurements not corrected for heavy interproximal and occlusal wear
U.W. 101-006	RM ₃ crown and roots	36A	3	5	13.4		
U.W. 101-010	RC ₁ crown and root	42	1	7			

	RP ₃ crown and roots	42	1	6–7		9.7
U.W. 101-037	RP ³ crown and roots	16A	3	2	8.3	10.8
U.W. 101-038	RI ¹ crown and root	10A	3	3–4	8.8	6.6
U.W. 101-039	RI ₁ crown and root	25A	3	4	5.9	5.5
U.W. 101-073	RI ² crown and root	11A	3	1	6.3	6.3
U.W. 101-144	LP ₃ crown and roots	30A	3	1	8.7	8.5
U.W. 101-145	LM ₂ crown	35A	3	1	13.3	10.8
U.W. 101-182	RP ³ crown and roots	16B	3	1–2	7.8	10.9
U.W. 101-184	LP ₄ crown and root	32A	3	1	9.0	8.5
U.W. 101-245	RC ₁ partial crown and root	28A	3	4		
U.W. 101-277	LP ⁴ crown and roots	18A	3	1–2	8.4	11.3
U.W. 101-284	LM ₂ crown and partial root	35B	3	1	13.8	11.4
U.W. 101-285	RM ₁ crown and partial root	33A	3	3	12.0	10.6
U.W. 101-293	C ¹ ? root	37A	3	8		

U.W. 101-294	LM ₁ mesial root	No figure	3	4			Described with U.W. 101-905
U.W. 101-297	RM ₁ crown and mesial root	33B	3	4	12.4		
U.W. 101-298	RP ₃ crown	30B	3	1	9.2	8.5	
U.W. 101-333	LP ⁴ crown	18B	3	1	8.0	11.1	
U.W. 101-334	RP ⁴ crown and roots	18C	3	1	8.0	11.1	
U.W. 101-335	RI ₂ crown and root	26A	3	2	6.7	5.9	
U.W. 101-337	RC ¹ crown and root	13A	3	1	7.7	8.3	
U.W. 101-339	RC ₁ crown and root	28B	3	1	7.0	7.4	
U.W. 101-357	mesial root of LM ₁ ?	No figure	3				
U.W. 101-358	LP ₃ crown and roots	30C	3	6+	(7.2) ^c	(9.6) ^c	Measurements not corrected for heavy interproximal and occlusal wear
U.W. 101-359	LC ₁ root	28C	3	7			

U.W. 101-361	LP ₄ root?	No figure	3				
	LM ₂	43	1	8			
	LM ₃	43	1	5	13.2	11.8	
U.W. 101-377	RP ₃ crown and roots	44	1	1	9.0	8.6	
	RP ₄ crown	44	1	1	8.8	9.0	
	RM ₁ crown and roots	44	1	2	12.1	10.9	
	RM ₂ crown and roots	44	1	1	12.9	11.2	
U.W. 101-383	RP ₄ crown and partial root	32B	3	1	9.1	8.9	
U.W. 101-384	RdP ⁴ crown and partial roots	5A	3	4	9.3	10.3	
U.W. 101-388	Root fragment	37B	3				
U.W. 101-412	LC ¹ crown and root	13B	3	3–4	8.5	8.3	
U.W. 101-417	LI ² crown and root	11B	3	3	(6.3) ^c	6.4	MD length not corrected for incisal and interproximal wear

U.W. 101-418C	LM ³ crown	24A	3	1	12.0	12.8	
U.W. 101-445	LM ¹ crown and partial roots	20A	3	1	12.2	11.6	
U.W. 101-455	RP ⁴ crown and root	18D	3	1	8.1	10.7	
U.W. 101-501	LC ¹ crown and root	13C	3	1	7.7	8.4	
U.W. 101-505	LM ² germ	22B	3	1	12.3	12.6	
U.W. 101-506	RP ₃ crown and roots	30D	3	1	8.9	8.5	
U.W. 101-507	RM ₂ crown	35C	3	1	13.6	11.1	
U.W. 101-516	LM ₃ crown and roots	36B	3	3	13.6	11.9	
U.W. 101-525	RM ¹ crown and partial roots	20B	3	3	11.7	11.8	Refits to U.W. 101- 1574
U.W. 101-527	LM ³ crown and roots	24B	3	3	11.5	12.4	
U.W. 101-528	LM ² crown and roots	22C	3	5	(11.8) ^c	(12.9) ^c	Measurements not corrected for heavy interproximal and occlusal wear

U.W. 101-544A	RdP ⁴ germ	5B	3	1	9.7	9.5	
U.W. 101-544B	RC ¹ germ	13D	3	1	(7.3) ^c	(4.7) ^c	Measurements reflect current size of germ
U.W. 101-544C	RdI ¹ crown and root	1A	3	3	4.3	6.2	
U.W. 101-582	LM ₁ crown and roots	33C	3	2	12.3	10.6	
U.W. 101-583	RM ¹ crown and roots	20C	3	2	11.7	12.2	
U.W. 101-589	M _? root	37C	3				
U.W. 101-591	LI ¹ crown and root	10B	3	4	(7.6) ^c	6.4	
U.W. 101-593	RM ² crown	22D	3	1	12.4	13.0	
U.W. 101-594	RM ³ crown and roots	24C	3	1	11.9	12.6	
U.W. 101-595	LdC ¹ crown and roots	3A	3	2	5.2	6.5	
U.W. 101-601	LI ₁ crown and roots	25B	3	3	6.0	(5.4) ^c	LaL breadth approximated given cervical damage
U.W. 101-602	RM _? ?	37D	3	7–8			

U.W. 101-652	Developing cusp	38	3			
U.W. 101-653	Incisor root?	39A	3	7		
U.W. 101-654	LM ₂ root	39B		8		
U.W. 101-655	RM ₂ germ (likely RM ₂)	35D	3	1		
U.W. 101-680	M ² lingual root?	No figure	3			
U.W. 101-686	anterior tooth root	39C	3			
U.W. 101-706	LC ¹ crown and root	14A	3	1	8.5	8.2
U.W. 101-708	LM ¹ crown and roots	20D	3	1	11.6	11.6
U.W. 101-709	RI ² crown and root	11C	3	1	6.7	5.8
U.W. 101-728	RdC ¹ crown and root	3B	3	1	5.3	6.4
U.W. 101-729	RP ³ crown and roots	16C	3	1	7.9	9.9
U.W. 101-786	LP ³ crown and root	16D	3	1	7.9	10.0
U.W. 101-789	LM ₂ crown and partial roots	35E	3	1	13.3	10.8
U.W. 101-796	LM ¹ crown and roots	20E	3	7–8		
U.W. 101-800	RP ₃ crown and roots	31A	3	4–5	9.4	8.9

U.W. 101-808	LP ⁴ crown and root	18E	3	1	8.0	10.6	
U.W. 101-809	LM ₁ crown and roots	33D	3	2	12.5	10.6	
U.W. 101-814	LM ₁ crown and roots	33E	3	2	12.1	10.5	
U.W. 101-816	RC ¹ crown and root	14B	3	1	8.5	8.2	
U.W. 101-823	RdP ³ crown and roots	4A	3	2	9.4	9.0	
U.W. 101-824	LdC ₁ crown and root	7A	3	3–4	4.8	6.0	
U.W. 101-850	RP ₃ crown and roots	41	3	4	8.0	9.6	refit to U.W. 101-001
U.W. 101-864	Crown and root fragment	39D	3				
U.W. 101-867	RM ² crown and roots	22E	3	1	12.7	13.3	
U.W. 101-886	RC ₁ crown and root	28D	3	1	7.1	7.1	
U.W. 101-887	LP ₄ crown and root	32C	3	1	8.7	8.9	
U.W. 101-889	LP ₃ crown and root	31B	3	1	9.1	8.5	
U.W. 101-905	LM ₁ crown	34A	3	4	(11.9) ^c	10.8	MD length not corrected for interproximal wear

U.W. 101-908	RC ¹ crown and root	14C	3	2	8.8	8.7	
U.W. 101-931	LI ¹ crown and root	10C	3	3–4	9.3	6.4	
U.W. 101-932	LI ² crown and root	11D	3	1	6.8	5.9	
U.W. 101-952	LI ² crown and root	12A	3	3	(6.1) ^c	6.4	MD length not corrected for interproximal wear
U.W. 101-985	LC ₁ crown and root	29A	3	1	7.3	7.2	
U.W. 101-998	LI ₂ crown and root	26B	3	2	7.3	6.0	
U.W. 101-999	RM ¹ crown and roots	21A	3	1	12.2	11.8	
U.W. 101-1002	RM ₂ ? germ	35F	3		(13.0) ^c	(11.3) ^c	Measurements reflect observed size of germ
U.W. 101-1004	RP ³ crown and root	17A	3	1	7.9	9.9	
U.W. 101-1005A	LI ₁ crown and root	25C	3	2	6.0	5.4	
U.W. 101-1005B	RI ₁ crown and root	25D	3	2	6.3	5.5	

U.W. 101-1005C	RI ₂ crown and root	26C	3	2	7.1	6.0	
U.W. 101-1006	RM ² crown	23A	3	1	12.5	12.4	
U.W. 101-1012	RI ¹ crown and root	10D	3	2	9.3	6.3	
U.W. 101-1014	RC ₁ crown and root	44	1,2,3	1	6.6	7.0	Refit to U.W. 101- 377
U.W. 101-1015	LM ² crown and partial root	23B	3	1	12.6	12.4	
U.W. 101-1063	LM ² germ?	23C	3		(11.2) ^c	(11.4) ^c	Measurements reflect size of crown incomplete germ
U.W. 101-1075	RI ₂ crown and root	27A	3	1	6.6	6.0	
U.W. 101-1076	LC ₁ crown and root	29B	3	1	7.4	6.9	
U.W. 101-1107	LP ³ crown and roots	17B	3	1	8.0	10.9	
U.W. 101-1126	LC ₁ crown and root	20C	3	1	7.1	7.2	
U.W. 101-1131	LI ₂ crown and root	27B	3	1	6.5	6.2	
U.W. 101-1132	LI ₁ crown and root	25E	3	1	5.7	5.4	

U.W. 101-1133	RI ₁ crown and root	25F	3	1	5.7	5.3	
U.W. 101-1135	RM ² germ?	23D	3		(11.0) ^c	(11.9) ^c	Measurements reflect size of crown incomplete germ
U.W. 101-1142	RM ₂ crown and roots	45	1	2	13.6	12.1	
	RM ₃ crown and roots	45	1	1	13.9	12.7	
	LI ₁ crown and root	46	1	4–5	(4.9) ^c	6.0	MD length not corrected for interproximal wear.
	RI ₁ crown and root	46	1	4–5	(4.8) ^c	5.9	MD length not corrected for interproximal wear.
	LI ₂ crown and root	46	1	4–5	(5.8) ^c	6.1	MD length not corrected for interproximal wear.
U.W. 101-1261							interproximal wear.

RI ₂ crown and root	46	1	4–5	(6.1) ^c	6.0	MD length not corrected for interproximal wear.
LC ₁ crown and root	46	1	4	7.1	7.0	
RC ₁ crown and root	46	1	4	7.2	7.0	
LP ₃ crown and roots	46	1	2	8.7	8.4	
RP ₃ crown and roots	46	1	2	8.6	8.6	
LP ₄ crown and roots	46	1	3	8.7	9.0	
RP ₄ crown and roots	46	1	3	8.3	8.9	
LM ₁ crown and roots	46	1	4	11.3	10.8	
RM ₁ crown and roots	46	1	4	11.2	10.7	
LM ₂ crown and roots	46	1	2	12.2	11.1	
RM ₂ crown and roots	46	1	2	12.4	11.0	
LM ₃ crown and roots	46	1	1	13.1	12.3	
RM ₃ crown and roots	46	1	1	13.0	11.6	

U. W. 101-1269	LM ³ crown and roots	24D	2,3	1	11.5	12.2	
U.W. 101-1277	LI ¹ crown and root	40	1	4–5	(8.1) ^c	6.4	MD length not corrected for interproximal wear
	LI ² crown and root	40	1	4	(6.2) ^c	6.0	MD length not corrected for interproximal wear
	L ^C crown and root	40	1	3	7.9	8.2	
	LP ³ crown and roots	40	1	2–3	8.0	10.2	
	LP ⁴ crown and roots	40	1	2	8.6	11.2	
	LM ¹ crown and roots	40	1	3–4	11.0	11.3	
	LM ² crown and roots	40	1	1	12.1	12.5	
U.W. 101-1287A	LdC ¹ crown and root	3C	3	2	6.5	5.4	

U.W. 101-1287B	RM ₁ crown and roots	34B	3	4	(12.3) ^c	11.4	MD length not corrected for interproximal wear
U.W. 101-1304	LdI ²	2	3	1	4.9	4.1	
U.W. 101-1305	LM ¹ germ	21B	3		12.3	11.8	
U.W. 101-1331	LdI ¹ crown and root	1B	3	3	6.1	4.2	
U.W. 101-1362	LP ⁴ crown and roots	19A	3	7			
U.W. 101-1376	LdP ⁴ crown and roots	5C	3	1	10.3	10.1	
U.W. 101-1377	LdP ³ crown and roots	4B	3	2	9.3	8.7	
U.W. 101-1396	RM ¹ crown and roots	21C	3	5	(11.3) ^c	12.4	MD length not corrected for interproximal wear
U.W. 101-1398A	RM ³ crown and roots	24E	3	1–2	12.7	13.1	
U.W. 101-1398B	I ² root?	No Figure	3				
U.W. 101-1400	LdC ₁ crown and root	47	1	1	5.7	5.0	

	LdP ₃ crown and roots	47	1	2	9.5	7.1	
	LdP ₄ crown and roots	47	1	1	11.4	9.0	
	Ll ₂ germ	27C	1				
	LC ₁ germ	No figure	1				
	LM ₁ germ	34C	1		12.7	10.9	
U.W. 101-1401	RP ⁴ crown and roots	19B	3	5	(7.5) ^c	11.1	MD length not corrected for interproximal wear
U.W. 101-1402	RP ³ crown and roots	17C	3	4–5	8.3	10.9	
U.W. 101-1403	RC ¹ root	114D	3				
U.W. 101-1463	RM ¹ crown and roots	21D	3	3	11.1	11.7	
U.W. 101-1471	LM ³ crown and roots	24F	3	2	12.7	13.1	
U.W. 101-1510	RC ¹ crown and root?	15A	3	7			
U.W. 101-1522	LM ² crown and roots	23E	3	2	12.9	13.6	

U.W. 101-1548	LC ¹ germ	15B	3		(7.3) ^c	(4.6)	Measurements reflect size of crown incomplete germ
U.W. 101-1556	LC ¹ crown and root	15C	3	5	(7.5) ^c	9.4	MD length not corrected for interproximal wear
U.W. 101-1558	RI ¹ crown and root	10E	3	5	(7.9) ^c	7.1	MD length not corrected for interproximal wear
U.W. 101-1560	LP ³ crown and roots	17D	3	4–5	8.4	10.8	
U.W. 101-1561	LP ⁴ crown and roots	19C	3	5	(7.4) ^c	11.0	MD length not corrected for interproximal wear
U.W. 101-1565	LP ₃ crown and partial root	31C	3	1	9.1	8.6	
U.W. 101-1571	LdC ₁ crown and partial root	7B	3	4	6.0	4.6	

U.W. 101-1574	RM ¹ distobuccal root	No figure	3				Refits to U.W. 101- 525
U.W. 101-1588	LI ² crown and root	12B	3	1	6.2	6.3	
U.W. 101-1605	LM _? germ?	No figure	3				
U.W. 101-1610	RC ₁ germ	29D	3				
U.W. 101-1611	RdC ₁ crown and root	7C	3	1	5.8	5.0	
U.W. 101-1612	RdI ₂ crown and root	6	3	1	4.7	4.2	
U.W. 101-1676	LM ¹ crown	21E	3	3–4	11.7	11.9	
U.W. 101-1684	LI ² crown and root	12C	3	5	(6.5) ^c	6.8	
U.W. 101-1685	RdP ₃ crown and roots	8	1	2	9.3	7.0	
U.W. 101-1686	RdP ₄ crown and root	9	3	1	11.4	9.0	
U.W. 101-1687	RdP ⁴ crown and roots	5D	3	1	10.4	10.1	
U.W. 101-1688	RM ¹ germ	21F	3		12.1	12.0	
U.W. 101-1689	RM ₁ germ	34D	3		12.6	11.2	

Abbreviations: ID = identification to class and side; L = left; R = right; M[?] = maxillary molar (unknown position); M_? = mandibular molar (unknown position).

^a Basis for ID codes are as follows: (1) in situ; (2) associated based on interproximal contact facets; (3) based on morphology.

^b Wear stages are based on Smith (1984).

^c Values in parentheses are uncorrected for wear, are observed measurements for incompletely formed crowns or broken crowns or are estimated values; please see accompanying Notes for each specimen for further details. Measurements reported in parentheses are not intended to be included in comparative analyses of tooth size.

Table 2

Proposed associations among the Dinaledi teeth. Specimens for each proposed association are arranged by specimen number.

Association	Associated teeth
1	U.W. 101-544B (RC ¹ germ), U.W. 101-544C (dI ¹), U.W. 101-728 (RdC ¹), U.W. 101-1287A (LdC ¹), U.W. 101-1305 (LM ¹), U.W. 101-1376 (LdP ⁴), U.W. 101-1377 (LdP ³), U.W. 101-1331 (dI ¹), U.W. 101-1400 (LdC ₁ , LdP ₃ , LdP ₄ , LI ₂ germ, and LM ₁ germ in situ), U.W. 101-1548 (LC ¹ germ), U.W. 101-1610 (RC ₁ germ), U.W. 101-1611 (RdC ₁), U.W. 101-1612 (RdI ₂), U.W. 101-1685 (RdP ₃), U.W. 101-1686 (RdP ₄), U.W. 101-1687 (RdP ⁴), U.W. 101-1688 (RM ¹ germ), U.W. 101-1689 (RM ₁ germ)
2	U.W. 101-377 (RP ₃ –RM ₂), U.W. 101-789 (LM ₂), U.W. 101-809 (LM ₁), U.W. 101-887 (LP ₄), U.W. 101-889 (LP ₃), U.W. 101-998 (RI ₂), U.W. 101-1005A (LI ₁), U.W. 101-1005B (RI ₁), U.W. 101-1005C (RI ₂), U.W. 101-1014 (R _C), U.W. 101-1076 (L _C),
3	U.W. 101-706 (LC ¹), U.W. 101-709 (RI ²), U.W. 101-816 (RC ¹), U.W. 101-931 (LI ¹), U.W. 101-932 (LI ²), U.W. 101-1012 (RI ¹)

- 4 U.W. 101-886 (RC₁), U.W. 101-1075 (RI₂), U.W. 101-1126 (LC₁), U.W. 101-1131 (LI₂),
U.W. 101-1132 (LI₁), U.W. 101-1133 (RI₁)
- 5 U.W. 101-277 (LP⁴), U.W. 101-418C (LM³), U.W. 101-1522 (LM²), U.W. 101-1676
(LM¹), and possibly U.W. 101-525 (RM¹) and U.W. 101-594 (RM³)
- 6 U.W. 101-1396 (RM¹), U.W. 101-1401 (RP⁴), U.W. 101-1402 (RP³), U.W. 101-1403
(RC¹), U.W. 101-1556 (LC¹), U.W. 101-1560 (LP³), U.W. 101-1561 (LP⁴), and possibly
U.W. 101-1684 (LI²)
- 7 (DH1) U.W. 101-1261 (complete mandibular dentition), U.W. 101-1269 (LM³), U.W. 101-1277
(LI¹–LM² in situ), and U.W. 101-1463 (RM¹)
- 8 (DH3) U.W. 101-357 (mesial root of LM₁), U.W. 101-358 (LP₃), U.W. 101-359 (LC₁), and U.W.
101-361 (LP₄–LM₃ in situ)
- 9 U.W. 101-527 (LM³), U.W. 101-528 (LM²), U.W. 101-796 (LM¹), U.W. 101-1362 (LP⁴),
and possibly U.W. 101-005 (RM²)

Abbreviations: L = left; R = right.